Identification of new molecular targets and antibiotics as novel strategies against filarial infections: Characterization of lipid II biosynthesis in *Wolbachia* endobacteria

Dissertation
zur
Erlangung des Doktorgrades (Dr. rer. nat.)
der
Mathematisch-Naturwissenschaftlichen Fakultät
der
Rheinischen Friedrich-Wilhelms-Universität Bonn

vorgelegt von
Kirstin Anne Meier
aus
Bonn

Bonn 2018

Angefertigt mit Genehmigung der Mathematisch-Naturwissenschaftlichen Fakultät der Rheinischen Friedrich-Wilhelms-Universität Bonn

1. Gutachter: Prof. Dr. Achim Hörauf

2. Gutachter: Prof. Dr. Albert Haas

Tag der Promotion: 06.05.2019

Erscheinungsjahr: 2019

Table of Contents

Summary

Filarial nematodes are prevalent in tropical regions worldwide with some species pathogenic to humans. Filarial diseases include lymphatic filariasis (68 million infected people) and onchocerciasis (37 million infected people) that can result in severe symptoms and are a health problem in affected communities. Anthelmintic drugs must be applied for years as the substances do not act against the adult worms. Moreover, reported side effects and suspected reduced efficacy of the currently used anthelmintics are worrisome. The development of novel substances effective against all life stages of the filariae and suitable for mass drug administration programs is substantial to successfully eliminate filarial diseases. *Wolbachia* are obligate intracellular Gram-negative bacteria that are widespread in arthropods and found in several filarial nematode species. In filarial worms, *Wolbachia* are obligate mutualistic endosymbionts required for survival of their hosts and for embryogenesis in the female worms. Thus, filariasis can be effectively treated with antibiotics targeting *Wolbachia.* However, the currently used antibiotics are not suitable for mass drug administration programs and new substances, which are well-tolerated by patients, are required. A better understanding of *Wolbachia* biology is crucial to identify novel potential antibiotic targets. The genome of *Wolbachia* is highly reduced due to adaption to their hosts and in contrast to free-living bacteria, they do not need a protective cell wall composed of the macromolecule peptidoglycan. However, the peptidoglycan precursor lipid II has already been shown to be synthesized and required for cell division in *Wolbachia*. Until now, it is unclear if and how lipid II is modified and peptidoglycan has never been detected in these endobacteria.

To provide insight into wolbachial lipid II processing, the putative penicillin-binding proteins (PBPs) PBP2 and PBP6a from *Wolbachia* endosymbionts of the filarial nematode *Brugia malayi* (*w*Bm) were analyzed in this study. Also, the activity of AmiD and PBP3 from *Wolbachia* endosymbionts of *Drosophila melanogaster* (*w*Mel) were characterized, two lipid II processing enzymes additionally present in genomes of *Wolbachia* residing in arthropods. Binding studies were performed to measure a potential interaction between the peptidoglycan-associated outer membrane lipoprotein (Pal) from *w*Bm and lipid II as well as PBP2. To detect a putative peptidoglycan-like structure in *Wolbachia,* lipid II was labeled in *Wolbachia* from *Aedes albopictus* using dipeptide analogues. Moreover, an established cell-free *Wolbachia* culture was further studied regarding potential growth facilitating factors and impact of antibiotics.

The results of the present study demonstrate PBP activity in dependence on functional serines of the active site motifs SXXK. PBPs are typically blocked by β-lactam antibiotics that bind to the serine of the highly conserved SXXK motif. Nevertheless, the PBPs were resistant to β-lactams. Contrary to their *E. coli* orthologs, all examined wolbachial PBPs encode additional SXXK motifs which might contribute to enzyme functionality and might explain β-lactam resistance. *In silico* analyses predicted that due to protein folding, β-lactams might not have access to all active site motifs. Therefore, in contrast to canonical systems like *E. coli*, these enzymes are not appropriate targets to deplete *Wolbachia*. AmiD showed zinc-dependent amidase activity and cleaved intact peptidoglycan, monomeric lipid II and additionally anhydromuropeptides, substrates that are generated by cleaved glycosidic bonds of glycan strands. The conservation of the capability of AmiD to cleave anhydromuropeptides gives a hint that at least insect *Wolbachia* may contain a peptidoglycan-like structure with connected glycan strands. Lipid II and PBP2 both interacted with the outer membrane protein Pal from *w*Bm suggesting that lipid II and PBP2 are present in the *Wolbachia* periplasmic space. These results together with the active PBPs from *w*Bm indicate that lipid II might be processed to a peptidoglycan-like structure also in *Wolbachia* residing in filarial nematodes. The dipeptide labeling provided visual evidence of a lipid II-containing structure in *Wolbachia* for the first time, which was absent in fosfomycin-treated cells with impaired lipid II synthesis. Moreover, fosfomycin led to an aberrant phenotype of cell-free *Wolbachia* resulting in enlarged cells. None of the other applied antibiotics including β-lactams showed an effect on morphology providing further evidence that *Wolbachia* are resistant to this class of antibiotics.

In conclusion, the results of this study together with latest research findings regarding peptidoglycan in intracellular bacteria indicate that *Wolbachia* are not cell wall-less bacteria, but rather have a physical structure composed of lipid II that can interact with outer membrane proteins and that is necessary for coordinated cell division.

Zusammenfassung

Filarien kommen weltweit in den Tropen vor und einige humanpathogene Arten verursachen Krankheiten wie die lymphatische Filariose (68 Millionen Infizierte) oder Onchozerkose (37 Millionen Infizierte). Diese Infektionen können zu schweren Pathologien führen und stellen ein erhebliches Gesundheitsproblem in betroffenen Gebieten dar. Die zur Verfügung stehenden Antiwurmmittel müssen jahrelang verabreicht werden, da die Medikamente nicht gegen die adulten Würmer wirken. Außerdem besteht bei den Antiwurmmitteln das Risiko möglicher Nebenwirkungen und Resistenzentwicklungen. Um Filarioseerkrankungen komplett einzudämmen, werden neue Medikamente benötigt, die gegen alle Entwicklungsstadien der Filarien wirksam sind und in Massenanwendungsprogrammen eingesetzt werden können. *Wolbachien* sind obligat intrazelluläre Gram-negative Bakterien, die sowohl in Arthropoden als auch in einigen Filarienarten vorkommen. In Filarien sind *Wolbachien* mutualistisch und essentiell für das Überleben ihres Wirtes sowie für die Embryogenese der weiblichen Würmer. Daher können Filariosen durch die Gabe von Antibiotika, die die *Wolbachien* abtöten, effektiv behandelt werden. Die momentan verwendeten Antibiotika sind jedoch nicht für Massenanwendungsprogramme geeignet. Um neue potentielle Angriffspunkte für Antibiotika zu finden, die für die Behandlung von Filariosen verwendet werden können, ist die Grundlagenforschung über *Wolbachien* unerlässlich. Das Genom von *Wolbachien* ist aufgrund ihrer endosymbiontischen Lebensweise bis auf die Gene reduziert, die essentiell zum Überleben sind. Die intrazellulären *Wolbachien* benötigen im Gegensatz zu freilebenden Bakterien keine schützende Zellwand bestehend aus einer Peptidoglykanmatrix. Jedoch wurde gezeigt, dass das Peptidoglykan Vorläufermolekül Lipid II synthetisiert und für die Zellteilung von *Wolbachien* notwendig ist. Die weitere Modifikation von Lipid II ist aber unbekannt und ein Peptidoglykan-ähnliches Molekül wurde bisher nicht nachgewiesen.

Um einen Einblick in die mögliche Prozessierung von Lipid II zu bekommen, wurden in der vorliegenden Doktorarbeit die Penicillin-bindenden Proteine (PBPs) PBP2 und PBP6a aus *Wolbachien* des Fadenwurms *Brugia malayi* (*w*Bm) untersucht. Des Weiteren wurden AmiD und PBP3 aus *Wolbachien* der Fruchtfliege *Drosophila melanogaster* (*w*Mel) charakterisiert. Diese beiden Lipid II-prozessierenden Enzyme sind zusätzlich in *Wolbachien* aus Arthropodenspezies annotiert. Außerdem wurden Bindungsstudien durchgeführt, um mögliche Interaktionen zwischen dem Peptidoglykan-assoziierten äußeren Membran Lipoprotein Pal aus *w*Bm und Lipid II bzw. PBP2 zu detektieren. Um eine potentielle

zellwandartige Struktur in *Wolbachien* nachzuweisen, wurde Lipid II in *Wolbachien* aus *Aedes albopictus* mit Hilfe von Dipeptidanalogen markiert. Außerdem wurde eine etablierte zellfreie *Wolbachien* Kultur in Hinblick auf mögliche wachstumsfördernde Substanzen sowie die Wirkung von Antibiotika untersucht.

Die Ergebnisse belegen enzymatische Aktivitäten der PBPs in Abhängigkeit von funktionalen Serinen des SXXK Motivs im aktiven Zentrum. β-Lactam-Antibiotika binden an das Serin des hochkonservierten SXXK Motivs und hemmen normalerweise die Aktivität von PBPs. Allerdings waren alle untersuchten PBPs aus *Wolbachien* resistent gegen β-Lactam-Antibiotika. Im Gegensatz zu ihren Orthologen aus *E. coli* haben alle in dieser Arbeit analysierten PBPs mehr als ein SXXK Motiv in ihrer Sequenz, die zur Enzymaktivität beitragen und die beobachtete Resistenz erklären könnten. *In silico* Analysen prognostizierten, dass β-Lactame aufgrund der Proteinfaltung der PBPs nicht an alle Motive des aktiven Zentrums gelangen. Daher sind β-Lactame ungeeignet, um die *Wolbachien* PBPs zu hemmen und somit die Bakterien abzutöten. AmiD zeigte eine zinkabhängige Amidaseaktivität und spaltete Peptidoglykan, Lipid II sowie Anhydromuropeptide, die durch die Teilung von Glykanketten entstehen. Die konservierte Funktion des AmiD Anhydromuropeptide zu spalten, weist auf eine zellwandartige Struktur mit verknüpften Glykanketten hin, zumindest in *Wolbachien*, die in Insektenzellen leben. Sowohl Lipid II als auch PBP2 interagierten mit dem äußeren Membranprotein Pal aus *w*Bm, was darauf hindeutet, dass Lipid II und PBP2 vermutlich im periplasmatischen Raum der *Wolbachien* präsent sind. Diese Ergebnisse zusammen mit den aktiven PBPs aus *w*Bm indizieren, dass möglicherweise auch *Wolbachien* aus Filarienspezies Lipid II zu einer peptidoglykanartigen Struktur prozessieren. Die markierten Dipeptide wiesen zum ersten Mal eine sichtbare Lipid II-beinhaltende in *Wolbachien* nach, die bei Fosfomycin-behandelten Zellen mit gehemmter Lipid II Synthese nicht mehr nachweisbar war. Zellfreie *Wolbachien* waren nach Fosfomycin Behandlung außerdem vergrößert. Keine der anderen verabreichten Antibiotika inklusive β-Lactame führten zu einer veränderten Morphologie. Dies bestätigt weiter, dass *Wolbachien* resistent gegen β-Lactame sind.

Die Ergebnisse dieser Arbeit, unterstützt durch neuere Forschungsergebnisse bezüglich nachgewiesener peptidoglykanartiger Strukturen in anderen intrazellulären Bakterien, deuten darauf hin, dass *Wolbachien* keineswegs zellwandlos sind. Sie haben vermutlich eine aus Lipid II bestehende physikalische Struktur, die mit der äußeren Membran interagiert und notwendig für eine koordinierte Zellteilung ist.

1 Introduction

1.1 Neglected tropical diseases and filariasis

Around one billion people in 149 countries are affected by so-called neglected tropical diseases caused by a variety of pathogens including bacteria, helminths, protozoa and viruses (Mackey et al., 2014). Neglected tropical diseases are mainly prevalent in the tropical regions of Africa, Asia and Latin America and play a minor role in research in high-income western countries. Diagnostics, medication and vaccines either do not exist or are outdated and unsuitable for use in areas with poor infrastructure (Mueller-Langer, 2013). Infected people suffer from severe illness, disability, social exclusion and mortality, the economic impact includes low productivity and high health care costs. As neglected tropical diseases are a constraint to economic growth and lower the already low standard of living in affected areas, the gap in equality between developed and developing countries widens further (Gallup and Sachs, 2000). In the past few years, the World Health Organization (WHO) has raised awareness of this topic, for example by publishing a roadmap to accelerate work on neglected tropical diseases (WHO, 2012). Subsequently, private and public partners signed up to the London Declaration on neglected tropical diseases in 2012 which commits them to work on the WHO targets, in particular by funding or supply of drugs. Additionally, the Sustainable Developmental Goals by the United Nations also include neglected tropical diseases as a target to "end the epidemics […] by 2030" (UN, 2015). New and ongoing efforts to control, eliminate and eradicate neglected tropical diseases represent key elements for achieving these goals (Hotez et al., 2016).

Neglected tropical diseases include lymphatic filariasis and onchocerciasis caused by filarial nematodes of the order *Spirurida*, which are endemic in tropical regions worldwide with around one billion people living in risk areas mainly in Africa and Southeast Asia (WHO, 2016a). Currently, around 68 million people have lymphatic filariasis provoked by *Wuchereria bancrofti*, *Brugia malayi* and *Brugia timori* (Ramaiah and Ottesen, 2014). Infectious third-stage (L3) larvae are transmitted from the intermediate host, mosquitoes of the genera *Aedes*, *Anopheles*, *Culex* and *Mansonia* during a blood meal onto the skin of the mammalian host (Figure 1). The larvae migrate to and penetrate through the bite wound into their definitive host, where they enter the lymphatic system and molt two more times as they develop into adult worms (Wenk and Renz, 2003). The adult worms reside in lymphatic vessels, mostly of the extremities and male genitalia where they can breed and, in case of *Wuchereria bancrofti*, survive up to ten years in humans (Wenk and Renz, 2003). After mating, the female worms

release microfilariae which migrate through the lymph into the blood stream, where they are ingested by a mosquito vector taking a blood meal. Inside the mosquito, the microfilariae lose their sheaths and migrate from the midgut into the thoracic musculature where they pass through first-stage (L1) and second-stage (L2) larval stages before becoming infective L3 larvae which migrate into the proboscis (Wenk and Renz, 2003).

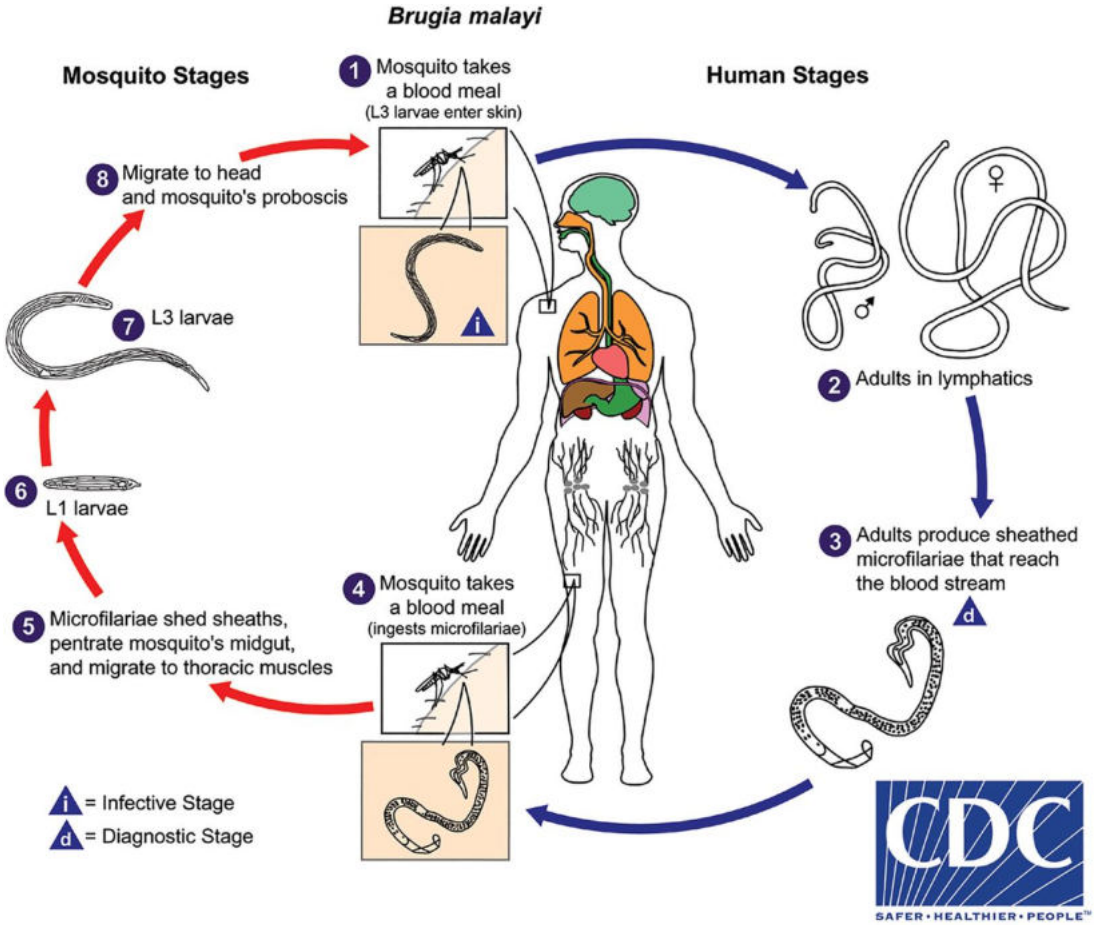

Figure 1: Life cycle of *Brugia malayi* exemplary for filarial nematodes causing lymphatic filariasis (Center for Disease Control and Prevention, https://www.cdc.gov/parasites/lymphaticfilariasis/biology_b_malayi.html). Infected mosquitoes are the intermediate host and transmit third-stage (L3) filarial larvae during a blood meal onto the skin of the human definitive host. The L3 larvae penetrate through the bite wound and enter the lymphatic system. After developing into adults, the worms commonly reside in the lymphatics and produce microfilariae. The microfilariae migrate actively into lymph and blood channels where a mosquito ingests the microfilariae during a blood meal. The microfilariae lose their sheaths, penetrate the mosquito's midgut and migrate to the thoracic muscles. There, the microfilariae develop into first-stage (L1), then second-stage (L2) larvae and subsequently into infectious L3 larvae. The L3 larvae migrate to the mosquito's head and proboscis and can infect another human when the mosquito takes a blood meal.

Due to the death of the adult worms severe pathologies like hydrocele and lymphedema (elephantiasis) can occur in infected individuals (Figure 2A) (Hoerauf et al., 2001; Taylor et al., 2010). Around 36 million cases of hydrocele and lymphedema are reported and affected people are predisposed to secondary bacterial infections, which can be life-threatening when untreated (Dreyer et al., 2000; Ramaiah and Ottesen, 2014). Lymphatic filariasis-caused

lymphedema is the second leading cause of global disability and moreover, the disfigurement of body parts leads to social stigmatization and marginalization (Ramaiah and Ottesen, 2014).

Onchocerciasis in humans is caused by the filarial worm *Onchocerca volvulus* and is transmitted through the bites of infected blackflies of the genus *Simulium*. Around 37 million people are infected with more than 99 % of cases located in Sub-Saharan African countries (Noma et al., 2013; WHO, 2016b). When a blackfly is taking a blood meal on an infected human, microfilariae are ingested and penetrate the blackfly's midgut and migrate to the thoracic musculature where they pass through L1 and L2 larval stages before they develop into infective L3 larvae which migrate to the head and blackfly's proboscis (Wenk and Renz, 2003). During another blood meal, the infected blackfly introduces L3 filarial larvae onto the skin of the human host, where they penetrate through the bite wound. In subcutaneous tissues the larvae develop into adult worms, which commonly reside in nodules. Notably, adult filariae causing onchocerciasis can breed and survive up to 15 years in humans (Ōmura and Crump, 2004). The ovoviviparous female adult worms release up to 1000 microfilariae per day, which migrate through skin tissues and the eyes. The death of microfilaria induces immune responses that can cause a variety of pathologies in the human body including blindness (river blindness), skin rashes, lesions, intense itching and skin depigmentation (Sowda) (Figure 2B) (Taylor et al., 2010). River blindness is the second leading cause of vision loss induced by infections (Boatin and Richards, 2006). Moreover, recent studies reveal an association between the nodding syndrome and the infection with *O. volvulus* (Foltz et al., 2013; Idro et al., 2016). This seizure disorder, mostly affecting children in Eastern Africa, may be an autoimmune epilepsy induced by *Onchocerca* worms (Johnson et al., 2017).

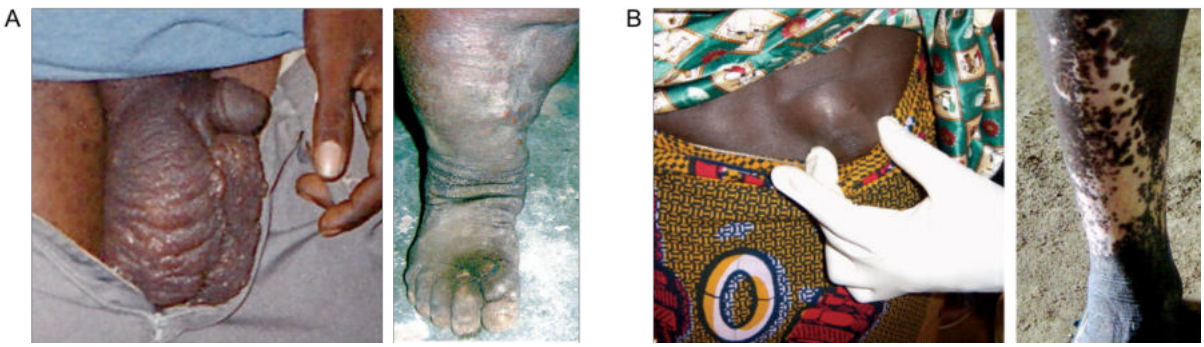

Figure 2: Severe pathologies of lymphatic filariasis and onchocerciasis (adapted from Taylor et al., 2010). A) In lymphatic filariasis, the dead adult worms (*Wuchereria bancrofti*, *Brugia malayi* or *Brugia timori*) inside the lymphatic vessels can lead to hydrocele (left) or lymphedema (right). B) Worms of the species *Onchocerca volvulus* reside in subcutaneous skin nodules (left). Released microfilariae migrate through the skin and can cause depigmentation (right).

Although not lethal per se, lymphatic filariasis and onchocerciasis cause 3.9 million disability-adjusted life years (DALYs) annually (WHO, 2016a, 2016b). DALYs regard the

immense limitations of life quality of infected people and measure the impact of the disease on the affected community. Thus, filarial diseases play a major social as well as economic role in endemic countries and infections have an enormous impact on the life of millions of people (Ottesen, 2000; Ramaiah and Ottesen, 2014).

1.2 Treatment of filarial diseases

Currently, there are no approved vaccinations available against filarial diseases (Khatri et al., 2018). Thus, alternative approaches are needed to interrupt the life cycle of the worms and to stop transmission. One possibility is the protection against infectious mosquito bites by repellents or bed nets, but the feasibility for residents of endemic areas is mixed (Sangoro et al., 2014). Another possibility is vector control, but this requires the use of chemicals like dichlorodiphenyltrichloroethane (DDT), which persists in the environment, accumulates in fatty tissues and can cause adverse health effects in humans (Turusov et al., 2002). For people already infected with filariasis, mainly the anthelmintic drugs albendazole (ALB), diethylcarbamazine (DEC) and ivermectin (IVM) are applied (Fischer et al., 2017). William C. Campbell and Satoshi Ōmura were awarded the Nobel Prize in Physiology or Medicine in 2015 for discovering the compound avermectin produced by *Streptomyces avermitilis*, which was chemically modified to the more effective drug IVM (reviewed by Campbell, 2012). IVM has radically lowered the incidence of onchocerciasis as well as lymphatic filariasis and, moreover, has shown efficacy against various other parasitic diseases like strongyloidiasis and also ectoparasitic infections like scabies (Crump and Ōmura, 2011; Tambo et al., 2015).

The WHO has launched programs to eliminate lymphatic filariasis and onchocerciasis by 2020 and 2025, respectively (Ramaiah and Ottesen, 2014). The current mass drug administration (MDA) strategy to treat lymphatic filariasis is to provide repeated, annual doses of ALB with either DEC or IVM for the lifespan of adult worms (Tisch et al., 2005; Fischer et al., 2017). Remarkably, it is estimated that about 97 million cases of lymphatic filariasis were prevented or cured since the beginning of MDA treatments in 2000 leading to a 59 % reduction of initial infection levels (Ramaiah and Ottesen, 2014). A pilot study reveals that a DEC, IVM and ALB single-dose triple-drug regimen is safe and more effective than the standard DEC plus ALB combination (Thomsen et al., 2015). These findings will potentially accelerate efforts to eradicate lymphatic filariasis (Fischer et al., 2017). DEC has been phased out as the drug of choice in treating of onchocerciasis as the sudden death of enormous numbers of microfilariae in the skin can cause serious side effects in patients (Bird et al., 1980; Francis et al., 1985; Awadzi and Gilles, 1992). Onchocerciasis is treated with IVM in MDA programs (Komlan et

al., 2018). In Latin America, MDA programs were successful achieving that four countries are verified free of onchocerciasis transmission (WHO, 2016b).

Unfortunately, apart from possible side effects and suspected resistance development, one major disadvantage of the presently used anthelmintic drugs is that all of them mainly have microfilaricidal effects and do not act against the adult worms (Osei-Atweneboana et al., 2011). Since these can survive and breed several years in humans, it is necessary to assure the administration of drugs for years, but for example 22 African countries are still challenged with the start, scale-up and continuation of MDA (WHO, 2016a). Moreover, in regions endemic for onchocerciasis with high prevalence it has been shown that transmission is likely to reappear when administration is stopped even after 17 years of annual treatment (Katabarwa et al., 2011). Additionally, IVM or DEC treatment in regions that are co-endemic for the filarial nematode species *Loa loa* can result in progressive neurologic decline and encephalopathy, thus excluding MDA in these areas (Gardon et al., 1997; Kamgno et al., 2009; Bockarie and Deb, 2010). Despite much progress, a major effort is needed to achieve the WHO goals. For the successful elimination of filarial infections novel drugs with macrofilaricidal or sterilization effects are required, which can be applied in short-term MDA programs and in areas with emerging IVM resistance or *L. loa* co-endemicity (Klarmann-Schulz et al., 2017).

1.3 *Wolbachia* endosymbionts as targets for anti-filarial treatment

Obligate α-proteobacterial endosymbionts of the genus *Wolbachia*, present in many filarial nematodes, have been investigated as a novel approach for chemotherapy to treat filarial diseases (Taylor and Hoerauf, 1999; Bandi et al., 2001; Hoerauf et al., 2003; Walker et al., 2015). These bacteria were first described as "*Rickettsia*-like organisms in insects" in 1924 by the scientists Marshall Hertig and Samuel Wolbach, and later named *Wolbachia* (Hertig and Wolbach, 1924; Hertig, 1936). *Wolbachia* are pleomorphic and cell size usually varies between 0.5 and 1.3 µm (Hertig, 1936). Subsequently, it has been shown that *Wolbachia* indeed belong to the order Rickettsiales and are widespread in arthropods, infecting at least 40 % of species (Zug and Hammerstein, 2012). Unlike members of the related genera *Anaplasma, Ehrlichia* and *Rickettsia*, *Wolbachia* do not routinely infect vertebrates (Werren et al., 2008). *Wolbachia* have attracted considerable interest in the last two decades, primarily because of their effects on their hosts, which range from reproductive manipulation to mutualism, and potential applications in pest and disease vector control (Werren et al., 2008).

Wolbachia intracellularly reside in host-derived Golgi-related vacuoles in the cytoplasm of some somatic tissues as well as in cells of the host germline (Tram et al., 2003; Cho et al.,

2011). A general characteristic feature of intracellular bacteria is a highly reduced genome due to the adaption to their host (Stepkowski and Legocki, 2001). Sequenced genomes of different *Wolbachia* strains range from 0.9–1.5 Mb and they have lost many genes compared to free-living bacteria, particularly those involved in biosynthetic pathways (Wu et al., 2004; Foster et al., 2005; Lindsey et al., 2016).

In arthropods, *Wolbachia* are facultative endosymbionts and as survival of the host is not necessarily dependent on the bacteria, manipulating the host by inducing cytoplasmic incompatibility, parthenogenesis, feminization and male killing are strategies of the *Wolbachia* to ensure vertical transmission and survival (Clark, 2007). However, there are exceptions and in some cases the arthropod host requires *Wolbachia* for oogenesis and positive benefits to fitness have also been demonstrated in terms of resistance to different pathogens and in nutrient provisioning (Zug and Hammerstein, 2015). Interestingly, several filarial nematode species also harbor *Wolbachia* (Sironi et al., 1995). Here, the *Wolbachia* are obligate mutualistic endosymbionts required for survival of their hosts and embryogenesis of microfilariae (Bandi et al., 1998; Bandi et al., 1999; Hoerauf et al., 2000).

The current hypothesis is that *Wolbachia* provide their host with essential metabolites and vice versa. For instance, the nematode host is not able to generate flavin adenine dinucleotide, purine, pyrimidine, riboflavin and heme and therefore needs to obtain these compounds by external sources or from its endosymbiont that is able to synthesize them (Foster et al., 2005; Slatko et al., 2010). In turn, *Wolbachia* strains residing in filarial nematodes have a smaller genome than strains living in arthropods and thus need essential compounds provided by their host (Foster et al., 2005). They lack almost all biosynthetic pathways to produce amino acids *de novo* and retained only incomplete pathways for the synthesis of certain vitamins and cofactors such as nicotinamide adenine dinucleotide, biotin, lipoic acid, ubiquinone, folate, pyridoxal phosphate, and Coenzyme A, making them dependent on external sources (Slatko et al., 2010).

Wolbachia are predominantly found in the hypodermal cells of the lateral cords in both male and female nematodes as well as in all larval stages (Hoerauf et al., 2001). Their presence in oocytes, developing eggs and microfilaria indicates that the bacteria are maintained in the population by vertical transmission. *Wolbachia* are essential for worm development, fertility and survival (Bandi et al., 1998). In addition, they were shown to be a major driver of the inflammatory pathogenesis in filarial diseases (Tamarozzi et al., 2011).

Several studies have demonstrated that the depletion of *Wolbachia* by the antibiotics doxycycline and rifampicin leads to sterility and degeneration of adult worms, revealing

Wolbachia as an effective target for anti-filarial therapy (Hoerauf et al., 2000; Hoerauf et al., 2003; Volkmann et al., 2003; Specht et al., 2008) (Figure 3). As *L. loa* do not harbor *Wolbachia* endosymbionts, these antibiotics could be used in co-endemic areas without the risk of severe adverse reactions (Bockarie and Deb, 2010). Moreover, anti-wolbachial treatment decreases immune responses that appear when *Wolbachia* are released after death of filariae, thus having a beneficial effect on treated patients (Pfarr et al., 2009).

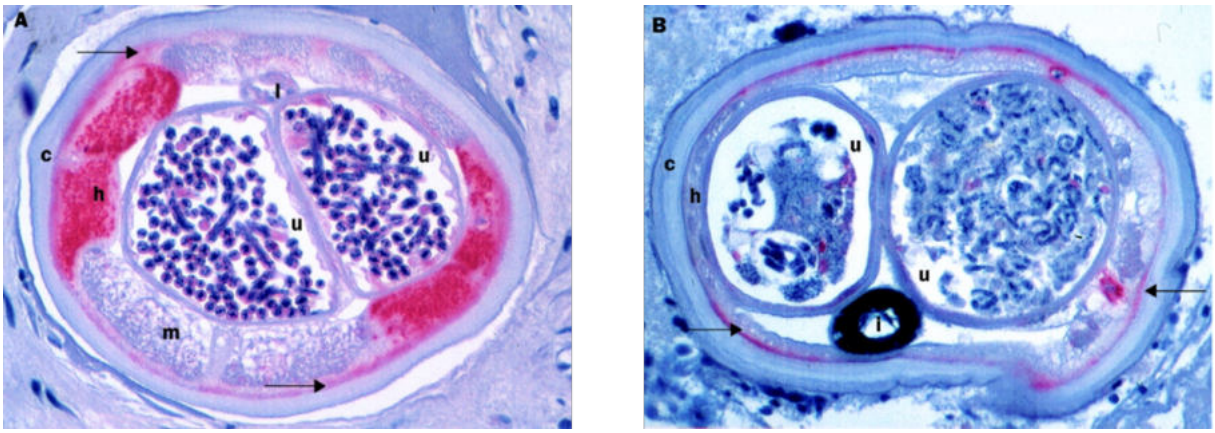

Figure 3: Impact of the depletion of endosymbiotic *Wolbachia* by doxycycline to *Onchocerca volvulus* (adapted from Hoerauf et al., 2000). A) A midbody cross-section of a female *Onchocerca volvulus* worm containing *Wolbachia* found mainly in the hypodermal chords and in embryos (*Wolbachia* are stained in red). B) *Wolbachia* are depleted after treatment with doxycycline and embryos are degenerated. h: hypodermal chords, c: cuticle, m: musculature, i: intestine, u: uterus epithelium, arrows: non-corpuscular, less intense staining possibly of nematode mitochondrial hsp-60.

Rifampicin is an essential back-up antibiotic for the treatment of tuberculosis, which is also endemic in many of the areas where filarial diseases occur, thus presenting a risk of selecting for rifampicin-resistant tuberculosis pathogens (*Mycobacterium spp.*) when broadly applied as an anti-wolbachial drug (Smits, 2009). The use of doxycycline in MDA programs is constrained by contraindications in children under eight years as well as pregnant or breast feeding women and the logistics of a relatively lengthy course of treatment (4–6 weeks) (Hoerauf et al., 2008; Taylor et al., 2014). However, doxycycline can be used for individual drug administration (Taylor et al., 2010). A recent clinical phase two pilot study suggests that the combination of doxycycline (200 mg/day 3 weeks) with ALB (800 mg/day 3 days) leads to an additive effect on top of that of doxycycline alone and might be a promising step forward to reduce treatment time (Klarmann-Schulz et al., 2017). Nevertheless, the development of substances suitable for short-term MDA and targeting all stages of the filarial worms is urgently needed.

Comparative genomics, bioinformatics and experimental analyses have identified a number of potential interactions which may be drug targets in *Wolbachia* including membrane proteins, ankyrins, lipoprotein biosynthesis, enzymes of undecaprenyl-pyrophosphoryl-

Mur*N*Ac-pentapeptide-Glc*N*Ac (lipid II) biosynthesis, heme biosynthesis, the glycolytic enzymes pyruvate phosphate dikinase and cofactor-independent phosphoglycerate mutase (Slatko et al., 2010). For example, treatment with globomycin, which inhibits lipoprotein biosynthesis, led to a reduced *Wolbachia* load in an infected insect cell culture and significant reductions in motility and viability in *B. malayi* in *in vitro* experiments (Johnston et al., 2010). The benzimidazole compound *w*ALADin1 selectively targets the δ-aminolevulinic acid dehydratase of *Wolbachia* (*w*ALAD), an enzyme of heme biosynthesis. *w*ALADin1 also exhibits macrofilaricidal effects on *Wolbachia*-containing filarial worms *in vitro* (Lentz et al., 2013). Currently, the most promising drug is corallopyronin A, a non-competitive inhibitor of the bacterial deoxyribonucleic acid (DNA)-dependent ribonucleic acid (RNA) polymerase which is synthesized by *Corallococcus coralloides* (Irschik et al., 1985). *In vivo*, corallopyronin A depletes *Wolbachia*, resulting in impeded worm development (Schiefer et al., 2012). Resistance development in *Staphylococcus aureus* due to mutations were reported (Mariner et al., 2011). However, recombination rates were shown to be slow in *Wolbachia* from nematodes (Jiggins, 2002). Thus, corallopyronin A is an antibiotic to be developed further in clinical studies for filariasis elimination without concern for cross-resistance development in tuberculosis as this antibiotic has low efficacy against *Mycobacterium spp.* (Schäberle et al., 2014). The approach with an antibiotic-based therapy shows promising results in defeating filariasis and preventing the painful and disfiguring symptoms of elephantiasis (Rebollo and Bockarie, 2014; Walker et al., 2015).

1.4 *Wolbachia* as an intracellular model organism: the benefit of basic research to identify new targets against filariasis

Wolbachia pipientis is the most common bacterial infection in the animal world and has a vast influence on invertebrate reproduction, sex determination, speciation and behavior (LePage and Bordenstein, 2013). From a biodiversity perspective, *Wolbachia* infections are one of the great pandemics in the history of life (LePage and Bordenstein, 2013). The discoveries that *Wolbachia*-infected mosquitoes show lower susceptibility or even resistance to viruses causing dengue, chikungunya, yellow fever and zika as well as malaria-causing *Plasmodium spp.* create a potentially cheap and sustainable system in which this pandemic can be used as a tool to control vector-borne diseases (Moreira et al., 2009; Bian et al., 2010; Dutra et al., 2016). For instance, in an effort to eliminate dengue, a technology was developed with the stable introduction of *W. pipientis* into the mosquito *Aedes aegypti* to reduce its ability to transmit

dengue fever due to life shortening and inhibition of viral replication effects (Hoffmann et al., 2011). Other research areas have focused on the mutualistic role between *Wolbachia* and filarial nematodes aiming to eliminate the bacterial infection and thereby reducing the fitness of the worms that depend on it. The evolutionary distance of *Wolbachia* from mammals is far greater than that from nematodes, affording opportunities for treating filarial infections by specifically targeting its endosymbiont (Slatko et al., 2010).

Due to their obligate intracellular lifestyle and reduced genome, *Wolbachia* represent an organism in which essential processes like cell elongation and cell division are functionally organized in a minimal set-up. One of the most significant challenges to the experimental investigation of *Wolbachia* biology is the reliance on a eukaryotic host cell for bacterial proliferation (Rasgon et al., 2006). Attempts to establish a cell line containing nematode *Wolbachia* strains were not successful so far (Slatko et al., 2014), but *Wolbachia*-infected insect cell lines like *Aedes albopictus* Aa23 or C6/36 are established *in vitro* models to simulate filarial *Wolbachia* strains (O'Neill et al., 1997; Turner et al., 2006). Notably, insect *W. pipientis* strain *A. albopictus* B (*w*AlbB) can be purified from host cells and maintained extracellularly up to one week in a cell culture, but without replication (Rasgon et al., 2006). A better understanding of *Wolbachia* biology and particularly host-symbiont interactions is a key for future development of drugs against filarial diseases and therefore an excellent example of how basic research can be translated to biomedical science.

1.5 Bacterial cell wall

Free-living bacteria are dependent on a cell surrounding envelope which regulates bacterial size, shape, internal pressure and diffusion of molecules from the environment (Cloud-Hansen et al., 2006). The bacterial cell wall consists of a peptidoglycan polymer, which, as the name implies, is made of long linear glycan chains that are cross-linked by short peptides (Figure 4) (Höltje, 1998). The glycan chains are composed of alternating β-1,4 linked amino sugar units of N-acetylglucosamine (Glc*N*Ac) and N-acetylmuramic acid (Mur*N*Ac). Pentapeptides, usually consisting of the amino acids L-alanine (L-Ala), D-glutamic acid (D-Glu), meso-diaminopimelic acid (m-DAP) or L-lysine (L-Lys), and two terminal D-alanine (D-Ala), are attached to the carboxy-group of Mur*N*Ac (Schwechheimer and Kuehn, 2015). The amino acid m-DAP, an intermediate product of the bacterial lysine biosynthesis pathway, is typically found in the peptide chains of Gram-negative bacteria and the Gram-positive bacilli, while L-Lys is found in most Gram-positive bacteria (Schwechheimer and Kuehn, 2015). The terminal D-Ala of the pentapeptide is removed during the crosslinking transpeptidation process,

which takes place between the carboxyl group of the D-Ala at position four and the amino group of the m-DAP/L-Lys at position three of an adjacent peptide chain (Typas et al., 2012). Gram-positive bacteria have an inner membrane and are surrounded by several peptidoglycan layers of about 40–80 nm. The predominantly single-layered peptidoglycan of Gram-negative bacteria is much thinner at around 7–8 nm and located in the periplasm between the inner and the outer membrane (Malanovic and Lohner, 2016).

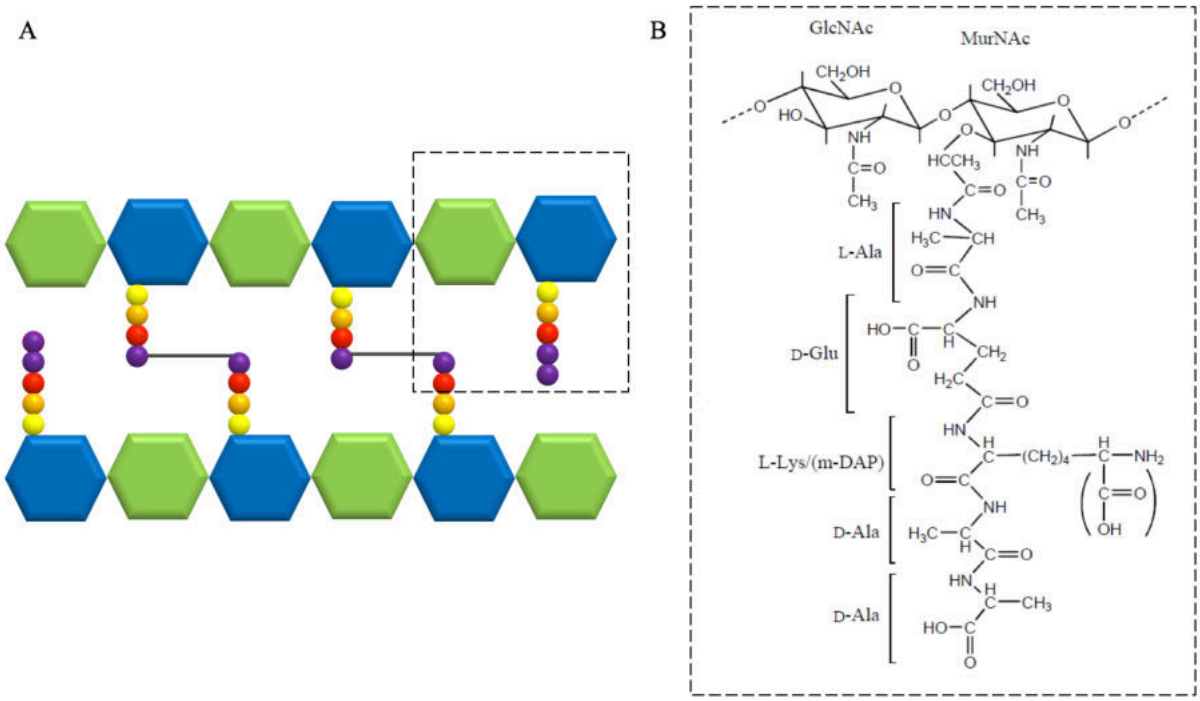

Figure 4: Structure of peptidoglycan. A) Simplified scheme of peptidoglycan consisting of linear glycan strands interlinked via peptide side chains. Green hexagons represent the sugar moiety N-acetylglucosamine (Glc*N*Ac), blue hexagons represent N-acetylmuramic acid (Mur*N*Ac). Circles represent the amino acids L-alanine (L-Ala; yellow), D-glutamic acid (D-Glu; orange), L-lysine (L-Lys; red) or meso-diaminopimelic acid (m-DAP; red) and D-alanine (D-Ala; purple). B) Chemical structure of a peptidoglycan monomer unit composed of Glc*N*Ac and Mur*N*Ac, and a pentapeptide containing L-Ala, D-Glu, L-Lys or m-DAP and two D-Ala (Olrichs, 2010).

1.5.1 Cell wall synthesis and breakdown in bacteria

Peptidoglycan biosynthesis is a multi-step process that takes place in three different cellular compartments: the cytoplasm, the cytoplasmic membrane and the periplasm (Figure 5) (Typas et al., 2012). It starts in the cytoplasm with the synthesis of uridine diphosphate N-acetyl-glucosamine (UDP-Glc*N*Ac) by the conversion of fructose-6-phosphate via the activity of the enzymes GlmS, GlmM and GlmU (Misra et al., 2015). The precursor UDP-N-acetylmuramic acid pentapeptide (UDP-Mur*N*Ac-pentapeptide) is synthesized from UDP-Glc*N*Ac and is catalyzed by the six enzymes MurA to MurF. Subsequently, the UDP-Mur*N*Ac-pentapeptide moiety is attached to the membrane-bound lipid carrier undecaprenyl phosphate (C_{55}-P) by the enzyme MraY, yielding lipid I. The lipid I molecule

serves as a substrate for the enzyme MurG to add an UDP-Glc*N*Ac molecule forming the final cell wall precursor lipid II (Typas et al., 2012). After synthesis, lipid II is flipped across the cytoplasmic membrane into the periplasm. To date, the identity of the enzyme translocating lipid II across the cell membrane remains a matter of debate. There are several candidates including MurJ, FtsW and RodA which might function as a flippase, but these are controversially discussed (Ruiz, 2016).

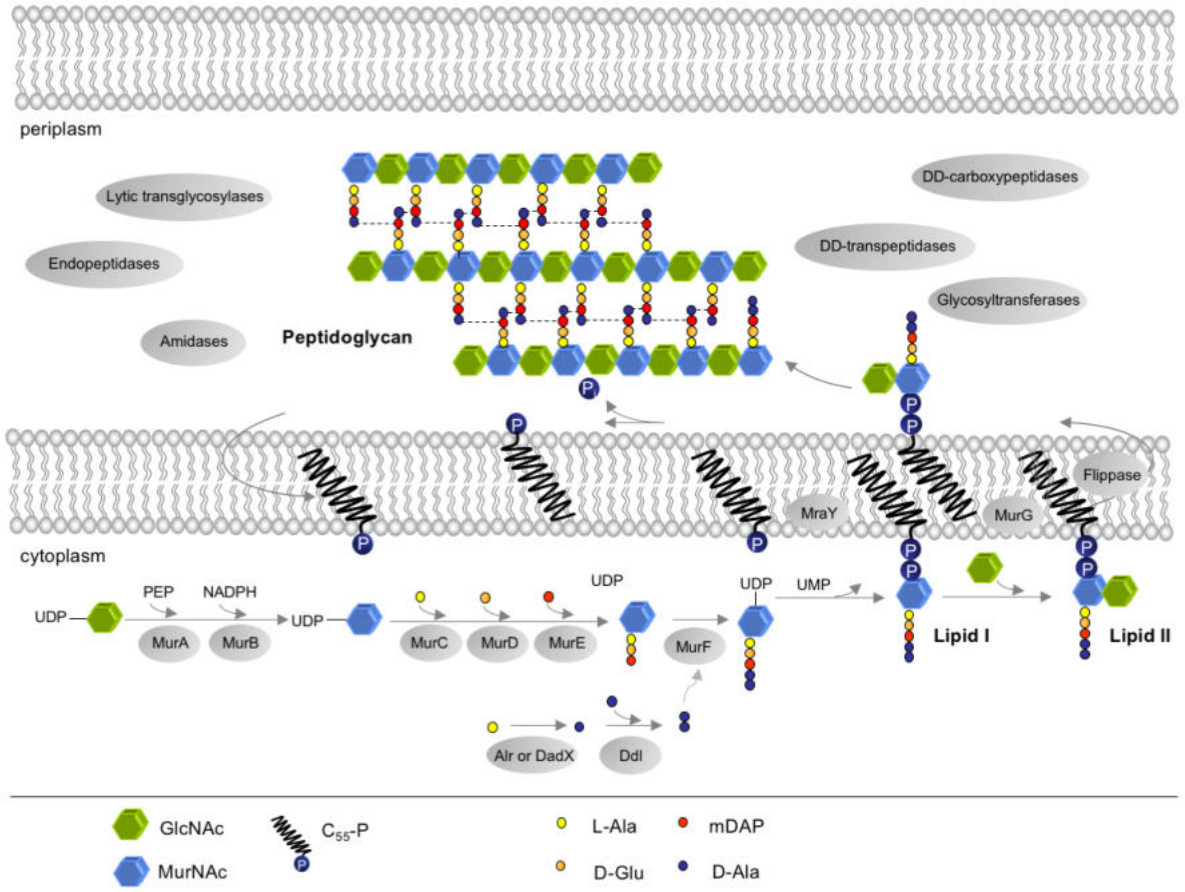

Figure 5: Peptidoglycan synthesis in Gram-negative bacteria. The peptidoglycan precursor lipid II is synthesized by the enzymes MurA-MurG and MraY. After translocation into the periplasm, lipid II is incorporated into the growing chain by various synthesizing and hydrolyzing enzymes building peptidoglycan.

Once in the periplasm, lipid II is incorporated into the growing peptidoglycan by a multi-enzyme complex, the elongasome, as exemplarily shown for the Gram-negative bacterium *Escherichia coli* (*E. coli*) (Typas et al., 2012) (Figure 6). The enzymes of the elongasome are highly regulated to avoid disturbing the equilibrium between synthesizing and hydrolyzing enzymes, which would ultimately lead to cell death if not tightly controlled.

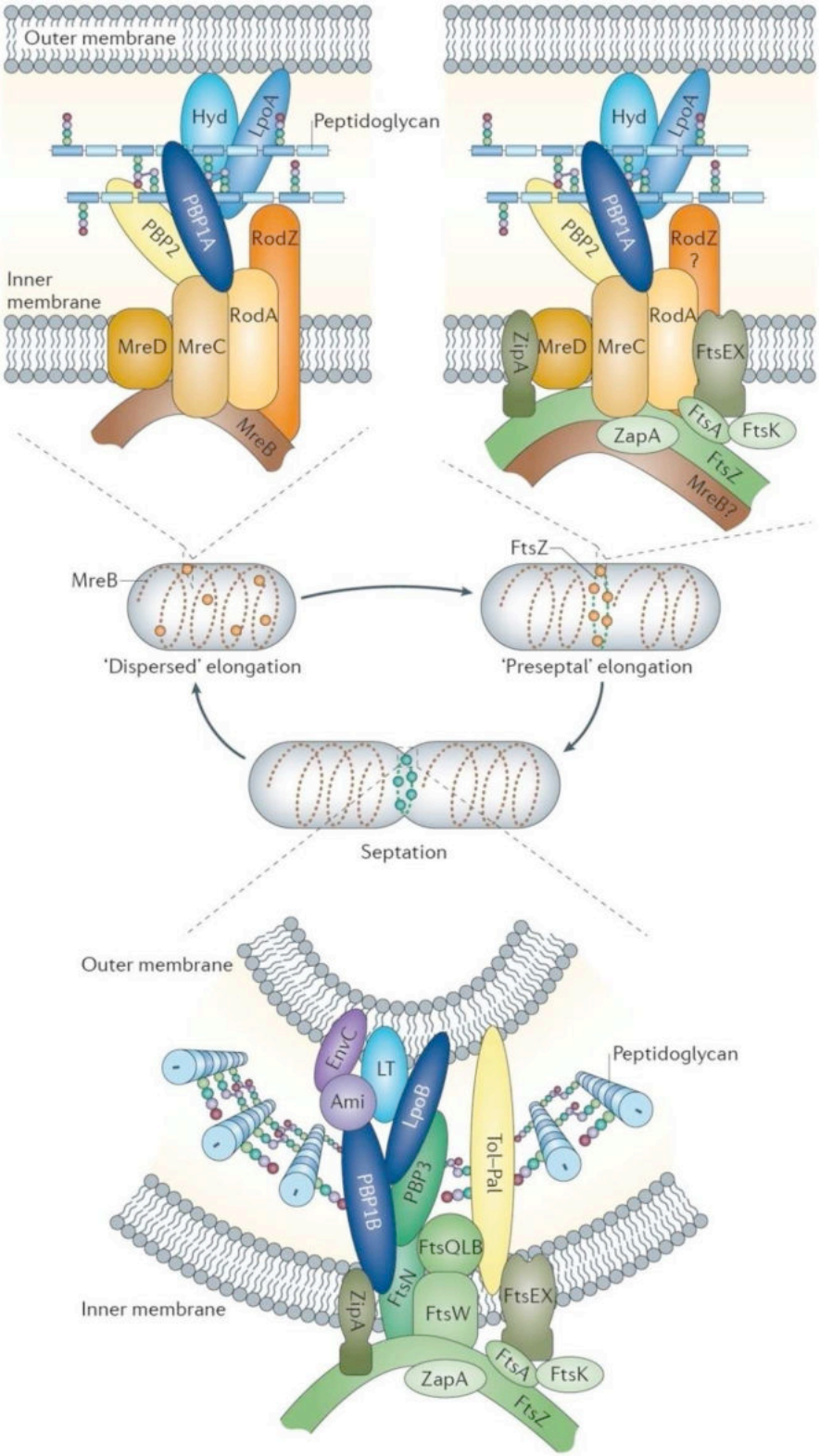

Figure 6: Different peptidoglycan synthesis complexes are active during the cell cycle of *E. coli* (Typas et al., 2012). MreB and associated membrane proteins control the position and activity of peptidoglycan synthases PBP1A and PBP2 as well as so far unknown hydrolases (Hyd) during dispersed elongation. During a preseptal mode of elongation, which is located to the midcell, FtsZ forms the Z-ring and is associated with ZapA, ZipA, FtsA, FtsEX and FtsK. It is unknown whether MreB and associated proteins participate at this time point. The cell division complex contains essential, inner membrane-localized cell division proteins, the peptidoglycan synthases PBP1B and PBP3, lytic transglycosylases (LT) and amidase enzymes (Ami) with their activators as well as proteins of the Tol-Pal complex for constriction of the outer membrane.

The sugar moieties are linked to the nascent glycan chains by glycosyltransferases, while D-alanyl-D-alanine (DD)-transpeptidases catalyze the formation of peptide cross-links. The degree of cross-linking is regulated by DD-carboxypeptidases that cleave the terminal D-Ala of the pentapeptide side chains to maintain cell shape by controlling the amount of pentapeptide substrates available to the peptidoglycan synthetic DD-transpeptidases (Peters et al., 2016). The DD-transpeptidases and DD-carboxypeptidases belong to the family of penicillin-binding proteins (PBP) named after their capacity to covalently bind penicillin (Suginaka et al., 1972) (see chapter 1.5.2). The insertion of a new peptidoglycan strand into the existing sacculus requires the degradation of mature peptidoglycan by lytic enzymes referred to as cell wall hydrolases (Vollmer et al., 2008). Cell wall hydrolases such as lytic transglycosylases, endopeptidases and amidases are capable of cleaving different bonds within the net-like peptidoglycan structure. Lytic transglycosylases cleave the glycosidic bond between Mur*N*Ac and Glc*N*Ac units, endopeptidases cut various amide bonds between the amino acids of the peptide chains and amidases hydrolyze the amide bond between Mur*N*Ac and the N-terminal L-Ala residue of the peptide chain (Vollmer et al., 2008). The degradation process is essential for proper cell division in which septal peptidoglycan needs to be cleaved but on the other hand also produced at the same time to allow separation of the daughter cells. This complex machinery, the divisome, consists of various synthesizing, hydrolyzing, cytoskeletal and regulating proteins as well as proteins of the Tol-Pal complex (Typas et al., 2012).

1.5.2 Penicillin-binding proteins (PBP)

PBPs belong to the protein family of acyl serine transferases and are essential enzymes for the final steps of peptidoglycan biosynthesis and are also required for proper cell division (Scheffers and Pinho, 2005). These enzymes play a crucial role in β-lactam susceptibility which is based on their high affinity for binding these antibiotics (Suginaka et al., 1972). Usually, PBPs have a PBP and serine/threonine kinase associated domain (PASTA) which forms a stable covalent adduct with β-lactam antibiotics (Yeats et al., 2002). Amino acid sequences of PBPs characteristically harbor the three conserved motifs SXXK, SX(D/N) and K(S/T)G with X denoting a variable amino acid residue. Occasionally, SXN is substituted by SXD and KTG is substituted by KSG, while SXXK is invariant (Goffin and Ghuysen, 2002). The SXXK motif contains the active site serine and is involved in binding of the substrate forming an acyl-enzyme intermediate and reacts with β-lactams. Subsequent deacylation is catalyzed by serine of the SX(D/N) motif and polarized by lysine of the K(S/T)G motif (Dougherty and

Pucci, 2011). Secondary and tertiary structures show that the SXXK motif is located in an α-helix, while SX(D/N) is in a loop connecting two α-helices and K(S/T)G is found in a β-sheet (Kelly and Kuzin, 1995; Goffin and Ghuysen, 1998). Four different physiological functions are assigned to PBPs (Egan et al., 2015) (Figure 7): first, transglycosylation, where PBPs catalyze the polymerization of disaccharide units with simultaneous removal of undecaprenyl pyrophosphate (C_{55}-PP; bactoprenol) probably leaving one C_{55}-PP at the terminal Mur*N*Ac residue of the new glycan strand; second, DD-carboxypeptidation, where PBPs cleave the terminal D-Ala of a pentapeptide chain regulating the extent of peptidoglycan cross-linking; third, transpeptidation, in which PBPs catalyze the cross-linking of the peptide chains; and fourth, endopeptidation, in which PBPs hydrolyze the cross-linked peptide chains.

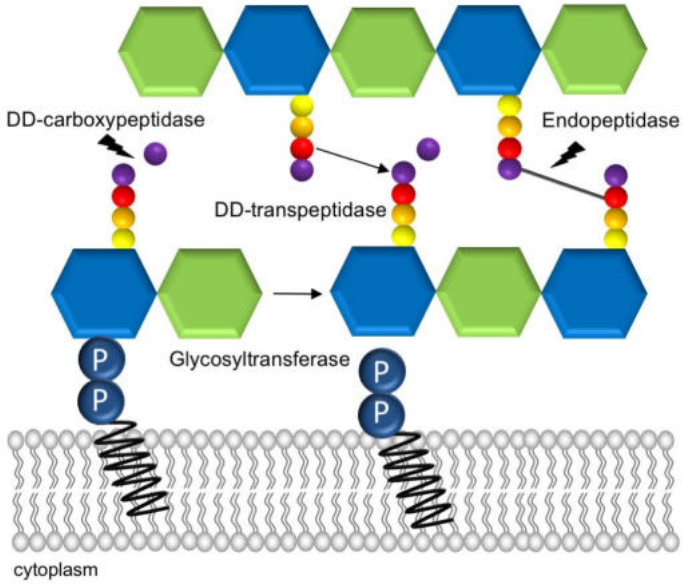

Figure 7: Schematic presentation of identified PBP activities. PBPs can catalyze transglycosylation reactions to connect the sugar units with simultaneous removal of undecaprenyl pyrophosphate (C_{55}-PP) probably leaving one C_{55}-PP at the terminal Mur*N*Ac residue of the new glycan strand (Egan et al., 2015). They can also exhibit DD-carboxypeptidase activity by cleaving the terminal D-Ala in a pentapeptide chain. PBPs can further act as DD-transpeptidases by cross-linking the peptide chains (with simultaneous DD-carboxypeptidase activity) or as endopeptidases by cleaving the cross-linked peptide chains. Green hexagons represent Glc*N*Ac, blue hexagons Mur*N*Ac. Circles represent the amino acids L-Ala (yellow), D-Glu (orange), L-Lys or m-DAP (red) and D-Ala (purple).

PBPs are divided into high molecular weight (HMW) PBPs and low molecular weight (LMW) PBPs (Sauvage et al., 2008). HMW-PBPs are usually anchored to the outer surface of the cytoplasmic membrane and are responsible for peptidoglycan polymerization (Goffin and Ghuysen, 1998; Born et al., 2006). Depending on their structure and activity, they are further classified into class A and class B PBPs. While the C-terminal domain of all HMW-PBPs shows DD-transpeptidase activity, the N-terminal domain of class A provides glycosyltransferase activity (Sauvage et al., 2008). Thus, they are bifunctional PBPs (Höltje, 1998). In class B, the

N-terminal domain is thought to be involved in maintaining cell shape by providing a recognition site for interaction with other proteins during the cell cycle (Den Blaauwen et al., 2008; Zapun et al., 2008). Class B PBPs in *E. coli* are monofunctional DD-transpeptidases (Sauvage et al., 2008). LMW-PBPs are described by the general term of class C PBPs. They are monofunctional and exhibit DD-carboxypeptidase or endopeptidase activity (Ghuysen, 1991; Massova and Mobashery, 1998). Bacteria have a variable number of PBPs which are historically numbered according to their migration on protein gels. For instance**,** *E. coli* have twelve known PBPs: PBP1a, PBP1b and PBP1c (class A HMW-PBPs); PBP2 and PBP3 (class B HMW-PBPs); PBP4a, PBP4b, PBP5, PBP6a, PBP6b, PBP7 and AmpH (class C LMW-PBPs) (Sauvage et al., 2008). Although the biochemical activities from of all these PBPs are well studied, control mechanisms and their exact roles within cells are not fully understood (Markovski et al., 2016).

1.5.3 Interaction between peptidoglycan and outer membrane proteins

In Gram-negative bacteria, the predominantly single-layered peptidoglycan sacculus is connected to the outer membrane by covalent and noncovalent interactions with various outer membrane proteins (Typas et al., 2010). The peptidoglycan-associated lipoprotein (Pal) is an outer membrane protein which specifically binds to uncross-linked m-DAP and is part of the membrane-spanning Tol-Pal complex (Parsons et al., 2006). The N-terminus of Pal containing the lipid moiety is anchored to the inner side of the outer membrane, with the C-terminus binding to peptidoglycan via a pocket for m-DAP residues (Bos et al., 2007). Pal interacts with the transmembrane protein TolA that, together with TolQ and TolR, forms a sub-complex in the inner membrane. TolB is a periplasmic protein which competes with peptidoglycan to bind Pal and thus regulates this association (Gerding et al., 2007). The Tol-Pal complex also interacts with other outer membrane proteins and builds a connection between the outer membrane, inner membrane and peptidoglycan layer facilitating membrane integrity (Godlewska et al., 2009). However, the Tol-Pal complex has not only been shown to play a role in cell wall stabilization but is also essential for proper constriction of the outer membrane during cell division (Gerding et al., 2007).

Apart from that, it was demonstrated in *E. coli* that certain outer membrane-anchored lipoproteins control peptidoglycan synthases (Paradis-Bleau et al., 2010; Typas et al., 2010). Each so-called Lpo protein stimulates the DD-transpeptidase activity of its cognate PBP by binding and inducing conformational changes (Egan et al., 2014; Markovski et al., 2016). Lpo proteins are limited to γ-proteobacteria (LpoA) and enterobacteria (LpoB). They evolved

independently and have no sequence homology (Typas et al., 2010). The additional level of regulation provided by Lpo proteins may enable niche-specific adaptation and other bacterial groups may have proteins with regulatory roles similar to Lpo proteins (Typas et al., 2012).

1.5.4 Host response to cell wall fragments

In *E. coli*, around 40–50 % of the peptidoglycan sacculus is removed during each generation and either translocated to the cytoplasm or liberated into the environment (Typas et al., 2012). To keep resources, most of the degradation products are recovered, translocated into the cytoplasm via permeases and recycled by several enzymes to be available again for the synthesis of new peptidoglycan (Park and Uehara, 2008). The release of cell wall fragments has important messenger functions in bacterial communication and, in infections, liberated fragments can also be detected by the host leading to an immune response (Johnson et al., 2013; Wheeler et al., 2014). To identify pathogens, eukaryotes have evolved different pattern-recognition-receptors (PRRs). One group of PRRs are Toll-Like-Receptors (TLRs) which are part of the innate immune system and recognize pathogen-associated molecular patterns (PAMPs). TLRs sense a variety of PAMPs like bacterial lipopolysaccharides (TLR4), lipopeptides and peptidoglycan (TLR2, TLR6) (Kawai and Akira, 2007). Another group of PRRs are the nucleotide-binding oligomerization domain receptors (NOD). They sense bacterial cell wall fragments, i.e. anhydromuropeptides, and subsequently activate the transcription factor NFκB, which plays a key role in regulating the immune response to infection (Wheeler et al., 2014). NOD 1 has been shown to be specifically activated by m-DAP typically found in Gram-negative bacteria, while NOD 2 binds N-acetyl-muramyl-L-alanyl-D-glutamate (Mur*N*Ac-dipeptide) fragments of the cell wall from Gram-positive and Gram-negative bacteria (Lee et al., 2009). Hence, peptidoglycan and cell wall fragments are major players in pathogenesis by contributing to fever, sleepiness and loss of appetite that are symptomatic for many bacterial infections (Wheeler et al., 2014).

1.5.5 Cell wall biosynthesis as a target for antibiotics

Currently, cell wall biosynthesis inhibitors are the most clinically used antibiotics worldwide (Sarkar et al., 2017). The precursor lipid II is essential, highly conserved and difficult to modify, thus resistance to lipid II-targeting antibiotics develops more slowly compared to other antibiotics, e.g. protein biosynthesis inhibitors (Schneider and Sahl, 2010). In particular, easy access outside the cytoplasm makes lipid II and peptidoglycan attractive antibiotic targets from the early identification of penicillin to the recent discovery of teixobactin

(Ling et al., 2015). For this reason, peptidoglycan synthesis is called the Achilles' heel of bacteria (Schneider and Sahl, 2010).

1.6 Lipid II metabolism in *Wolbachia*

The genome of *Wolbachia* is highly reduced due to their obligate endosymbiotic lifestyle and it is hypothesized that retained genes and metabolic pathways are crucial for survival (Foster et al., 2005). The characterization of preserved pathways that are essential for *Wolbachia* is necessary to better understand *Wolbachia* biology and possibly their interaction with their different hosts. As for other intracellular bacteria, *Wolbachia* are protected by the host cell and therefore do not need peptidoglycan to withstand osmotic challenges. Interestingly, the *Wolbachia* genomes that have been sequenced and annotated encode all proteins required for the synthesis of lipid II, but endopeptidases and almost all peptidoglycan recycling enzymes are not annotated (Foster et al., 2005) (Figure 8). Also bifunctional PBPs with glycosyltransferase activity were not identified leading to the assumption that *Wolbachia* might have an unusual cell wall without connected glycan subunits (Vollmer et al., 2013). However, a cell wall has not been detected (Kozek, 1977; Louis and Nigro, 1989) and the question remains why *Wolbachia* should keep the high resource consuming process of lipid II synthesis. It has been shown that recombinant *Wolbachia* proteins and purified *Wolbachia* membranes synthesize lipid I and II, supporting the hypothesis that lipid II is required during cell division (Henrichfreise et al., 2009; Vollmer et al., 2013). When lipid II synthesis was blocked by the antibiotic fosfomycin, *Wolbachia* in a C6/36 insect cell culture could not separate properly resulting in enlarged cells (Vollmer et al., 2013). These findings indicate that *Wolbachia* might have kept the energy consuming process of lipid II synthesis, because cell wall biosynthesis and cell division are tightly connected and cannot be separately eliminated in the course of evolution. Additionally, it was demonstrated that *Wolbachia* lipid II likely contains D-Ala obtained by the racemase MetC (Vollmer et al., 2013). It is unclear whether lipid II is further processed and any attempts to detect peptidoglycan in *Wolbachia* have not been successful (Henrichfreise et al., 2009). Therefore, the exact composition of a possible *Wolbachia* cell wall is of great interest in order to find potential targets for the treatment of filarial diseases.

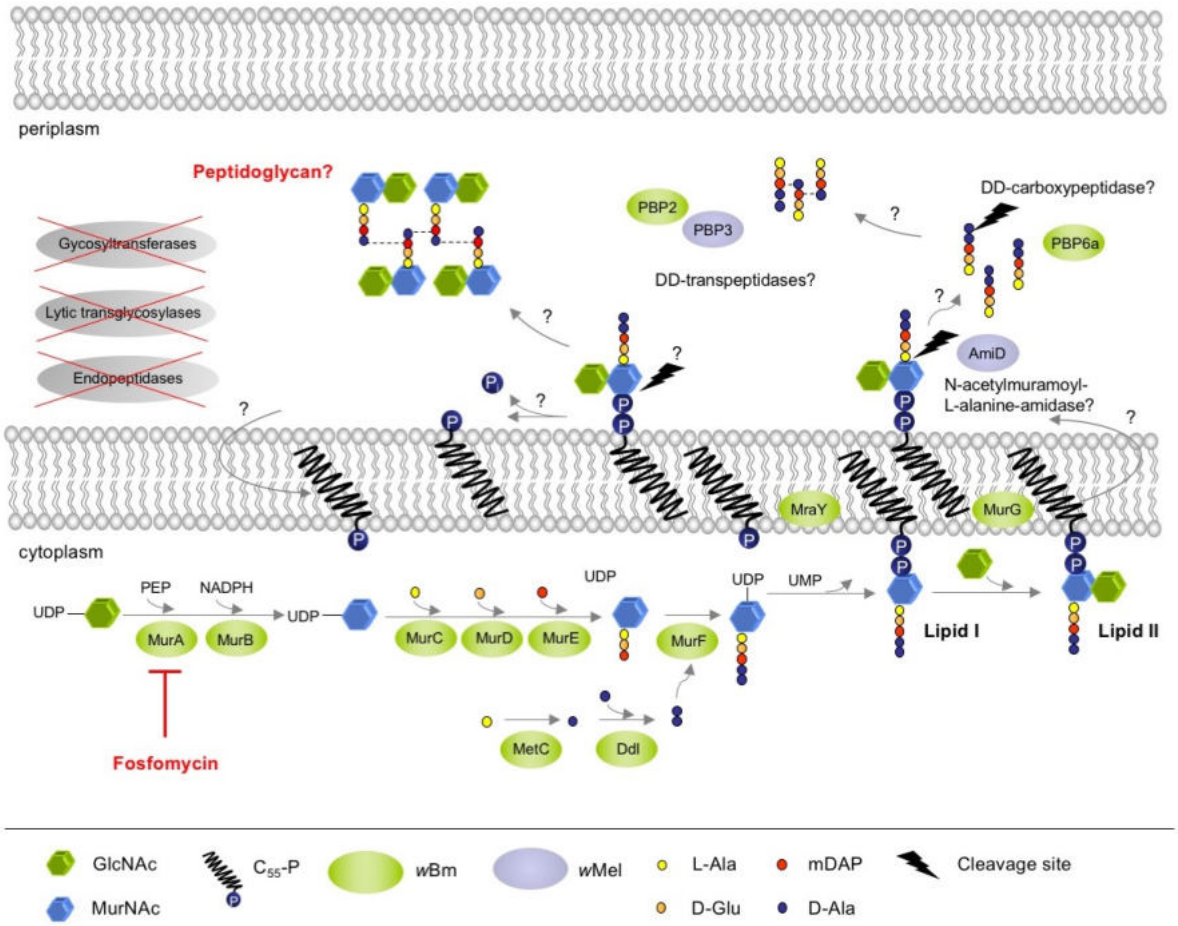

Figure 8: Proposed lipid II pathway in *Wolbachia* (adapted from Henrichfreise et al., 2009). Lipid II biosynthesis takes place in the cytoplasm and is catalyzed by the enzymes MurA to MurF, MraY and MurG. Lipid II synthesis can be inhibited by fosfomycin and MetC has been shown to function as a racemase that generates D-amino acids which might be connected to dipeptides via the D-alanine-D-alanine ligase Ddl, which is expressed in *Wolbachia* (Vollmer et al., 2013). Lipid II might be flipped into the periplasm where it could be cross-linked by the action of DD-carboxypeptidases and DD-transpeptidases. *Wolbachia* from *Brugia malayi* (*w*Bm) only encode genes for PBP2 and PBP6a, while *Wolbachia* from *Drosophila melanogaster* (*w*Mel) additionally encode for PBP3 and AmiD. Genes that are not annotated in the *Wolbachia* genome are depicted with red X's. Question marks indicate yet unidentified or uncharacterized metabolic steps.

1.6.1 Retained lipid II processing enzymes in *Wolbachia*

Although almost all peptidoglycan recycling enzymes and glycosyltransferases are not annotated, there are still peptidoglycan synthesizing enzymes encoded in the genome of *Wolbachia*. PBP2 and PBP6a are found in filarial and insect *Wolbachia*, while PBP3 is only annotated in insect *Wolbachia*. PBP2 and PBP3 in free-living bacteria are known to provide DD-transpeptidase activity and catalyze the cross-linking of peptide stems, the DD-carboxypeptidase PBP6a regulates the degree of crosslinking by cleaving the terminal D-Ala of the pentapeptide (Höltje, 1998). The annotated genomes of *Wolbachia* from arthropods (e.g. *w*Mel, *Wolbachia* from *Drosophila melanogaster*; *w*Ri, *Wolbachia* from *Drosophila simulans*; *w*PiP, *Wolbachia* from *Culex quinquefasciatus* Pel) have retained one cell wall hydrolase that shows homology to the *E. coli* N-acetylmuramoyl-L-alanine-amidase

AmiD. Vollmer et al. (2013) showed that lipid II processing enzymes are not only encoded in the wolbachial genome, but they are indeed expressed in *w*AlbB. However, the activity of these enzymes has not been studied in *Wolbachia* and it is unknown if and how lipid II is processed.

A new cell wall labeling technique revealed that obligate intracellular bacteria of the genus *Chlamydia* synthesize a peptidoglycan-like structure after decades of debates between scientists (Liechti et al., 2014). With the same technique, a peptidoglycan-like structure was also detected in free-living *Planctomycetes* for the first time and recently also in *Orientia tsutsugamushi*, which are closely related to *Wolbachia* also belonging to the order Rickettsiales (Atwal et al., 2017).

1.6.1.1 Penicillin-binding protein PBP2

PBP2 (synonyms: MrdA, pbpA) is a HMW class B PBP DD-transpeptidase involved in cell elongation and maintenance of cell shape. These proteins have an N-terminal, non-penicillin-binding domain, which might be involved in protein-protein interactions and a C-terminal domain with the active site motifs (Höltje, 1998). Inhibition of PBP2 by specific antibiotics, like mecillinam, leads to spherical cells instead of rods in *E. coli* (Spratt and Pardee, 1975). As shown for *S. aureus*, PBP2 localizes at the septum in the presence of lipid II. When the lipid II synthesis pathway is inhibited by the antibiotic D-cycloserine, PBP2 delocalizes from the septum (Pinho and Errington, 2005). PBP2 was also found in the lateral wall and at mid-cell during cell division suggesting that it might have an additional housekeeping role (Den Blaauwen et al., 2003). The filarial *Wolbachia* DD-transpeptidase homolog PBP2 from *w*Bm was re-annotated on the database of the National Center for Biotechnology Information (NCBI) and is now listed as a putative PBP3, a monofunctional DD-transpeptidase involved in cell division. The characterization of this enzyme is part of this work.

1.6.1.2 Penicillin-binding protein PBP3

In free-living bacteria, PBP 3 (synonym: FtsI) is part of the divisome and responsible for correct septation (Goffin et al., 1996). In *E. coli*, the protein is a HMW class B PBP, which consists of an N-terminal non-penicillin-binding domain with a short intracellular part, a membrane anchor responsible for correct localization, and the C-terminal penicillin-binding domain which harbors the active site motifs (Goffin et al., 1996; Weiss et al., 1999). Up to now, no transpeptidation activity could be detected for PBP3 *in vitro*, but purified protein from *E. coli* has been shown to hydrolyze artificial thioester compounds, which might at least indicate the presence of an accessible active site (Adam et al., 1991; Egan et al., 2015). The specific inhibition of PBP3 by the antibiotic aztreonam leads to the arrest of cell division and a

filamentous phenotype which facilitates *in vivo* activity assays (Weiss et al., 1997). Filarial *Wolbachia* only harbor the putative monofunctional DD-transpeptidase PBP2 (see chapter 1.6.1.1), whereas *Wolbachia* residing in insect cells encode PBP2 and PBP3. The function of this additional PBP in *Wolbachia* biology is unknown. Thus, the putative PBP3 enzyme from *w*Mel was investigated in this thesis.

1.6.1.3 Penicillin-binding protein PBP6a

The final reaction in cell wall synthesis is the cleavage of the terminal D-Ala residue accompanied by the formation of an interpeptide bridge. The degree of cross-linking is regulated by DD-carboxypeptidases which belong to LMW class C PBPs. In *E. coli*, three periplasmic monofunctional DD-carboxypeptidases have been identified: PBP5, PBP6a (synonym: DacC, formerly known as PBP6) and PBP6b (Peters et al., 2016). To date, the exact function of these proteins, especially PBP6a, is poorly understood. They seem to play a vital role in controlling cell diameter and septum formation as well as in modulating the mature peptidoglycan meshwork (Ghosh et al., 2008; Sarkar et al., 2011). DD-carboxypeptidases are dispensable for the survival of *E. coli* and the deletion of the corresponding genes does not affect cell growth or morphology except for PBP5, which is considered to act as the main DD-carboxypeptidase (Nelson and Young, 2001). Due to their high amino acid sequence similarity, a potential substitution of PBP5 by PBP6a was investigated, but PBP6a did not compensate growth defects of PBP5-lacking cells (Chowdhury et al., 2010). Additionally, PBP6 was shown to have an *in vitro* enzyme activity five times weaker than PBP5 (Chowdhury et al., 2010). Contrary to PBP5, which is produced primarily during early exponential growth in *E. coli*, PBP6a is highly expressed in the stationary phase (Baquero et al., 1996). This leads to the hypothesis of a functional difference between PBP5 and PBP6a *in vivo*, suggesting a role for the latter in the stabilization of peptidoglycan during the stationary phase (Van der Linden et al., 1992). Of note, overexpressed PBP6a from *E. coli* was able to restore cell division of a PBP3-repressed *E. coli* strain, which shows a filamentous phenotype when grown at the non-permissive temperature of 42 °C (Begg et al., 1990). This growth defect can be complemented by the overexpression of a DD-carboxypeptidase cleaving the terminal D-Ala of the pentapeptide chains. The subsequent cleavage of the tetrapeptides by a second carboxypeptidase (LD-carboxypeptidase A) results in increased levels of available tripeptide chains in peptidoglycan. These are the preferred substrates for the residual activity of the impaired PBP3 and cell division can be complemented partially (Botta and Park, 1981; Pisabarro et al., 1986; Begg et al., 1990; Dai et al., 1993). Restoration of growth in the same

PBP3-repressed *E. coli* strain has also been performed with PBP6 from *Chlamydia pneumoniae* and provides an established assay for the determination of *in vivo* DD-carboxypeptidase activity (Otten, 2014). The elucidation of the putative cell wall active enzyme PBP6a from *w*Bm is part of this work.

1.6.1.4 N-acetylmuramoyl-L-alanine-amidase AmiD

In *E. coli*, four periplasmic N-acetylmuramoyl-L-alanine-amidases are described (Uehara and Park, 2007; Kerff et al., 2010). All of them are zinc-dependent and can be blocked by metal chelators like ethylenediaminetetraacetic acid (EDTA). AmiA, AmiB and AmiC belong to the amidase 3 family and play a role in septum cleavage leading to separation of the daughter cells at the end of cell division (Heidrich et al., 2001). These enzymes hydrolyze the amide bond between the Mur*N*Ac lactyl group and the L-alanine of the peptide but they have no activity when the Mur*N*Ac is in its anhydro form as a result of glycan chain cleavage by lytic transglycosylases (Heidrich et al., 2001). AmiD, the last N-acetylmuramoyl-L-alanine amidase identified in *E. coli*, is a periplasmic lipoprotein anchored in the outer membrane belonging to the amidase 2 family. It exerts its broader hydrolytic activity on the intact peptidoglycan and soluble fragments containing Mur*N*Ac regardless of its anhydro form (Uehara and Park, 2007). AmiD is not involved in cell separation during the bacterial division, and its exact role in the cell has not been identified (Kerff et al., 2010). It has been proposed that AmiD is part of a secondary strategy to prevent immune responses in the host organism by degrading cell wall fragments in the periplasm (Uehara and Park, 2007). The genomes of arthropod *Wolbachia* (e.g. *w*Mel, *w*Ri, *w*PiP) all contain only one predicted periplasmic cell wall hydrolase. Sequenced genomes of filarial *w*Bm and *O. volvulus* (*w*Ov) show that these strains have lost the ability to synthesize any of these enzymes, e.g. *w*Bm0682 might encode an amidase, but genome analysis has concluded that it is a pseudogene (Wu et al., 2004; Foster et al., 2005). Recently, the only identified chlamydial amidase AmiA has been shown to perform a novel bifunctional activity on lipid II as an amidase as well as a DD-carboxypeptidase *in vitro* and this amidase is essential for cell division (Klöckner et al., 2014). In this thesis, the putative hydrolyzing activity of AmiD from *w*Mel was analyzed.

1.6.2 Interaction of *Wolbachia* lipid II and outer membrane proteins

Bioinformatic analysis of the *w*Bm genome using distinct databases consistently identified two lipoproteins in the outer membrane: *Wolbachia* Pal and *Wolbachia* VirB6, which is a core component of the bacterial Type IV secretion system (Turner et al., 2009; Voronin et al., 2014). Analysis of the proteome of adult female *B. malayi* revealed that Pal is one of the

most abundant proteins in *Wolbachia* (Voronin et al., 2014). *Wolbachia* do not encode Tol genes located in the inner membrane. Only some of the annotated *Wolbachia* strains (e.g. *w*AlbB, *w*Mel, *w*Pip) found in arthropods possess the gene for the periplasmic protein TolB which is assumed to modulate Pal by competing for peptidoglycan (Gerding et al., 2007). However, it is possible that Pal is necessary to connect the inner and outer membrane, especially during cell division, and this interaction partner might be lipid II (Vollmer et al., 2013). First evidence for this was demonstrated in fosfomycin-treated *Wolbachia* (blocking of lipid II synthesis) resulting in enlarged cells unable to divide and a perturbed localization of the lipoprotein Pal (Vollmer et al., 2013).

1.6.3 Host response to *Wolbachia* cell wall fragments

In filarial infections, the pro-inflammatory activity of *B. malayi* and *O. volvulus* is higher when *Wolbachia* are present, and lipoproteins have been identified as key ligands (Hise et al., 2007; Turner et al., 2009; Tamarozzi et al., 2011). It was shown that *Wolbachia* activate TLR 2/6 in filariasis, and Pal recruits neutrophils, macrophages and other innate immune cells, stimulating their activation and the production of an array of pro-inflammatory cytokines and mediators (Saint André et al., 2002; Hise et al., 2007; Tamarozzi et al., 2011). Additionally, *Wolbachia* lipoproteins also drive adaptive Th1 immunity through activation of dendritic cells (Turner et al., 2009). Thus, Pal is likely a major driver of *Wolbachia*-mediated inflammatory immunity. With protein extract of *Litomosoides sigmodontis*, a filarial nematode infecting rodents used as a mouse model for human filarial infections, it was demonstrated that both NOD 1 and NOD 2 receptors were activated in stimulated human embryonic kidney cells expressing the specific receptor (Ajendra et al., 2016). When *Wolbachia* residing in the nematodes were depleted by tetracycline, the receptors were not activated after incubation with *L. sigmodontis* extract. The activation of NOD 1 and NOD 2 receptors further confirm that at least cell wall precursors are synthesized by *Wolbachia* which likely contain m-DAP (Ajendra et al., 2016).

1.7 Objectives

Wolbachia endobacteria are not challenged by osmotic pressure and peptidoglycan has never been detected. Still, *Wolbachia* encode almost all genes required for the synthesis of the cell wall precursor lipid II, which has been shown to be synthesized and to be essential for cell division (Henrichfreise et al., 2009; Vollmer et al., 2013). However, it is unknown if and how lipid II is processed. The investigation of *Wolbachia* enzymes involved in lipid II metabolism and the exact composition of a putative *Wolbachia* cell wall not only provides insight into *Wolbachia* biology but might also identify novel targets for the development of antibiotics for use in depleting these essential endobacteria from filarial nematodes. Since the role of lipid II in *Wolbachia* biology is poorly understood, the function of the retained lipid II modifying enzymes in cell wall biosynthesis and cell separation were examined. The overall objective of the present thesis was to elucidate the processing of lipid II in *Wolbachia*. In particular, the functionality as well as antibiotic susceptibility of putative lipid II processing enzymes were investigated *in vivo* and *in vitro*. The main goals of the thesis were:

1. Characterization of the following proteins:
   (I) AmiD$^{w\text{Mel}}$, a putative N-acetylmuramoyl-L-alanine-amidase from *Wolbachia* endosymbionts of *D. melanogaster*
   (II) PBP2$^{w\text{Bm}}$, a putative DD-transpeptidase from *Wolbachia* endosymbionts of *B. malayi*
   (III) PBP3$^{w\text{Mel}}$, a putative DD-transpeptidase involved in cell division from *Wolbachia* endosymbionts of *D. melanogaster*
   (IV) PBP6a$^{w\text{Bm}}$, a putative DD-carboxypeptidase from *Wolbachia* endosymbionts of *B. malayi*
   (V) Pal$^{w\text{Bm}}$, peptidoglycan-associated lipoprotein from *Wolbachia* endosymbionts of *B. malayi*
2. By labeling lipid II *in vivo*, it was investigated whether *Wolbachia* from an infected C6/36 insect cell culture have a peptidoglycan-like structure.
3. In interaction assays, it was examined *in vitr*o whether Pal$^{w\text{Bm}}$ interacts with lipid II and PBP2$^{w\text{Bm}}$.
4. An established cell-free *Wolbachia* culture was further studied and supplemented with substances in order to enhance stability and growth (Vollmer, 2012). Moreover, cell-free *Wolbachia* were incubated with different antibiotics to test the efficacy and impact on proliferation and morphology.

2 Materials and methods

2.1 Equipment and consumables

2.1.1 Chemicals and solvents

Table 1: List of chemicals used in this thesis.

Name	Manufacturer
1,10-Phenanthroline	Sigma-Aldrich, Steinheim, Germany
Anhydrotetracycline	IBA Lifesciences, Göttingen, Germany
(L-)Arginine	Sigma-Aldrich, Steinheim, Germany
(L-)Ascorbic acid	Sigma-Aldrich, Steinheim, Germany
β-Mercaptoethanol	Merck Millipore, Darmstadt, Germany
BCIP	Carl Roth, Karlsruhe, Germany
Betaine	Sigma-Aldrich, Steinheim, Germany
Biotin	Sigma-Aldrich, Steinheim, Germany
Biotin Blocking Buffer	IBA Lifesciences, Göttingen, Germany
Bovine Serum Albumin Fraction V	Fisher Scientific, Schwerte, Germany
Bradford reagent	Cytoskeleton, Denver, USA
Bromophenol blue	Sigma-Aldrich, Steinheim, Germany
C_{55}-P	Larodan Fine Chemicals, Malmö, Sweden
CENTA™	Calbiochem, Darmstadt, Germany
Chloroform	J.T. Baker, Griesheim, Germany
(D-)Desthiobiotin	IBA Lifesciences, Göttingen, Germany
DMF	Sigma-Aldrich, Steinheim, Germany
DMSO	Sigma-Aldrich, Steinheim, Germany
EDTA	Carl Roth, Karlsruhe, Germany
Ethanol	Merck Millipore, Darmstadt, Germany
Ethynyl-D-alanyl-D-alanine	Pepmic Co., Ltd., Suzhou, China
Ethynyl-L-alanyl-L-alanine	Pepmic Co., Ltd., Suzhou, China
Glycerol	Sigma-Aldrich, Steinheim, Germany
HCl	Sigma-Aldrich, Steinheim, Germany
KH_2PO_4	Sigma-Aldrich, Steinheim, Germany
LE-Agarose	Biozym, Hamburg, Germany
(D-)Mannitol	Sigma-Aldrich, Steinheim, Germany
Methanol	J.T. Baker, Griesheim, Germany
$MgCl_2$	Sigma-Aldrich, Steinheim, Germany
Midori Green Advanced	Nippon Genetics Europe, Düren, Germany
MOPS	Sigma-Aldrich, Steinheim, Germany
NaOH	Carl Roth, Karlsruhe, Germany
Na_2HPO_4	Sigma-Aldrich, Steinheim, Germany
NBT	Carl Roth, Karlsruhe, Germany
Novex™ sharp prestained protein ladder	Thermo Scientific, Waltham, USA
PAGEruler prestained protein ladder 1kb	Thermo Scientific, Waltham, USA
PAGEruler unstained protein ladder 1kb	Thermo Scientific, Waltham, USA
Perchloric acid 70 %	Merck Millipore, Darmstadt, Germany

Name	Manufacturer
Paraformaldehyde	Merck Millipore, Darmstadt, Germany
Quick-Load 1kb DNA ladder	New England Biolabs, Ipswich, USA
Remazol Brilliant Blue Dye	Sigma-Aldrich, Steinheim, Germany
SDS	Carl Roth, Karlsruhe, Germany
Strep-Tactin® Sepharose	IBA Lifesciences, Göttingen, Germany
Sucrose	Sigma-Aldrich, Steinheim, Germany
SYBR Green	Fermentas, St. Leon-Rot, Germany
TEMED	Roth, Karlsruhe, Germany
(D-)Trehalose	Sigma-Aldrich, Steinheim, Germany
Triton X-100	Sigma-Aldrich, Steinheim, Germany
Tri-Track loading dye	Thermo Scientific, Waltham, USA
Uridine 5′-diphospho-N-acetylglucosamine sodium salt	Sigma-Aldrich, Steinheim, Germany
Vectashield Mounting Medium	Vector Laboratories, Burlingame, USA
$ZnCl_2$	Sigma-Aldrich, Steinheim, Germany

2.1.2 Enzymes

Table 2: List of enzymes used in this thesis.

Name	Manufacturer
α-Amylase from *Aspergillus oryzae*	Sigma-Aldrich, Steinheim, Germany
α-Chymotrypsin	Sigma-Aldrich, Steinheim, Germany
Alkaline phosphatase conjugate	IBA Lifesciences, Göttingen, Germany
Benzonase	Novagen, Darmstadt, Germany
BamHI	New England Biolabs, Ipswich, USA
BsaI HF	New England Biolabs, Ipswich, USA
EcoRI HF	New England Biolabs, Ipswich, USA
NcoI HF	New England Biolabs, Ipswich, USA
D-amino acid oxidase (DAAO)	Sigma-Aldrich, Steinheim, Germany
Lysozyme	Novagen, Darmstadt, Germany
Phusion® HF Polymerase	Thermo Scientific, Waltham, USA
T4 Ligase	New England Biolabs, Ipswich, USA

2.1.3 Kits

Table 3: List of kits used in this thesis.

Name	Manufacturer
Click-iT® Cell Reaction Buffer Kit	Thermo Scientific, Waltham, USA
HotStarTaq® DNA Polymerase Kit	Qiagen, Hilden, Germany
LIVE/DEAD® *Bac*Light™ Bacterial Viability Kit	Molecular Probes, Carlsbad, USA
Nucleospin Gel and PCR Clean-up Kit	Macherey Nagel, Düren, Germany
QIAamp DNA Mini Kit	Qiagen, Hilden, Germany
QIAprep Spin Miniprep Kit	Qiagen, Hilden, Germany
QIAquick PCR purification Kit	Qiagen, Hilden, Germany
QuantaBlu™ Fluorogenic Peroxidase	Thermo Scientific, Waltham, USA

Name	Manufacturer
Substrate Kit	
QuikChange Lightning Site-Directed Mutagenesis Kit	Agilent Technologies, Waldbronn, Germany
Strep Tactin Miniprep Spin Column Kit	IBA Lifesciences, Göttingen, Germany

2.1.4 Technical equipment

Table 4: List of technical equipment and devices used in this thesis.

Name	Manufacturer
96-well cell culture well plates, clear, flat bottom, with lid	Greiner, Frickenhausen, Germany
Bench-top centrifuge 5417R	Eppendorf, Hamburg, Germany
Bench-top centrifuge Mikro 200	Hettich, Tuttlingen, Germany
Biacore® T100	GE Healthcare, Chicago, USA
Binocular Leitz Diavert	Leitz, Wetzlar, Germany
BLItz® system device	Pall ForteBio, Fremont, USA
Borosilicate glass beads 3mm	Sigma-Aldrich, Steinheim, Germany
Cellstar standard cell culture flasks	Greiner, Frickenhausen, Germany
CM5 sensor chip	GE Healthcare, Chicago, USA
Corning cell lifter	Sigma-Aldrich, Steinheim, Germany
Electrophoresis power supply consort EV243	Thermo Scientific, Waltham, USA
Falcon™ Chambered Cell Culture Slides	BD Falcon, Corning, USA
FastGene Led Illuminator	Nippon Genetics Europe, Düren, Germany
Fraction Collector FC204	Gilson, Middleton, USA
Freeze dryer Alpha 2-4 LSC	Martin Christ, Osterode am Harz, Germany
Gel Doc™ EZ Imager	Bio-Rad, München, Germany
Heraeus Multifuge 1 S-R	Heraeus Instruments, Hanau, Germany
Hi-Trap DEAE FF column	Amersham Biosciences, Freiburg, Germany
HPLC	Gilson, Middleton, USA
Incubator Type B6120	Heraeus Instruments, Hanau, Germany
MicroPulser™	Bio-Rad, München, Germany
Mini-PROTEAN® 12 % Precast Gels	Bio-Rad, München, Germany
Mini-PROTEAN® Tetra Electrophoresis System	Bio-Rad, München, Germany
Nanophotometer TM 7122v1.6.1	Implen, München, Germany
Neubauer counting chamber improved	Laboroptik, Bad Homburg, Germany
Nitrocellulose blotting membrane	Amersham Biosciences, Freiburg, Germany
PCR cycler	MWG-Biotech, Ebersberg, Germany
Pierce™ Streptavidin Coated Plates	Thermo Scientific, Waltham, USA
Polypropylene column	Qiagen, Hilden, Germany
QIAcube robotic workstation	Qiagen, Hilden, Germany
Rotavapor RE11	Büchi Labortechnik, Flawil, Switzerland
Rotorgene 6000	Corbett Life Sciences, Sydney, Australia
Shaker MaxQ 5000 Mod4360	Thermo Scientific, Waltham, USA
Silica plate TLC Silica Gel 60	Merck Millipore, Darmstadt, Germany
Sorvall Discovery M120 SE	Fisher Scientific, Schwerte, Germany
Sorvall Evolution EC Superspeed Centrifuge	Fisher Scientific, Schwerte, Germany
Spark™ 10M multimode microplate reader	Tecan, Männedorf, Switzerland

Name	Manufacturer
Spectramax® 340PC	Molecular Devices, Biberach an der Riss, Germany
Streptavidin biosensors	Pall ForteBio, Fremont, USA
Sunrise™ microplate reader	Tecan, Männedorf, Switzerland
Teflon tubes	Nalgene, Rochester, USA
Trans-Blot Turbo™ Transfer System	Bio-Rad, München, Germany
UviLine 9400 photometer	SI Analytics, Mainz, Germany
Vortexer RS-VA10	Phoenix Instruments, Garbsen, Germany
Zeba Spin Desalting Columns 7K MWCO	Thermo Scientific, Waltham, USA
ZeissAxio VertA.1 Epifluorescence microscope	Carl Zeiss AG, Oberkochen, Germany
Zeiss Laser Scanning Microscope 710	Carl Zeiss AG, Oberkochen, Germany

2.1.5 Culture media and supplements

Table 5: Culture media and agar plates used in this thesis.

Name	Composition/Manufacturer
ATCC medium: 200 YM medium	3 g yeast extract, 3 g malt extract, 10 g dextrose, 5 g peptone, ad 1 l aqua dest.; pH 6.2
L15 Leibovitz medium	Invitrogen, Darmstadt, Germany
Lysogeny broth (LB) medium	10 g tryptone, 5 g yeast extract, 10 g NaCl, ad 1 l aqua dest.; pH 7.5
LB agar	10 g tryptone, 5 g yeast extract, 10 g NaCl, 15 g agar, ad 1 l aqua dest.; pH 7.5
Mueller-Hinton agar	Becton Dickinson GmbH, Heidelberg, Germany
Mueller-Hinton broth	Carl Roth, Karlsruhe, Germany
NaCl-free LB broth	10 g tryptone, 5 g yeast extract, ad 1 l aqua dest.; pH 7.5
Super optimal broth (SOC) medium	Thermo Scientific, Waltham, USA
Tryptone soya broth (TSB)	Thermo Scientific, Waltham, USA

Table 6: Culture media supplements used in this thesis.

Name	Manufacturer
α-cardiac actin from bovine cardiac muscle	Hypermol, Bielefeld, Germany
Bacto™-Yeast extract	Becton Dickinson, Heidelberg, Germany
Bacto™-Tryptone	Becton Dickinson, Heidelberg, Germany
Biotin	Sigma-Aldrich, Steinheim, Germany
Cholesterol	Sigma-Aldrich, Steinheim, Germany
Fetal Calf Serum (FCS)	PAA Laboratories, Colbe, Germany
Lipid Mixture	PeproTech Inc, Hamburg, Germany
MEM non-essential amino acids	PAA Laboratories, Colbe, Germany
Penicillin/Streptomycin	PAA Laboratories, Colbe, Germany
Sodium pyruvate	Sigma-Aldrich, Steinheim, Germany
Tryptose phosphate broth	PAA Laboratories, Colbe, Germany

2.1.6 Antibiotics

Table 7: Antibiotics used in this thesis.

Name	Manufacturer
Aztreonam	Sigma-Aldrich, Steinheim, Germany
Ampicillin	Sigma-Aldrich, Steinheim, Germany
Bacitracin	AppliChem GmbH, Darmstadt, Germany
Bocillin™ FL penicillin	Thermo Scientific, Waltham, USA
Clindamycin	Alfa Aesar, Ward Hill, USA
Chloramphenicol	Sigma-Aldrich, Steinheim, Germany
Doxycycline	Calbiochem, Darmstadt, Germany
Fosfomycin	Infectopharm, Heppenheim, Germany
Mecillinam	Sigma-Aldrich, Steinheim, Germany
Penicillin G	Sigma-Aldrich, Steinheim, Germany
Polymyxin B	Sigma-Aldrich, Steinheim, Germany
Rifampicin	Sigma-Aldrich, Steinheim, Germany
Sulfamethoxazol	Sigma-Aldrich, Steinheim, Germany
Tetracycline	Sigma-Aldrich, Steinheim, Germany
Trimethoprim	Sigma-Aldrich, Steinheim, Germany
Vancomycin	Sigma-Aldrich, Steinheim, Germany

2.1.7 Antibodies and fluorophores

Table 8: Antibodies and fluorophores used in this thesis.

Name	Manufacturer
Alexa Fluor® 488 azide	Thermo Scientific, Waltham, USA
Alexa Fluor® 594 azide	Thermo Scientific, Waltham, USA
DAPI	Sigma-Aldrich, Steinheim, Germany
Goat anti-Rabbit IgG (H+L) secondary antibody, Alexa Fluor® 488 conjugate	Thermo Scientific, Waltham, USA
Goat anti-Rabbit IgG (H+L) secondary antibody, Alexa Fluor® 594 conjugate	Thermo Scientific, Waltham, USA
Nile red	Sigma-Aldrich, Steinheim, Germany
Rabbit *w*PAL anti-serum	Taylor Laboratory, Liverpool School of Tropical Medicine, Liverpool, UK
Rabbit *Wolbachia* FtsZ anti-serum	Sullivan Laboratory, University of California, Santa Cruz, USA
Strep-MAB-Immo monoclonal antibody	IBA Lifesciences, Göttingen, Germany
Strep-Tactin® Alkaline phosphatase conjugate	IBA Lifesciences, Göttingen, Germany

2.2 Strains, expression vectors and primers

2.2.1 Cell lines, yeast and bacterial strains

Table 9: Cell lines, yeast and bacterial strains used in this thesis.

Strain	Description	Reference
Aedes albopictus C6/36	Cell line	Turner, Langley et al. 2006
Aedes albopictus C6/36 infected with *Wolbachia pipientis*	*Wolbachia pipientis* strain *Aedes albopictus* B (*w*AlbB)	Turner, Langley et al. 2006
Bacillus cereus T	Indicator strain	Provided by AG Bierbaum, Bonn, Germany
Escherichia coli (*E. coli*) ADE24 +PBAD33	Δ *amiA, amiB, amiC* amidase triple mutant, harboring pBAD33-amiCEc, glucose induced chain forming phenotype	Klöckner, Otten et al. 2014; Provided by AG Vollmer, Newcastle, UK
E. coli C43	B F dcm ompT hsdS(rBmB) Gal λ (DE3)	Lucigen, Middleton, USA
E. coli JM83	rpsL ara Δ(lac-proAB) Φ80dlacZΔM15	DSM 3947
E. coli MCI23	[araD139]B/r, leu-260::Tn10, ftsI23(ts), Δ(argF-lac)169, λ-, e14-, flhD5301, Δ(fruKyeiR) 725(fruA25), relA1, rpsL150(strR), rbsR22, Δ(fimBfimE) 632(::IS1), deoC1: FEGSC	CGSC; Provided by AG Henrichfreise, Bonn, Germany
E. coli ML-35 pYC	*ΔlacI*, constitutive β-galactosidase expression, plasmid-encoded (pBR-22) β-lactamase, Amp^R	Lehrer, Barton et al. 1988
E. coli W3110	Sex(Hfr,F+,F-,or F'): F-F-mrcAΔ/mrr-hsdRMS-mrcBC) Φ80lacZΔM15VlacX74deoRrec A1araD139Δ(ara-leu) 7697galUgalKrpsLendA1nupG	DSM5911
One Shot TOP10® chemically competent *E. coli*		Invitrogen, Darmstadt, Germany
Micrococcus flavus	Indicator strain	Provided by AG Schneider, Bonn, Germany
Rhodotorula minuta var. *texensis*	Yeast strain	ATCC, Manassas, USA; Phaff, Mrak et al. 1952
Staphylococcus simulans 22	Indicator strain	Sahl and Brandis 1981; Provided by AG Bierbaum, Bonn, Germany

2.2.2 Expression vectors

pASK-IBA plasmids are Strep-tag II expression vectors manufactured by IBA Lifesciences, Germany. These vectors carry the promoter region from the *tetA* resistance gene in front of the multiple cloning site, thus overexpression of heterologous proteins can be induced by adding anhydrotetracycline (AHT) at a concentration that is antibiotically ineffective (200 ng/ml). Strep-tag II is a short peptide, which selectivity binds to Strep-Tactin, an engineered streptavidin. In this thesis, four different pASK-IBA vectors were used (Table 10).

pASK-IBA2 contains an N-terminal OmpA leader-sequence for periplasmic overexpression of the target protein and a C-terminal Strep-tag II. In this work, both pASK-IBA2 and pASK-IBA2C were used, which encode an ampicillin or a chloramphenicol resistance gene, respectively.

pASK-IBA3 encodes a C-terminal Strep-tag II fused to the gene of interest, is used for cytoplasmic overexpression and contains an ampicillin resistance gene.

pASK-IBA6 harbors an N-terminal OmpA leader-sequence and Strep-tag II for periplasmic expression of the target protein. In this work pASK-IBA6C was used, which encodes a chloramphenicol resistance gene.

Table 10: List of pASK-IBA expression vectors used in this thesis.

Feature	Position (bp)
Promoter	37 to 72
Forward primer binding site	57 to 76
OmpA signal sequence	139 to 201
Multiple cloning site	202 to 282
Strep-tag®	283 to 312
Reverse primer binding site	368 to 384
F1 origin	397 to 835
AmpR resistance gene	984 to 1844
Tet-repressor	1854 to 2477

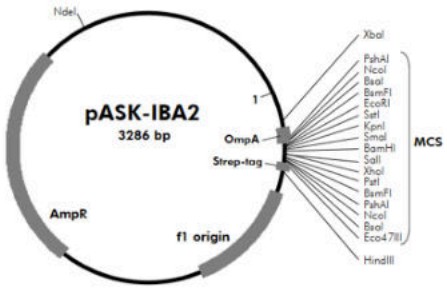

Feature	Position (bp)
Promoter	37 to 72
Forward primer binding site	57 to 76
OmpA signal sequence	139 to 201
Multiple cloning site	202 to 282
Strep-tag®	283 to 312
Reverse primer binding site	368 to 384
F1 origin	397 to 835
CamR resistance gene	957 to 1616
Tet-repressor	1629 to 2252
Col E1origin	2405 to 2993

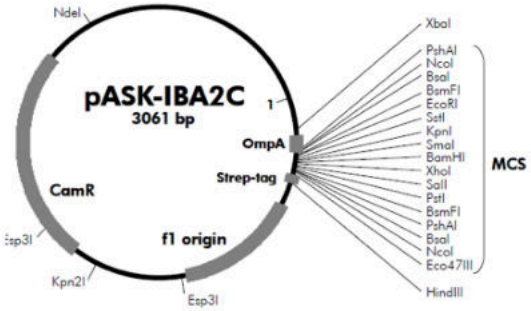

Feature	Position (bp)
Promoter	37 to 72
Forward primer binding site	57 to 76
Multiple cloning site	160 to 243
Strep-tag®	244 to 273
Reverse primer binding site	329 to 345
F1 origin	358 to 796
AmpR resistance gene	945 to 1805
Tet-repressor	1815 to 2438

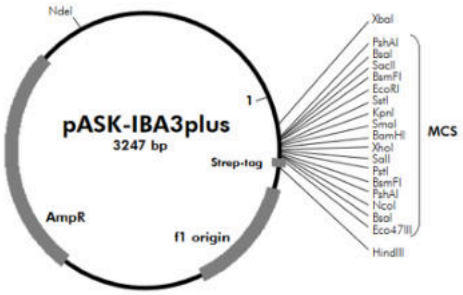

Feature	Position (bp)
Promoter	37 to 72
Forward primer binding site	57 to 76
OmpA signal sequence	139 to 201
Strep-tag®	202 to 231
Factor Xa cleavage site	232 to 243
Multiple cloning site	244 to 320
Reverse primer binding site	388 to 404
F1 origin	417 to 855
CamR resistance gene	977 to 1636
Tet-repressor	1649 to 2272
Col E1origin	2425 to 3013

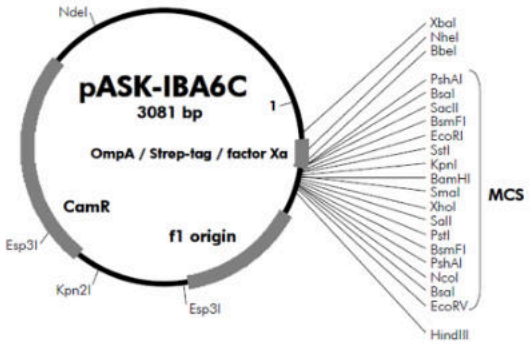

2.2.3 Primers

Table 11: Primers used for cloning into expression vectors and sequencing. Restriction sites are written in bold. Annealing temperatures used in PCRs and restriction enzymes are shown in the right column.

Primer name		Sequence (5´→ 3´)	Restriction enzyme/ Annealing °T
IBA2C_amiD	for	ATGGTA**GGTCTC**AGGCCAAAATCCAACTATCTA AAGTCAAC	BsaI/ 57 °C
	rev	ATGGTA**GGTCTC**AGCGCTACGAATTTCTTCCTTT GCTTTTTCTAAATAC	
IBA2_amiDΔSP	for	ATGGTA**GGTCTC**AGGCCTCAAGCAATATCGAGA ATGATTTTCA	BsaI/ 57 °C
	rev	ATGGTA**GGTCTC**AGCGCTACGAATTTCTTCCTTT GCTTTTTCTA	
IBA2C_pbp2	for	ATGGTA**GGTCTC**AGGCCATGTGGATAAAAAAC AAAGTCTTTAATC	BsaI/ 57.2 °C
	rev	ATGGTA**GGTCTC**AGCGCTCCCTTTAAGCATATA CCGCAATATT	
IBA2C_pbp2ΔTM	for	ATGGTA**GGTCTC**AGGCCCGAAACAGACAAAAA TACGAAAAGC	BsaI/ 57.2 °C
	rev	ATGGTA**GGTCTC**AGCGCTCCCTTTAAGCATATA CCGCAATATT	
IBA2C_pbp6a	for	ATGGTA**CCATGG**TAGTATATTAGACAAATTGGT AATCCTGCTG	NcoI/ 59.3 °C
	rev	ATGGTA**CCATGG**TCAAACAATATTCTAAAAAAC TTTTCTACGTAATTTAATTCC	
IBA2C_pbp6aΔSP	for	ATTCTTC**CCATGG**TTACCAATTTAGAACTAAAG CA	NcoI/ 59 °C
	rev	ATGGTA**CCATGG**TCAAACAATATTCTAAAAAAC TTTTCTACGTAATTTAATTCC	
IBA3_amiD	for	ATGGTA**GGTCTC**AAATGATGAAAATCCAACTAT CTAAAGTCAAC	BsaI/ 57 °C
	rev	ATGGTA**GGTCTC**AGCGCTACGAATTTCTTCCTTT GCTTTTTCTA	
IBA6C_pbp2	for	ATGGTA**GGTCTC**AGCGCTGGATAAAAAACAAA GTCTTTAATCGT	BsaI/ 57.2 °C
	rev	ATGGTA**GGTCTC**ATATCACCCTTTAAGCATATA CCGCAATATT	
IBA6C_pbp2ΔTM	for	ATGGTA**GGTCTC**AGCGCCGAAACAGACAAAAA TACGAAAAGC	BsaI/ 57.2 °C
	rev	ATGGTA**GGTCTC**ATATCACCCTTTAAGCATATA CCGCAATATT	
IBA2C_pbp3	for	ATGGTA**GGTCTC**AGGCCCAAGCATTACTTAAAA ATAAGCTCCG	BsaI/ 58 °C
	rev	ATGGTA**GGTCTC**AGCGCTCATCTCAGGTGTAAC ATTTAGTATAG	
IBA_sequencing	for	GAGTTATTTTACCACTCCCT	
	rev	CGCAGTAGCGGTAAACG	

Table 12: Primers used for mutagenesis of the active site residues. Mutated positions are underlined.

Primer name		Sequence (5´→ 3´)
amiD_mut1 (H79A)	for	GGTTATAGTTCACGCGACTGAAACATCAAC
	rev	GTTGATGTTTCAGTCGCGTGAACTATAACC
amiD_mut2 (S83A)	for	CACCATACTGAAACAGCAACACTAAAAGGTAC
	rev	GTACCTTTTAGTGTTGCTGTTTCAGTATGGTG
amiD_mut3 (D207A)	for	GCTATACAATGCGTAAACCAGCGCCACACAAATTGTTTGATTG
	rev	CAATCAAACAATTTGTGTGGCGCTGGTTTACGCATTGTATAGC
amiD_mut4 (S400A)	for	AGATATCGCATATGGTCTGCCCTCTATAAACCATTTAAGC
	rev	GCTTAAATGGTTTATAGAGGGCAGACCATATGCGATATCT
pbp2_mut1 (S107A)	for	GTAACAAAATCGGCGGAAACAAAAATAACCGCTC
	rev	GAGCGGTTATTTTTGTTTCCGCCGATTTTGTTAC
pbp2_mut2 (S265A)	for	CGTATCAAATTCCACCTGGTGCGATATTTAAAATAATAGTTG
	rev	CAACTATTATTTTAAATATCGCACCAGGTGGAATTTGATACG
pbp3_mut1 (S107A)	for	GAGTACTTACTGCCGAAAAGAAATTTGCTTGG
	rev	CCAAGCAAATTTCTTTTCGGCAGTAAGTACTC
pbp3_mut2 (S256A)	for	GGGGTATATGAGATGGGGGCGGTATTAAAATACTTTAC
	rev	GTAAAGTATTTTAATACCGCCCCCATCTCATATACCCC
pbp3_mut3 (S339A)	for	GCTATGAAGCTATTTGCGCCTTTGAAAATAGAAATACC
	rev	GGTATTTCTATTTTCAAAGGCGCAAATAGCTTCATAGC
pbp3_mut4 (S445A)	for	GAGGAAAAACTGGAGCGGCGGAAAAAGTTG
	rev	CAACTTTTTCCGCCGCTCCAGTTTTTCCTC
pbp6a_mut1 (S48A)	for	GTTCATTTTTGAGCATAATGCCGACGAAAAGATGTCTCC
	rev	GGAGACATCTTTTCGTCGGCATTATGCTCAAAAATGAAC
pbp6a_mut2 (S56A)	for	CGAAAAGATGTCTCCATCTGCAATGAGCAAGCTAATGAC
	rev	GTCATTAGCTTGCTCATTGCAGATGGAGACATCTTTTCG

Table 13: Primers used for quantitative real-time PCR.

Primer name	Sequence (5´→ 3´)
16S rRNA-for	TTGCTATTAGATGAGCCTATATTAG
16S rRNA-rev	GTGTGGCTGATCATCCTCT

2.3 Microbiological methods

2.3.1 General cultivation of bacterial strains

Material from glycerol stocks (see chapter 2.3.5) was streaked out on LB agar plates with the appropriate antibiotic, incubated overnight at 30 °C or 37 °C and afterwards kept at 4 °C. For bacterial growth in liquid media, a single colony from an LB agar plate was inoculated in fresh LB medium containing the appropriate antibiotic and grown at 30 °C or 37 °C under shaking (120–180 rpm) overnight. To prepare a main culture, 1 % inoculum from the overnight culture was applied unless otherwise indicated. Selective media were supplemented with 30 µg/ml chloramphenicol or with 50 µg/ml ampicillin.

2.3.2 Preparation of competent *E. coli* cells

2.3.2.1 Chemically competent *E. coli* cells

50 ml TYM medium (Table 14) was inoculated with 2 % of an *E. coli* C43, JM83 or W3110 overnight pre-culture in LB medium and incubated at 37 °C under shaking at 120 rpm until the optical density at 600 nm (OD_{600}) reached 0.6. Cells were kept cool for 10 min on ice, transferred into a pre-chilled 50 ml falcon tube and centrifuged (Heraeus Multifuge, HighConic Rotor, 2,500 rpm, 10 min, 4 °C). The cell pellet was resuspended in 5 ml cold TFB I buffer and centrifuged again. The pellet was resuspended in 2 ml cold TFB II buffer and cells were aliquoted in a final volume of 50 µl, shock frozen in liquid nitrogen and stored at -80 °C.

Table 14: Medium and buffers for the preparation of chemically competent cells.

TYM medium	**TFB I**	**TFB II**
10 g Tryptone	30 mM KAc, pH 5.8	100 mM MOPS, pH 7
2.5 g Yeast extract	50 mM $MnCl_2$	7.5 mM $CaCl_2$
100 M NaCl	100 mM KCl	10 mM KCl
10 mM $MgSO_4$	10 mM $CaCl_2$	15 % Glycerol
	15 % Glycerol	
ad 500 ml Aqua dest.	ad 250 ml Aqua dest.	ad 250 ml Aqua dest.

2.3.2.2 Electro-competent *E. coli* cells

500 ml LB medium was inoculated with 1 % of an overnight *E. coli* MCI23 pre-culture and incubated at 30 °C and 120 rpm until $OD_{600} = 0.5$. Cells were chilled for 15 min on ice and afterwards harvested by centrifugation (Sorvall Evolution, Rotor SLC 4000, 6,000 rpm, 4 °C, 15 min). The pellet was resuspended in 150 ml ice-cold sterile distilled water. After a second centrifugation step, the pellet was resuspended in 10 ml ice-cold water with 10 % sterile glycerol (v/v) and transferred into a cold 50 ml falcon tube. The pellet was again harvested by centrifugation and finally resuspended in 800 µl ice-cold distilled water with 10 % sterile glycerol (v/v). Aliquots of 50 µl were prepared, frozen in liquid nitrogen and stored at -80 °C.

2.3.3 Transformation of chemically competent *E. coli* cells

A 50 µl aliquot of chemically competent cells was thawed on ice and mixed with 100 ng of plasmid DNA. The mixture was incubated for 30 min on ice, subsequently heat-shocked for 30 s at 42 °C and immediately cooled on ice for 5 min. Cells were mixed with 950 µl of SOC medium and incubated at 37 °C and 120 rpm for 2 h. Afterwards, cells were spread on LB plates containing the desired antibiotic and incubated overnight at 37 °C.

2.3.4 Transformation of electro-competent *E. coli* cells

Transformation of plasmid DNA into *E. coli* MCI23 using electroporation instead of a heat-shock was necessary due to high temperature-sensitivity of the strain. Electro-competent cells were thawed on ice, mixed with 100 ng of plasmid DNA and incubated for 1 min on ice. The suspension was transferred into a pre-cooled 2 mm electroporation cuvette and placed into an electroporation apparatus (MicroPulser^{TM}, Bio-Rad). Cells were pulsed for 5 ms, immediately mixed with 950 µl of pre-warmed SOC medium and incubated for 2 h at 30 °C under shaking at 120 rpm. Cells were spread on fresh LB plates containing the desired antibiotic and incubated at 30 °C overnight.

2.3.5 Preparation of glycerol stocks

For long term storage of bacterial strains and clones, 5 ml LB medium containing the appropriate antibiotic was inoculated with a single colony and grown overnight under shaking. The next day, 800 µl of the suspension was mixed with 200 µl of sterile glycerol and subsequently stored in cryovials at -80 °C.

2.3.6 *In vivo* activity assays

2.3.6.1 *In vivo* complementation assay of *E. coli* MCI23 with AmiD$^{w\text{Mel}}$, PBP2$^{w\text{Bm}}$, PBP3$^{w\text{Mel}}$ and PBP6a$^{w\text{Bm}}$

One colony of *E. coli* MCI23 containing a pASK-IBA vector with *amiD*^{wMel}, *pbp2*^{wBm}, *pbp3*^{wMel} or *pbp6a*^{wBm} was inoculated in 5 ml LB medium with the desired antibiotic and grown at 30 °C and 120 rpm overnight. The next day, 2 % of the culture was transferred into fresh LB medium supplemented with antibiotic and grown at 30 °C and 120 rpm until $OD_{600} = 0.4$. 100 ng/ml tetracycline dissolved in ethanol was added inducing expression of the pASK-IBA vector and the culture was split into two conical flasks. One culture was further incubated at 30 °C, the other one transferred to 42 °C where *E. coli* MCI23 cannot divide anymore as the activity of its essential cell division protein PBP3 is repressed at that temperature (Begg et al., 1990; Dai et al., 1993). *E. coli* MCI23 expressing the empty vector or *pal*^{wBm} served as controls. 120 min after induction, 1 µl of the culture was applied to a 1 % agarose slide and complementation was monitored by microscopy. Five randomly chosen pictures were taken from each sample and cell size was measured using ImageJ (Version 2.0.0-rc-43/1.50e, https://imagej.nih.gov/ij/). Cells were categorized in single/dividing cells (< 7 µm^2) and elongated cells (≥ 7 µm^2).

2.3.6.2 *In vivo* complementation assay of *E. coli* ADE24 ΔamiABC with AmiD^{wMel}

To investigate whether AmiD^{wMel} is involved in cell separation, complementation assays were carried out using the *E. coli* ADE24 ΔamiABC- triple knockout mutant (kindly provided by AG Vollmer, Newcastle, UK, Table 9). This mutant harbors an arabinose-inducible pBAD33 plasmid with *amiC* from *E. coli* (Klöckner et al., 2014). By adding 0.8 % glucose, the expression of AmiC is repressed and the *E. coli* cells cannot separate any longer resulting in long chains (Guzman et al., 1995). 10 ml LB with the appropriate antibiotic were inoculated with a 2 % overnight culture of *E. coli* ADE24 ΔamiABC harboring *amiD^{wMel}* in pASK-IBA2, pASK-IBA2C or pASK-IBA3. 100 ng/ml tetracycline were added to induce AmiD^{wMel} expression and cells were grown at 30 °C to the exponential phase (OD_{600} = 0.5). 1 µl of the culture was applied on 1 % agarose slides and visualized under a microscope (ZeissAxio VertA.1, Carl Zeiss AG). *E. coli* ADE24 ΔamiABC expressing the empty vector served as a control.

2.3.6.3 Growth kinetics

E. coli cultures harboring pASK-IBA expression vectors were grown in LB medium supplemented with the desired antibiotic at 25 °C and 120 rpm. Protein expression was induced with 200 ng/ml AHT at OD_{600} = 0.6 and the optical density was measured hourly after induction. Growth was recorded to control the viability of the production strain after the induction of protein expression.

2.3.6.4 *In vivo* complementation assay with PBP2^{wBm} and PBP3^{wMel} in the presence of antibiotics

Inhibition of PBP2 by the β-lactam mecillinam leads to spherical cells instead of rods in *E. coli* (Spratt and Pardee, 1975). Aztreonam is a β-lactam with high affinity for PBP3 leading to arrested cell division and a filamentous phenotype (Georgopapadakou et al., 1982). To investigate if these antibiotics affect PBP2^{wBm} and PBP3^{wMel}, *E. coli* MCI23 were prepared as described (see chapter 2.3.6.1) and 30 min after induction, the appropriate antibiotic was added (PBP2^{wBm}: 16 µg/ml mecillinam; PBP3^{wMel}: 8 µg/ml aztreonam). The cultures were further incubated at 30 °C (PBP3^{wMel}) or 42 °C (PBP2^{wBm}) for 120 min and subsequently visualized via microscopy. Uninduced *E. coli* MCI23 as well as cultures with the induced empty vector supplemented with aztreonam or mecillinam served as controls.

2.3.7 Preparation of Remazol Brilliant Blue (RBB)-peptidoglycan sacculi

To analyze if AmiD^{wMel} is capable of cleaving polymeric peptidoglycan, Remazol Brilliant Blue (RBB)-dyed peptidoglycan was used as a substrate. During the reaction, which

takes place in an alkaline environment at elevated temperature, the vinylsulphone function of the dye reacts with free hydroxyl groups of peptidoglycan (Broadbent, 2001). When used in enzyme assays, the subsequent cleavage of N-acetyl-anhydromuramoyl-L-alanine bonds within RBB-peptidoglycan by an amidase releases stained fragments of different lengths, which are visible with the naked eye and can be quantified at 595 nm (Figure 9).

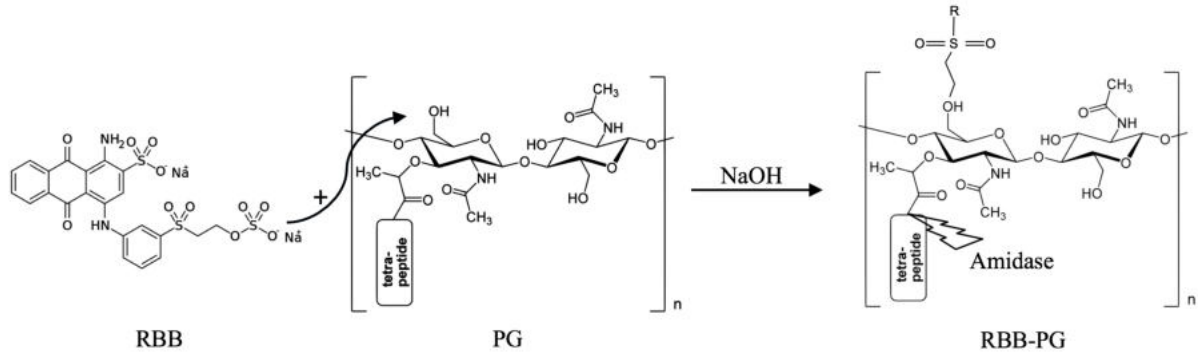

Figure 9: Reaction of Remazol Brilliant Blue (RBB) with peptidoglycan (PG) building an RBB-PG complex. This complex can be cleaved by enzymes, e.g. N-acetyl-anhydromuramoyl-L-alanine amidases releasing stained fragments of different lengths, which can be quantified at 595 nm.

An *E. coli* W3110 overnight pre-culture was inoculated 1 % in 2 l LB medium and incubated at 37 °C and 130 rpm until $OD_{600} = 0.6$. The culture was harvested (Sorvall Evolution, Rotor SLC 4000, 6,000 rpm, 4 °C, 12 min) and the pellet was resuspended in 20 ml phosphate buffered saline (PBS) (4 mM KH_2PO_4, 16 mM Na_2HPO_4, 115 mM NaCl, pH 7.4). The mixture was transferred to an 80 ml boiling 5 % sodium dodecyl sulfate (SDS)-solution and incubated for 30 min under stirring. Afterwards, the mixture was further incubated overnight at room temperature (RT) under stirring to completely lyse bacterial cells. To separate peptidoglycan sacculi from other cell components and to remove SDS, the mixture was centrifuged (Sorvall Discovery, Rotor S80-AT3, 12,600 rpm, 20 min, RT) and washed three times with 1 ml distilled water. The sacculi were further incubated with 300 µg/ml α-chymotrypsin overnight at 37 °C. Then, 250 µl of a 5 % SDS-solution was added and the mixture was incubated for 2 h at 95 °C. Sacculi were centrifuged (Sorvall Discovery, Rotor S80-AT3, 21,000 rpm, 20 min, RT) and washed three times with 2 ml distilled water. The sacculi were incubated with 200 µg/ml α-amylase for 2 h at 37 °C, centrifuged (Sorvall Discovery, Rotor S80-AT3, 21,000 rpm, 20 min, RT) and washed two times with 1 ml distilled water. *E. coli* W3110 sacculi were stained with 20 mM RBB and 250 mM NaOH in PBS buffer at 37 °C overnight. To adjust the RBB-peptidoglycan to pH 7, 1 M HCl was added. The dyed sacculi were centrifuged (Sorvall Discovery, Rotor S80-AT3, 21,000 rpm, 20 min, RT) and washed several times with distilled water until the supernatant was completely colorless. Then, the pellet was resuspended in 1 ml

distilled water and 50 µl aliquots were prepared. After shock freezing in liquid nitrogen, the RBB-peptidoglycan aliquots were lyophilized overnight and stored at -20 °C.

2.4 Molecular Biological Methods

2.4.1 Isolation of genomic and plasmid DNA

Genomic DNA (gDNA) from *w*Bm (NCBI RefSeq NC_006833.1) was kindly provided by Dr. Kenneth Pfarr (IMMIP). gDNA from *w*Mel (NCBI RefSeq NC_002978) was kindly provided by Dr. Benjamin Makepeace, Liverpool School of Tropical Medicine, UK and by Dr. Benjamin Loppin, Université de Lyon, France. gDNA from the C6/36 insect cell culture infected with *W. pipientis* strain *A. albopictus* B (*w*AlbB) (NCBI RefSeq NZ_CAGB00000000.1, Table 9) was extracted using the QIAamp DNA Mini Kit (Qiagen) following the manufacturer's instructions for DNA purification from blood or body fluids with an adjusted elution volume of 50 µl. Plasmid DNA was purified using the QIAprep® Miniprep-Kit (Qiagen) according to the manufacturer's instructions with an adjusted elution volume of 30 µl. Genomic and plasmid DNA of multiple samples was extracted using a QIAcube robotic workstation (Qiagen).

2.4.2 Polymerase chain reaction (PCR)

The polymerase chain reaction (PCR) is a broadly-used standard technique to produce high amounts of any desired DNA sequence *in vitro* (Mullis et al., 1986). The reaction needs a DNA template, a thermo-stabile DNA polymerase (e.g. *Taq* or *Pfu*), two primers binding on the opposite strands on the regions outside the target DNA sequence, magnesium chloride, and deoxynucleotides (dNTPs). The reaction includes several cycles and each cycle consists of three steps. First step is the denaturation of the double stranded DNA by increasing the temperature up to 98 °C. Second, the temperature is decreased enabling the primers to anneal to the DNA template. Last step is extension, where temperature is increased to 72 °C, which is the optimal temperature for the polymerase to synthesize the new filament of DNA. Here, PCR was used to amplify *w*Bm or *w*Mel genes for further cloning into an expression vector, the corresponding primers with annealing temperatures are listed in Table 11. The standard reaction mixture and PCR cycling parameters are shown in Table 15.

Table 15: PCR reaction mixture and cycling parameters.

1x PCR reaction mixture		**PCR cycling parameters**		
Component	Volume [µl]	Cycles	Temperature	Time
5x Reaction buffer (including $MgCl_2$)	10	1 cycle	98 °C	5 min
dNTP-mix (10 mM)	1		98 °C	10 s
Primer forward (10 µM)	2.5	30 cycles	Table 11	30 s
Primer reverse (10 µM)	2.5		72 °C	30 s/kb
gDNA (100 ng)	X			
Phusion® HF (2 U/µl)	0.5	1 cycle	72 °C	10 min
Ultrapure water	ad 50		8 °C	∞

2.4.3 Agarose gel electrophoresis

Agarose gel electrophoresis is a method to separate nucleic acid fragments by their length. In an agarose gel, the negatively charged DNA fragments migrate along an applied electrical field from the cathode to the anode and the speed of migration depends on the fragment's size (Sambrook et al., 1989). The gels used in this study contained 1 % agarose and Midori Green advanced, which allows visualization of DNA bands under UV light. Agarose gels were placed into a running chamber containing 0.5x TBE buffer (Table 16). DNA samples were mixed with Tri-Track loading dye and applied to the gel. Agarose gels were run at 120 V for 45 min and subsequently visualized using an automated gel imaging instrument (Gel Doc™ EZ Imager, Bio-Rad). The length of the analyzed DNA fragments was determined with a 1kb DNA ladder.

Table 16: 0.5x TBE buffer used for agarose gel electrophoresis.

Component	**Concentration**
Tris base	4.45 mM
Boric acid	44.5 mM
$Na_2EDTA \cdot 2H_2O$	1.25 mM
Aqua dest.	ad 1 liter

2.4.4 Quantitative real-time PCR

Quantitative real-time PCR (qPCR) is an established method to amplify specific parts of DNA and to quantify the products at the same time using a fluorescent dye or a fluorescent reporter. The principle of DNA amplification is identical to a standard PCR reaction (see chapter 2.4.2), but with an additional fluorophore in the reaction mixture. Here, SYBR Green was used which intercalates in double-stranded DNA emitting fluorescent light that is detectable in the appropriate channel of a thermal cycler (Rotorgene 6000, Corbett Life Sciences). *w*AlbB cell numbers were calculated by the quantification of 16S rRNA gene copies by qPCR as previously described (Makepeace et al., 2006) using the HotStar Taq Polymerase

Kit (Qiagen). A qPCR reaction contained 1 x HotStar Taq polymerase buffer, 3 mM $MgCl_2$, 200 µM dNTPs, 0.2 µl SYBR Green 1:1000 dilution in dimethyl sulfoxide (DMSO), 0.5 µM 16S rRNA gene specific forward and reverse primers (see Table 13), 0.5 U HotStar Taq polymerase and 2 µl of extracted gDNA. Standard qPCR cycling conditions are shown in Table 17. Melt curve analysis confirmed a specific peak for all positive samples. Data were analyzed using Rotorgene 6000 software version 1.7.

Table 17: qPCR cycling parameters.

Cycles	Temperature	Time
1	95 °C	15 min
45	95 °C	10 s
	55 °C	15 s
	72 °C	20 s
1	72 °C	10 min

2.4.5 Cloning

AmiD$^{w\text{Mel}}$, PBP2$^{w\text{Bm}}$, PBP3$^{w\text{Mel}}$ and PBP6a$^{w\text{Bm}}$ were amplified from gDNA of *w*Bm or *w*Mel, with specific primers (see Table 11). Primers were designed following the manufacturer's instructions using the software "Primer D'Signer" (IBA Lifesciences). During the PCR, BsaI or NcoI restriction sites were added at the 5' and 3'-ends of the respective products. The amplified products were controlled for correct size and purity by agarose gel electrophoresis, purified and cloned into pASK-IBA expression vectors (see Table 10). Correct cloning of the inserts into the vectors was confirmed by sequencing (Microsynth Seqlab, Göttingen, Germany). Wolbachial PBPs were only cloned into vectors which encode a chloramphenicol resistance cassette as ampicillin is a β-lactam and might interfere with the PBPs when added to the LB medium during expression.

2.4.5.1 Purification of DNA fragments

To remove compounds from the reaction mixtures and other contaminants, DNA fragments were purified after PCR (see chapter 2.4.2), after restriction digest (see chapter 2.4.5.2) and after dephosphorylation (see chapter 2.4.5.3) with a Nucleospin Gel and PCR Clean-up Kit following the manufacturer's instructions (Macherey Nagel).

2.4.5.2 Restriction digest

Restriction enzymes are endonucleases which recognize specific sites in DNA and degrade it by the hydrolysis of the phosphate backbone producing double-stranded fragments with either blunt or sticky ends with terminally unpaired bases (Pham et al., 1998). The

restriction enzymes BsaI and NcoI used in this work produce sticky-ends which facilitates the correct insertion of the DNA fragments into the vector during the ligation process. The reaction scheme is summarized in Table 18. The vector and the PCR product were digested by incubating the mixture for 60 min at 37 °C and subsequently incubating for 20 min at 65 °C (BsaI) or 80 °C (NcoI) to heat-inactivate the restriction enzyme. After restriction digest, the gene of interest was purified (see chapter 2.4.5.1), while the vector was dephosphorylated (see chapter 2.4.5.3).

Table 18: Restriction digest mixture.

Components	**Volume [µl]**
1 µg purified PCR product/vector DNA	X
10x CutSmart buffer	5
Restriction enzyme	1
Aqua dest.	ad 50

2.4.5.3 Dephosphorylation

To avoid re-ligation of the restricted and linearized vector, the phosphate of the 5' ends can be removed by a phosphatase. Here, 5 µl of 10x Phosphatase reaction buffer and 1 µl of Antarctic Phosphatase were applied to the 50 µl restriction mixture of the vector and incubated for 1 h at 37 °C. Subsequently, the dephosphorylated vector was purified (see chapter 2.4.5.1).

2.4.5.4 Ligation

The ligation step inserts the gene of interest into the vector building a construct that can be transformed into *E. coli* cells (see chapter 2.3.3 and 2.3.4). A ligase catalyzes the formation of the phosphodiester bond between the 3' hydroxyl group of the sugar and the 5' phosphate group of two adjacent DNA strands (Sambrook et al., 1989). The T4 ligase used in this work catalyzes the reaction of both blunt-ended and sticky-ended DNA fragments (Rusche and Howard-Flanders, 1985). The molar ratio of insert:plasmid was 3:1, the standard reaction is shown in Table 19. The ligation mixture was either incubated for 15 min at RT or overnight at 16 °C and subsequently heat inactivated at 70 °C for 5 min.

Table 19: Scheme of the ligation reaction mixture.

Components	**Volume [µl]**
Insert	X
50 ng Vector	X
10x T4 ligase Buffer	2
T4 DNA ligase	1
Aqua dest.	ad 50

2.4.5.5 Suicide cut

Restriction with BsaI or NcoI removes the multiple cloning site from the pASK-IBA vector and during ligation, the desired gene is inserted. To further decrease the level of false positive clones caused by undigested re-ligated empty vectors, they were cut with a suitable restriction enzyme after ligation. BamHI was selected as a suitable restriction enzyme for AmiD$^{w\text{Mel}}$, which targets a recognition site in the multiple cloning site of pASK-IBA vectors, but not in the sequence of AmiD$^{w\text{Mel}}$. For PBP2$^{w\text{Bm}}$ and PBP6a$^{w\text{Bm}}$, EcoRI was used. The ligation mixture was supplemented with 5.6 µl CutSmart buffer and 1 µl BamHI/EcoRI and incubated for 1 h at 37 °C. EcoRI was inactivated at 65 °C for 20 min (not required for BamHI) and 5 µl of the mixture were used for transformation in chemically competent *E. coli* cells (see chapter 2.3.3).

2.4.6 Site-directed mutagenesis

Putative active site motifs in the gene sequences of wolbachial AmiD and PBPs were changed using the QuikChange Lightning Site-Directed Mutagenesis Kit (Agilent Technologies). This technique is used to specifically introduce point mutations into a gene of interest. Two complementary primers harboring the mutation bind to the plasmid and are amplified in a PCR with a PfuUltra high-fidelity DNA polymerase leading to the formation of a mutated and non-methylated version of the vector. DpnI digestion of the amplification products cuts the original plasmid in contrast to the newly synthesized mutated one due to missing methylation (Figure 10). In this thesis, primers were designed using the software "PrimerX automated design of mutagenic primers for site-directed mutagenesis" (http://www.bioinformatics.org/primerx/) according to the manufacturer's guidelines for primer design. The site-directed mutagenesis was performed following the manufacturer's instructions (Tables 20 and 21) with one modification. Instead of using the provided chloramphenicol resistant *E. coli* XLGold cells, 5 µl of the mixture was transformed into *E. coli* TOP10 cells since the used pASK-IBA vectors harbor a chloramphenicol selection marker. After transformation, correct base changes were confirmed by sequencing (see Table 11).

Table 20: Reaction mixture of site-directed mutagenesis.

Components	Volume [µl]
10x Reaction buffer	5
100 ng dsDNA template	X
125 ng oligonucleotide primer forward	X
125 ng of oligonucleotide primer reverse	X
dNTP mix	1
QuikSolution reagent	1.5
Aqua dest.	ad 50
QuikChange Lightning Enzyme	1

Table 21: Cycling parameters for site-directed mutagenesis.

Cycles	Temperature	Time
1	95 °C	2 min
18	95 °C	20 s
	60 °C	10 s
	68 °C	30 s/kb of plasmid length
1	68 °C	5 min

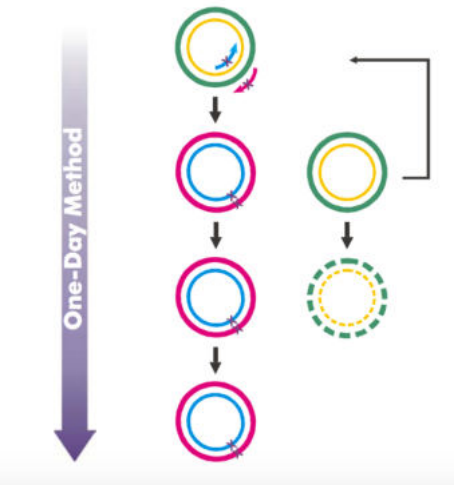

Figure 10: Principle of QuikChange Site-Directed mutagenesis (Agilent technologies). Primers harboring the mutation bind to the plasmid and are amplified in a PCR leading to the formation of a mutated and non-methylated version of the vector (purple-blue). DpnI only cuts the methylated non-mutated plasmid (green-yellow).

2.5 Biotechnological methods

2.5.1 Overproduction using Strep-tagged proteins

2.5.1.1 Overproduction pre-tests

By carrying out pre-tests, the optimal conditions for protein overexpression were determined for each protein used in this study. Overproduction was tested in different *E. coli* strains (C43, JM83 and W3110), different temperatures (25 °C and 30 °C), time points of induction (OD_{600} = 0.5 and OD_{600} = 1.2) and length of expression (4 h and overnight). Overproduction pre-tests were performed in 50 ml LB medium containing chloramphenicol. Medium was inoculated with 1 % of an *E. coli* overnight culture containing a pASK-IBA vector with the gene of interest. 1 ml samples were collected before induction of protein expression with 200 ng/ml AHT and after 4 h or overnight expression. The samples were lysed (see chapter 2.5.1.3) and analyzed via SDS-PAGE and Western Blot (see chapter 2.6). Cells containing the induced empty vector served as a control.

2.5.1.2 Small-scale co-solvent screen

The substitution of NaCl in LB medium with co-solvents has been shown to improve production, folding and stability of proteins expressed in the periplasm (Otten et al., 2015). Therefore, it was tested if co-solvent assisted overproduction also had positive effects on the

proteins investigated in this thesis. To prevent osmotic stress, the amount of co-solvent was adjusted to an osmotic pressure elicited by 10 g/l NaCl. 171 mM NaCl which are equivalent to 342 osm/l of dissociated Na^+ and Cl^- ions were replaced by 342 mM of non dissociating co-solvents (equivalent to 342 osm/l) (Otten et al., 2015). All co-solvents had a final concentration of 342 mM, except for arginine, which was observed to be toxic for bacteria in high concentrations. Thus, arginine was used in a final concentration of 100 mM. After addition of co-solvents to the NaCl-free LB medium, the pH was adjusted to 7.5 and the medium was sterile filtered. After optimal expression conditions were determined (see chapter 2.5.1.1), 50 ml NaCl-free LB medium was supplemented with different co-solvents (Table 22), inoculated with 1 % from an overnight *E. coli* culture, grown until $OD_{600} = 0.5$ and then induced with 200 ng/ml AHT. The harvested pellets were lysed and analyzed by SDS-PAGE and Western Blot (see chapter 2.5.1.3 and 2.6).

Table 22: Used co-solvents for the substitution of NaCl.

Co-solvent	Molecular mass [g/mol]	Amount [g/l]	Molarity [mM]
L-Arginine	174.20	17.42	100
Betaine	117.15	40.09	342
Glycerol	92.09	31.52	342
D-Mannitol	182.17	62.34	342
Sucrose	342.30	117.15	342
D-Trehalose	342.30	117.15	342

2.5.1.3 Protein overproduction and purification

NaCl-free LB medium containing the appropriate antibiotic and co-solvent was inoculated with 1 % from an overnight culture and grown under the optimal induction conditions as determined previously (see chapter 2.5.1.1 and 2.5.1.2).

Purification of Strep-tagged proteins was performed according to the manufacturer´s instructions (IBA Lifesciences) with slight adjustments. Cell pellets were resuspended in 10 ml Buffer P per liter *E. coli* culture, supplemented with 1 mg/ml lysozyme (Table 23) and lysed for 30 min at 4 °C under gentle rotation. For $PBP2^{wBm}$ with its native transmembrane domain, 2 % Tween 200 was added to the lysis Buffer P as a detergent to increase solubility. To reduce viscosity, benzonase (20 U/ml) and $MgCl_2$ (3 mM) were added and the suspension was incubated for additional 15 min on ice. Cleared lysate containing soluble proteins was prepared by centrifugation (38,800 g, 15 min, 4 °C) and Strep-tagged proteins were purified by gravity flow chromatography at 4 °C. For this, 1 ml Strep-Tactin® Sepharose was applied to a 1 ml polypropylene column and equilibrated with 2 ml Buffer W (Table 23). The cleared lysate was loaded onto the column and washed five times with 1 ml Buffer W. Finally, the proteins were

eluted eight times with 0.5 ml Buffer E (Table 23). As AmiD^{wMel} is a putative metalloprotein, adjusted buffers were used following the manufacturer's recommendations. Briefly, ethylenediaminetetraacetic acid (EDTA) in Buffer P was substituted by 2 mg/ml polymyxin B, while Buffer W and Buffer E were prepared without EDTA. To test if amidase activity of AmiD^{wMel} is deacreased in the presence of EDTA, some batches of overexpressed protein were prepared with EDTA. Purified proteins were kept at 4 °C for up to five days and, in case of AmiD^{wMel}, for long-time storage in 50 % sterile glycerol at -20 °C.

Table 23: Buffers used for cell lysis and purification of Strep-tagged proteins.

Buffer P	**Buffer W**	**Buffer E**
100 mM TrisHCl, pH 8	100 mM TrisHCl, pH 8	100 mM TrisHCl, pH 8
500 mM Sucrose	150 mM NaCl	150 mM NaCl
1 mM EDTA	1 mM EDTA	1 mM EDTA
1 mg/ml Lysozyme		2.5 mM D-Desthiobiotin

2.6 Electrophoretic methods

2.6.1 Sodium dodecyl sulfate polyacrylamide gel electrophoresis

Sodium dodecyl sulfate polyacrylamide gel electrophoresis (SDS-PAGE) separates proteins equivalent to their molecular weight, based on their differential rates of migration through a sieving matrix under the influence of an applied electrical field (Laemmli and Favre, 1970). Proteins are denaturated by the addition of a loading buffer containing β-mercaptoethanol as a reducing agent and by heating. The internal charge, which is a consequence of the different properties of the contained amino acids, is overlaid by the association of negatively charged SDS. The intensity of this constant negative charge is proportional to the length of the peptide chain and therefore indirectly to molecular weight of the polypeptides (Laemmli and Favre, 1970). Polyacrylamide polymerization results in a matrix in which the denaturated protein samples can be separated driven by an electric field. Protein samples are concentrated first in an upper stacking gel with large pores in the matrix due to a lower concentration of acrylamid. In the lower separation gel protein samples are fragmented by their molecular weight. In this thesis, Mini-PROTEAN® Stain-free™ 12 % Precast Gels (Bio-Rad) were used. Alternatively, self-made gels were prepared. A 4 % stacking gel contained 3 ml distilled water, 1.25 ml upper buffer (0.5 M Tris-HCl, 0.4 % SDS, pH 6.8) and 750 µl acrylamide/bisacrylamide. Polymerization was initiated by adding 15 µl 10 % ammonium persulphate (APS) and 10 µl Tetramethylethylenediamine (TEMED). TEMED induces free radical formation from APS which transfers electrons to the acrylamide/bisacrylamide

monomers causing a vinyl addition and resulting in a polyacrylamide chain. For a 12.5 % separation gel, 4 ml of lower buffer (1.5 M Tris-HCl, 0.4 % SDS, pH 8.8) were mixed with 5.3 ml distilled water and 6.7 ml acrylamide/bisacrylamide, 80 µl of 10 % APS and 8 µl TEMED. 5 µl of 5x SDS sample buffer was added to 20 µl of the sample (Table 24). Samples were mixed, heated 10 min at 70 °C and subsequently applied to the SDS gel. The SDS gel was run at 160 V for 45 min in buffer (25 mM Tris-HCl, 192 mM glycine, 0.1% SDS, pH 8.3).

Table 24: 5x SDS sample buffer.

Component	Concentration
Tris-HCl, pH 6.8	25 mM
Glycerol	25 %
SDS	7.5 %
Bromophenol blue	0.04 %
β-Mercaptoethanol	12.5 %

2.6.2 Western Blot

Western Blot is a technique to transfer proteins from a polyacrylamid gel to a membrane to specifically visualize tagged proteins (Renart et al., 1979). Western Blots can be detected with chemiluminescent, colorimetric or fluorescent methods. Here, Strep-tagged proteins were visualized using a colorimetric method. After separating proteins by SDS-gelelectrophoresis (see chapter 2.6.1), they were transferred to a nitrocellulose membrane. The nitrocellulose membrane and blotting paper were pre-wetted in Towbin running buffer (25 mM Tris Base, 192 mM glycine, 20 % methanol, pH 8.3). For blotting, the Trans-Blot® TurboTM Transfer System (Bio-Rad) was used for 80 min at 15 V. Chromogenic detection of Strep-tagged proteins with Strep-Tactin Alkaline Phosphatase (AP) conjugate was performed following the manufacturer's instructions (IBA Lifesciences, Figure 11). Briefly, the membrane was incubated in 20 ml PBS blocking buffer (4 mM KH_2PO_4, 16 mM Na_2HPO_4, 115 mM NaCl, pH 7.4, with 3 % bovine serum albumin (w/v, BSA) and 0.5 % Tween 20 (v/v)) for 1 h at RT under gentle shaking. PBS-blocking buffer was removed by washing three times with 20 ml PBS-Tween buffer (PBS buffer with 0.1 % Tween 20 (v/v)) for 5 min at RT and gentle shaking. After the last washing step, 10 ml PBS-Tween buffer plus 10 µl of Biotin blocking buffer were added to the membrane to block

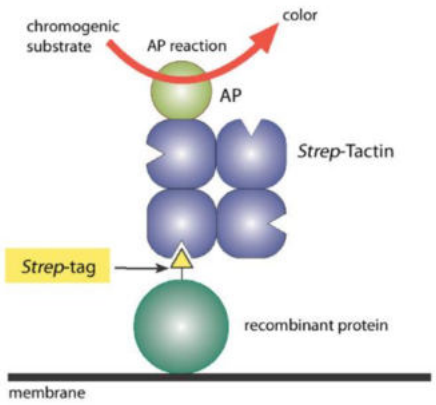

Figure 11: Detection of recombinant Strep-tagged fusion proteins (IBA Lifesciences). Immobilized proteins on a nitrocellulose membrane are linked to Strep-Tactin-Alkaline-Phosphatase (AP) conjugate and detected by colorimetric detection after the addition of chromogenic substrates.

endogenously biotinylated proteins of the expression strain. 5 µl Strep-Tactin alkaline phosphatase conjugate (1:2000) was added and incubated for 1 h and subsequently washed two times with PBS-Tween buffer for 1 min. After washing, the membrane was transferred to 20 ml reaction buffer (100 mM NaCl, 5 mM $MgCl_2$, 100 mM Tris-HCl, pH 8.8). Specific staining of Strep-Tactin motifs of recombinant proteins was visualized by addition of 10 µl 7.5 % nitro blue tetrazolium (w/v, NBT) solution and 60 µl of 5 % 5-bromo-4-chloro-3-indolyl-phosphate (w/v, BCIP) solution. The reaction was stopped with tap water.

2.7 Biochemical methods

2.7.1 Protein determination via Bradford assay

The Bradford assay is a quantitative method to determine the protein concentration in a solution (Bradford, 1976). Coomassie Brilliant Blue G-250 dye builds complexes with cationic and unpolar side chains of polypeptides in an acidic environment shifting the absorption maximum of the dye from 465 to 595 nm. Using a BSA standard curve with known concentrations allows determination of the relative protein concentration of the samples. Quantification is based on the positive correlation of the absorption rate of the dye and the amount of protein in the samples. In this thesis, a standard curve with defined concentrations of BSA between 7.5 µg/ml up to 2 mg/ml was used. 3 µl of protein samples were applied in triplicates to a 96-well plate and 300 µl of 1x Bradford reagent was added to each sample. The plate was subsequently measured in a photometric plate-reader at 595 nm (Spectramax® 340PC, Molecular Devices) and analyzed with Softmax® Pro Version 6.3.

2.7.2 *In vitro* DD-carboxy- and DD-transpeptidase activity assays using lipid II as a substrate

Lipid II is the precursor of peptidoglycan and the natural substrate of PBPs. To perform *in vitro* assays, lipid II containing either m-DAP or Lys was synthesized (see chapter 2.9) and used to study wolbachial protein activity.

Standard *in vitro* activity assays for wolbachial PBPs were carried out in a final volume of 70 µl containing 0.5 nmol purified protein, 2 nmol lipid II, 50 mM MES (pH 5.5), 2 mM $MgCl_2$ and 20 % DMSO. The reaction mixture was incubated for 4 h or overnight at 30 °C. To test the impact of β-lactam antibiotics on PBP activity, penicillin G or ampicillin were added to the reaction mixture in a molar ratio of 1:10. Reaction products were extracted with 70 µl of n-butanol/pyridine acetate (2:1, v/v, pH 4.2). For the extraction solution, 6 M glacial acetic acid

was adjusted to pH 4.2 by the addition of pyridine and mixed with two volumes of n-butanol according to Anderson (1967). The mixture was vortexed for 1 min and centrifuged (21,000 g, 5 min, RT). The upper phase containing lipids was analyzed via TLC and MALDI-TOF (see chapter 2.7.5 and 2.8.1) as described previously (Klöckner et al., 2014). For DD-transpeptidase activity assays, TLC bands were quantified by Image Quant^{TM} TL (GE Healthcare).

Standard *in vitro* activity assay mixtures for AmiD^{wMel} contained 4 µg purified protein, 2 nmol lipid II, 50 mM Tris (pH 7.5) and 5 % DMSO in a volume of 40 µl and were incubated for 4 h at 30 °C. Reaction products were extracted with 40 µl of n-butanol/pyridine acetate (2:1, v/v, pH 4.2), centrifuged (21,000 g, 5 min, RT) and analyzed by TLC and MALDI-TOF (see chapter 2.7.5 and 2.8.1). To inhibit amidase activity of AmiD^{wMel}, the protein was lysed and purified in the presence of 1 mM of the non-specific metal chelator EDTA (see chapter 2.5.1.3). As a second approach, 5 mM of the zinc-specific inhibitor 1,10-phenanthroline was added to the reaction mixtures of the activity tests.

2.7.3 *In vitro* activity of AmiD^{wMel} using peptidoglycan as a substrate

For the RBB-PG dye-release assay, 20 µl of stained peptidoglycan sacculi (see chapter 2.3.7) were incubated at 30 °C overnight with 4 µM of purified AmiD^{wMel} in a final volume of 200 µl containing 50 mM Tris (pH 7.5) and 5 % DMSO. Samples were centrifuged (20,000 g, 20 min, RT) and absorbance of the supernatants was measured at 595 nm in a nanophotometer (TM 7122v1.6.1, Implen).

2.7.4 Cleavage of anhydromuropeptides by AmiD^{wMel}

The cleavage of anhydromuropeptides was performed by the research group of Prof. Vollmer, University of Newcastle, United Kingdom. Briefly, *E. coli* sacculi were prepared as described previously (Glauner et al., 1988). Peptidoglycan (750 µg) was digested with the lytic transglycosylase Slt (1 µM) in a final volume of 210 µl containing 10 mM HEPES (pH 7.5) and 150 mM NaCl for 18 h at 37 °C. The reaction mixture was heated for 10 min at 100 °C and centrifuged for 20 min. The supernatant containing the 1,6-anhydro-muropeptides was collected and stored at 2–8 °C. 1,6-anhydro-muropeptides (15 µl) were incubated with AmiD^{wMel} (2 µM) in a final volume of 50 µl containing 50 mM Tris (pH 7.5) and 5 % DMSO for 4 h at 30 °C. Samples were boiled for 10 min and centrifuged for 20 min, and the supernatant was recovered. The pH of the supernatant was adjusted to pH 4 with 20 % phosphoric acid. HPLC analysis was carried out as described previously (Glauner et al., 1988) and selected peaks were collected and analyzed by mass spectrometry (Bui et al., 2009).

2.7.5 Thin layer chromatography (TLC)

Thin layer chromatography (TLC) is a method to separate mixtures of non-volatile compounds according to their different solubility in a mobile and a stationary phase (Gordon et al., 1943). The various applications of TLC include the determination of the purity of samples, the identification of compounds and the examination of reactions. The mobile phase (a solvent) moves by capillary action along the stationary phase (silica plate) transporting the compounds. Here, the upper phase of lipid extracts was spotted onto a silica plate and dried. The TLC plate was placed in a glass chamber containing chlorophorm:methanol:water:ammonia (88:48:10:1, v/v/v/v) as the mobile phase according to Rick (1998). After separating the compounds up to 60 min, the plate was removed and dried. To visualize lipid bands, the TLC plate was dipped into a phosphomolybdic acid (PMA) staining solution (2.5 % phosphomolybdic acid (w/v), 1 % ceric IV sulfate (w/v), 6 % sulfuric acid (v/v)) and dried again. The silica plate was developed at 140 °C in an oven until stained blue bands were visible.

2.8 Instrumental methods

2.8.1 Matrix assisted laser desorption/ionization (MALDI)

Matrix assisted laser desorption/ionization (MALDI) is routinely used for the analysis of biomolecules (e.g. DNA, proteins, peptides and sugars) and large organic molecules (e.g. polymers, dendrimers and other macromolecules) (Karas et al., 1987). The target molecules are embedded in a defined matrix and ionized via a pulse laser. In this thesis, MALDI was combined with a time-of-flight detector (MALDI-TOF). For detection of reaction products from AmiD$^{w\mathrm{Mel}}$ and PBP6a$^{w\mathrm{Bm}}$ activity assays using lipid II (see chapter 2.7.2), 1 µl of the sample was placed onto a ground steel MALDI-TOF target plate and dried at RT. Each sample was then overlaid with 1 µl of matrix (saturated solution of 6-Aza-2-thiothymine in 50 % ethanol/20 mM diammonium citrate or alpha-cyano-cinnamic acid in 33 % acetonitril/0.1 % trifluoroacetic acid) and air dried at RT again. Spectra were recorded in the reflector negative mode on a Biflex III mass spectrometer (Bruker Daltonik). MALDI-TOF measurements were performed by Michaele Josten, AG Schneider, IMMIP, University of Bonn.

2.8.2 Biomolecular binding interaction studies

Surface plasmon resonance (SPR) and Biolayer interferometry (BLI) are two established techniques for label-free measurement of biomolecular binding interactions. SPR

and BLI use light to measure the interaction between two molecules in real-time. In this thesis, both techniques were used to examine interactions between wolbachial proteins and lipid II.

2.8.2.1 Surface plasmon resonance (SPR)

SPR is a method to determine specificity, affinity and kinetic parameters of the interaction between two macromolecules for example protein-protein, protein-DNA or lipid membrane-protein (Karlsson et al., 1991; Nguyen et al., 2015). This optical technique measures the refractive index changes in the vicinity of metal layers, i.e. a gold layer in a sensor chip, in response to biomolecular interactions (Figure 12). The sensor chip consists of a glass surface coated with a thin layer of gold. This is the basis for a range of specialized surfaces designed to optimize the binding of a variety of molecules. One of the interaction partners, the ligand, is coupled to the surface of a sensor chip. The analyte, the potential interaction partner of the ligand, is dissolved in running buffer and flows over the sensor surface continuously. Binding between the ligand and the analyte changes the detectable resonance signal; when molecules in a solution bind to a target molecule the mass increases, when they dissociate the mass falls. This principle forms the basis of the sensorgram, which monitors the association and dissociation of the interacting molecules in real-time. The sensorgram provides quantitative information on specificity of binding, kinetics and affinity. In this thesis, the interaction between Pal^{wBm} and lipid II with either m-DAP or Lys was investigated using a Biacore® T100 (GE Healthcare). Purified Pal^{wBm} was immobilized on a CM5 sensor chip using a Strep-tag II specific Strep-MAB-Immo monoclonal antibody (IBA Lifesciences) following the manufacturer's protocol. As CM5 sensor chips have a carboxy-methylated dextran matrix attached to a gold layer, molecules can be covalently coupled to the sensor surface via amine, thiol, aldehyde or carboxyl groups. StrepMAB-Immo antibody nearly irreversibly captures Strep-tag® II fusion proteins on solid phases. Lipid II (0–12.5 µM) dissolved in HBS-EP running buffer (Table 25) was used as the analyte of the binding reaction. Data were analyzed using the provided Biacore® T100 software.

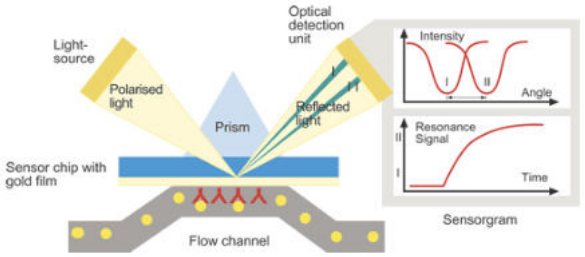

Figure 12: Principle of surface plasmon resonance (SPR) (University of Chicago, USA). SPR detects changes in the refractive index at the surface of a sensor which is comprised of a glass substrate and a thin gold coating.

Table 25: Biacore HBS-EP running buffer.

Component	Concentration
HEPES, pH 7.4	10 mM
NaCl	150 mM
EDTA	3 mM
Surfactant P20	0.005 % v/v

2.8.2.2 Biolayer interferometry (BLI)

BLI is a label-free technology for measuring biomolecular interactions (Cooper, 2006). The binding between a ligand immobilized on a biosensor surface and an analyte in solution produces an increase in optical thickness at the biosensor resulting in a wavelength shift (Figure 13). Any changes in the number of molecules bound to the biosensor can be measured in real-time, whereas unbound molecules or changes in the refractive index of the surrounding medium do not affect the interference pattern. This feature of BLI allows application of crude samples for protein-protein interaction, quantitation, affinity and kinetic measurements. In this thesis, a BLItz® system device (Pall ForteBio) was used to measure interactions between Pal^{wBm} and PBP2^{wBm}. 50 µg Pal^{wBm} was biotinylated and purified using Zeba Spin Desalting Columns (Thermo Scientific) according to the manufacturer's instructions. In a basic kinetic assay, biotinylation was confirmed. For interaction measurements, a streptavidin sensor (Pall ForteBio) was incubated with 1 µl biotinylated Pal^{wBm} (ligand) for 1 min. The sensor was measured in analysis buffer for 30 s to get a baseline before starting the interaction measurements. 1 µl PBP2^{wBm} (analyte) or the empty vector, which served as a negative control, were applied and measured for 2 min. The sensor was incubated with analysis buffer for 1 min to measure dissociation. Data were analyzed using the provided BLItz® Pro software (version 1.2.0.49).

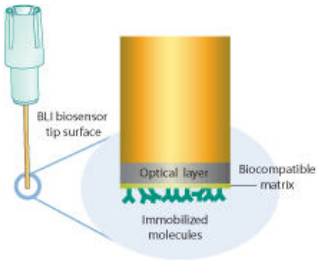

Figure 13: Principle of Biolayer interferometry (BLI) (Pall ForteBio). A biosensor with a coated matrix can immobilize molecules (ligand). An analyte in solution which binds to the ligand results in a wavelength shift of the optical layer.

2.9 Chromatographic methods

2.9.1 Lipid II Synthesis

2.9.1.1 Isolation of UDP-Mur*N*Ac-pentapeptide substrate

UDP-Mur*N*Ac-pentapeptide is a cytoplasmic, soluble precursor of peptidoglycan (see chapter 1.5.1), which can be accumulated and subsequently purified. In this thesis,

Staphylococcus simulans 22 and *Bacillus cereus* T were used to accumulate and isolate UDP-Mur*N*Ac-pentapeptide with either Lys or m-DAP at position three of the pentapeptide side chain for lipid II synthesis. 4 l Mueller-Hinton broth was inoculated with 1 % of *S. simulans* 22 or *B. cereus* T overnight cultures and incubated at 37 °C and 120 rpm until $OD_{600} = 0.75$. To inhibit protein biosynthesis, 130 µg/ml chloramphenicol was added for 15 min. Chloramphenicol prevents the *de novo* synthesis of enzymes that may interfere, e.g. through induction of cellular autolysis, with the accumulation of the UDP-linked peptidoglycan precursor in the cytoplasm (Dai and Ishiguro, 1988). Afterwards, the 10x minimal inhibitory concentration of vancomycin (*S. simulans* 22: 5 µg/ml, *B. cereus* T: 10 µg/ml) was added. Vancomycin binds to the terminal D-alanyl-D-alanine (D-Ala-D-Ala) residues of the pentapeptide and therefore blocks the regeneration of the lipid-carrier C_{55}-P, leading to an accumulation of the UDP-Mur*N*Ac-pentapeptide in the cytoplasm (Anderson et al., 1967). After 1 h of incubation, cells were harvested (Sorvall Evolution, Rotor SLC-4000, 10 min, 8,000 rpm, 4 °C) and the pellet was resuspended in 20 ml distilled water. The suspension was slowly transferred to 80 ml boiling distilled water under stirring in a 500 ml Erlenmeyer flask. After 15 min boiling, the suspension was chilled on ice and centrifuged again (Sorvall Evolution, Rotor SS-34, 18,000 rpm, 30 min, 4 °C) to remove insoluble cell parts. The supernatant containing the UDP-Mur*N*Ac-pentapeptide substrate was shock frozen with liquid nitrogen, lyophilized in a freeze dryer and stored at -20 °C. For lipid II synthesis, UDP-Mur*N*Ac-pentapeptide was resolved in 4 ml distilled water and added to the reaction mixture (see chapter 2.9.1.3).

2.9.1.2 Membrane preparation

As the enzymes MraY and MurG are necessary to build lipid II (see chapter 1.5.1), the membranes of *Micrococcus flavus* were isolated as described previously (Schneider et al., 2004). Briefly, 2 l TSB were inoculated with 1 % of an overnight culture of *M. flavus* and incubated at 37 °C and 120 rpm overnight. The next morning, cells were harvested (Sorvall Evolution, Rotor SLC 4000, 7,500 rpm, 15 min, 4 °C), the pellet was washed in 700 ml Tris-buffer (50 mM Tris-HCl, 10 mM $MgCl_2$, pH 7.5) and centrifuged again. The pellet was resuspended in the Tris-buffer containing 800 µg/ml lysozyme and 80 µg/ml benzonase and incubated on ice for 60 min. The suspension was heated up in a water bath to 35 °C and afterwards cooled again on ice. Membranes were obtained through centrifugation (Sorvall Evolution, Rotor SLC 4000, 13,000 rpm, 20 min, 4 °C). Finally, pellets were resuspended in 8 ml Tris-buffer and stored at -80 °C until further use.

2.9.1.3 *In vitro* lipid II-synthesis

To synthesize lipid II *in vitro*, the isolated membranes from *M. flavus* were incubated with UDP-Mur*N*Ac-pentapeptide from *S. simulans* or *B. cereus* T, C_{55}-P and UDP-Glc*N*Ac. For every synthesis, the optimal conditions had to be titrated in an analytical assay before preparing lipid II in a larger scale for purification. Lipid II was obtained by mixing 20–30 µl isolated membranes (see chapter 2.9.1.2), 7.5–15 µl UDP-Mur*N*Ac-pentapeptide (see chapter 2.9.1.1), 5 nmol C_{55}-P, 1 mM UDP-Glc*N*Ac, 5 mM $MgCl_2$, 60 mM Tris-HCl (pH 7.5), 0.5 % Triton X-100 (v/v) in a final volume of 75 µl. C_{55}-P (dissolved in 10 µl chloroform/methanol, 1:1, v/v) was vacuum-dried in a desiccator and subsequently re-dissolved by adding 0.5 % Triton X-100 and vortexed vigorously. The remaining components were added and the mixture was incubated for 4 h at 30 °C and under shaking. To verify that lipid II was synthesized, bactoprenol-containing products were extracted and visualized via TLC (see chapter 2.7.5). Lipid II synthesis in a larger scale was achieved by using the 200-fold volume of the optimal analytical scale. Extraction was done in two steps by first extracting the lipids in 15 ml and then in 10 ml of n-butanol/pyridine acetate (2:1, v/v, pH 4.2). The two upper phases containing soluble lipids were combined and washed with ice-cold, acidic ultrapure water (1:1, v/v, pH 4.2). The mixture was centrifuged (Heraeus Multifuge, HighConic Rotor, 10.000 rpm, 10 min, 4 °C) and the upper phase was used for HPLC purification of lipid II.

2.9.1.4 Purification of lipid II via high performance liquid chromatography (HPLC)

High performance liquid chromatography (HPLC) is a separation technique for chemical and biological compounds which is mainly used to identify, quantify or purify compounds from a mixture (Horvath and Lipsky, 1966; Jadaun et al., 2017). HPLC pumps a liquid mobile phase through a stationary phase, usually a column, which separates the sample components. During the chromatographic separation, a pump can either deliver a constant mobile phase composition (isocratic) or an increasing mobile phase composition (gradient). In this thesis, the liquid mixture containing *in vitro* synthesized lipid II was applied to a 5 ml HiTrap DEAE FF-Agarose-column with Buffer A (Table 26) and a flow rate of 3 ml/min for 1 h. Lipid II was eluted by creating a linear ammonium bicarbonate gradient flow with up to 25 % Buffer B (Table 26) and a flow rate of 5 ml/min for 3 h. Fractions of 5 ml were collected in glass tubes and the ones containing purified lipid II were identified via TLC (see chapter 2.7.5). These fractions were combined and separated from the organic solvents with a rotating evaporator (Büchi Labortechnik). The remaining solution was transferred to a teflon tube, dried in an exsiccator to remove chloroform, then frozen with liquid nitrogen and lyophilized

overnight. The dried material was resolved in 500 µl chloroform/methanol (1:1, v/v) and centrifuged (Eppendorf 5417R, Rotor FA45-24-11, 10 min, 5,000 rpm, RT) to remove salts. The supernatant was applied to a glass tube and stored at -20 °C. Lipid II concentration was determined by its phosphate content (see chapter 2.9.1.5).

Table 26: Buffers used for HPLC purification of lipid II.

Buffer	Components
Buffer A	Chloroform, methanol, ultrapure aqua dest. (2:3:1, v/v/v)
Buffer B	Chloroform, methanol, 300 mM ammonium bicarbonate (2:3:1, v/v/v)

2.9.1.5 Determination of phosphate concentration

As lipid II contains two phosphate residues, the amount synthesized *in vitro* can be quantified by determination of the phosphate concentration. In this thesis, the method according to Rouser (1970) was used. This assay is based on the principle that free inorganic phosphate (Pi) is released when phospholipids are hydrolyzed. In an acidic environment, Pi binds to molybdate resulting in yellowish phosphomolybdic acid. Ascorbic acid reduces phosphomolybdic acid to molybdenum blue which can be measured at 797 nm. To determine the phosphate concentration of the synthesized lipid II, two different volumes (5 µl and 10 µl) were applied to clean and phosphate-free glass tubes, 0–90 nmol Pi of 1 mM monopotassium phosphate (KH_2PO_4) served as a standard. The tubes were dried at 140 °C for 20 min and afterwards 300 µl of 70–72 % perchloric acid ($HClO_4$) was added to each tube. The mixture was incubated for 3 h at 180 °C to hydrolyze the lipid II or the standard and afterwards cooled down to RT. 1 ml phosphate-free ultrapure water, 400 µl of 1.25 % ammonium heptamolybdate and 400 µl of 5 % ascorbic acid were added, the mixture was vigorously vortexed and boiled for 5 min in a water bath. The absorption was measured at 797 nm (UviLine 9400, Schott Instruments) and the concentration of lipid II was calculated based on the standard curve.

2.10 Fluorometric methods

2.10.1 QuantaBlu assay

To examine whether wolbachial PBPs or AmiD exhibit DD-carboxypeptidase activity *in vitro*, a fluorescent-linked enzyme assay to detect free D-Ala was performed using QuantaBlu Substrate solution (Thermo Scientific). Free D-Ala, which is released through the activity of a DD-carboxypeptidase, can be converted into pyruvate, ammonia and hydrogen peroxide by a D-amino acid oxidase (DAAO). The hydrogen peroxide can be used by horseradish peroxidase (HRP) to oxidize a suitable fluorogenic substance. In this thesis, the substrate from QuantaBlu

Substrate solution (QBS) was converted into a chromophore detectable at 420 nm following the reaction scheme:

$$\text{D-Ala} + O_2 \xrightarrow{\text{DAAO}} \text{Pyruvate} + NH_3 + H_2O_2$$
$$2H^+ + H_2O_2 + \text{QBS} \xrightarrow{\text{HRP}} 2H_2O + \text{QBS}^{2+}\ (A_{420})$$

Purified protein was incubated with synthesized lipid II (see chapter 2.9). A DD-carboxypeptidase (VanY) from *S. aureus* served as a positive control and the pASK-IBA empty vector as a negative control. After overnight incubation, every sample was supplemented with 150 pmol D-Ala due to the detection limit of this assay and the reaction was stopped by adding 360 µl of a detection mixture (55 mg/ml ampicillin, 10 µl QuantaBlu substrate solution, 2.78 µg/ml FAD, 100 mM Tris-HCl, 1U HRP and 0.06 U DAAO). The samples were further incubated for 1 h at RT and subsequently measured (excitation/emission 325/420 nm) in a luminescence photometer (Spark™ 10M, Tecan).

2.10.2 *In vivo* β-lactamase activity assay

To examine whether wolbachial PBPs or AmiD possess β-lactamase activity, an assay using CENTA™ as a substrate was performed. CENTA™ is a chromogenic β-lactamase substrate suitable for both Gram-positive and Gram-negative bacteria (Jones et al., 1982). The hydrolysis of the β-lactam ring causes a shift in absorption maxima (λ_{max}) from 340 nm to 405 nm. Permeabilization of the outer membrane with the pore forming compound polymyxin B enables the substrate access to the enzyme and vice versa. *E. coli* ML-35 pYC constitutively expressing a β-lactamase served as a positive control (Lehrer et al., 1988). PBP2^{wBm} and PBP6a^{wBm} were expressed in *E. coli* JM83 and PBP3^{wMel} was expressed in *E. coli* C43, two strains deficient in native β-lactamases. Fresh LB medium supplemented with chloramphenicol was inoculated with 2 % of the respective *E. coli* pre-culture harboring a pASK-IBA expression vector with a wolbachial PBP or AmiD. Cells were grown at 30 °C until $OD_{600} = 0.4$ and then induced with 200 ng/ml AHT. After 4 h of expression, cells were diluted 1:10 and supplemented with 150 µM CENTA™ (dissolved in DMSO) and 1 µg/ml polymyxin B (dissolved in ultrapure water) in 200 µl LB medium in a flat bottom 96-well plate. The mixture was incubated for 16 h in a plate reader (Tecan Sunrise™, Tecan) at 30 °C and λ_{405} was measured every 10 min. All samples were prepared in duplicates, the empty vector served as a negative control.

2.10.3 Penicillin-binding assay

To test whether *Wolbachia* AmiD or PBPs bind to penicillin, the fluorescent derivative Bocillin™ FL was used (Zhao et al., 1999). 4 µg purified protein, 10 µM Bocillin™ FL, 20 mM

potassium phosphate, pH 7.5 and 140 mM NaCl in a total volume of 20 µl were incubated in the dark at 20–35 °C for 30 min up to 16 h. Afterwards, SDS-PAGE was performed (see chapter 2.6.1) and the protein bound to Bocillin™ FL was visualized with a FastGene Led Illuminator (Nippon Genetics Europe GmbH).

2.11 Cell biological methods

2.11.1 C6/36 insect cell culture

Culture experiments were performed with an *A. albopictus* C6/36 insect cell line uninfected or stably infected with *w*AlbB (Turner et al., 2006). Cells were grown at 26 °C and split every seven days as described previously (Turner et al., 2006; Henrichfreise et al., 2009). Culture medium consisted of L15 Leibovitz medium supplemented with 5 % fetal calf serum (FCS), 2 % tryptose phosphate broth, 1 % MEM non-essential amino acids and 1 % penicillin/streptomycin. In later experiments, the standard 5 % FCS in the culture media was switched to 20 % as this was shown to increase the percentage of infected cells by *Wolbachia* (Clare et al., 2015).

2.11.2 Isolation of *w*AlbB from C6/36 insect cells

*Wolbachia w*AlbB were purified from infected C6/36 cells as described (Vollmer, 2012). Briefly, cells were grown to ~90 % confluence, harvested in 10 ml cell culture medium and lysed by vortexing with 100 sterile 3 mm borosilicate glass beads (Sigma-Aldrich) for 5 min. Cell debris was removed by centrifugation at 2,500 g for 10 min at 4 °C and the supernatant was filtered through a 5 µm syringe filter. The number of *Wolbachia* was determined by qPCR of the *Wolbachia* 16S rRNA single copy gene (see chapter 2.4.4).

2.11.3 Cell-free *w*AlbB culture

The cell-free *w*AlbB culture consisted of culture medium (see chapter 2.11.1), isolated *w*AlbB (see 2.11.2) and fractionated insect cell lysate from uninfected C6/36 cells (Vollmer, 2012). The amount of uninfected insect cells was calculated using a Neubauer counting chamber. Subsequently, uninfected cells were lysed by vortexing with 100 sterile 3 mm borosilicate glass beads for 5 min. Cell debris was removed by centrifugation at 2,500 g for 10 min at 4 °C and the supernatant was filtered through a 5 µm syringe filter. Additionally, the uninfected insect cell lysate was centrifuged at 20,000 g, 4 °C for 30 min. The supernatant containing cytosol, microsomes and plasma membranes was retained and used to prepare cell-

free *w*AlbB cultures. The final concentration of insect cell lysate fraction added to the culture was equivalent to 0.95 x 10^6 insect cells/ml. Purified *Wolbachia* were added in a final concentration of 0.5–1 x 10^3 16S rRNA gene copies/µl. Prepared cell-free *Wolbachia* cultures of 200 µl were incubated in triplicates in 96-well plates for twelve days at 26 °C. *Wolbachia* numbers were calculated by qPCR on day 0 and then every three days by harvesting three wells.

2.11.4 Cell-free *w*AlbB with modified growth conditions

As *Wolbachia* are obligate intracellular bacteria, there is a high dependence on substances from their hosts to ensure survival and proliferation (see chapter 1.3). Isolated cell-free *w*AlbB were incubated with culture medium and additionally supplemented with insect cell lysate (see chapter 2.11.3), which has been shown to facilitate growth (Vollmer, 2012). However, the cell-free *w*AlbB culture decreased after twelve days as shown in qPCR and thus likely needs modified growth conditions to keep viable and to proliferate (Vollmer, 2012). In this work, several conditions were tested whether they could enhance growth and stability of the culture. Apart from that, cell-free *w*AlbB were incubated with different antibiotics to test the efficacy and impact on proliferation and morphology.

2.11.4.1 Incubation in a lowered oxygen environment

As shown for other intracellular bacteria, culturing in a lowered oxygen environment can increase cell-free growth (Omsland et al., 2009). Here, a carbonic gas chamber with 3 % oxygen, 5 % carbonic gas and 77 % nitrogen was used to examine whether proliferation of cell-free *Wolbachia* could be enhanced under these conditions. Cells were prepared as described in chapter 2.11.3 and fresh gas was applied every three days after harvesting three samples.

2.11.4.2 Incubation of cell-free *w*AlbB on actin-coated streptavidin plates

Pal^{wBm} specifically binds to actin filaments of *B. malayi* and might be crucial in maintenance of endosymbiosis (Melnikow et al., 2013). As cell-free *w*AlbB show no adherence in the 96-well plate (J. Vollmer, pers. communication), culturing on a plate with actin was used to examine if the bacteria bind to the substrate to facilitate medium change. Here, a streptavidin plate was coated with biotin-labeled α-cardiac actin from bovine cardiac muscle according to the manufacturer's protocol (Hypermol). Briefly, biotin-labeled actin was adjusted to 10 µg/ml with wash buffer (25 mM Tris, 150 mM NaCl; pH 7.2, 0.1% BSA (w/v), 0.05% Tween 20 (v/v)). Each well of the streptavidin plate was washed three times with 200 µl wash buffer and was then incubated with 100 µl of biotin-labeled actin for two hours under shaking at RT. The plates were washed three times with 200 µl wash buffer and subsequently washed three times

with 200 µl Leibovitz medium. Cell-free *w*AlbB were prepared (see chapter 2.11.3) and medium change was performed on day six.

2.11.4.3 Supplementation of cell-free *w*AlbB culture medium

An optimized culture medium was designed for cell-free growth of the obligate endobacteria *Coxiella burnetii* (Omsland et al., 2009). The cell-free *w*AlbB standard medium was compared to the medium for *C. burnetii*. Substances, which were only present in the medium for *C. burnetii* were supplemented to the cell-free *w*AlbB medium including biotin, cystine, glucose, pyridoxal 5-phosphate (PLP) and sodium bicarbonate (Table 27). Moreover, insufficient amounts of cholesterol were considered being a potential limiting factor of cell-free growth. *Wolbachia* do not synthesize lipid A and it was proposed that cholesterol might be necessary to promote membrane stability as a substitute for lipopolysaccharide (Lin and Rikihisa, 2003; Wu et al., 2004). Therefore, cholesterol was also added to the cell-free *w*AlbB standard medium. Lipid Mixture Solution (PeproTech) contains non-animal-derived fatty acids and lipids to improve cell growth in serum-free media, but the exact formulation is proprietary of PeproTech. The lipid mixture solution was added to the cell-free *w*AlbB culture to examine any beneficial effects regarding proliferation.

Table 27: Supplements tested in cell-free *w*AlbB culture.

Compound	**Concentration**	**Solvent**
Biotin	25 mg/l	1N NaOH (adjusted to pH 7)
Cholesterol	0.1 mg/l and 1 mg/ml	H_2O
D-Glucose	500 mg/l	H_2O
L-Cystine	30 mg/l	1M HCl (adjusted to pH 7)
Lipid mixture	1x, 2.5x and 5x	H_2O
PLP	0.247 mg/l	H_2O
Sodium bicarbonate	250/500/2500 mg/l	H_2O

2.11.4.4 Growth of cell-free *w*AlbB co-cultured with yeast

B. malayi and *B. pahangi* infective-stage larvae co-cultured *in vitro* with the yeast *Rhodotorula minuta* have been shown to support consistent and reproducible molting to the fourth larval stage (Smith et al., 2000). It was assumed that the larvae are benefiting from an unknown secreted product of the yeast. *R. minuta* were cultured in YM medium (see Table 5) at 24 °C. Cell-free *Wolbachia* were prepared (see chapter 2.11.3) and co-cultured with different concentrations of *R. minuta* ranging from 10^4–10^7 cells/ml. Proliferation rates were examined via qPCR (see chapter. 2.4.4).

2.11.4.5 Antibiotic treatment

Cell-free *w*AlbB were prepared (see chapter 2.11.3) and additionally treated with antibiotics (Table 28). All antibiotics were applied freshly every three days during the assay, except for fosfomycin, which had to be given daily due to its short half-life in solution (Kirby, 1977). Growth was detected via qPCR every three days and changes in morphology were examined using immunohistochemistry (see chapter 2.12.1).

Table 28: Antibiotics tested in the cell-free *w*AlbB culture.

Compound	Antibiotic class	Target	Concentration	Solvent
Ampicillin	β-lactam	Cell wall synthesis	512 µg/ml	H_2O
Bacitracin	Cyclic peptide	Cell wall synthesis	512 µg/ml	H_2O
Ciprofloxacin	Fluoroquinone	DNA synthesis	512 µg/ml	0.1 M HCl
Clindamycin	Lincosamide	Protein synthesis	512 µg/ml	H_2O
Corallopyronin A	Alpha-pyrone	RNA synthesis	1 µg/ml	DMSO
Doxycycline	Tetracycline	Protein synthesis	4 µg/ml	H_2O
Fosfomycin	Phosphonic	Cell wall synthesis	512 µg/ml	H_2O
Rifampicin	Ansamycin	RNA synthesis	512 µg/ml	Ethanol
Sulfamethoxazol	Sulfonamide	Folic acid synthesis	512 µg/ml	Ethanol
Trimethoprim	Sulfonamide	Folic acid synthesis	512 µg/ml	DMSO
Vancomycin	Glycopeptide	Cell wall synthesis	512 µg/ml	DMSO

2.12 Immunohistochemistry

2.12.1 Fluorescence microscopy of antibiotic treated cell-free *w*AlbB

For viability assays, *Wolbachia* were pelleted by centrifugation at 18,400 g for 5 min and suspended in ultrapure water, PBS or Leibovitz medium, respectively. To test for lysozyme sensitivity, isolated *w*AlbB were resuspended in 5 mg/ml lysozyme. Bacteria were stained with the LIVE/DEAD® *Bac*Light™ Bacterial Viability Kit (Molecular Probes) as previously described (Rasgon et al., 2006) and examined with a fluorescence microscope (ZeissAxio VertA.1, Carl Zeiss AG).

To test the effect of antibiotics on growth of cell-free *w*AlbB, cultures were prepared (see chapter 2.11.3), cultured in 96-well plates and treated with the respective antibiotic for twelve days (see chapter 2.11.4.5). Cell-free *w*AlbB were stained with the LIVE/DEAD® *Bac*Light™ Bacterial Viability Kit as described previously (Rasgon et al., 2006). Additionally, cell-free *w*AlbB were fixed, stained and visualized as described for C6/36 *w*AlbB infected cells (Vollmer et al., 2013). Briefly, 50 µl *w*AlbB were dried on a microscope slide and fixed in ice-cold 4 % paraformaldehyde (w/v) for 15 min. Then, samples were washed three times with 1x PBS (137 mM NaCl, 2.7 mM KCl, 10 mM Na_2HPO_4, 2 mM KH_2PO_4, pH 7.4) and cells were

permeabilized with 1x PBS + 0.25 % Triton X-100 (v/v) for 15 min. Subsequently, slides were washed three times and blocked with 1x PBS + 10 % BSA (w/v) for 1 h at RT. Samples were washed again three times with 1x PBS and incubated with a *Wolbachia*-specific FtsZ/Pal antibody diluted 1:1000 in PBS overnight at 4 °C in a humid chamber. The next day, samples were washed three times with 1x PBS and incubated with secondary antibody conjugated to Alexa Fluor® 488 diluted 1:200 in PBS for 1 h at RT in the dark. After three washing steps with 1x PBS, 0.25 µg/ml DAPI was applied and incubated for 10 min at RT. Cells were washed again three times with 1x PBS and stored at 4 °C until fluorescence microscopy was performed.

2.12.2 Lipid II labeling of *w*AlbB

Liechti *et al.* (2014) developed a novel peptidoglycan labeling approach that bypasses the bacterial Ddl enzyme using D-Ala-D-Ala dipeptide analogues modified with alkyne functional groups (Ethynyl-D-alanyl-D-alanine; EDA-DA) and click chemistry. With this technique, a peptidoglycan-like structure was revealed for the first time in intracellular *Chlamydia trachomatis*, in free-living *Planctomycetes* and in the closely to *Wolbachia*-related *O. tsutsugamushi* (Liechti et al., 2014; Jeske et al., 2015; Van Teeseling et al., 2015; Atwal et al., 2017). Here, the labeling technique was applied to the C6/36 *w*AlbB infected culture to investigate if *Wolbachia* residing in insect cells also have a peptidoglycan-like structure. Cells were harvested, counted in a Neubauer chamber and inoculated to a final concentration of 50.000 cells/ml in chamber slides. To block lipid II synthesis, 512 µg/ml fosfomycin was applied daily for 12 days to the C6/36 *w*AlbB infected culture before harvesting and seeding the cells to chamber slides. Cells were incubated with 1 mM EDA-DA or ELA-LA (synthesized by Pepmic Co., Ltd.) for 72 h and subsequently prepared for fluorescence microscopy. Cells were fixed in ice-cold 4 % paraformaldehyde (w/v) for 15 min, washed three times with 1x PBS (136 mM NaCl, 2.68 mM KCl, 10 mM Na_2HPO_4-$2H_2O$, 1.98 mM KH_2PO_4, pH 7.4) and were incubated for 10 min with 1x PBS + 0.15 % Tween 20 (v/v). Cells were washed again three times and blocked with 1x PBS + 3 % BSA (w/v) for 1 h at RT. Click chemistry was performed using the Click-iT® Cell Reaction Buffer Kit (Thermo Scientific) following the manufacturer's instructions with a concentration of 10 mM Alexa Fluor® 594 azide. Cells were washed again three times with 1x PBS and incubated with a *Wolbachia*-specific FtsZ or Pal antibody diluted 1:1000 in PBS overnight at 4 °C in the dark. The next day, samples were washed three times with 1x PBS and incubated with secondary antibody conjugated to Alexa Fluor® 488 diluted 1:200 in PBS for 1 h at RT in the dark. After three washing steps with 1x PBS, 0.25 µg/ml DAPI was applied and incubated for 10 min at RT. Cells were washed again three times with

1x PBS and observed with a fluorescence microscope (ZeissAxio VertA.1, Carl Zeiss AG). Fosfomycin treated cells were visualized using a confocal microscope (Zeiss LSM710, Carl Zeiss AG).

2.13 Bioinformatics

2.13.1 *In silico* analyses

BLAST analysis (http://blast.ncbi.nlm.nih.gov/Blast.cgi) was used to identify sequences similar to Wbm0075 (*pal*), Wbm0152 (*pbp2*), Wbm0290 (*pbp6a*), WD1073 (*amiD*) and WD1273 (*pbp3*) and the sequence alignment tool Clustal Omega (http://www.ebi.ac.uk/Tools/msa/clustalo/) to align wolbachial and *E. coli* sequences. The presence of transmembrane domains and a signal peptide for secretion in the periplasm was predicted using TMHMM 2.0 (http://www.cbs.dtu.dk/services/TMHMM/) and SignalP 4.1 (http://www.cbs.dtu.dk/services/SignalP/). Protein structure prediction of the proteins was generated by Phyre^2 (protein homology/analogy recognition engine V2.0) based on secondary structure prediction by recognition of similar sequences and related 3D structures (www.sbg.bio.ic.ac.uk). Potential ligand binding sites were predicted by 3DLigandSite (http://www.sbg.bio.ic.ac.uk/~3dligandsite/) (Wass et al., 2010). 3D-models of the proteins with highlighted putative active sites were illustrated using Jmol 14.28.3 (http://jmol.sourceforge.net/).

2.13.2 Statistical analyses

For statistical analyses, GraphPad Prism 5 software (GraphPad Software Inc., La Jolla, USA) was used. Normality tests were performed using Shapiro-Wilk tests. For normal distributed data, parametric t-tests were applied (comparison of two groups), whereas non-parametric data were analyzed using Mann-Whitney tests (comparison of two groups) or Kruskal-Wallis tests (comparison of more than two groups) with subsequent Dunn's comparison post-hoc test with a significance level of $P < 0.05$.

3 Results

3.1 Functional analysis of PBP6a$^{w\text{Bm}}$

3.1.1 Primary structure analysis of PBP6a$^{w\text{Bm}}$

The genome of *w*Bm encodes the putative DD-carboxypeptidase PBP6a$^{w\text{Bm}}$ (NCBI: WP_041571552.1) which consists of 370 amino acids with a predicted molecular mass of 42.21 kDa. PBP6a$^{w\text{Bm}}$ shares 84 % sequence similarity with PBP6a from *w*Mel (NCBI: AAS13855.1) having identical conserved PBP active site motifs SXXK, SX(D/N) and K(S/T)G (Supplementary Figure 1). PBP6a$^{w\text{Bm}}$ and PBP6a from *E. coli* (NCBI: WP_032169860.1) have 35 % sequence identity (Figure 14). Notably, the wolbachial PBP6a has one more SXXK motif which might harbor the active site serine than its *E. coli* homolog, but only the second SXXK (S^{56}MSK), SXN (S^{116}GN) and the KTG (K^{218}TG) motifs align to *E. coli* PBP6a. PBP6a$^{w\text{Bm}}$ has a predicted signal peptide ranging from amino acid 1–22, but no predicted transmembrane domain suggesting the enzyme being localized in the periplasm (Supplementary Figure 2).

```
PBP6a wBm       ----MSILDK----LVILLLVSTLPFSSY--SYQFRTKAKQAVVLDLASDLFIFEHNSDE  50
PBP6a E. coli   MTQYSSLLRGLAAGSAFLFLFAPTAFAAEQTVEAPSVDARAWILMDYASGKVLAEGNADE  60
                     *:*       .:*:*.:   *::        ..*:  :::* **. .: * *:**

PBP6a wBm       KMSPSSMSKLMTLYVAFDYLKAGIIDMKDKFRVSRKAWER------KGSSMFLKEGQSVS  104
PBP6a E. coli   KLDPASLTKIMTSYVVGQALKADKIKLTDMVTVGKDAWATGNPALRGSSVMFLKPGDQVS  120
                *:.*:*::*:** **. : ***. *.:.* . *.:.**         .* **** *:.**

PBP6a wBm       VKELLEGVTTVSGNDACITLAEGIAGSEENFVVEMNEVAQNLNLSDSYFVNSSGWPDKDH  164
PBP6a E. coli   VADLNKGVIIQSGNDACIALADYIAGSQESFIGLMNGYAKKLGLTNTTFQTVHGLDAPGQ  180
                * :* :**   *******:**: ****:*.*:  **  *::*.*::: * .  *    .:

PBP6a wBm       FMSAKDLVVLAKRIFTDFPEYYDLFSKQYLTYNDIIQKNKNLLLF-HDIGVDGIKTGYTN  223
PBP6a E. coli   FSTARDMALLGKALIHDVPEEYAIHKEKEFTFNKIRQPNRNRLLWSSNLNVDGMKTGTTA  240
                * :*:*:.:*.* :: *.** * :..:: :*:*.* * *:* **:  ::.***:*** *

PBP6a wBm       AGGYGIVISAKRNDRRIFAVVNGLNTEKERIEEAKRLIQYSFNHFNTKKIFAKDSVVEEI  283
PBP6a E. coli   GAGYNLVASATQGDMRLISVVLGAKTDRIRFNESEKLLTWGFRFFETVTPIKPDATFVTQ  300
                ..**.:* **.:.* *:::** * :*:: *::*:::*: :.*..*:* . :  *:..

PBP6a wBm       NVLYGKERKVSATVANDVTITYNRNLRDKIKVR-VEYKDMIPAPIKKGQEVGKIFIEIPG  342
PBP6a E. coli   RVWFGDKSEVNLGAGEAGSVTIPRGQLKNLKASYTLTEPQLTAPLKKGQVVGTIDFQLNG  360
                .* :*.: :*.  ..:  ::*  *.  .:::*.  .  :  : **:**** **.* ::: *

PBP6a wBm       IEQQTIPLYAVNDVQELNYVEKFFRILF------------                      370
PBP6a E. coli   KSIEQRPLIVMENVEEGGFFGRVWDFVMMKFHQWFGSWFS                      400
                . :  ** .:::*:* .:. :.: :::
```

Figure 14: Primary structure and amino acid alignment of PBP6a$^{w\text{Bm}}$ and *E. coli* PBP6a. PBP6a$^{w\text{Bm}}$ (WP_041571552.1) shares 35 % similarity with its *E. coli* homolog (WP_032169860.1). Conserved SXXK, SX(D/N) and K(S/T)G motifs found in PBP6a$^{w\text{Bm}}$ are written in bold letters, motifs which align to *E. coli* PBP6a are additionally framed in black. The predicted signal peptide for periplasmic secretion ranging from amino acid 1–22 is highlighted gray. ***** fully conserved residue; **:** conservation between groups of strongly similar properties; **.** conservation between groups of weakly similar properties.

3.1.2 Secondary structure analysis of PBP6a^{wBm}

To get a deeper insight into the putative active site of PBP6a^{wBm}, secondary structure analysis was performed. Based on sequence alignments to *E. coli*, the conserved active site motifs found in PBP6a^{wBm} were localized (Figure 15). The first SXXK motif (S^{48}DEK) was predicted to be located on a loop, while the second SXXK motif (S^{56}MSK) is putatively found in an α-helix. S^{116}GN is likely localized in an α-helix and loop, whereas K^{218}TG is found in a β-sheet. The results of the structure analysis indicated that PBP6a^{wBm} has a catalytic center and might be an active DD-carboxypeptidase. The gene *pbp6a* from *w*Bm was cloned into pASK-IBA2C, transformed into different *E. coli* strains and tested in *in vivo* and *in vitro* activity assays.

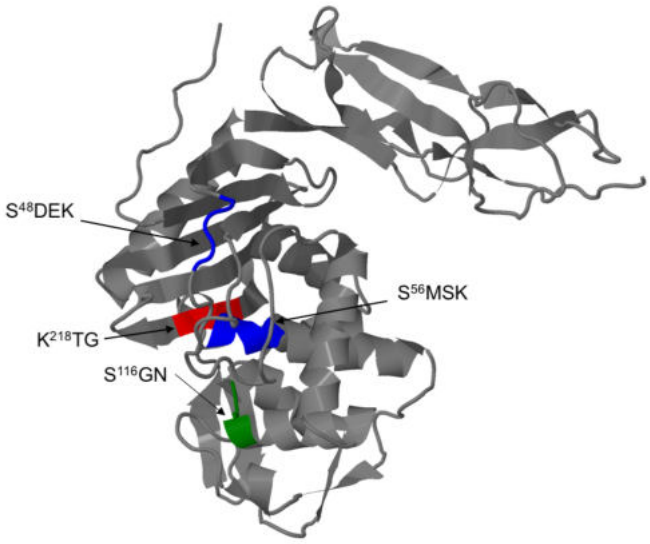

Figure 15: Secondary structure of PBP6a^{wBm} as predicted by Phyre^2. S^{48}DEK or S^{56}MSK (blue) might, together with S^{116}GN (green) and K^{218}TG (red), build the catalytic center of the enzyme. The molecular structure of PBP6a^{wBm} was illustrated by Jmol.

3.1.3 Characterization of PBP6a^{wBm} *in vivo*

The characterization of DD-carboxypeptidases *in vivo* is challenging as depletion in *E. coli* does not lead to an aberrant phenotype (Nelson and Young, 2001). However, the activity of DD-carboxypeptidases can be measured indirectly by complementation of *E. coli* MCI23. This strain encodes a temperature sensitive version of the essential cell division DD-transpeptidase PBP3 resulting in a filamentous phenotype when grown at the non-permissive temperature of 42 °C (Begg et al., 1990; Dai et al., 1993). This growth defect can be complemented by the overexpression of a DD-carboxypeptidase cleaving the terminal D-Ala of the pentapeptide chains of peptidoglycan. The subsequent cleavage of the tetrapeptides by the LD-carboxypeptidase A results in increased levels of available tripeptide

chains in peptidoglycan (Begg et al., 1990). These are the preferred substrates of PBP3 (Botta and Park, 1981; Pisabarro et al., 1986). This is sufficient to partially restore cell division by the residual activity of PBP3 (Begg et al., 1990). To test the *in vivo* activity of the putative DD-carboxypeptidase PBP6a^{wBm}, the encoded *pbp6a* gene from *w*Bm was cloned into the expression vector pASK-IBA2C. The native signal sequence of *pbp6a* was replaced by the *ompA* signal peptide of the expression vector pASK-IBA2C. Successful cloning was confirmed by sequencing (Supplementary Figure 3) and the construct was transformed into *E. coli* MCI23 and ready-to-use for *in vivo* assays. *E. coli* MCI23 expressing recombinant PBP6a^{wBm} showed short and dividing cells at 30 °C and PBP6a^{wBm} overproduction at the non-permissive temperature of 42 °C partially restored cell division (Figure 16A). Additional staining with DAPI displayed distinct DNA separation of PBP6a^{wBm} expressing cells, thus confirming the restoration of cell division in the temperature sensitive *E. coli* MCI23 strain. *E. coli* MCI23 with the induced empty vector pASK-IBA2C incubated at 30 °C had a normal phenotype with only single and dividing cells, whereas bacteria grown at 42 °C were unable to divide resulting in elongated cells (Figure 16B). In accordance, no partition of DNA was monitored in DAPI-stained cells. Consequently, each filament represents one viable elongated cell. Experiments were repeated six times and in each experiment five randomly chosen pictures were taken for quantitative analysis of cells at the non-permissive temperature. *E. coli* MCI23 expressing PBP6a^{wBm} were statistically shorter than and cells expressing the empty vector control at 42 °C (Figure 16C). In *E. coli* MCI23 expressing recombinant PBP6a^{wBm} at 42 °C, a mixed set of phenotypes was observed with 36.3 % (± 25.6 standard deviation (SD)) elongated cells and 63.7 % (± 25.6 SD) short cells able to divide (Figure 16D). *E. coli* MCI23 expressing the empty vector pASK-IBA2C at 42 °C resulted in 97.8 % (± 2.6 SD) elongated bacteria and only 2.2 % (± 2.6 SD) short single and dividing cells. In conclusion, these results give a first hint that PBP6a^{wBm} might act as a DD-carboxypeptidase *in vivo.*

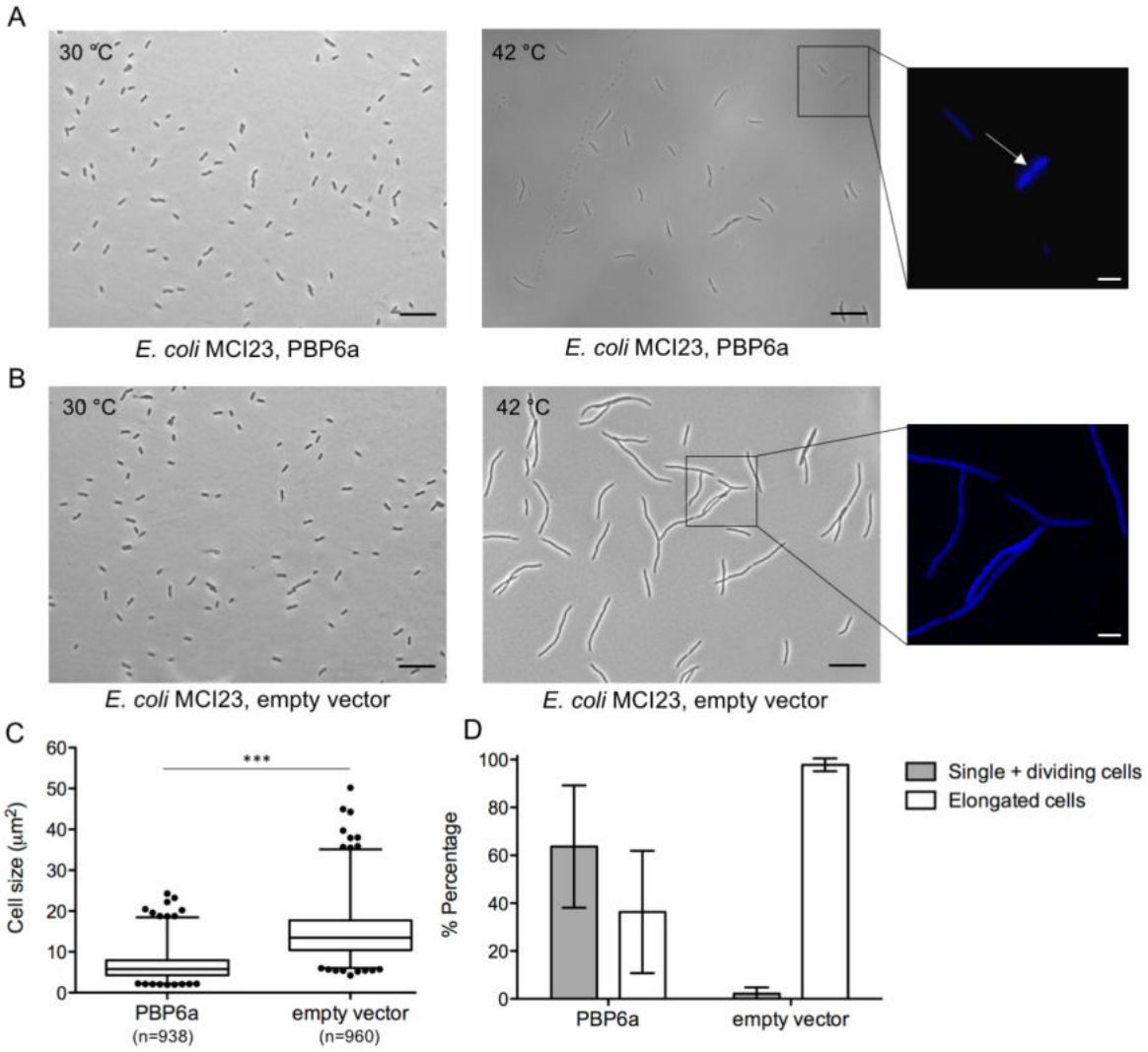

Figure 16: PBP6a^{wBm} rescues cell division in a temperature sensitive *E. coli* MCI23 mutant. *E. coli* MCI23 were grown in LB medium containing chloramphenicol until $OD_{600} = 0.4$. PBP6a^{wBm} expression was induced with 100 ng/ml tetracycline and cells were incubated for 120 min at 30 °C (endogenous PBP3 is expressed, cells divide normally; permissive temperature) or 42 °C (endogenous PBP3 is not expressed, cells do not divide normally and form long, filamentous strands; non-permissive temperature). A) *E. coli* MCI23 expressing recombinant PBP6a^{wBm} complement cell division at 30 °C and partially at the non-permissive temperature of 42 °C, scale bar = 20 µm. DAPI staining confirmed septa formation in *E. coli* MCI23 expressing PBP6a^{wBm}, scale bar = 5 µm. B) *E. coli* MCI23 expressing the empty vector pASK-IBA2C have short, single cells at 30 °C, but are not able to divide at 42 °C showing a filamentous phenotype. DAPI staining confirmed that septa were absent in cells with the empty vector control. C) At least 938 cells from 30 randomly chosen pictures taken from six independent assays per sample at 42 °C were measured by Image J. Boxes extend from the 25th to the 75th percentile. The line in the middle of the box is plotted at the median. Whiskers represent 1st and 99th percentiles, dots represent outliers. Statistical analysis was performed using Mann-Whitney test. *** = $P \leq 0.001$. D) Columns represent mean ± SD of relative occurrence of different phenotypes at 42 °C from 30 randomly chosen pictures in six independent experiments.

3.1.4 Active site analysis of PBP6a^{wBm} *in vivo*

The serine of the SXXK motif catalyzes the enzymatic reaction of PBPs and the mutagenesis of SXXK motifs in PBP6 from *C. pneumoniae* was shown to inhibit DD-carboxypeptidase activity *in vitro* (Otten, 2014). Since PBP6a^{wBm} contains two SXXK motifs, it was tested which of the serine residues from the conserved SXXK motifs is essential

for enzyme activity. Mutagenesis PCRs were performed to exchange serine from both SXXK motifs to alanine (S48A and S56A) (Figure 17). Successful mutagenesis was confirmed by nucleotide sequencing (Supplementary Figure 4).

```
  1    MSILDKLVILLLVSTLPFSSYSYQFRTKAKQAVVLDLASDLFIFEHNADEKMSPSAMSKL   60
 61    MTLYVAFDYLKAGIIDMKDKFRVSRKAWERKGSSMFLKEGQSVSVKELLEGVTTVSGNDA  120
121    CITLAEGIAGSEENFVVEMNEVAQNLNLSDSYFVNSSGWPDKDHFMSAKDLVVLAKRIFT  180
181    DFPEYYDLFSKQYLTYNDIIQKNKNLLLFHDIGVDGLKTGYTNAGGYGIVISAKRNDRRI  240
241    FAVVNGLNTEKERIEEAKRLIQYSFNHFNTKKIFAKDSVVEEINVLYGKERKVSATVAND  300
301    VTITYNRNLRDKIKVRVEYKDMIPAPIKKGQEVGKIFIEIPGIEQQTIPLYAVNDVQELN  360
361    YVEKFFRILF                                                     370
```

Figure 17: Primary structure of PBP6a^{wBm} in pASK-IBA2C after site-directed mutagenesis. Serine residues from SXXK motifs were substituted by alanine (red bold letters). The predicted native signal peptide (highlighted gray) was removed and replaced by OmpA from the pASK-IBA2C vector. The amino acid sequence is shown in single-letter code.

E. coli MCI23 cultures expressing mutated PBP6a^{wBm} were tested for their ability to rescue division at 42 °C. In control assays with *E. coli* MCI23 expressing recombinant PBP6a^{wBm} S48A, S56A or S48A-S56A at 30 °C, all cells were short and dividing (data not shown). Expression at 42 °C of PBP6a^{wBm} with one mutated SXXK motif (S48A or S56A) resulted in a mixed set of phenotypes similar to the expression of unmutated PBP6a^{wBm} at 42 °C (see chapter 3.1.1). In contrast, the expression of PBP6a^{wBm} S48A-S56A predominantly resulted in elongated cells (Figure 18A-C). Analysis of six independent experiments confirmed these observations showing that cells with only one SXXK mutation were significantly shorter than the double SXXK mutant (Figure 18D). Expression of single SXXK mutants resulted in 61.3 % (± 29.5 SD) (PBP6a^{wBm} S48A) and 59.7 % (± 31.2 SD) (PBP6a^{wBm} S56A) short cells able to divide (Figure 18E) similar to the unmutated PBP6a^{wBm} (see chapter 3.1.1). Expression of PBP6a^{wBm} S48A-S56A resulted in an increase of elongated cells to 91 % (± 8.1 SD) with a concomitant decrease of short, single and dividing cells to 9 % (± 8.1 SD).

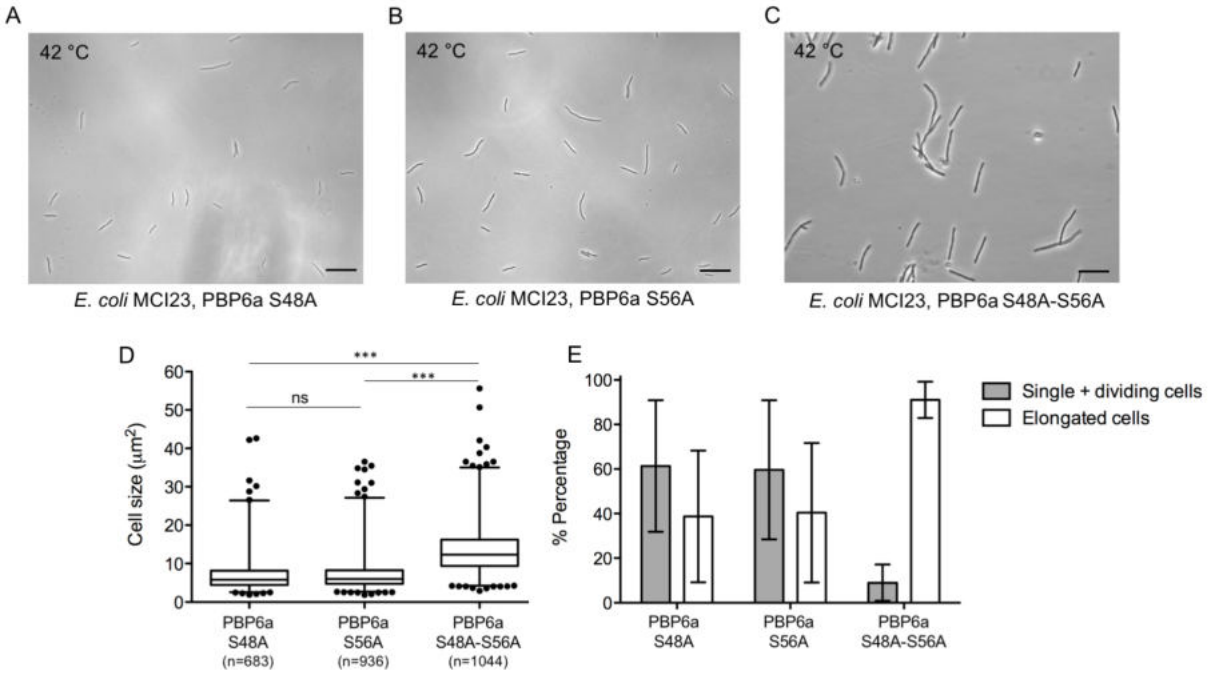

Figure 18: Complementation assay to test for the ability of PBP6a^{wBm} active site mutants to rescue cell division in a temperature sensitive *E. coli* MCI23 mutant. Cultures were grown in LB medium containing chloramphenicol at 30 °C and protein expression was induced with 100 ng/ml tetracycline at OD_{600} = 0.4. Cells were further incubated for 120 min at the non-permissive temperature of 42 °C. Phase-contrast micrographs show that *E. coli* MCI23 expressing A) PBP6a^{wBm} S48A and B) PBP6a^{wBm} S56A partially rescue cell division, while C) expression of PBP6a^{wBm} S48A-S56A leads to elongated cells unable to divide. Scale bars = 20 µm. D) At least 683 cells from 30 pictures taken from six independent assays per sample were measured by Image J. Boxes extend from the 25th to the 75th percentile. The line in the middle of the box is plotted at the median. Whiskers represent 1st and 99th percentiles. Statistical analysis was performed using Kruskal-Wallis test and Dunn's comparison post-hoc test. ns = not significant, *** = P ≤ 0.001. E) Columns represent mean ± SD of relative occurrence of different phenotypes at 42 °C from 30 randomly chosen pictures in six independent experiments.

Growth of *E. coli* was monitored to exclude that the different observed phenotypes resulted from potential cell arrests induced by protein induction. In three independent measurements, all cultures grew exponentially after induction (Figure 19).

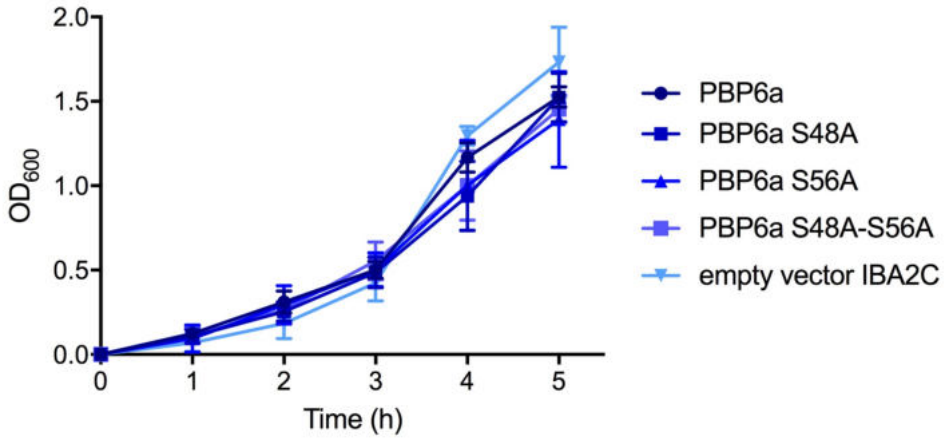

Figure 19: Growth kinetics of *E. coli* MCI23 during periplasmic expression of PBP6a^{wBm}. Protein expression was induced at OD_{600} = 0.4 with 100 ng/ml tetracycline. OD_{600} was measured every hour. Each point represents mean ± SD (n = 3).

As the number of single and dividing cells in PBP6a^{wBm} S48A-S56A (9 %) was still higher than cells expressing the empty vector (2.2 %), further control experiments with *E. coli* MCI23 expressing Pal^{wBm} were performed. This protein is not expected to have any DD-carboxypeptidase or DD-transpeptidase activity and was an appropriate control to exclude potential false positive results caused by expression stress of proteins after induction which could also contribute to reduced cell size. In six independent assays, cells expressing Pal^{wBm} were significantly shorter than the empty vector control, but only 8.32 % (± 2.42 SD) of cells were single and dividing, whereas 91.68 % (± 2.42 SD) of cells were elongated (Figure 20). This explains the apparent remaining activity of the PBP6a^{wBm} S48A-S56A which is likely caused by expression stress of the bacteria.

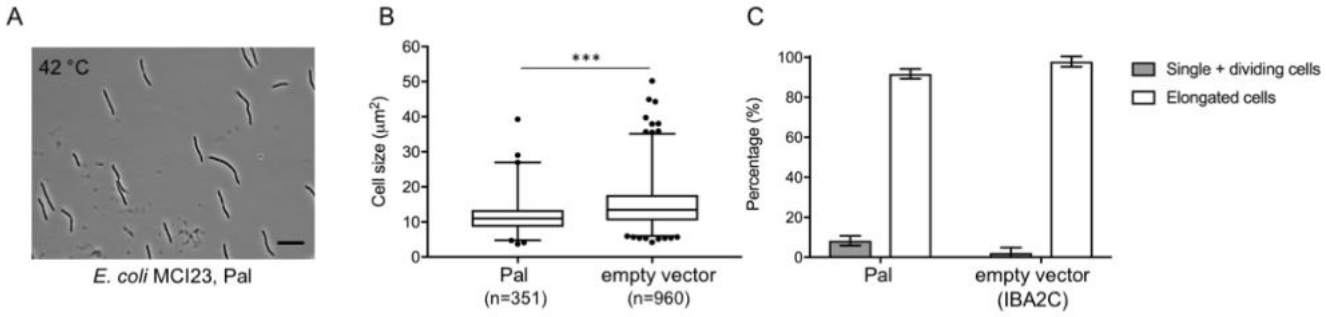

Figure 20: Lack of complementation of cell division defect of *E. coli* MCI23 with Pal^{wBm}. A) The phase-contrast micrograph shows that *E. coli* MCI23 expressing Pal^{wBm} predominantly have elongated cells unable to divide. Scale bar = 20 µm. B) At least 351 cells from 30 pictures taken from six independent assays per sample were measured by Image J. Boxes extend from the 25th to the 75th percentile. The line in the middle of the box is plotted at the median. Whiskers represent 1st and 99th percentiles. Statistical analysis was performed using Kruskal-Wallis test and Dunn's comparison post-hoc test. *** = P ≤ 0.001. C) Columns represent mean ± SD of relative occurrence of different phenotypes at 42 °C from 30 randomly chosen pictures in six independent experiments.

In conclusion, the results from the *in vivo* complementation assays in *E. coli* indicate that the serines in both SXXK motifs of PBP6a^{wBm} are most likely responsible for catalytic activity in this enzyme.

3.1.5 Periplasmic expression and purification of recombinant PBP6a^{wBm}

As previous attempts to obtain purified recombinant PBP6a^{wBm} by cytoplasmic overexpression were not successful (data not shown), *pbp6a* was cloned into pASK-IBA2C with *ompA* substituting the native signal peptide for periplasmic expression. This method has been shown to improve protein yields of expressed recombinant PBPs from intracellular bacteria of the genus *Chlamydia* (De Benedetti et al., 2014; Klöckner et al., 2014; Otten et al., 2015). For small-scale overexpression pre-tests, pASK-IBA2C containing *pbp6a* was transformed into the *E. coli* strains C43, JM83 and W3110. Pre-tests were carried out to identify conditions that facilitate the production of recombinant PBPs and yield the highest amounts of

soluble protein. PBP6a^{wBm} was expressed in all three strains and *E. coli* JM83 was chosen to be used for further overexpression as this strain yielded highest protein amounts. PBP6a^{wBm} overproduction was additionally optimized by co-solvent supplementation. Co-solvent assisted overproduction has been established for heterologous expression of recombinant proteins from intracellular *Chlamydia* (Otten et al., 2015). The co-solvent test revealed that 4 h expression at 25 °C in the presence of arginine resulted in the highest amount of soluble protein. Subsequently, the expression culture was scaled-up to 4 l and recombinant protein was purified using Strep-tag chromatography. Protein concentration of each eluate was measured (80–120 µg/ml) and purity of PBP6a^{wBm} was confirmed by Western Blot analysis (Figure 21). As a negative control, a mock purification of the empty vector pASK-IBA2C was performed, which is exemplarily shown in chapter 3.4.1.1.

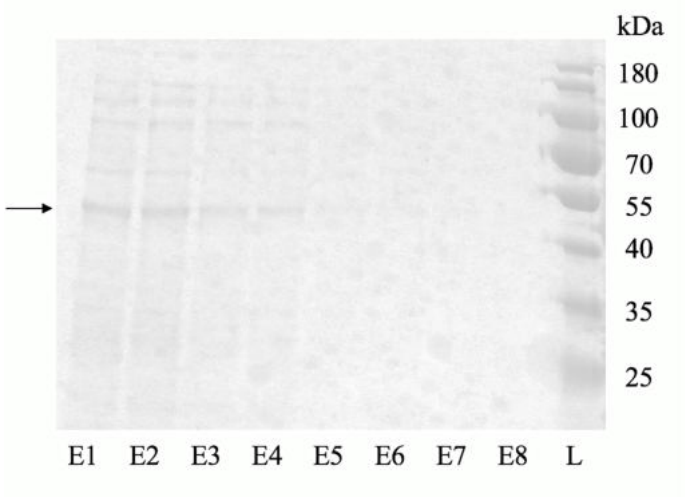

Figure 21: Overexpressed and purified PBP6a^{wBm} in pASK-IBA2C. Western Blot analysis of elution fractions (E1-E8) after PBP6a^{wBm} expression and Strep-tag purification. The arrow points to the recombinant protein with a predicted molecular weight of 42.21 kDa.

3.1.6 Activity of PBP6a^{wBm} *in vitro* using lipid II as a substrate

The arginine-assisted overproduction of recombinant PBP6a^{wBm} yielded in soluble protein accessible to biochemical characterization. The protein was incubated with the cell wall precursor lipid II for 4 h or overnight at 30 °C. To exclude false positive results from potentially contaminating *E. coli* DD-carboxypeptidases, the corresponding eluate of the overexpressed and purified empty vector pASK-IBA2C served as a negative control. The DD-carboxypeptidase VanY from *S. aureus* served as a positive control and was incubated with lipid II for 1 h. After incubation of PBP6a^{wBm} with lipid II for 4 h and separation of the reaction mixture by TLC, a lipid II band at the normal running level was detected. However, after overnight incubation, two bands at different levels were observed (Figure 22A). The lower band represents lipid II with a tetrapeptide, which is generated when the terminal D-Ala is cleaved

from the pentapeptide chain. This band was also detected when lipid II was incubated with VanY from *S. aureus*. The upper band represents lipid II with a pentapeptide, which was also observed in the empty vector. MALDI-TOF analysis of the reaction products confirmed the TLC results (Figure 22B). Lipid II (L-Lys) has a mass of around 1875 Da, which was detected in the empty vector control. When incubated with PBP6a^{wBm}, a mass of 1805 Da was measured due to the cleavage of the terminal D-Ala from the pentapeptide side chain. The enzyme activity of PBP6a^{wBm} was slower compared to VanY from *S. aureus*. Nevertheless, TLC as well as MALDI-TOF analysis of the reaction products indicated *in vitro* DD-carboxypeptidase activity of PBP6a^{wBm}.

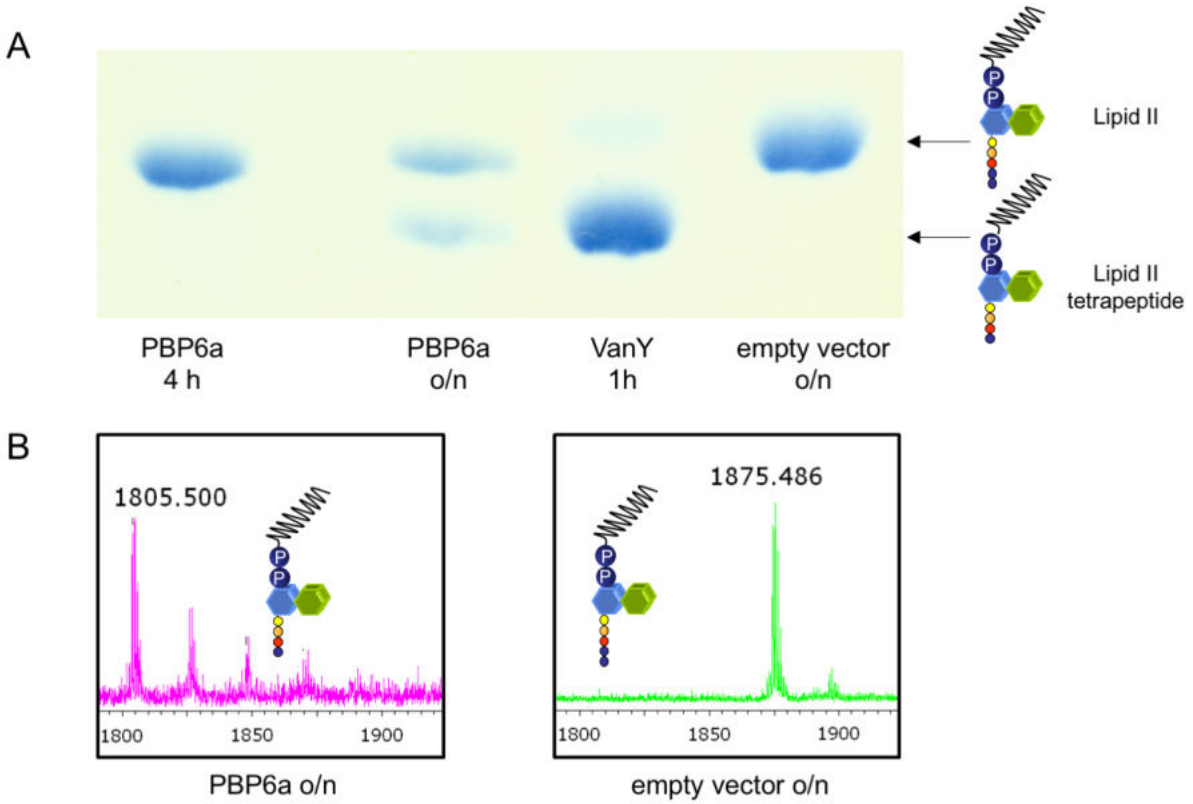

Figure 22: *In vitro* activity of PBP6a^{wBm}. The overexpressed recombinant PBP6a^{wBm} showed DD-carboxypeptidase activity on lipid II. A) TLC comparing DD-carboxypeptidase activity of PBP6a^{wBm} after 4 h and overnight (o/n) incubation with lipid II. The DD-carboxypeptidase VanY (*S. aureus*) was used as a positive control, the empty vector pASK-IBA2C served as a negative control. B) MALDI-TOF analysis of the lipid II reaction products after incubation with PBP6a^{wBm} and the empty vector pASK-IBA2C. Cleaving of terminal D-Ala from the pentapeptide side chain of lipid II (mass: 1875 Da) resulted in the formation of lipid II-tetrapeptide (mass: 1805 Da). MALDI-TOF analysis was performed by M. Josten, IMMIP.

3.1.7 Active site analysis of PBP6a^{wBm} *in vitro*

The expressed and purified PBP6a^{wBm} S48A-S56A protein, in which both active site serine residues of the SXXK motifs were replaced by alanine, was not capable of cleaving the terminal D-Ala from lipid II as shown by TLC and MALDI-TOF (Figure 23). The mass of the reaction products after overnight incubation of PBP6a^{wBm} S48A-S56A with lipid II was around 1877 Da, which corresponds to the mass of lipid II (L-Lys) with a pentapeptide confirming no DD-carboxypeptidase activity of the active site mutant.

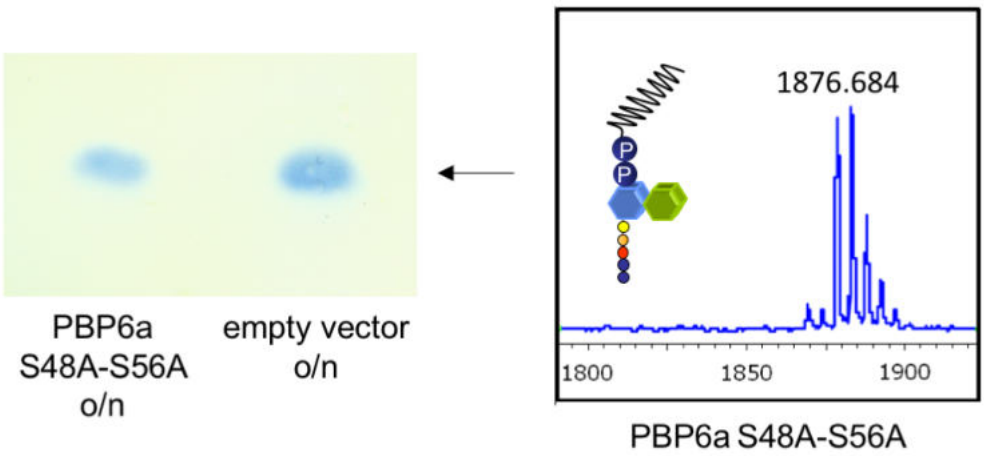

Figure 23: *In vitro* activity of PBP6a^{wBm} S48A-S56A active site mutant. TLC and MALDI-TOF analysis of the lipid II reaction products after incubation with overexpressed recombinant PBP6a^{wBm} S48A-S56A active site mutant did not reveal DD-carboxypeptidase activity on lipid II. MALDI-TOF analysis was performed by M. Josten, IMMIP.

3.1.8 Resistance of PBP6a^{wBm} to β-lactam antibiotics *in vitro*

As PBPs usually show a high penicillin-binding affinity, antibiotic susceptibility tests using β-lactam antibiotics were performed. These antibiotics bind to the active site serine in the SXXK motif of PBPs and inhibit cell wall synthesis by the formation of an acyl-enzyme complex due to structural similarity to the natural substrate D-Ala-D-Ala (Sauvage and Terrak, 2016). Neither penicillin G nor ampicillin abolished the DD-carboxypeptidase activity of PBP6a^{wBm} after incubation overnight in a molar ratio of 1:10 (Figure 24). A Bocillin^{TM} FL-binding assay confirmed that penicillin did not bind to the protein *in vitro* (Supplementary Figure 5). Additionally, a more sensitive assay with radiolabeled penicillin also did not reveal any binding to PBP6a^{wBm} (data not shown). Altogether, these results indicate that PBP6a^{wBm} is resistant to β-lactam antibiotics.

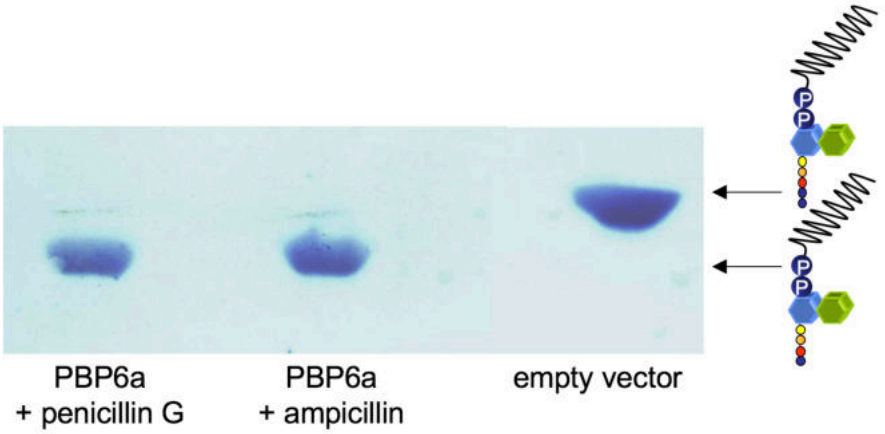

Figure 24: β-lactam susceptibility testing of PBP6a^{wBm}. The resistance of PBP6a^{wBm} to the β-lactams penicillin G and ampicillin (molar ratio 1:10) shown by TLC analysis.

3.1.9 *In vivo* β-lactamase activity assay of PBP6a^{wBm}

DD-carboxypeptidases and β-lactamases are members of the so-called serine proteases and have high structural similarities (Smith et al., 2013). Serine-β-lactamases hydrolyze the lactam ring by an active serine residue resulting in resistance to β-lactam antibiotics. A bifunctional DD-carboxypeptidase and β-lactamase activity was demonstrated in PBP5 from *Pseudomonas aeruginosa* explaining β-lactam resistance of these bacteria (Smith et al., 2013). As penicillin G and ampicillin were not able to inhibit PBP6a^{wBm} activity *in vitro* and penicillin-binding was not observed (see chapter 3.1.7), a β-lactamase assay was performed to examine if PBP6a^{wBm} cleaves β-lactam antibiotics. For this, PBP6a^{wBm} was expressed in *E. coli* JM83 cultures supplemented with CENTA^{TM} as a substrate and incubated for 16 h. Analysis of absorbance measurements of six independent assays showed an increase of λ_{405} from 0.48 (± 0.04 standard error of the mean (SEM)) to 1.36 (± 0.15 SEM) in cultures containing the positive control *E. coli* ML-35 pYC indicating successful CENTA^{TM} hydrolysis (Figure 25). In contrast, constant absorbance values around $\lambda_{405} = 0.38$ (± 0.02 SEM) were observed in cells expressing PBP6a^{wBm} in eight independent assays. Cultures expressing the empty vector control showed slightly increased λ_{405} levels from 0.4 (± 0.03 SEM) to 0.58 (± 0.07 SEM) after 16 h incubation in six independent assays. In conclusion, no β-lactamase activity for PBP6a^{wBm} was detected under the conditions tested.

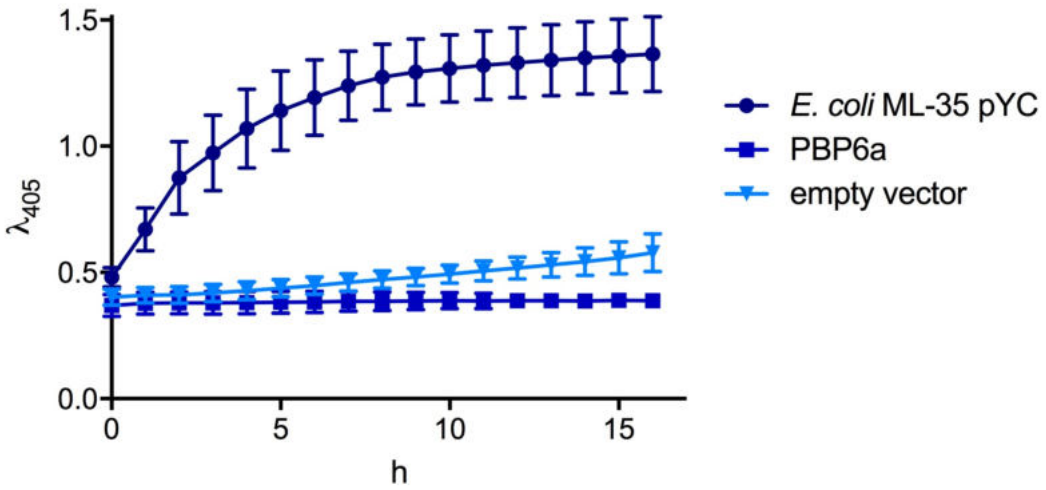

Figure 25: β-lactamase activity assay of PBP6a^{wBm} *in vivo*. *E. coli* JM83, carrying PBP6a^{wBm} in pASK-IBA2C were induced with 200 ng/ml AHT. β-lactamase activity was detected at λ_{405} using the chromogenic cephalosporin CENTA^{TM} as a substrate. *E. coli* ML35-pYC constitutively expressing a periplasmic β-lactamase were used as a positive control, pASK-IBA2C (empty vector) served as a negative control. PBP6a^{wBm} data represent means from eight independent assays, the positive and negative control were tested in six independent assays. Error bars represent ± SEM.

3.1.10 *In silico* binding of PBP6a^{wBm} to cefoxitin

In silico analysis predicted a binding of the β-lactam antibiotic cefoxitin to PBP6a^{wBm}, including the serine of the second SXXK motif S56 (Figure 26). Contrary to PBP6a from *E. coli*, PBP6a^{wBm} has two SXXK motifs allowing the enzyme to be active even when bound to a β-lactam. As the first SXXK serine is not involved in binding and *in vivo* assays indicate that SXXK motifs can substitute each other (see chapter 3.1.4), PBP6a^{wBm} might still be a functional DD-carboxypeptidase in the presence of a β-lactam.

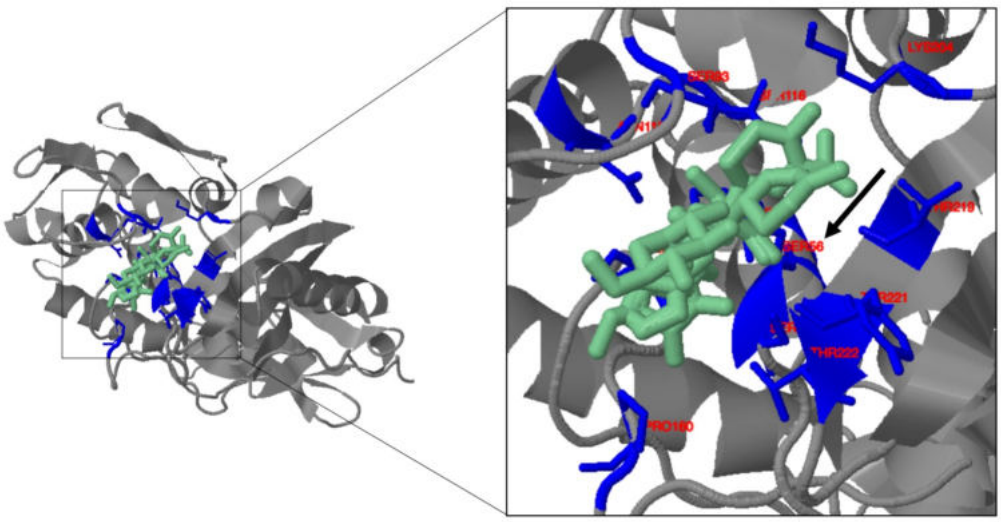

Figure 26: PBP6a^{wBm} bound to cefoxitin as predicted by 3DLigandSite. The residues S55, S56, K59, S93, S116, N118, S157, P160, K204, T219, Y221, T222 putatively involved in binding to cefoxitin (green) are labeled in red, their corresponding structures are marked in blue. The arrow points to the active site serine S56 of the SXXK motif predicted to be involved in binding.

3.2 Functional analysis of PBP2$^{w\mathrm{Bm}}$

3.2.1 Primary structure analysis of PBP2$^{w\mathrm{Bm}}$

In rod-shaped *E. coli*, PBP2 is an essential compound of the peptidoglycan biosynthesis multi-enzyme complex and promotes cell elongation as well as shape maintenance (Typas et al., 2012). The annotated wolbachial DD-transpeptidase homolog PBP2$^{w\mathrm{Bm}}$ (NCBI: WP_011256277) investigated in this thesis consists of 520 amino acids with an estimated size of 58 kDa. It harbors one predicted N-terminal transmembrane domain ranging from amino acids 1–35, but no signal peptide for periplasmic secretion (Supplementary Figure 6). PBP2$^{w\mathrm{Bm}}$ contains two SXXK, four SX(D/N) and one K(S/T)G motif. *E. coli* PBP2 (NCBI: WP_000776176.1) has only one SXXK motif, but four SX(D/N) and one KSG motif. A glycosyltransferase activity site was not identified in PBP2$^{w\mathrm{Bm}}$, thus it might be a monofunctional DD-transpeptidase like *E. coli* PBP2 (Sauvage et al., 2008). PBP2$^{w\mathrm{Bm}}$ was re-annotated on NCBI and is now listed as a putative PBP3, a DD-transpeptidase involved in cell division. PBP2$^{w\mathrm{Bm}}$ shares 28 % sequence identity with *E. coli* PBP2 and 24 % with *E. coli* PBP3 (NCBI: ARB43848.1) (Figure 27). Sequence alignment of PBP2$^{w\mathrm{Bm}}$ with PBP2$^{w\mathrm{Mel}}$ and PBP3$^{w\mathrm{Mel}}$ revealed a high similarity around 84 % to PBP2$^{w\mathrm{Mel}}$ and only 18 % to PBP3$^{w\mathrm{Mel}}$ (Supplementary Figures 7, 8). Thus, the term PBP2$^{w\mathrm{Bm}}$ was kept in this thesis as a description for this enzyme. However, the question remained whether this enzyme is involved in cell elongation or whether it is part of the cell division complex.

```
PBP2 wBm        ------------MWIKNKVFNRRAF-ILGGIQLTISTIFSCRLYSLQIRNRQKYEKLAD   46
PBP2 E. coli    ----MKLQNSFRDYTAESALFVRRAL-VAFLGILLLTGVLIANLYNLQIVRFTDYQTRSN   55
PBP3 E. coli    MKAAAKTQKPKR--QEEHANFISWRFALLCGCILLALAFLLGRVAWLQVISPDMLVKEGD   58
                              :   *    : :     *    .:  .:  **:       . .:

PBP2 wBm        NNRIRVAAIMPKRGRILDRNGIELAVDKISYIVLFDKQKISS-----EEVDWETLSEI--   99
PBP2 E. coli    ENRIKLVPIAPSRGIIYDRNGIPLALNRTIYQIEMMPEKVDN-----VQQTLDALRNVVD   110
PBP3 E. coli    MRSLRVQQVSTSRGMITDRSGRPLAVSVPVKAIWADPKEVHDAGGISVGDRWKALANALN   118
                . :::  :  .** * **.*  **:.     :    ::: .          .:* :

PBP2 wBm        -----------------------------------ESNVTKSSETKITALYKRHYPFGS   123
PBP2 E. coli    LTDDDIAAFRKERARSHRFTSIPVKTNLTEVQVARFAVNQYRFPGVEVKGYKRRYYPYGS   170
PBP3 E. coli    IPLDQLSARINANP-KGRFIYLARQVNP---DMA-DYIKKLKLPGIHLREESRRYYPSGE   173
                                                :  :    .:    :*:** *.

PBP2 wBm        ICSHTLGYTKKQQG-----------------INEAGISGIEYTYDHILKGKPGRSEQEIN   166
PBP2 E. coli    ALTHVIGYVSKINDKDVERLNNDGKLANYAATHDIGKLGIERYYEDVLHGQTGYEEVEVN   230
PBP3 E. coli    VTAHLIGFTN---------------------VDSQGIEGVEKSFDKWLTGQPGERIVRKD   212
                  :* :*:..                     .. *  *:*  ::. * *: *    . :

PBP2 wBm        SKKRIVRELSSIPQQDGQDVQLTIDIDLQEKIAEI-------FKGHKGSVTAIDVGNGEI   219
PBP2 E. coli    NRGRVIRQLKEVPPQAGHDIYLTIDLKLQQYIETL-------LAGSRAAVVVTDPRTGGV   283
PBP3 E. coli    RYGRVIEDISSTDSQAAHNLALSIDERLQALVYRELNNAVAFNKAESGSAVLVDVNTGEV   272
                   *::.:::..   * .::: *:**  **  :            .  .:..  *  .* :

PBP2 wBm        LTLYNSPSYDNNLFANKLSNEAWEG-LNTPSLPLVNRALSYQIPPGSIFKIIVALAGLKD   278
PBP2 E. coli    LALVSTPSYDPNLFVDGISSKDYSALLNDPNTPLVNRATQGVYPPASTVKPYVAVSALSA   343
PBP3 E. coli    LAMANSPSYNPNNL------------SGTPKEAMRNRTITDVFEPGSTVKPMVVMTALQR   320
                *:: .:***: * :             . *.  : **:      *.* .*  *.::.*.

PBP2 wBm        GIITPEEKFSCVGYMK---I--GERRFCCLKSKVHGYVSLNEAMALSCNTYFYNIGKKIS   333
PBP2 E. coli    GVITRNTSLFDPGWWQ---LPGSEKRYRDWKKWGHGRLNVTRSLEESADTFFYQVAYDMG   400
PBP3 E. coli    GVVRENSVLNTIPYTIPYRINGHEIK--DVA--RYSELTLTGVLQKSSNVGVSKLALAMP   376
                *::  :  :    :     :   * :        :. :.:.  :  *.:. . ::.  :

PBP2 wBm        VDSLVEMARKFGIGSGPLIGAFKEEAPGLLPDKDWRTRKLYSEWYLGDTVNLVIGQGYVL   393
PBP2 E. coli    IDRLSEWMGKFGYGHYTGID-LAEERSGNMPTREWKQKRFKKPWYQGDTIPVGIGQGYWT   459
PBP3 E. coli    SSALVDTYSRFGLGKATNLG-LVGERSGLYPQKQ--------RWSDIERVTFSFGYGL-M   426
                . * :   :** *    :. :  *  *  * ::         *   : : . :* *

PBP2 wBm        TTPLQLAVLAA-RIATGKEVIPRIEMSKTMQ----------DFPDID--IAHEHLSIVRK   440
PBP2 E. coli    ATPIQMSKALMILINDGIVKVPHLLMSTAEDGKQVPWVPPHEPPVGD--IHSGYWELAKD   517
PBP3 E. coli    VTPLQLARVYATIGSYGIYRPLSI--TK------------VDPPVPGERVFPESIVRTVV   472
                .**:*::         *      :  :.            : *  .  :       .

PBP2 wBm        AMFNMVNIKAGTYRKGLSS--IRIAGKTG--------------TPEINSKGESHKLFIAY   484
PBP2 E. coli    GMFGVANRPNGTAHKYFASAPYKIAAKSGTAQVFGLKANETYNAHKIAERLRDHKLMTAF   577
PBP3 E. coli    HMMESVALPGGGGVK-AAIKGYRIAIKTGTAKKVGPDGRYI--NK-------YIAYTAGV   522
                *:  .    *   *  :    :** *:*                              .

PBP2 wBm        GPYHDPRYAISVFIEYGKAPRQ---------DVAMANEILRYMLKG--------------   521
PBP2 E. coli    APYNNPQVAVAMILENGGAGPA---------VGTLMRQILDHIMLGDNNTDLPAENPAVT   628
PBP3 E. coli    APASQPRFALVVVINDPQAGKYYGGAVSAPVFGAIMGGVLRTMNIEPDALTTGDKNEFVI   582
                .*  :*: *: :.::   *              ::   :*  :

PBP2 wBm        ----------                                                    521
PBP2 E. coli    AAEDH-----                                                    633
PBP3 E. coli    NQGEGTGGRS                                                    592
```

Figure 27: Primary structure analysis and amino acid alignment of PBP2^{wBm} and *E. coli* PBP2 and PBP3. PBP2^{wBm} (WP_011256277.1) shares 28 % sequence identity to *E. coli* PBP2 (WP_000776176.1) and 24 % identity to *E. coli* PBP3 (ARB43848.1). Conserved SXXK, SX(D/N) and K(S/T)G motifs found in PBP2^{wBm} are written in bold letters, motifs which align to *E. coli* PBP2 and PBP3 are additionally framed in black. The predicted N-terminal transmembrane domain is highlighted gray. ***** fully conserved residue; **:** conservation between groups of strongly similar properties; **.** conservation between groups of weakly similar properties.

3.2.2 Secondary structure analysis of PBP2^{wBm}

To get a deeper insight into the putative active site of PBP2^{wBm}, secondary structure analysis was performed. Here, the three conserved motifs were localized based on sequence alignments to *E. coli*. Secondary structure analysis predicted that the first SXXK motif (S^{107}ETK) is outside the predicted catalytic center (Figure 28). The second motif (S^{265}IFK), which was found to be conserved in the *E. coli* PBP2, is probably localized in an α-helix and thus might comprise the active site with S^{320}CN (α-helix and loop) and K^{465}TG (β-sheet). The results of the structure analysis indicated that PBP2^{wBm} has a catalytic center and might be an active DD-transpeptidase. The gene *pbp2* from *w*Bm was cloned into pASK-IBA expression vectors, transformed into different *E. coli* strains and tested in *in vivo* and *in vitro* activity assays.

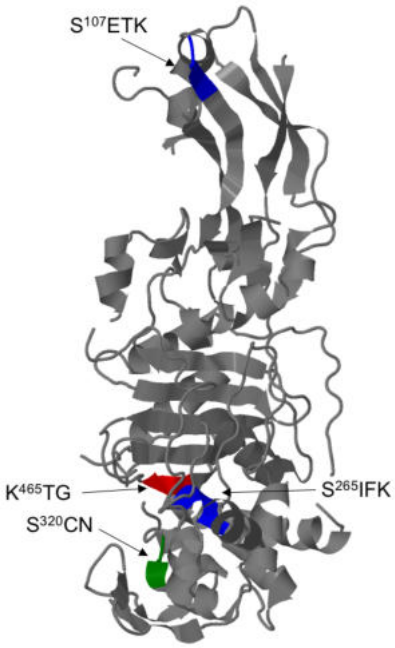

Figure 28: Secondary structure of PBP2^{wBm} as predicted by Phyre^2. S^{265}IFK (blue) might, together with S^{320}CN (green) and K^{465}TG (red), build the catalytic center of the enzyme, while S^{107}ETK is predicted to be located outside the active site (blue). The molecular structure of PBP2^{wBm} was illustrated by Jmol.

3.2.3 Characterization of PBP2^{wBm} *in vivo*

To gain a first insight into the function of the putative wolbachial DD-transpeptidase PBP2^{wBm}, *in vivo* complementation assays were performed with the PBP3 temperature sensitive *E. coli* MCI23 strain. As PBP2 and PBP3 have clearly distinct tasks in other bacteria like *E. coli*, a complementation of cell division deficiency would only be expected if PBP2^{wBm} was involved in cell division. PBP2^{wBm} with and without its predicted N-terminal transmembrane domain (PBP2ΔTM^{wBm}) was cloned into pASK-IBA6C and transformed into *E. coli* MCI23. Successful cloning and transformation were confirmed by sequencing (Supplementary Figures 9,10).

Additionally, *E. coli* MCI23 were transformed with the empty vector as a control for *in vivo* assays. *E. coli* MCI23 expressing recombinant PBP2ΔTM^{wBm}, PBP2^{wBm} or the empty vector control at 30 °C only had short and dividing cells (data not shown). At the non-permissive temperature of 42 °C, *E. coli* MCI23 expressing recombinant PBP2ΔTM^{wBm} were mainly short and dividing (Figure 29A), whereas *E. coli* MCI23 overexpressing PBP2^{wBm} and the empty vector control did not rescue cell division (Figure 29B,C). Analysis of six independent assays confirmed the observed results (Figure 29D,E). *E. coli* MCI23 expressing recombinant PBP2ΔTM^{wBm} were significantly shorter than PBP2^{wBm} and the empty vector control with 85.7 % (± 7.6 SD) short and dividing cells at 42 °C and 14.3 % (± 7.6 SD) elongated cells at 42 °C. In contrast, *E. coli* MCI23 overexpressing PBP2^{wBm} did not restore cell division with only 6 % (± 5.2 SD) short and 94 % (± 5.2 SD) elongated cells observed. Cells expressing the empty vector had 95.3 % (± 5.9 SD) filamentous and 4.6 % (± 5.9 SD) short cells. Possibly, the soluble PBP2ΔTM^{wBm} replaced the impaired *E. coli* PBP3 on the division site, while PBP2^{wBm} with its native transmembrane domain was not recruited to the divisome. In conclusion, the *in vivo* results indicated that PBP2^{wBm} might be an active DD-transpeptidase.

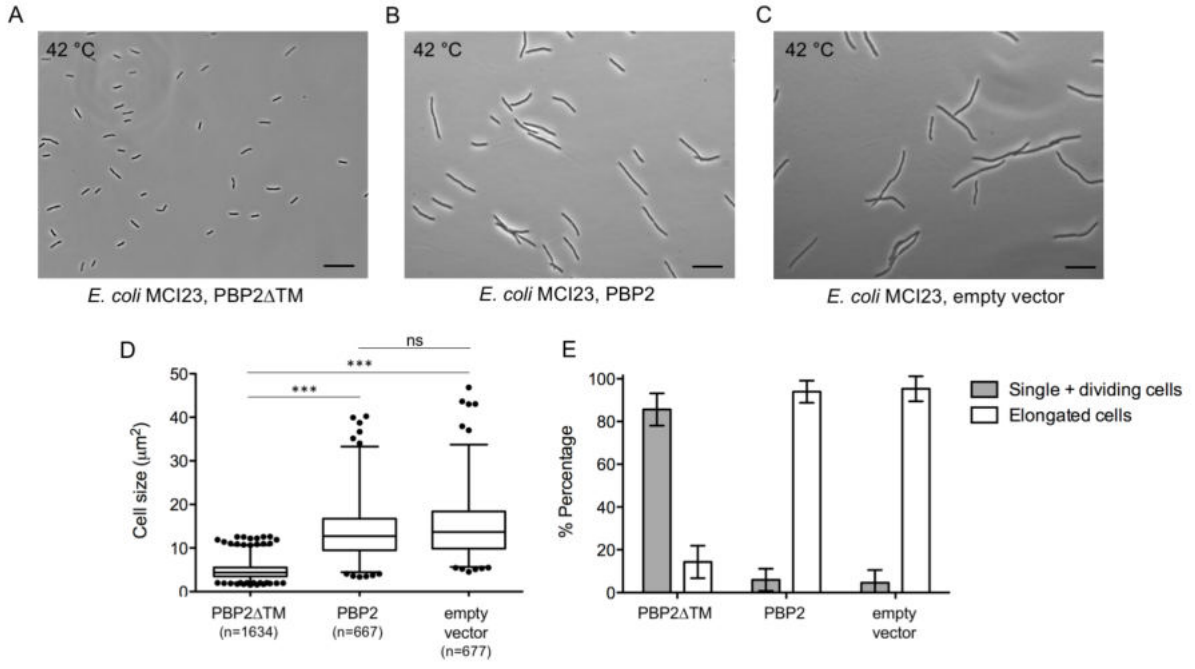

Figure 29: PBP2ΔTM^{wBm} rescues cell division in a temperature sensitive *E. coli* MCI23. A) Phase-contrast microscopy shows *E. coli* MCI23 expressing recombinant PBP2ΔTM^{wBm} are mainly short and dividing, while B) expressed PBP2^{wBm} are not able to restore cell division at 42 °C. C) The induced empty vector pASK-IBA6C is not able to restore cell division. Scale bars = 20 µm. D) At least 667 cells from 30 pictures taken from six independent assays per sample were measured by Image J. Boxes extend from the 25th to the 75th percentile. The line in the middle of the box is plotted at the median. Whiskers represent 1st and 99th percentiles. Statistical analysis was performed using Kruskal-Wallis test and Dunn's comparison post-hoc test. ns = not significant, *** = $P \leq 0.001$. E) Columns represent mean ± SD of relative occurrence of different phenotypes from five randomly chosen pictures in each experiment (n = 6).

3.2.4 Active site analysis of PBP2ΔTM^{wBm} *in vivo*

The serine of the SXXK motif catalyzes the enzymatic reaction of PBPs and the mutagenesis of SXXK motifs in PBP3 from *C. pneumoniae* was shown to inhibit enzyme activity (Otten, 2014). Thus, the active site serine of both SXXK motifs in PBP2ΔTM^{wBm} were changed to alanine (S107A and S265A) by mutagenesis PCR (Figure 30), successful amino acid substitution was confirmed by nucleotide sequencing (Supplementary Figure 11).

```
  1   MWIKNKVFNRRAFILGGIQLTISTIFSCRLYSLQIRNRQKYEKLADNNRIRVAAIMPKRG   60
 61   RILDRNGIELAVDKISYIVLFDKQKISSEEVDWETLSEIESNVTKSAETKITALYKRHYP  120
121   FGSICSHTLGYTKKQQGINEAGISGIEYTYDHILKGKPGRSEQEINSKKRIVRELSSIPQ  180
181   QDGQDVQLTIDIDLQEKIAEIFKGHKGSVTAIDVGNGEILTLYNSPSYDNNLFANKLSNE  240
241   AWEGLNTPSLPLVNRALSYQIPPGAIFKIIVALAGLKDGIITPEEKFSCVGYMKIGERRF  300
301   CCLKSKVHGYVSLNEAMALSCNTYFYNIGKKISVDSLVEMARKFGIGSGPLIGAFKEEAP  360
361   GLLPDKDWRTRKLYSEWYLGDTVNLVIGQGYVLTTPLQLAVLAARIATGKEVIPRIEMSK  420
421   TMQDFPDIDIAHEHLSIVRKAMFNMVNIKAGTYRKGLSSIRIAGKTGTPEINSKGESHKL  480
481   FIAYGPYHDPRYAISVFIEYGKAPRQDVAMANEILRYMLKG                     520
```

Figure 30: Primary structure analysis of PBP2ΔTM^{wBm} in pASK-IBA6C after site-directed mutagenesis. Serine residues from SXXK motifs were substituted by alanine (red bold letters). The predicted transmembrane domain (highlighted gray) was removed to increase solubility of the protein. The amino acid sequence is shown in single-letter code.

The plasmid containing mutated PBP2ΔTM^{wBm} was transformed into *E. coli* MCI23 and activity assays were performed (see chapter 3.2.3). *E. coli* MCI23 expressing PBP2ΔTM^{wBm} S107A, S265A or S107A-S265A were exclusively short or dividing at 30 °C (data not shown). At 42 °C, single mutation of the SXXK motifs did not impair PBP2ΔTM^{wBm} activity, still restoring division in 84.1 % (± 14.3 SD) (S107A) and 82.3 % (± 21.7 SD) (S265A) of cells (Figure 31). Expression of a PBP2ΔTM^{wBm} double active site mutant (S107A-S265A) revealed functional dependency of at least one functional serine of the SXXK motif as an increase to 72.5 % (± 13.6 SD) of elongated cells unable to divide was observed.

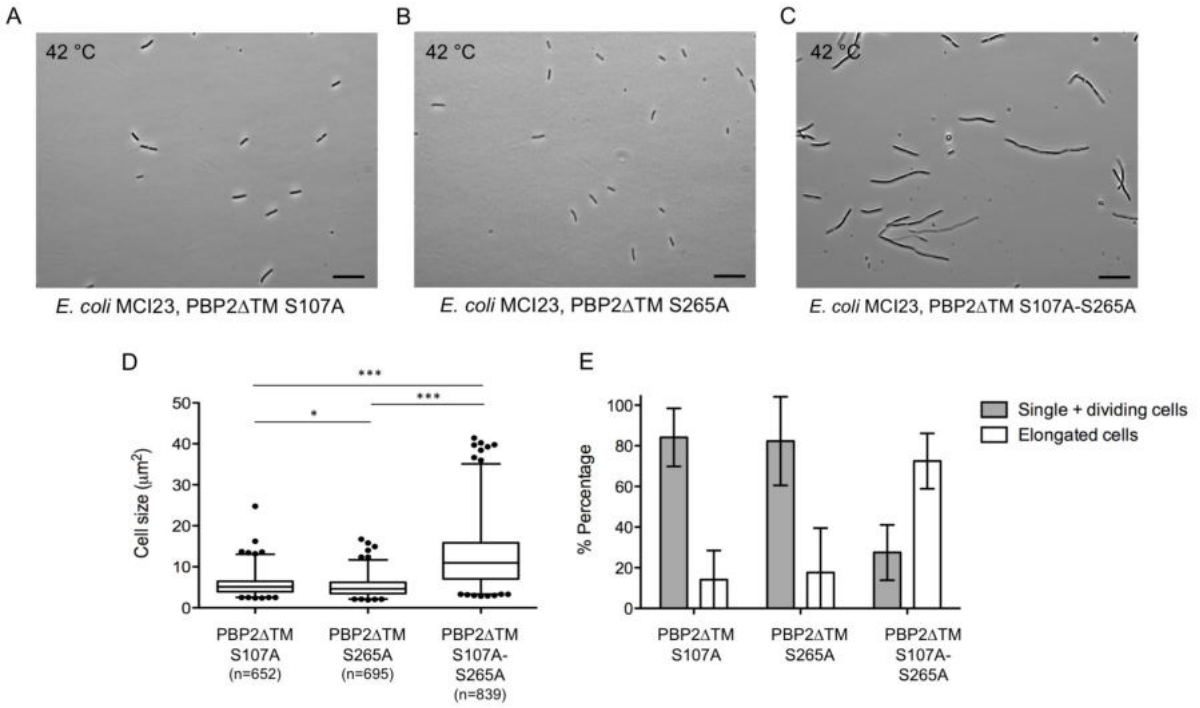

Figure 31: Complementation assay to test for the ability of PBP2ΔTM^{wBm} active site mutants to rescue cell division in a temperature sensitive *E. coli* MCI23 mutant. Phase-contrast micrographs shows *E. coli* MCI23 expressing PBP2ΔTM^{wBm} active site mutants A) PBP2ΔTM S107A and B) PBP2ΔTM S265A partially rescue cell division, while C) PBP2ΔTM S107A-S265A cannot restore growth defects resulting in elongated cells. Scale bars = 20 µm. D) At least 652 cells from 30 pictures taken from six independent assays per sample were measured by Image J. Boxes extend from the 25th to the 75th percentile. The line in the middle of the box is plotted at the median. Whiskers represent 1st and 99th percentiles. Statistical analysis was performed using Kruskal-Wallis test and Dunn's comparison post-hoc test. * = $P \leq 0.05$, *** = $P \leq 0.001$. E) Columns represent mean ± SD relative occurrence of different phenotypes at 42 °C from five randomly chosen pictures in each experiment (n = 6).

Growth of *E. coli* was monitored to exclude that the different observed phenotypes resulted from potential cell arrests induced by protein induction. In three independent measurements, all cultures grew exponentially after induction (Figure 32).

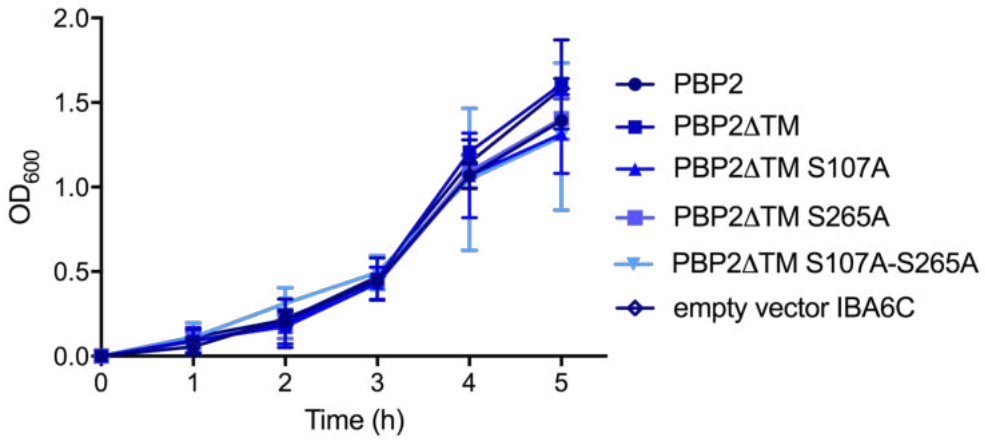

Figure 32: Growth kinetics of *E. coli* MCI23 during periplasmic expression of PBP2^{wBm}. Protein expression was induced at OD_{600} = 0.4 with 100 ng/ml tetracycline. OD_{600} was measured every hour. Each point represents mean ± SD (n = 3).

3.2.5 Mecillinam treatment of PBP2^{wBm} *in vivo*

Specific inhibition of PBP2 by the β-lactam mecillinam leads to spherical cells instead of rods in *E. coli* (Spratt and Pardee, 1975). Thus, the potential sensitivity of PBP2ΔTM^{wBm} to this antibiotic was examined. *In vivo* complementation assays using *E. coli* MCI23 at the non-permissive temperature of 42 °C were conducted (see chapter 3.2.3) in the presence of mecillinam in six independent assays. *E. coli* MCI23 overexpressing PBP2ΔTM^{wBm} were mainly short and rod-shaped indicating that mecillinam did not affect the activity of this enzyme (Figure 33A). Control cultures with uninduced PBP2ΔTM^{wBm} had spherical cells due to the inhibition of PBP2 from *E. coli* by mecillinam (Spratt and Pardee, 1975) (Figure 33B). Cultures overexpressing the empty vector showed an altered phenotype with elongated, but also spherical cells in the presence of mecillinam (Figure 33C). *E. coli* MCI23 with the uninduced empty vector served as a further control resulting in spherical cells after mecillinam treatment (Figure 33D). These results suggest that PBP2^{wBm} is not inhibited by mecillinam.

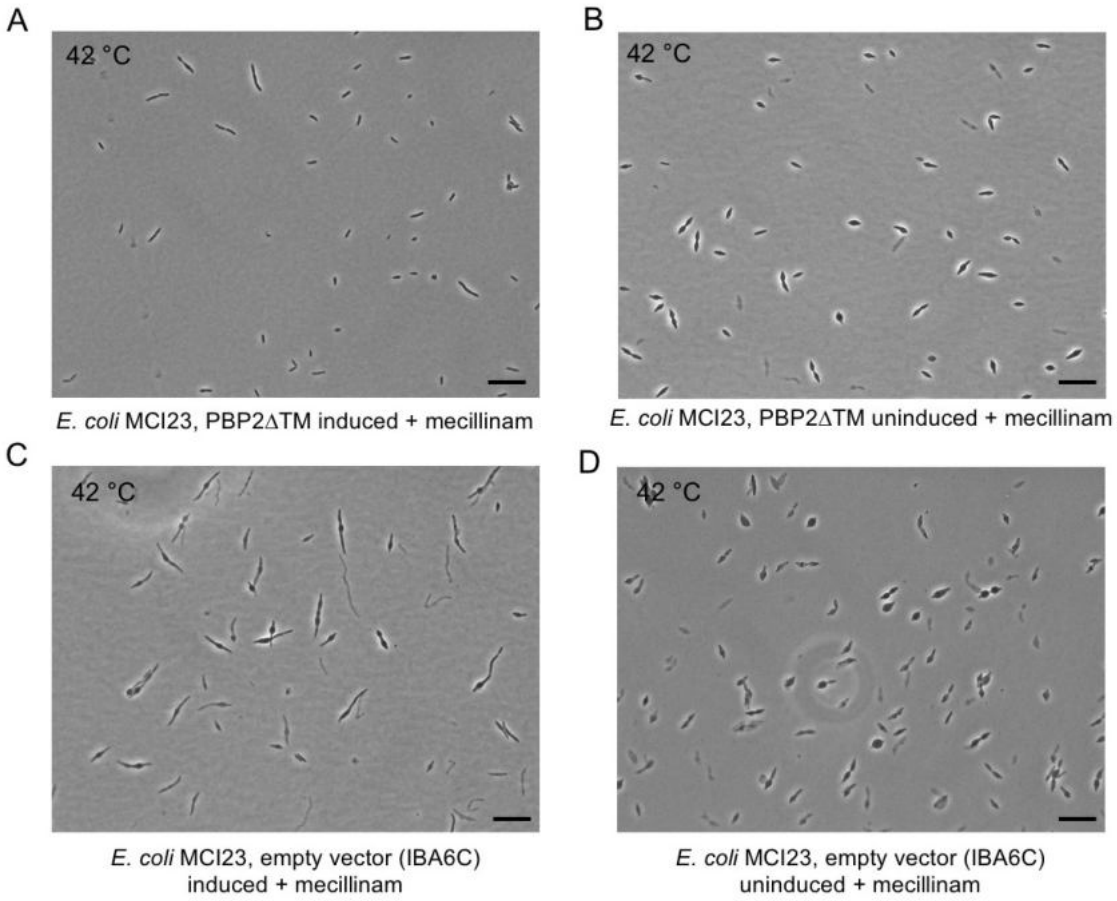

Figure 33: Cell division of *E. coli* MCI23 expressing PBP2ΔTM^{wBm} is not inhibited by mecillinam, a specific inhibitor of PBP2. A) *E. coli* overexpressing PBP2ΔTM^{wBm} complement cell division in the presence of mecillinam, while B) uninduced cells show a spherical phenotype. C) *E. coli* expressing the empty vector pASK-IBA6C are partially elongated, but also show a spherical phenotype. D) Uninduced cultures harboring the empty vector are spherical after mecillinam treatment.

3.2.6 Periplasmic expression and purification of recombinant PBP2^{wBm}

As previous attempts to get soluble protein by cytoplasmic overexpression in pET vectors were unsuccessful (data not shown), the PBP2^{wBm} encoding gene was cloned into pASK-IBA vectors for co-solvent assisted periplasmic expression (Otten et al., 2015). *Ppb2* was cloned with and without its predicted transmembrane domain (ΔTM). This modification was performed to allow the protein to accumulate in the periplasm in a soluble and correctly folded state. In the following step, small-scale overexpression pre-tests in different *E. coli* strains (C43, JM83 and W3110) and in the presence of different co-solvents were carried out to identify conditions that facilitate the production of recombinant PBP2^{wBm} and yield the highest amounts of soluble protein. Taken together, the overproduction and purification conditions were optimized regarding expression strain, addition of co-solvents and detergents, and recombinant PBP2^{wBm} was successfully purified for the first time (Figure 34). Although the largest proportion of recombinant protein was found in flow-through and wash fractions, mannitol-assisted overproduction in *E. coli* JM83 for 4 h at 25 °C resulted in soluble PBP2ΔTM^{wBm}. By adding the detergent Tween 20 to the lysis Buffer P, also soluble PBP2^{wBm} with its native transmembrane domain was purified. Protein concentrations of single elution fractions were around 100 µg/ml (PBP2^{wBm}) or 200 µg/ml (PBP2ΔTM^{wBm}) respectively, which was sufficient for biochemical characterization.

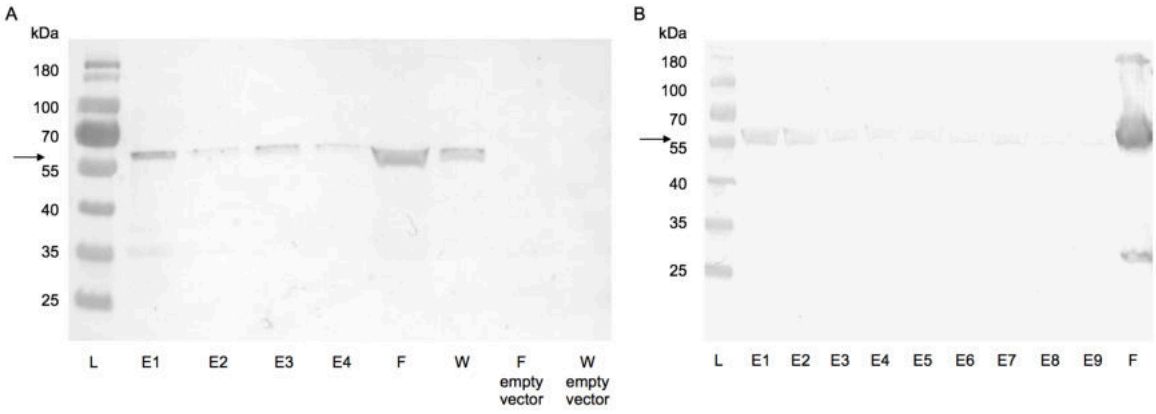

Figure 34: Purification of PBP2ΔTM^{wBm} and PBP2^{wBm} via Strep-Tactin affinity chromatography. Western Blot analysis shows recombinant protein from different steps of the purification procedure of A) PBP2ΔTM^{wBm}, the empty vector pASK-IBA2C and B) PBP2^{wBm}. L = Ladder, E = Elution fractions, F = Flow through, W = Wash Fraction, F empty = Flow through of the empty vector control, W empty = Wash fraction of the empty vector control. Arrows point to expected protein size.

3.2.7 Characterization of PBP2^{wBm} *in vitro*

3.2.7.1 DD-transpeptidase activity test using lipid II as a substrate

The cross-linking of lipid II stem peptide moieties by monofunctional DD-transpeptidases is poorly characterized *in vitro* even in well investigated bacteria due to a lack of established assays (Dougherty and Pucci, 2011). Still, the presence or absence of monomeric lipid II on a TLC plate can indicate DD-transpeptidation since polymerized lipid II cannot be extracted by butanol-pyridine acetate and is consequently not detectable on the TLC plate. PBP2^{wBm} was incubated with 2 nmol synthesized lipid II overnight and reaction products were analyzed by TLC. The corresponding elution fraction of the empty vector served as a negative control, PBP2 from *S. aureus*, which is a bifunctional PBP with DD-transpeptidase and glycosyltransferase activity, served as a positive control. In first assays, a bright lipid II band was detectable on the TLC plate after overnight incubation with PBP2^{wBm} (Figure 35). In the positive control with PBP2 from *S. aureus*, no lipid II was detectable indicating polymerization of lipid II. In contrast, the lipid II band was still present after incubation with the empty vector elution fraction, implying that lipid II was not polymerized in this sample.

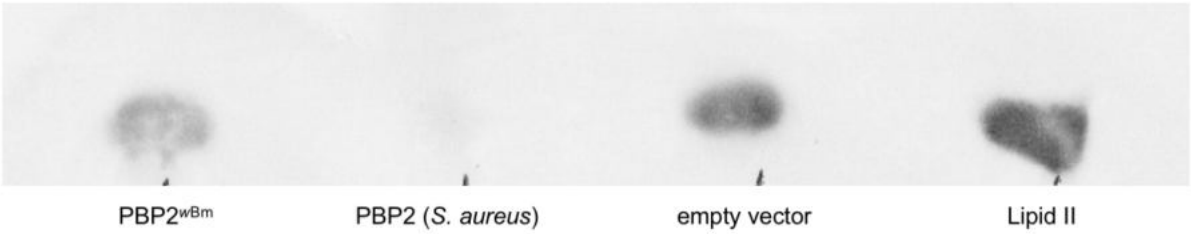

Figure 35: *In vitro* activity assay of PBP2^{wBm}. PBP2^{wBm} was incubated with lipid II and incubated overnight. The mixture was applied on a TLC and stained bands were quantified using Image Quant^{TM} TL. Polymerization of the monomeric lipid II results in extinction of the lipid II band on a TLC as shown here for the positive control PBP2 from *S. aureus* with only 0.18 nmol detectable residual lipid II. PBP2^{wBm} shows a slight band containing 0.78 nmol lipid II. The overexpressed and purified empty vector containing 1.43 nmol lipid II after overnight incubation served as a negative control to exclude activity of potentially contaminating *E. coli* DD-transpeptidases. 2 nmol pure lipid II were applied to the TLC as a reference of band intensity for quantification.

These observations were confirmed by quantification of the bands (Image Quant^{TM} TL). As a reference, 2 nmol pure lipid II were applied to the TLC. Based on the intensity of this band, the amount of monomeric lipid II in the other samples was calculated. The mixture with the positive control PBP2 from *S. aureus* had 0.18 nmol residual lipid II after overnight incubation. In the PBP2^{wBm} containing sample, 0.78 nmol lipid II were detected, while the mixture with the empty vector contained 1.43 nmol lipid II. Assays were repeated under different conditions (time, temperature, pH, increased protein concentration), but none of them resulted in increased extinction of the lipid II band in the presence of PBP2^{wBm}.

3.2.7.2 Penicillin-binding assays

Penicillin-binding was tested by incubating cleared lysates, wash fractions and elution fractions of overexpressed PBP2^{wBm} with Bocillin^{TM} FL. While 4 µg of purified PBP2 from *S. aureus* (positive control) was sufficient to observe a distinct fluorescent band, no bands were detectable in lanes containing PBP2^{wBm} (Supplementary Figure 5). Further, a more sensitive assay using radiolabeled penicillin also did not reveal binding to PBP2^{wBm} (data not shown). These results indicate that PBP2^{wBm} might not bind to β-lactam antibiotics.

3.2.8 *In vivo* β-lactamase activity assay of PBP2^{wBm}

As PBP2^{wBm} was resistant to mecillinam *in vivo* (see chapter 3.2.5) and no penicillin-binding of was observed *in vitro* (see chapter 3.2.7.2), a potential β-lactamase activity of PBP2^{wBm} was examined using CENTA^{TM} as a substrate. PBP2^{wBm} and PBP2ΔTM^{wBm} were expressed in *E. coli* JM83, supplemented with CENTA^{TM} and incubated for 16 h. In six independent experiments, absorbance λ_{405} increased of from 0.48 (± 0.04 SEM) to 1.36 (± 0.15 SEM) in cultures containing the positive control *E. coli* ML-35 pYC indicating CENTA^{TM} hydrolysis (Figure 36). Cultures expressing PBP2^{wBm} only slightly increased from $\lambda_{405} = 0.4$ (± 0.02 SEM) to 0.54 (± 0.04 SEM) in seven independent assays. Similar values were observed in cells expressing PBP2ΔTM^{wBm} with a slight increase from $\lambda_{405} = 0.4$ (± 0.02 SEM) to 0.52 (± 0.05 SEM) in seven experiments. Cultures expressing the empty vector control slightly increased from $\lambda_{405} = 0.4$ (± 0.03 SEM) to 0.58 (± 0.07 SEM) in six independent assays. No β-lactamase activity of PBP2^{wBm} or PBP2ΔTM^{wBm} was detected under these conditions.

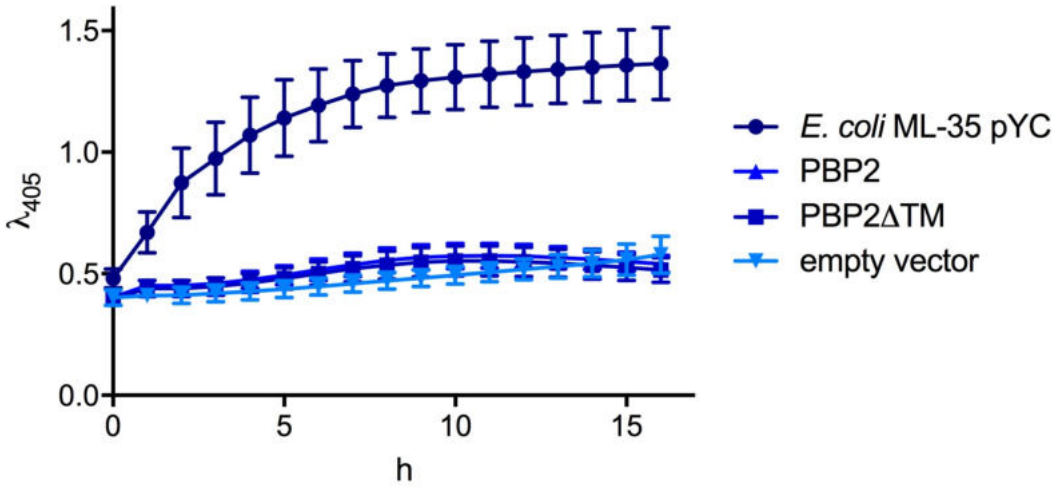

Figure 36: β-lactamase activity assay of PBP2^{wBm} *in vivo*. *E. coli* JM83 with PBP2^{wBm} in pASK-IBA6C or PBP2ΔTM^{wBm} in pASK-IBA2C were induced with 200 ng/ml AHT. β-lactamase activity was detected at λ_{405} using CENTA^{TM} as a substrate. *E. coli* ML35-pYC were used as a positive control, pASK-IBA2C (empty vector) served as a negative control. PBP2^{wBm} and PBP2ΔTM^{wBm} data represent means from seven independent assays, the positive and negative control were tested in six independent assays. Error bars represent ± SEM.

3.2.9 *In silico* modeling of PBP2^{wBm}

In silico analysis predicted a binding of the β-lactam antibiotic cefoxitin, including the serine of the second SXXK active site motif S265 (Figure 37). As the first SXXK motif is not involved in binding, PBP2^{wBm} might still be active in the presence of a β-lactam with inactivated S265 as indicated by *in vivo* assays (see chapter 3.2.2 and 3.2.3).

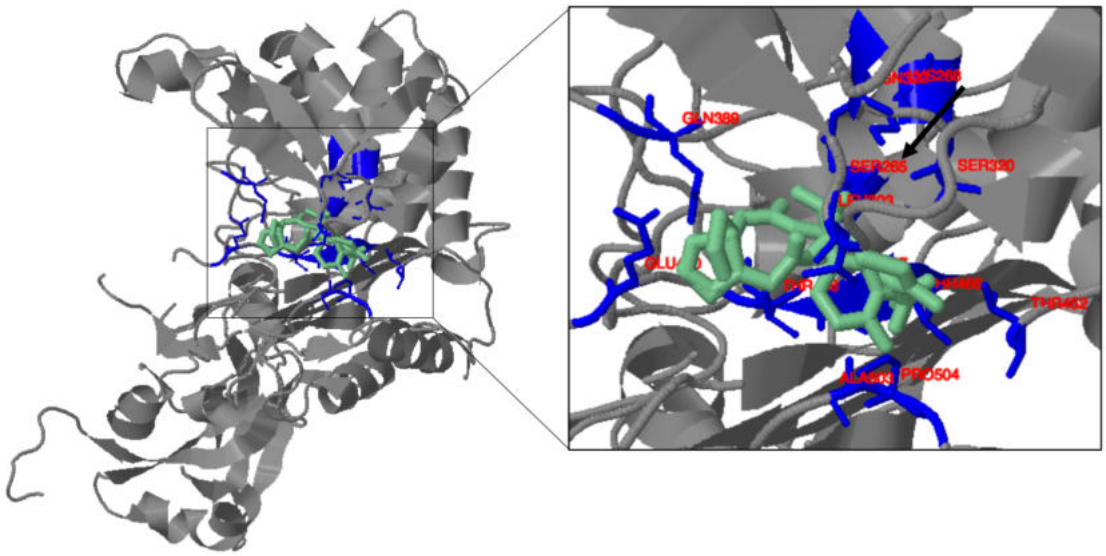

Figure 37: 3D structure of PBP2^{wBm} bound to cefoxitin as predicted by 3DLigandSite. The residues S265, K268, L303, S320, N322, 389, T452, T466, G467, T468, E470, A503, P504 putatively involved in binding to cefoxitin (green) are marked in blue. The arrow points to the active site serine S265 of the SXXK motif.

3.3 Functional analysis of Pal^{wBm}

3.3.1 Primary structure analysis of Pal^{wBm}

Peptidoglycan-associated lipoprotein Pal^{wBm} is among the most abundant proteins in *Wolbachia* (Voronin et al., 2014). Pal^{wBm} (NCBI: AAW70743.1) consists of 159 amino acids with a predicted molecular mass of 18.5 kDa and shares 37 % sequence identity with *E. coli* Pal (NCBI: WP_001560401.1) (Figure 38). Pal^{wBm} contains a signal peptide ranging from amino acid 1–24 suggesting the enzyme being localized in the periplasm (Supplementary Figure 12). Fosfomycin treatment of *Wolbachia* (blocking of lipid II synthesis) results in enlarged cells and a perturbed localization of wolbachial Pal indicating that this protein is necessary to connect the inner and outer membrane, in particular during cell division (Vollmer et al., 2013). The interaction partner of Pal might be lipid II. In *E. coli,* outer membrane-anchored lipoproteins control PBP activity by binding and inducing conformational changes (Paradis-Bleau et al.,

2010; Typas et al., 2012; Egan et al., 2014). Thus, a potential binding between Pal^{wBm} and PBP2^{wBm} as well as Pal^{wBm} and lipid II were investigated in *in vitro* experiments in this thesis.

```
Pal wBm        -MWSRLVAMCCFCLLLTGVSSCSKR----------------------GVNA---INKMNF     34
E. coli Pal    MQLNKVLKGLMIALPVMAIAACSSNKNASNDGSEGMLGAGTGMDANGGNGNMSSEEQARL     60
                  .:::    :.* : .:::**..                          * .     :: .:

Pal wBm        VVKQ-MKEKRVFFDYDKSDISEAGADTLLDVMEVLQDDPNVKVTLIGHTDNRGSYEYNVA     93
E. coli Pal    QMQQLQQNNIVYFDLDKYDIRSDFAQMLDAHANFLRSNPSYKVTVEGHADERGTPEYNIS    120
               ::*  ::: *:** ** ** .  *: *    :.*:.:*. ***: **:*:**: ***::

Pal wBm        LGARRADAAKNFMVSCTPYLENRIKTASKGETEPLVYVADDSKNSKYEKEHAKNRRVEFS    153
E. coli Pal    LGERRANAVKMYLQGKG-VSADQISIVSYGKEKPVVLGHDEAA-------YAKNRRAVLV    172
               ** ***:*.* :: .      ::*. .* *: :*:*   *::        :*****. :

Pal wBm        FSGMKK                                                          159
E. coli Pal    Y-----                                                          173
               :
```

Figure 38: Amino acid alignment of Pal^{wBm} and *E. coli* Pal. Pal^{wBm} (AAW70743.1) shares 37 % sequence identity with *E. coli* Pal (WP_001560401.1). The predicted signal peptide ranges from amino acids 1–24 (highlighted gray). ***** fully conserved residue; **:** conservation between groups of strongly similar properties; **.** conservation between groups of weakly similar properties.

3.3.2 Pal^{wBm} interaction with PBP2^{wBm}

To measure a potential interaction between Pal^{wBm} and PBP2^{wBm} *in vitro*, biolayer interferometry was performed. Biotinylated Pal^{wBm} was immobilized on a streptavidin biosensor. Purified PBP2ΔTM^{wBm} or the empty vector control was used as the analyte and applied to the biosensor. Here, a concentration-dependent interaction of PBP2ΔTM ^{wBm} with Pal^{wBm} was observed, but not from supernatant of the overexpressed empty vector control, as exemplarily shown (Figure 39). In five independent assays using purified protein from two different expressions, the interaction of Pal^{wBm} and PBP2ΔTM ^{wBm} had a dissociation constant with a mean of 12.1 (±3.4 nM SD), indicating a high affinity between the proteins.

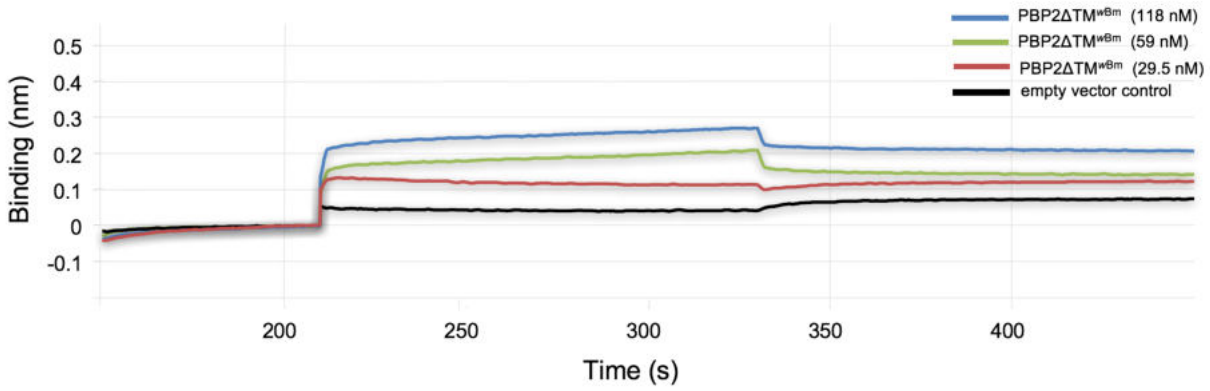

Figure 39: Interaction between PBP2ΔTM^{wBm} and Pal^{wBm} detected by biolayer interferometry (BLI). Biotinylated Pal^{wBm} was immobilized on a streptavidin biosensor PBP2ΔTM^{wBm} (29.5 nM – 118 nM) was used as an analyte. Calculated dissociation constant in this assay was 9.7 nM. The empty vector served as a negative control. The graph is representative for five experiments using purified PBP2ΔTM^{wBm} from two different expressions.

3.3.3 Pal^{wBm} interaction with lipid II

Surface plasmon resonance was used to measure a possible protein-lipid II interaction between Pal^{wBm} and lipid II (either mDAP or L-Lys). Pal^{wBm} was immobilized on a CM5 chip using a strep-tag II specific monoclonal antibody. Lipid II was dissolved in running buffer and used as the analyte of the binding reaction. Pal^{wBm} showed a higher affinity for lipid II with an mDAP residue at position 3 in the pentapeptide side chain typically found in Gram-negative bacteria compared to lipid II with an L-Lys residue at position 3 typically found in Gram-positive bacteria (Figure 40).

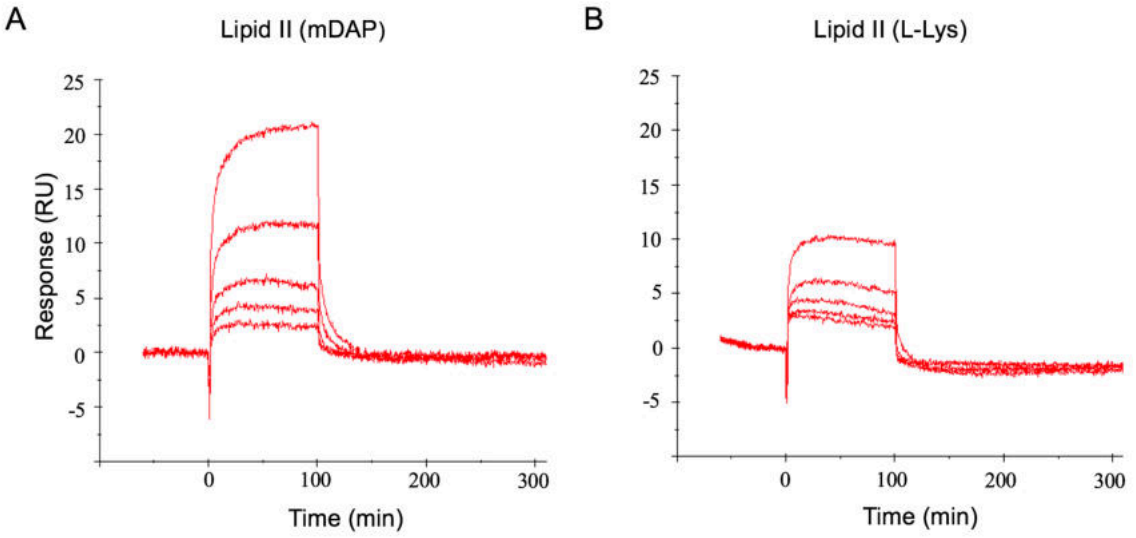

Figure 40: Binding of Pal^{wBm} to lipid II. Pal^{wBm} has a higher affinity for A) lipid II with an mDAP residue compared to B) lipid II with an L-Lys residue at position 3 in the pentapeptide side chain as revealed by surface plasmon resonance. Pal^{wBm} was immobilized on a CM5 chip using a strep-tag II specific monoclonal antibody. Lipid II dissolved in running buffer (0–12.5 µM) was used as the analyte of the binding reaction.

3.4 Functional analysis of AmiD^{wMel}

3.4.1 Primary structure analysis of AmiD^{wMel}

The genomes of insect *Wolbachia* such as *w*Mel encode a putative peptidoglycan hydrolase, the N-acetylmuramoyl-L-alanine amidase AmiD, although a functional cell wall has not been detected. AmiD^{wMel} (NCBI: AAS14728) has 497 amino acids and is almost double the size of AmiD from *E. coli* (NCBI: NP_415388) with 257 amino acids (Kerff et al., 2010) (Figure 41). Sequence alignments with periplasmic *E. coli* AmiA, AmiB, AmiC and AmiD reveal the highest homology to *E. coli* AmiD with 27 % sequence identity. AmiD^{wMel} contains an N-terminal predicted signal sequence from amino acids 1–30 for the transport into the periplasm (Supplementary Figure 13). However, the signal sequence lacks a typical lipobox

motif with a conserved cysteine residue for lipidation and insertion into the outer membrane suggesting that AmiD^{wMel} is not a lipoprotein. A putative amidase catalytic site with three conserved zinc-binding residues is present (H^{79}, H^{187} and D^{207}). Additionally, two SXXK, two SX(D/N) and one K(S/T)G motif are conserved in AmiD^{wMel}.

```
AmiD wMel      MKIQLSKVNKYLLVLLITVSAFLISGQVSSSSNIENDFQDLQEKLPLLKDQDLLFLDPAS    60
AmiD E. coli   -------MRRFF---WLVAAALLLAGCAGEKGIVEKEGYQLDTRR---------------    35
                      :.:::    :..:*:*::* ..... :*::  :*: :

AmiD wMel      ALNYGDRAGKKVLMVIVHHTETSTLKGTKDTLNARGLSVHFIVD-------RDGSITLMV   113
AmiD E. coli   ----QAQAAYPRIKVLVIHYTADDFDSSLATLTDKQVSSHYLVPAVPPRYNGKPRIWQLV    91
                     :*.   : *:* *  :. :..:  **. : :* *::*         .  *  :*

AmiD wMel      PLEKEAWHAGISYARVKVDSKLEELRKLNNYSVGIEIVNTGLE---------PFPEEQMR   164
AmiD E. coli   PEQELAWHAGISAWRG--------ATRLNDTSIGIELENRGWQKSAGVKYFAPFEPAQIQ   143
               * :: *******  *           :**: *:***: * * :          **   *::

AmiD wMel      SVKELILYLMERFKIKRDMIFSHSEIGTIVYDPELGYTMRKPDPHKLFDWELLEKNEIGL   224
AmiD E. coli   ALIPLAKDIIARYHIKPENVVAHADIA----------PQRKDDPGPLFPWQQLAQQGIGA   193
               ::  *   :: *::** : :.:*::*.            ** **  ** *: * :: **

AmiD wMel      HISDRINPKDAKHKMGKTLYKAGDRNEG---ILKLKQRLNRFFYKIEPWNDKRGNVIFPD   281
AmiD E. coli   WPDAQR----------VNFYLAGRAPHTPVDTASLLELLARYGYDVKPDMTPREQ-----   238
                 . :            .:* **   .      .* : * *: *.::*    * :

AmiD wMel      NNADYSDEFDENFVWVIYQFSIHNLPREIRKDLPLKLEQADIFPEFFSEYSHGISSSYLT   341
AmiD E. coli   -------------RRVIMAFQMHFRPTLYNGEA--DAETQAIAEALLEKYGQD-------   276
                          **  *.:*  *   . :   . *   *   ::.:*.:.

AmiD wMel      FSEKIKSTLQPCLSKVDYENLLSSLAQYENNISPDASTTLMYKIKLYYGSYLRYRIWSSL   401
AmiD E. coli   ------------------------------------------------------------   276

AmiD wMel      YKPFKLNVLEELEILKSGVLSLKSLDSSKAAEVSSLIDSFKVDISLEFQGFEKQWFQEFK   461
AmiD E. coli   ------------------------------------------------------------   276

AmiD wMel      NAWRQEFIPSLEEQITWTALHEAILEYLEKAKEEIR                           497
AmiD E. coli   -----------------------------------                            276
```

Figure 41: Sequence alignment of AmiD^{wMel} with *E. coli* AmiD. AmiD^{wMel} (AAS14728) shares 27 % sequence identity to *E. coli* AmiD (NP_415388). The signal peptide of AmiD^{wMel} (highlighted gray) was predicted by SignalP and lacks a cysteine-containing lipobox motif that mediates the insertion into the outer membrane as found in *E. coli* (LAGC, underlined). The three conserved zinc-coordinating residues of the amidase active site are shaded in black. AmiD^{wMel} additionally contains two SXXK, two SX(D/N) and one K(S/T)G motif (bold letters).

3.4.2 Secondary structure analysis of AmiD^{wMel}

The active site of AmiD^{wMel} comprises three conserved zinc-coordinating residues (H79, H187, D207). *In silico* analysis of AmiD^{wMel} predicted that these residues indeed bind to zinc, thus it is highly possible that they are essential for N-acetylmuramoyl-L-alanine amidase activity (Figure 42). However, the modeling was incomplete because it was based on homologies to the presumed *E. coli* ortholog which is half the size of AmiD^{wMel} (see chapter 3.4.1). Thus, the putative DD-carboxypeptidase active site could not be analyzed as it is located in the C-terminus outside the predicted secondary structure of AmiD^{wMel}. For functional analysis of AmiD^{wMel}, the gene was cloned and transformed into expression strains by

Dr. Miriam Wilmes, IMMIP. As part of this thesis, the enzyme was overproduced in *E. coli* JM83 by co-solvent assisted periplasmic expression which has been established for chlamydial proteins (Otten et al., 2015). Activity was tested by *in vivo* and *in vitro* assays. The potential dependency on zinc was tested by mutation of the respective residues in the enzyme.

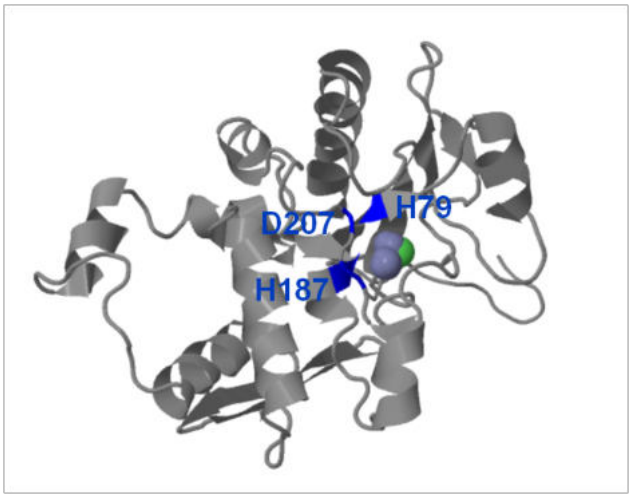

Figure 42: 3D structure of AmiD^{wMel} bound to zinc as predicted by 3DLigandSite. The zinc-coordinating residues H79, H187 and D207 are marked in blue, zinc ions are marked in green-gray.

3.4.3 Characterization of AmiD^{wMel} *in vivo*

3.4.3.1 AmiD^{wMel} complementation assay with an *E. coli* amidase mutant

E. coli AmiD is not involved in cell separation and it has been hypothesized that the insertion into the outer membrane prevents movement of AmiD to the septum (Uehara et al., 2010). As AmiD^{wMel} lacks a lipobox motif, the enzyme might be soluble in the periplasm after cleavage of its predicted signal peptide and thus might be involved in cell division. Hence, it was tested if AmiD^{wMel} can restore the normal phenotype of an *E. coli* ADE24 Δ*amiABC* triple knockout mutant. *E. coli* ADE24 is characterized by long chains of cells due to the deletion of all three periplasmic amidases involved in cell separation (Klöckner et al., 2014). To prevent impaired growth of cultures, *E. coli* ADE24 harbor pBAD33-amiC which restores cell division defects and which can be blocked by glucose. AmiD^{wMel} without its native signal peptide was cloned in pASK-IBA2 and IBA2C by Dr. M. Wilmes and transformed into *E. coli* ADE24 for periplasmic expression. As part of this thesis, AmiD^{wMel} was cloned with its native signal peptide in pASK-IBA3 and transformed into *E. coli* ADE24 for cytoplasmic expression. Expression of *E. coli* AmiC was blocked by adding 0.8 % glucose to the culture, which resulted in long chains (Figure 43A). Expression of AmiD^{wMel} in three independent assays did not rescue cell separation in the *E. coli* Δ*amiABC* triple mutant in none of the pASK-IBA vectors (Figure 43B-D). The induced empty vector served as a control for all constructs.

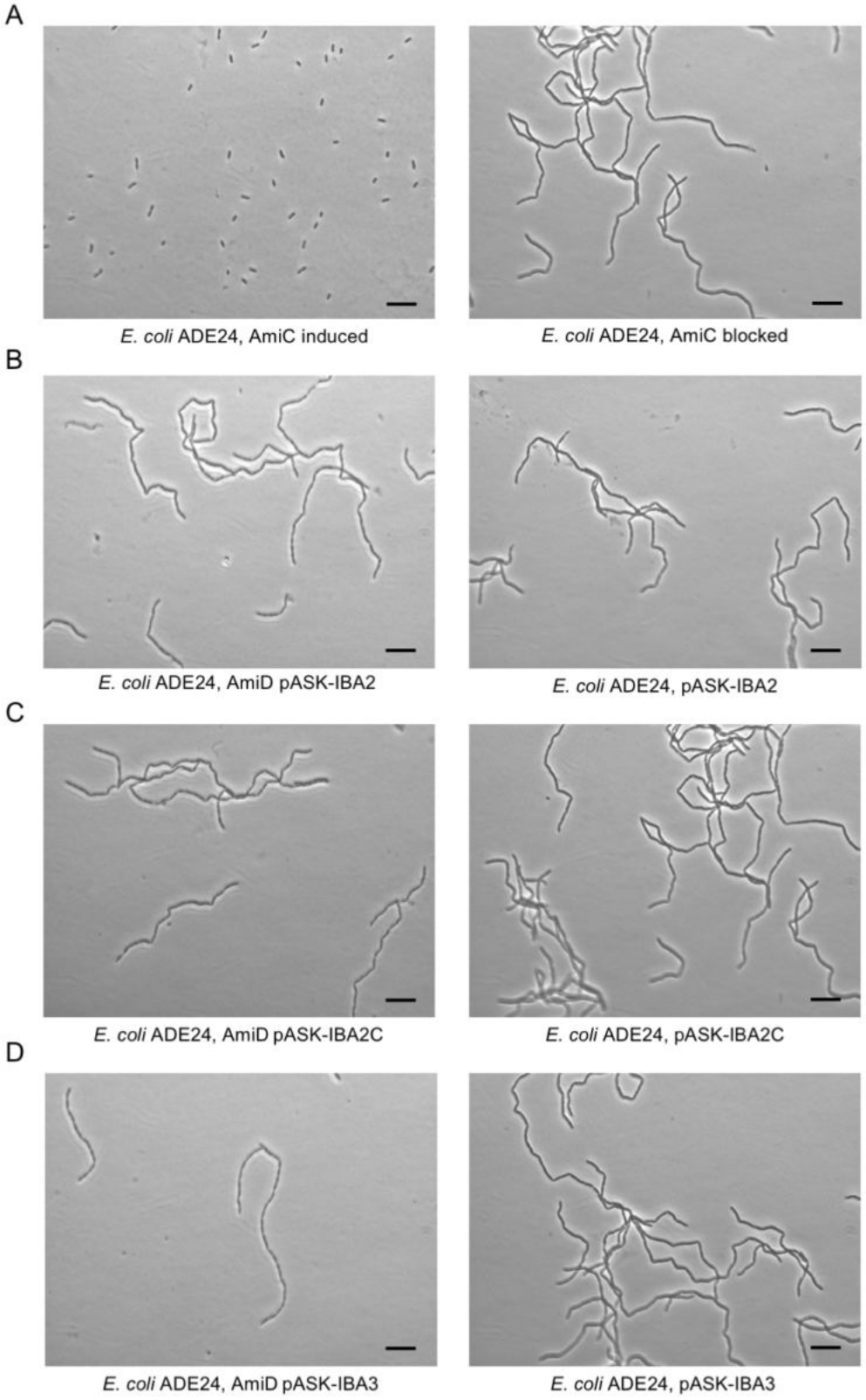

Figure 43: Complementation assay of *E. coli* Δ*amiABC* triple-knockout mutant ADE24 with AmiD^{wMel}. A) *E. coli* ADE24 harbor an arabinose-inducible plasmid with *amiC* (*E. coli*). In the presence of 0.8 % glucose, *amiC* expression is blocked resulting in long chains of cells. In the presence of glucose and 100 ng/ml tetracycline, expression of AmiD^{wMel} with either B) and C) the OmpA leader sequence (pASK-IBA2, pASK-IBA2C) or D) its native signal sequence (pASK-IBA3) did not complement cell division. Cells transformed with the empty vectors pASK-IBA2, pASK-IBA2C and pASK-IBA3 were used as controls. Scale bars = 20 µm.

To confirm that AmiD^{wMel} was expressed in *E. coli* ADE24, cultures were harvested and proteins were extracted. Western Blot analysis revealed that the protein was expressed, but it was half the expected size already after 1 h of expression (Figure 44). Due to the high proteolytic activity of *E. coli* ADE24, no conclusion could be drawn if AmiD^{wMel} is able to restore the normal phenotype in this strain.

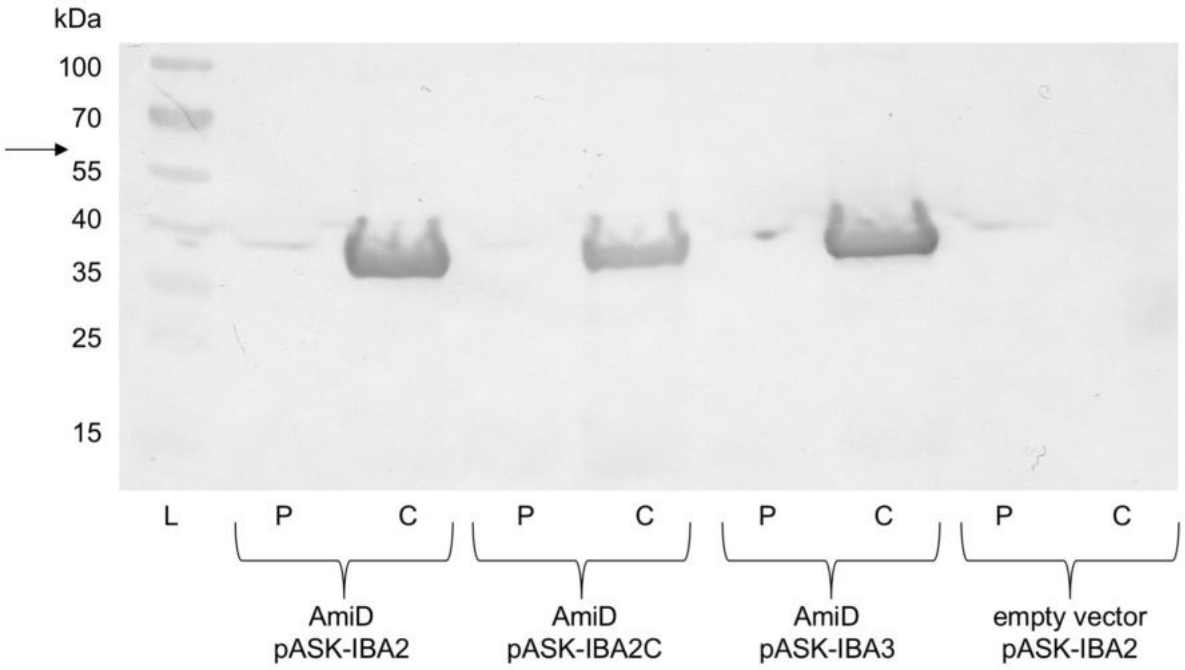

Figure 44: Western Blot analysis of expressed AmiD^{wMel} in *E. coli* ADE24. Western Blot analysis confirmed the presence of degraded AmiD^{wMel} in the periplasm after 1 h of expression. The outer membrane and cell wall were disrupted and cells were centrifuged at 18,000 g and 4 °C to separate the periplasmic contents (found in the supernatant) from cytoplasmic contents (found in the pellet). The different fractions were separated by SDS-PAGE and detected using Strep-Tactin Alkaline Phosphatase conjugate. The picture is representative of three expressions. L: Ladder, P: Periplasmic fraction, C: Cytoplasmic Fraction. Arrow points to expected protein size of recombinant AmiD^{wMel}.

3.4.3.2 AmiD^{wMel} localization

The presence of an N-terminal signal peptide (see chapter 3.4.1) indicated a periplasmic localization of AmiD^{wMel}. To test whether AmiD^{wMel} is transported into the periplasm after expression, the protein was overproduced in *E. coli* JM83 with its native signal sequence in the cytoplasm via pASK-IBA3. The cells were harvested and the outer membrane and cell wall were disrupted by polymyxinB and lysozyme, respectively, to release periplasmic proteins. Western Blot confirmed the presence of AmiD^{wMel} in the periplasm in three independent expressions (Figure 45).

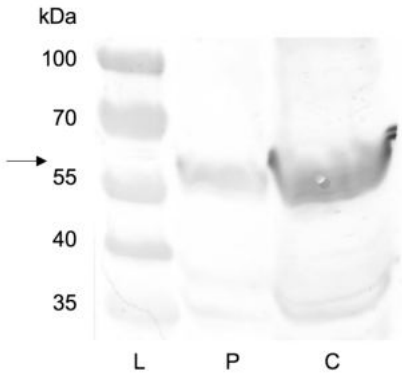

Figure 45: Cellular distribution of AmiD^{wMel} after cytoplasmic expression in *E. coli* JM83. Western Blot analysis confirmed the presence of AmiD^{wMel} in the periplasm after expression. The outer membrane and cell wall were disrupted and cells were centrifuged at 18,000 g and 4 °C to separate the periplasmic contents (found in the supernatant) from cytoplasmic contents (found in the pellet). The different fractions were separated by SDS-PAGE and detected using Strep-Tactin Alkaline Phosphatase conjugate. The picture is representative of three expressions experiments. L: Ladder, P: Periplasmic fraction, C: Cytoplasmic Fraction. Arrow points to expected protein size of recombinant AmiD^{wMel}.

3.4.3.3 Growth kinetics of *E. coli* JM83 overexpressing AmiD^{wMel}

When AmiD^{wMel} was overexpressed in *E. coli* JM83, the turbidity of the culture decreased gradually (Figure 46). This might be the result of AmiD^{wMel} hydrolytic activity on peptidoglycan and subsequent lysis of the host strain. In contrast, cells expressing the empty vector did not show growth defects. To validate that lysis was induced by AmiD^{wMel} activity, the zinc-coordinating active sites H^{97} and D^{207} of the enzyme were mutated to alanine by Dr. M. Wilmes. The overexpressed mutants did not decrease turbidity of the *E. coli* cultures suggesting that bacteria lysis was indeed caused by hydrolytic activity of AmiD^{wMel}.

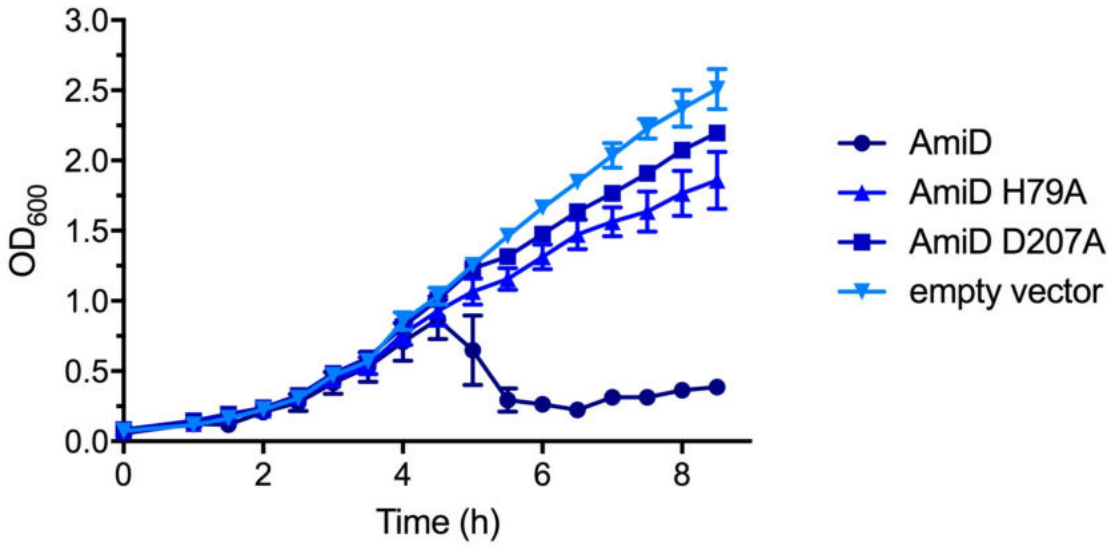

Figure 46: *In vivo* activity of AmiD^{wMel} and active site mutants expressed in *E. coli* JM83. Periplasmic overexpression of AmiD^{wMel} resulted in lysis of *E. coli* JM83 compared to the amidase active site mutants AmiD^{wMel} H79A and AmiD^{wMel} D207A and the empty vector control pASK-IBA2C. OD_{600} was measured every 30 min for 8.5 h. Each point represents mean ± SD (n = 3).

3.4.4 Characterization of AmiD^{wMel} *in vitro*

3.4.4.1 Overexpression and purification of AmiD^{wMel}

For functional analysis of AmiD^{wMel}, the enzyme was produced in *E. coli* JM83 by co-solvent assisted periplasmic expression in NaCl-free LB medium containing D-mannitol. The turbidity of the *E. coli* JM83 culture decreased gradually when AmiD^{wMel} was overexpressed (see chapter 3.4.3.3). Thus, cells were harvested around two hours after induction when they started lysing. AmiD^{wMel} was purified by Strep-tag affinity chromatography and recombinant protein was detected by Western Blot (Figure 47). A mock purification of the empty vector served as a control. Protein concentration of eluates ranged between 500–1000 µg/ml making the recombinant AmiD^{wMel} accessible for *in vitro* activity assays. Contrary to the other investigated wolbachial enzymes in this thesis, AmiD^{wMel} could be stored in 50 % glycerol at -20 °C and was stable for at least 8 months in activity assays (data not shown).

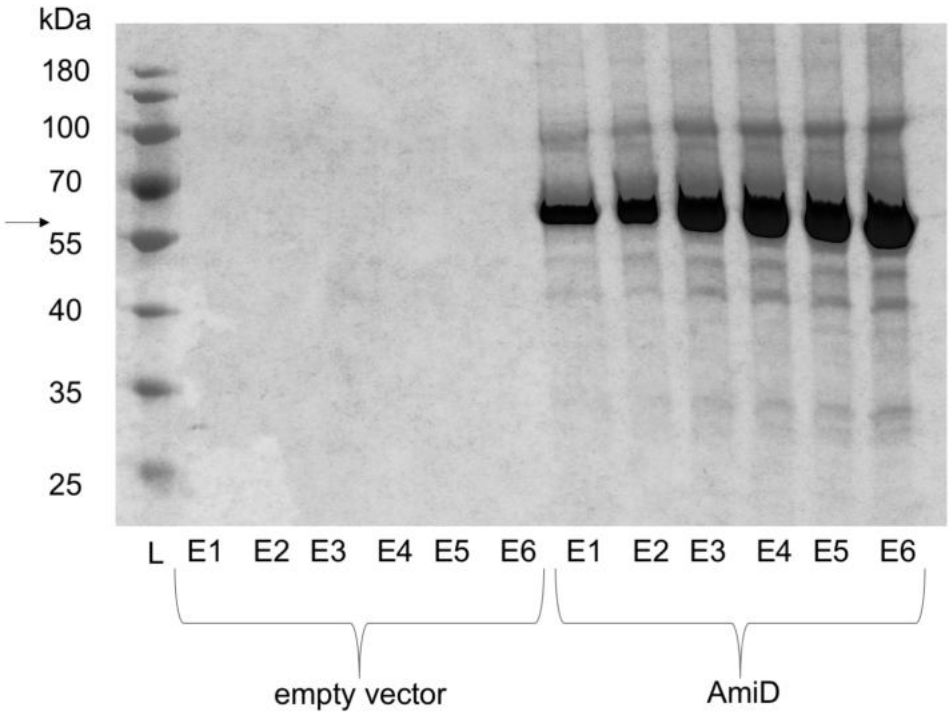

Figure 47: Overexpressed and purified AmiD^{wMel} in pASK-IBA2C. Western Blot analysis of six elution fractions after AmiD^{wMel} expression and Strep-tag purification. A mock expression and purification of the empty vector pASK-IBA2C served as a negative control. L: Ladder, E: Eluate. The arrow points to expected protein size of AmiD^{wMel}.

3.4.4.2 Peptidoglycan as a substrate for AmiD^{wMel}

The activity of purified AmiD^{wMel} using peptidoglycan as a substrate was analyzed in a dye-release assay by incubating the enzyme with RBB-stained peptidoglycan. Released reaction products in the supernatant resulting from peptidoglycan cleavage were quantified by

absorbance measurements. Recombinant AmiD^{wMel} was fully active at pH 7–9 (Figure 48A) and temperatures ranging from 20 °C–37 °C (Figure 48B). For all further *in vitro* activity tests a temperature of 30 °C and a pH of 7.5 were chosen.

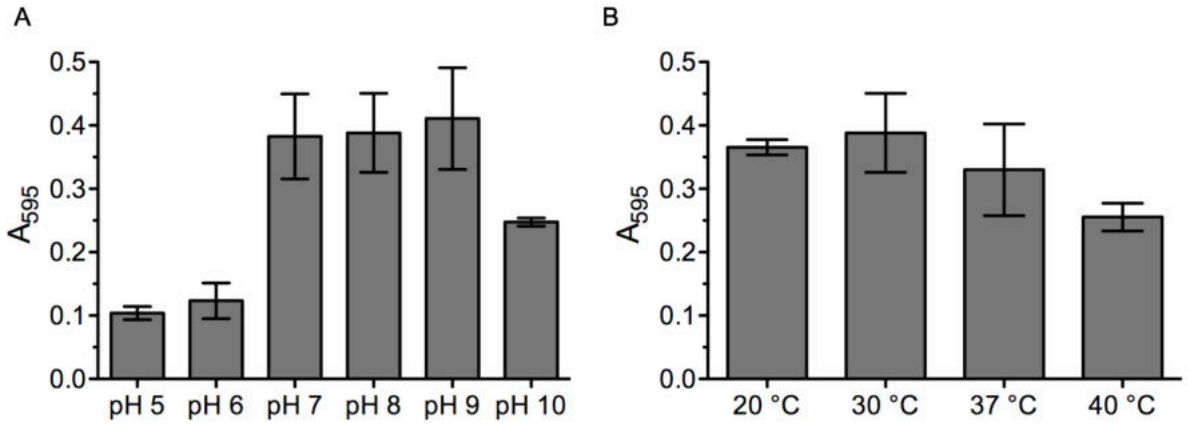

Figure 48: Peptidoglycan-degrading activity of AmiD^{wMel} at different pH and temperatures. To find the optimal conditions for AmiD^{wMel} activity, degradation of peptidoglycan was measured by monitoring the absorbance at 595 nm of Remazol Brilliant Blue dye released into the supernatant after incubation with AmiD^{wMel} overnight at different conditions regarding pH (5–10) and temperature (20–40 °C). Bars represent mean ± SD (n = 3).

Released RBB-stained reaction products in the supernatant resulting from peptidoglycan cleavage were quantified by absorbance measurements. After incubation with AmiD^{wMel} overnight at 30 °C and pH 7.5, significantly more products were released compared to the empty vector control in six independent assays (Figure 49).

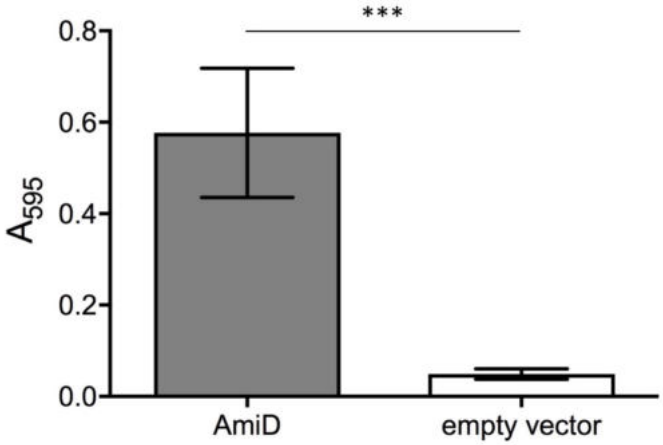

Figure 49: AmiD^{wMel} can use peptidoglycan as a substrate *in vitro*. Degradation of peptidoglycan was detected by monitoring the absorbance at 595 nm of Remazol Brilliant Blue-dye reaction products released into the supernatant after incubation with AmiD^{wMel} overnight at 30 °C and pH 7.5. Product from cells containing the empty vector pASK-IBA2C was used as a negative control. Bars represent mean ± SD (n = 6). Statistical difference was determined using the Unpaired student's t-test, two tailed, *** = P ≤ 0.001.

3.4.4.3 Lipid II as a substrate for AmiD^{wMel}

It was tested whether AmiD^{wMel} can remove the pentapeptide side chain of lipid II. Lipid II was incubated with AmiD^{wMel} and the reaction products were extracted and analyzed by TLC and MALDI-TOF. Contrary to *E. coli* AmiD (Pennartz et al., 2009), AmiD^{wMel} was able to use lipid II as a substrate and hydrolyzed the amide bond between Mur*N*Ac and L-Ala (Figure 50).

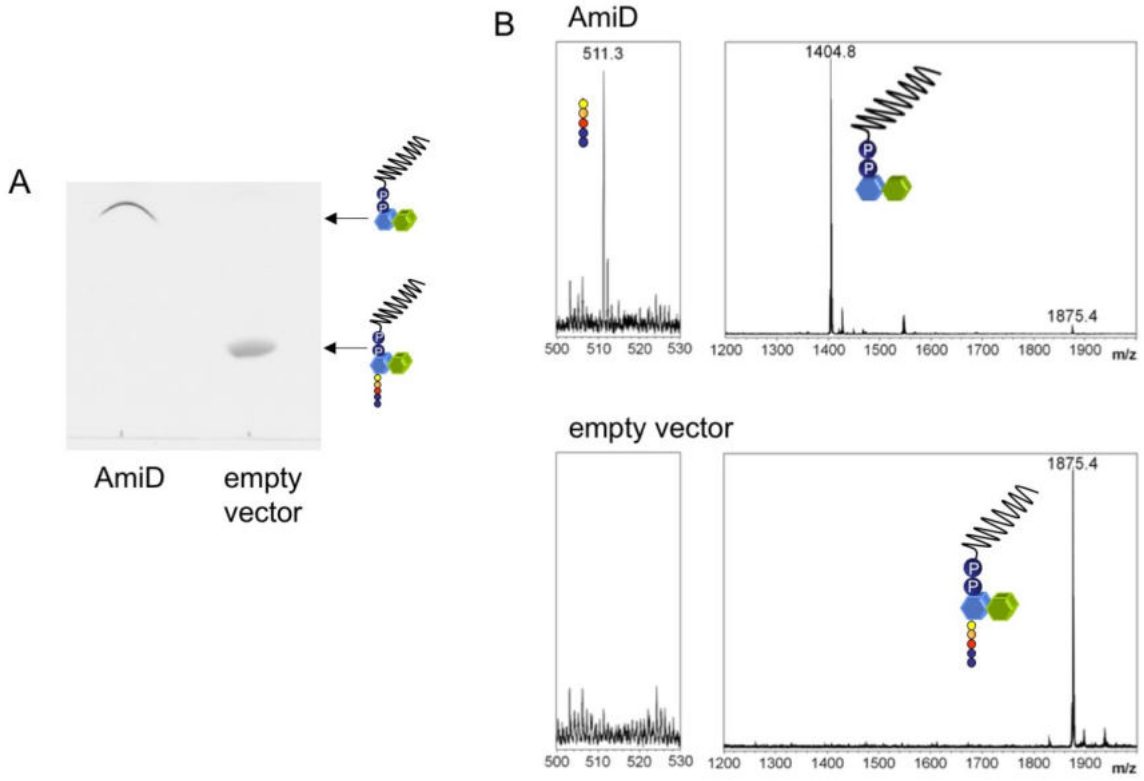

Figure 50: AmiD^{wMel} can use lipid II as a substrate *in vitro*. Lipid II was incubated with AmiD^{wMel} for 4 h at 30 °C. The reaction products were analyzed by A) TLC and B) MALDI-TOF (m/z - lipid II: 1875.4; undecaprenyl-pyrophosphoryl-Mur*N*Ac-Glc*N*Ac: 1404.8; pentapeptide (sodium adduct): 511.3). MALDI-TOF analysis was performed by M. Josten, IMMIP.

3.4.4.4 Inhibition of AmiD^{wMel} activity *in vitro*

Peptidoglycan cleavage by AmiD^{wMel} was partially impaired in the presence of EDTA and the specific zinc-chelator 1,10-phenanthroline (Figure 51A), while lipid II cleavage was completely blocked in EDTA samples and decreased in the presence of 1,10-phenanthroline (Figure 51B). Consistently to the *in vivo* results (see chapter 3.4.3.3), the mutation of one of the residues involved in zinc-binding to alanine (H79A or D207A) resulted in decreased peptidoglycan cleavage and AmiD^{wMel} D207A was not able to hydrolyze the Mur*N*Ac-L-Ala bond in lipid II.

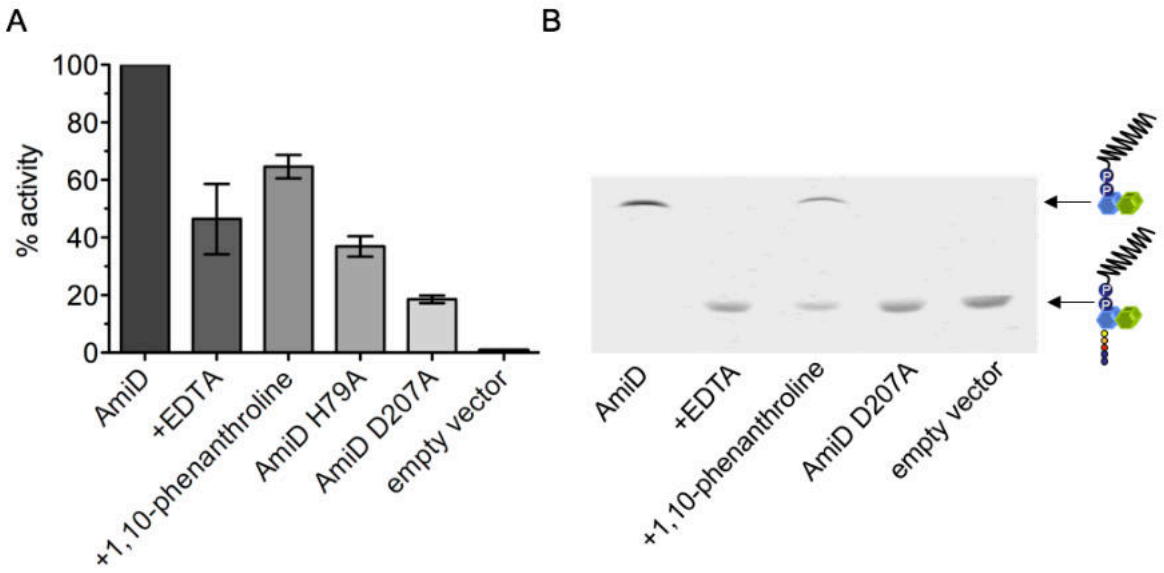

Figure 51: Inhibition of AmiD^{wMel} activity. The zinc-dependent amidase activity was inhibited in the presence of 1 mM of the non-specific metal chelator EDTA and 5 mM of the Zn^{2+}-specific chelator 1,10-phenanthroline as shown by A) Remazol Brilliant Blue dye-release assay on peptidoglycan and B) TLC on lipid II. Moreover, the exchange of one of the zinc-coordinating residues with alanine (H79A or D207A) decreased amidase activity. Bars represent means ± SD. The graph is representative of three experiments with different batches of purified enzyme.

3.4.4.5 Cleavage of anhydromuropeptides

AmiD from *E. coli* has a broad substrate specificity and can also cleave anhydroMur*N*Ac-L-Ala-bonds produced by lytic transglycosylases during cell growth (Uehara and Park, 2007). Anhydromuropeptides (TetraAnh and TetraTetradiAnh) resulting from peptidoglycan digest with the *E. coli* lytic transglycosylase Slt70 were incubated with AmiD^{wMel}. The products were separated by HPLC and confirmed by mass spectrometry. AmiD^{wMel} hydrolyzed TetraAnh and TetraTetradiAnh in a dose-dependent manner (Figure 52A), whereas the mutant protein AmiD^{wMel} D207A was inactive (Figure 52B). The results were obtained and analyzed by Dr. Christian Otten in a cooperation project with the University of Newcastle, UK.

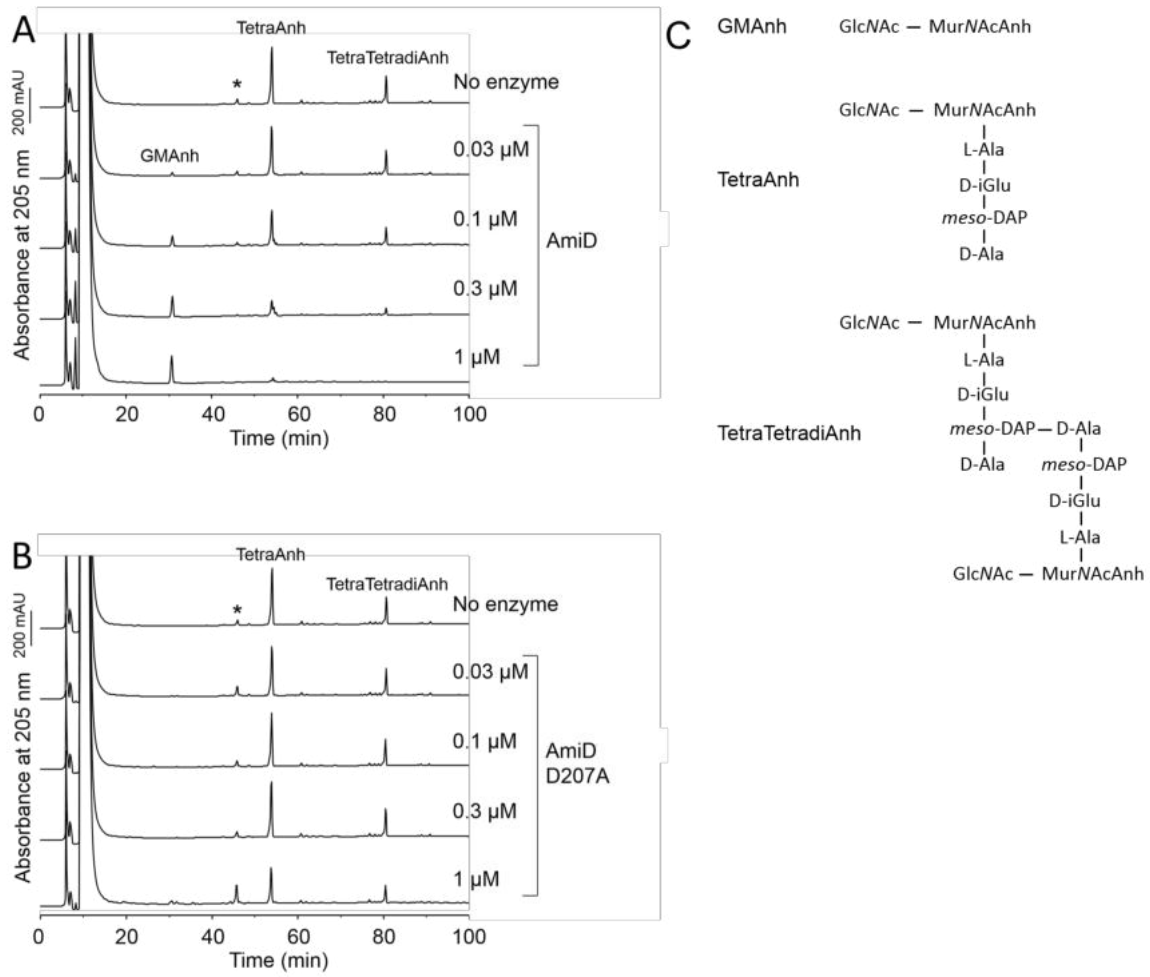

Figure 52: Cleavage of anhydromuropeptides by AmiD^{wMel} *in vitro*. A) Anhydromuropeptides (TetraAnh, TetraTetradiAnh) derived from peptidoglycan digested with the *E. coli* lytic transglycosylase Slt70 were incubated for 4 h at 30 °C with AmiD^{wMel} or B) the amidase active site mutant AmiD^{wMel} (D207A) at different concentrations. The samples were analyzed by HPLC and mass spectrometry. The main product was identified as Glc*N*Ac-Mur*N*AcAnh (m/z = 479.1866, H^+ form; theoretical value: 479.1877). C) Structures of the muropeptides and the reaction products analyzed in A) and B). * = unknown compound unrelated to the reaction. Data and graphs were prepared by C. Otten, University of Newcastle, UK.

The data obtained from *in vivo* and *in vitro* assays demonstrated that AmiD^{wMel} is capable of cleaving monomeric lipid II, polymeric intact peptidoglycan as well as soluble peptidoglycan fragments including the anhydro form.

3.4.5 Characterization of a putative DD-carboxypeptidase activity of AmiD^{wMel}

Contrary to its *E. coli* homolog, AmiD^{wMel} is a relatively big protein and harbors two SXXK, two SX(D/N) and one K(S/T)G motif typically found in PBPs, catalyzing the final steps in cell wall biosynthesis. Of note, an SXXK and SX(D/N) motif are also present in AmiA of *Chlamydia pneumoniae,* an amidase that has been shown to have additional DD-carboxypeptidase activity (Klöckner et al., 2014). In this thesis, it was tested whether AmiD^{wMel} is also a bifunctional enzyme with additional DD-carboxypeptidase activity.

3.4.5.1 DD-carboxypeptidase activity of AmiD^{wMel} *in vivo*

To investigate the potential DD-carboxypeptidase activity of AmiD^{wMel} *in vivo*, the temperature sensitive *E. coli* mutant strain MCI23 was used in complementation assays as described for PBP6a^{wBm} (see chapter 3.1.3). AmiD^{wMel} D207 with impaired amidase activity was used to prevent hydrolysis of the exponentially growing *E. coli* cells. Cell division defects in the temperature sensitive *E. coli* mutant MCI23 overexpressing AmiD^{wMel} D207 at 42 °C were partially rescued with 58 % (± 0.3 SD) of cells being short and 42 % (± 0.3 SD) filamentous (Figure 53A,D). Notably, in some experiments cells showed a granulous structure implicating that the recombinant AmiD^{wMel} protein accumulated inclusion bodies. In contrast, 96 % (± 2.6 SD) of cells expressing the empty vector control were elongated (Figure 53B,D). These differences were confirmed by statistical analysis of cell size. Here, cells expressing AmiD^{wMel} D207 were significantly shorter than the empty vector control (Figure 53C).

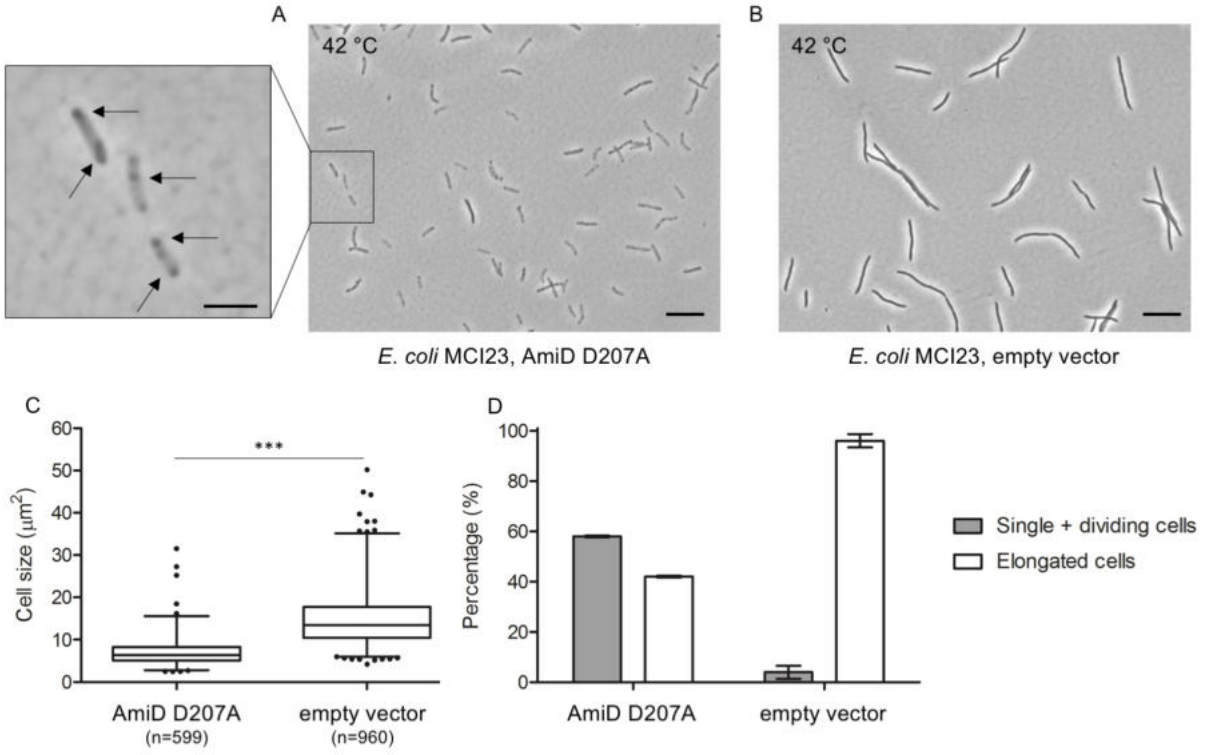

Figure 53: AmiD^{wMel} rescues cell division in a temperature sensitive *E. coli* MCI23 mutant. A) *E. coli* MCI23 expressing recombinant AmiD^{wMel} have a mixed set of phenotypes with short and dividing, but also filamentous cells. Scale bar = 20 µm. Arrows point to granulous structures inside the *E. coli* bacteria observed in some experiments. Scale bar of the zoomed picture = 5 µm. B) *E. coli* MCI23 expressing the empty vector pASK-IBA2C were unable to divide. Scale bar = 20 µm. C) At least 599 cells from 15 pictures taken from three independent assays per sample were measured by Image J. Boxes extend from the 25th to the 75th percentile. The line in the middle of the box is plotted at the median. Whiskers represent 1st and 99th percentiles. Statistical analysis was performed using Mann-Whitney test. *** = $P \leq 0.001$. D) Columns represent relative occurrence of different phenotypes from five randomly chosen pictures in each experiment (n = 3). Error bars represent ± SD.

3.4.5.2 Active site analysis of DD-carboxypeptidase activity of AmiD^{wMel} *in vivo*

Amino acid exchange of the serine residue from S^{83}TLK to alanine (S83A) did not abolish activity at 42 °C and *E. coli* MCI23 partially restored cell division with 48.3 % (± 2.5 SD) of cells being short and able to divide (Figure 54). In contrast, 95 % (± 5.1 SD) of cells were elongated and unable to divide when the AmiD^{wMel} S^{400}LYK (S400A) mutant was expressed indicating that S^{400}LYK harbors the active site serine. Analysis of cell size confirmed that cells expressing AmiD^{wMel} D207A-S400A were significantly longer compared to cells expressing AmiD^{wMel} S83A-D207A. Notably, S^{400}LYK is found nearby the K^{417}SG and S^{425}LD motifs, suggesting that the DD-carboxypeptidase catalytic center of AmiD^{wMel} might be assigned to the C-terminal part of the protein.

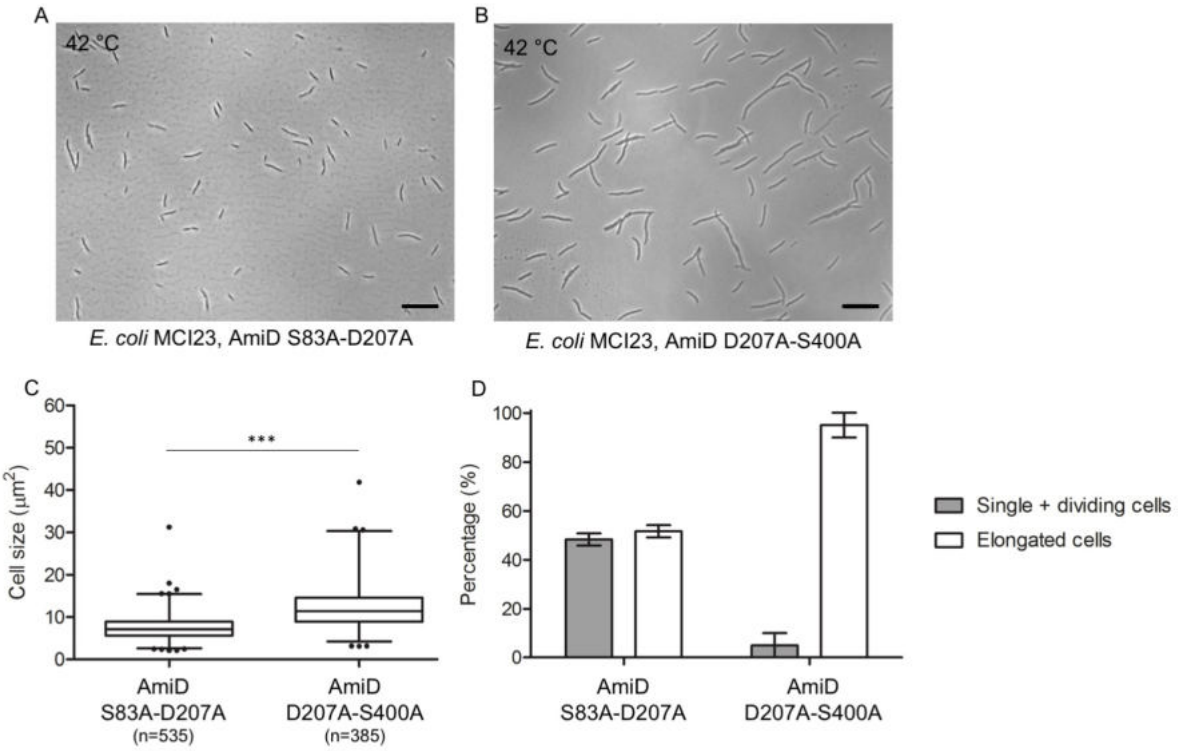

Figure 54: Complementation assay to test for the ability of AmiD^{wMel} active site mutants to rescue cell division in a temperature sensitive *E. coli* MCI23 mutant. Phase-contrast micrographs show A) *E. coli* MCI23 expressing AmiD^{wMel} S83A partially rescue cell division at 42 °C, while B) cells expressing AmiD^{wMel} S400A cannot restore division resulting in a filamentous phenotype. Scale bars = 20 µm. C) At least 385 cells from 15 pictures taken from three independent assays per sample were measured by Image J. Boxes extend from the 25th to the 75th percentile. The line in the middle of the box is plotted at the median. Whiskers represent 1st and 99th percentiles. Statistical analysis was performed using Mann-Whitney test. *** = P ≤ 0.001. D) Columns represent relative occurrence of different phenotypes at 42 °C from 15 randomly chosen pictures in three independent experiments. Error bars represent ± SD.

3.4.5.3 DD-carboxypeptidase activity of AmiD^{wMel} *in vitro*

In vivo results indicated DD-carboxypeptidase activity of AmiD^{wMel}. However, the analysis of the reaction products of *in vitro* AmiD^{wMel} activity assays by TLC or MALDI-TOF did not demonstrate the presence of lipid II with a tetrapeptide resulting from a cleaved D-Ala

(see chapter 3.4.4.3 and 3.4.4.4). Thus, a more sensitive fluorescent-linked activity assay using QuantaBlu substrate solution was used to quantify cleaved off D-Ala. As the empty vector control values were very high, DD-carboxypeptidase activity could not be evaluated under the conditions tested even with the positive control VanY from *S. aureus* (Figure 55).

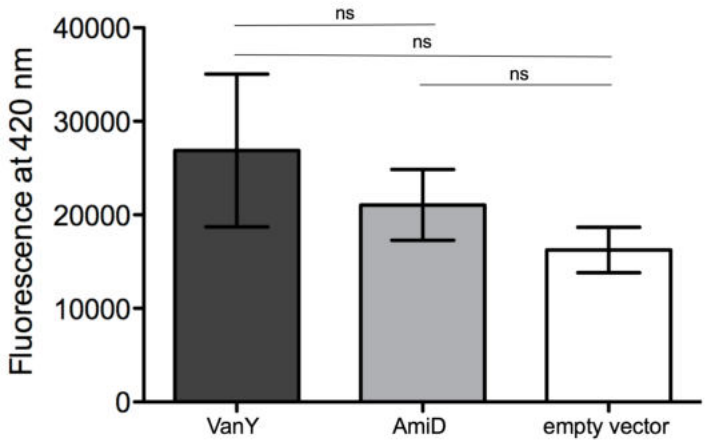

Figure 55: *In vitro* QuantaBlu DD-carboxypeptidase activity assay with VanY (*S. aureus*) and AmiD^{wMel}. D-Ala cleaved from lipid II after overnight incubation at 30 °C was detected by the activity of D-amino acid oxidase in the presence of QuantaBlu fluorescent substrate at 420 nm. Overexpressed VanY from *S. aureus* served as a positive control. Results show the mean ± SEM (n = 4–6). Statistical difference was determined using the Unpaired student's t-test, two tailed, ns = not significant.

3.4.5.4 Penicillin-binding assay of AmiD^{wMel}

Since AmiD^{wMel} has penicillin-binding motifs in its sequence that are targets for β-lactam antibiotics, a binding of AmiD^{wMel} to Bocillin^{TM} FL was tested. A weak binding was observed giving a hint that penicillin-binding motifs are accessible for β-lactam antibiotics at least in recombinant AmiD^{wMel} (Figure 56).

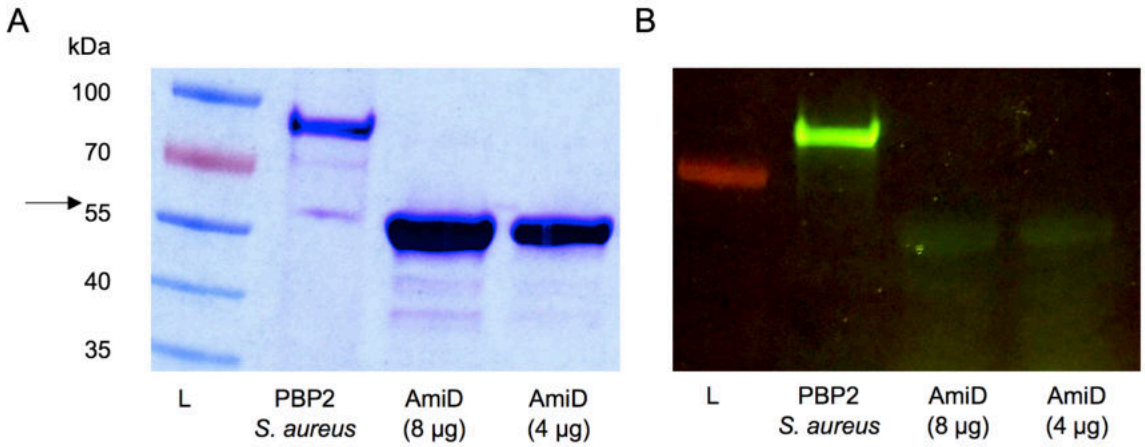

Figure 56: Detection of penicillin-sensitive PBP2 (*S. aureus*) and AmiD^{wMel} by Bocillin^{TM} FL binding assay. Purified AmiD^{wMel} (4 and 8 µg) was incubated with 10 µM Bocillin^{TM} FL at 30 °C for 1 h and separated by SDS-PAGE. PBP2 from *S. aureus* served as a positive control. A) Detection of proteins by Coomassie staining. The arrow points to expected protein size of AmiD^{wMel}. B) Detection of proteins bound to Bocillin^{TM} FL by UV light.

3.4.5.5 *In vivo* β-lactamase activity assay of AmiD^{wMel}

To test if AmiD^{wMel} has β-lactamase activity, the protein was expressed in *E. coli* JM83 cultures supplemented with CENTA^{TM} and incubated for 16 h. Analysis of absorbance measurements showed an increase of λ_{405} from 0.48 (± 0.04 SEM) to 1.36 (± 0.15 SEM) in cultures containing the positive control *E. coli* ML-35 pYC in six independent experiments, indicating CENTA^{TM} hydrolysis (Figure 57). In contrast, cultures expressing AmiD^{wMel} rarely increased from λ_{405} = 0.4 (±0.03 SEM) to 0.48 (± 0.09 SEM) in eight independent assays. Cultures expressing the empty vector control slightly increased from λ_{405} = 0.4 (± 0.03 SEM) to 0.58 (± 0.07 SEM) in six independent assays. In conclusion, β-lactamase activity of AmiD^{wMel} was not observed under the conditions tested.

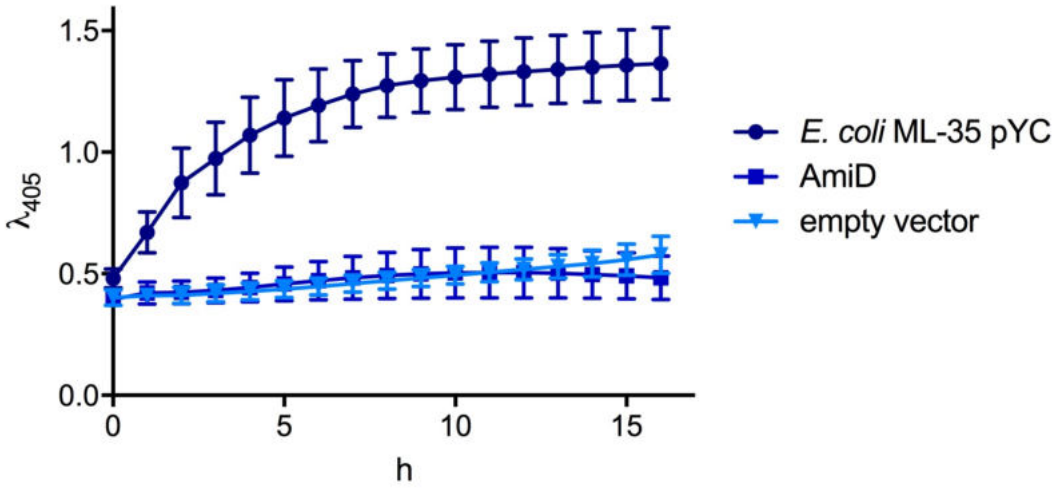

Figure 57: β-lactamase activity assay of AmiD^{wMel} *in vivo*. *E. coli* JM83 with AmiD^{wMel} in pASK-IBA2C were induced with 200 ng/ml AHT. *E. coli* ML35-pYC constitutively expressing a periplasmic β-lactamase were used as a positive control, pASK-IBA2C (empty vector) served as a negative control. AmiD^{wMel} data represent means from eight independent assays, the positive and negative control were tested six times. Error bars represent ± SEM.

3.5 Functional analysis of PBP3^{wMel}

3.5.1 Primary structure analysis of PBP3^{wMel}

Genome analysis of *w*Mel revealed the presence of two putative monofunctional DD-transpeptidases PBP2 and PBP3. Part of this thesis was the investigation of the additional PBP3 protein only found in *Wolbachia* residing in insect cells. PBP3^{wMel} (NCBI: WP_010963147.1) consists of 515 amino acids and the protein has a predicted molecular weight of 58.24 kDa with 26 % sequence identity to *E. coli* PBP3 (NCBI: ARB43848.1) (Figure 58). It possesses a set of four SXXK, five SX(D/N) and one K(S/T)G active site motifs. Like its *E. coli* homolog,

PBP3^{wMel} consists of a predicted N-terminal transmembrane domain ranging from amino acids 1–34, but no signal peptide (Supplementary Figure 14).

```
PBP3 wMel       ---------------MQALLKNKLRSLCFIVPLFIFYIIIIFR-IFSLTFDQLTT---SE  41
PBP3 E. coli    MKAAAKTQKPKRQEEHANFISWRFALLCGCILLALAFLLGRVAWLQVISPDMLVKEGDMR  60
                             ::. ::  **  : * : :::  .  :  :: * *..    .

PBP3 wMel       NFRKDNIVHKQPDILDRNGVVIATNVPTTSLYIDATKVKNPESIAAQLCS-TL---HDLE  97
PBP3 E. coli    SLRVQQVSTSRGMITDRSGRPLAVSVPVKAIWADPKEVHDAGGISVGDRWKALANALNIP  120
                .:* :::  .:  * **.*  :*..**..::: * .:*::  .*:.     :*    ::

PBP3 wMel       YKNL--YRVLTSEKKFAWIKRHLTPKELLAIKNAGVPGVNFDDDIKRIYPHSNLFSHVLG  155
PBP3 E. coli    LDQLSARINANPKGRFIYLARQVNPDMADYIKKLKLPGIHLREESRRYYPSGEVTAHLIG  180
                .:*      . : :* :: *::.*.    **:  :**::: :: :* ** .:: :*::*

PBP3 wMel       YTDIDGNGIAGVEAYISKN-------------------------NEQEKPIILSLDTRV  189
PBP3 E. coli    FTNVDSQGIEGVEKSFDKWLTGQPGERIVRKDRYGRVIEDISSTDSQAAHNLALSIDERL  240
                :*::*.:** ***  :.*                              .:  : : **:* *:

PBP3 wMel       QSIVHEELTKAVRRYQALGGVGIVLNVRNSEVISMVSLPDFNPNLQNKAEDVQKFNRASL  249
PBP3 E. coli    QALVYRELNNAVAFNKAESGSAVLVDVNTGEVLAMANSPSYNPNNLSGTPKEAMRNRTIT  300
                *::*:.**.:**   :* .* .::::*...**::*.. *.:***  . : .    **:

PBP3 wMel       GVYEMGSVLKYFTIAAALDANATKTSDLYD---VSTPITIGKYKIQDFHKSKIPKITVQD  306
PBP3 E. coli    DVFEPGSTVKPMVVMTALQRGVVRENSVLNTIPYTIPYRINGHEIKDV--ARYSELTLTG  358
                .*:* **.:* :.: :**: ...: ..: :    : *  *. ::*:*.  ::  ::*: .

PBP3 wMel       IFVKSSNIGAAKIAVKLGIEKQVEYFKAMKLFSPLKIEIPEKSTPI--IPDKWSETTLIT  364
PBP3 E. coli    VLQKSSNVGVSKLALAMPSSALVDTYSRFGLGKATNLGLVGERSGLYPQKQRWSDIERVT  418
                :: ****:*.:*:*: :  .  *: :. : * .  :: :  : : :    ::**:   :*

PBP3 wMel       ASYGYGIAVTPIHLAQTAAALINNGIFHNATLMLNK-RSIGEQIISRRTSREMRK-LLRA  422
PBP3 E. coli    FSFGYGLMVTPLQLARVYATIGSYGIYRPLSITKVDPPVPGERVFPESIVRTVVHMMESV  478
                *:***: ***::**:. *:: . **::  ::   .    **::: .   * : : :  .

PBP3 wMel       AVTDGTGRKAKIKAYSIGGKTGSAEKVVDGKYSKDANIASFIGVLTMLDPRYIVLIAIDE  482
PBP3 E. coli    ALPGGGGVKAAIKGYRIAIKTGTAKKVGPDGRYINKYIAYTAGVAPASQPRFALVVVIND  538
                *: .* * ** **.* *. ***:*:**  .    :  **   **    :**: :::.*::

PBP3 wMel       PQGMHHTGGIIAAPIVKNIINRIAPILNVTPEM----------------------        515
PBP3 E. coli    PQAGKYYGGAVSAPVFGAIMGGVLRTMNIEPDALTTGDKNEFVINQGEGTGGRS        592
                **. :: ** ::**:.  *:. :   :*: *:
```

Figure 58: Amino acid alignment of PBP3^{wMel} and *E. coli* PBP3. PBP3^{wMel} (WP_010963147.1) shares 26 % identity to *E. coli* PBP3 (ARB43848.1). Conserved SXXK, SX(D/N) and K(S/T)G motifs found in PBP3^{wMel} are written in bold letters, motifs which align to *E. coli* PBP3 are additionally framed in black. The predicted transmembrane domain is highlighted gray. ***** fully conserved residue; **:** conservation between groups of strongly similar properties; **.** conservation between groups of weakly similar properties.

3.5.2 Secondary structure analysis of PBP3^{wMel}

To get a deeper insight into the putative active site serine of the SXXK motif, secondary structure analysis was performed. Here, the three conserved motifs were localized based on sequence alignments to *E. coli*. The SXXK motifs S^{107}EKK and S^{339}PLK are predicted to be located outside the active site (Figure 59). S^{445}AEK is located in a β-sheet next to the K^{442}TG motif, while S^{256}VLK is found in an α-helix. Thus, one of these SXXK motifs might build the catalytic center together with S^{311}SN (α-helix and loop) and K^{442}TG (β-sheet). The gene *pbp3* from *w*Mel was cloned into pASK-IBA2C, transformed into different *E. coli* strains and tested in *in vivo* and *in vitro* activity assays.

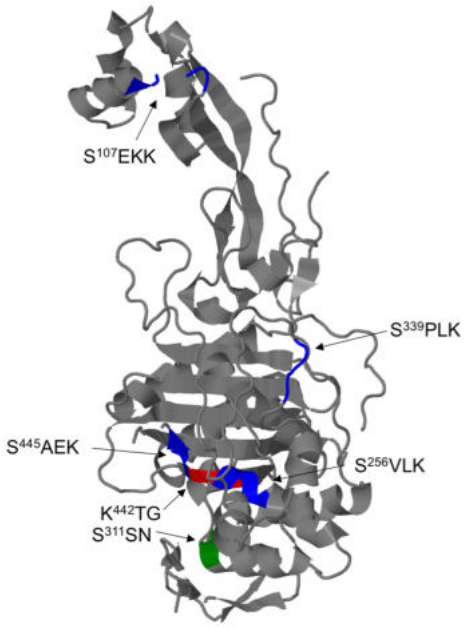

Figure 59: Secondary structure of PBP3^{wMel} as predicted by Phyre^{2}. S^{256}VLK or S^{445}AEK (blue) might, together with S^{311}SN (green) and K^{442}TG (red), build the catalytic center of the enzyme, while S^{107}EKK, S^{339}PLK are predicted to be located outside the active site (blue). The molecular structure was illustrated by Jmol.

3.5.3 Characterization of PBP3^{wMel} and active site analysis *in vivo*

Since PBP3^{wMel} is the homolog of *E. coli* PBP3, it was examined whether overexpression of PBP3^{wMel} is sufficient to restore cell division in *E. coli* MCI23 at the non-permissive temperature of 42 °C. To test dependency on functional SXXK motifs, site-directed mutagenesis was performed. Substitution of S107, S256, and S339 to alanine and *in vivo* activity assays of these mutants were part of a master thesis (Ritzmann, 2016). Mutagenesis PCR of serine from the fourth SXXK motif S445 was part of this thesis resulting in a PBP3^{wMel} S107A-S256A-S339A-S445A quadruple mutant (Figure 60). Successful amino acid substitution was confirmed by nucleotide sequencing of the PBP3^{wMel} gene (Supplementary Figure 15).

```
  1   MQALLKNKLRSLCFIVPLFIFYIIIIFRIFSLTFDQLTTSENFRKDNIVHKQPDILDRNG   60
 61   VVIATNVPTTSLYIDATKVKNPESIAAQLCSTLHDLEYKNLYRVLTAEKKFAWIKRHLTP  120
121   KELLAIKNAGVPGVNFDDDIKRIYPHSNLFSHVLGYTDIDGNGIAGVEAYISKNNEQEKP  180
181   IILSLDTRVQSIVHEELTKAVRRYQALGGVGIVLNVRNSEVISMVSLPDFNPNLQNKAED  240
241   VQKFNRASLGVYEMGAVLKYFTIAAALDANATKTSDLYDVSTPITIGKYKIQDFHKSKIP  300
301   KITVQDIFVKSSNIGAAKIAVKLGIEKQVEYFKAMKLFAPLKIEIPEKSTPIIPDKWSET  360
361   TLITASYGYGIAVTPIHLAQTAAALINNGIFHNATLMLNKRSIGEQIISRRTSREMRKLL  420
421   RAAVTDGTGRKAKIKAYSIGGKTGAAEKVVDGKYSKDANIASFIGVLTMLDPRYIVLIAI  480
481   DEPQGMHHTGGIIAAPIVKNIINRIAPILNVTPEM                           515
```

Figure 60: Primary structure analysis of PBP3^{wMel} in pASK-IBA2C after site-directed mutagenesis. Serine residues from SXXK motifs were substituted by alanine (red bold letters). The amino acid sequence is shown in single-letter code, the predicted transmembrane domain is highlighted in gray.

PBP3^{wMel} expression at 42 °C led to a mixed set of phenotypes of *E. coli* MCI23 (Figure 61A). Quantitative analysis of six independent assays showed that 66.7 % (± 27.5 SD) of observed cells expressing PBP3^{wMel} were single and dividing cells, while 33.3 % (± 27.5 SD) were elongated. Neither single nor simultaneous mutation of the serines S107, S256, and S339 of SXXK motifs had an impact on PBP3^{wMel} activity at 42 °C (Ritzmann, 2016). However, site-directed mutagenesis of all four SXXK motifs including S445 showed a decrease of PBP3^{wMel} *in vivo* activity resulting in 21.2 % (± 14.3 SD) single and dividing cells and concomitant increase of elongated cells to 78.8 % (± 14.3 SD) (Figure 61B,D). Statistical analysis of cell size showed that PBP3^{wMel} expressing *E. coli* were significantly shorter than the quadruple SXXK mutant and the empty vector control (Figure 61E).

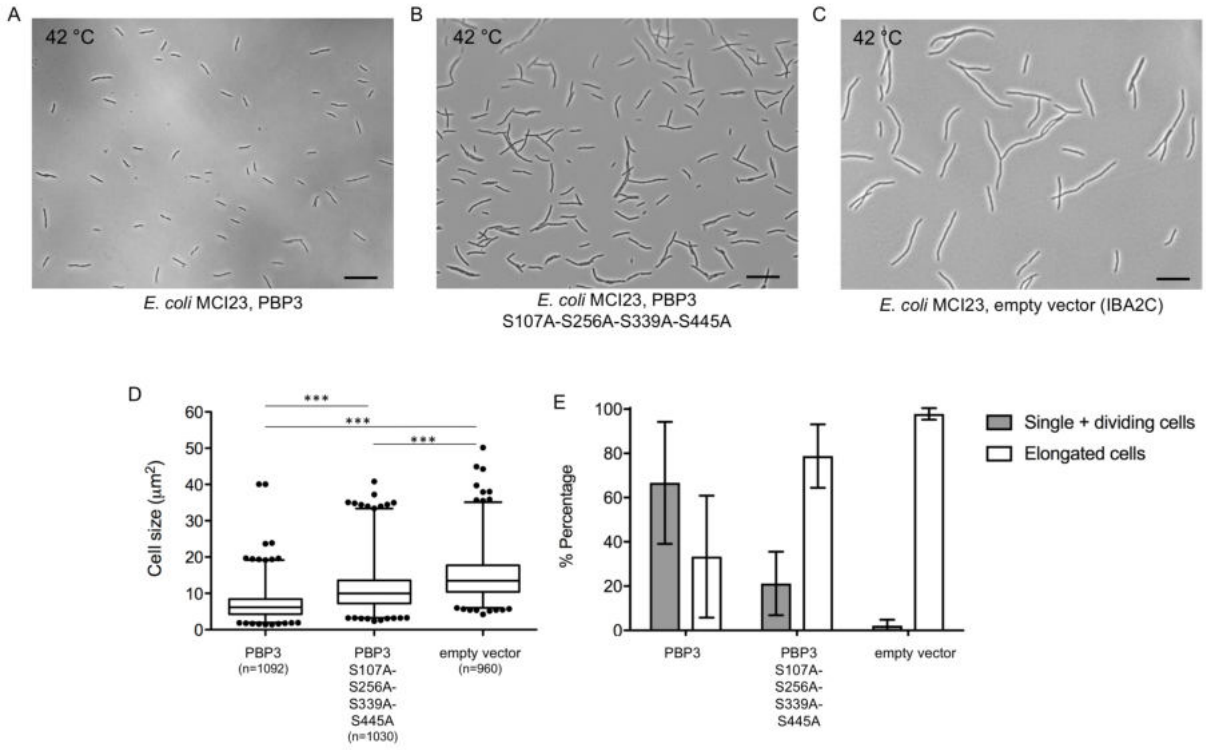

Figure 61: Complementation assay to test for the ability of PBP3^{wMel} and PBP3^{wMel} active site mutants to rescue cell division in a temperature sensitive *E. coli* MCI23 mutant. *E. coli* MCI23 were grown in LB medium containing chloramphenicol until OD_{600} = 0.4. Cultures were induced with 100 ng/ml tetracycline and incubated for 120 min 42 °C. A) *E. coli* MCI23 expressing recombinant PBP3^{wMel} are mainly short and dividing, while B) cells expressing PBP3^{wMel} S107A-S256A-S339A-S445A are predominantly filamentous. C) *E. coli* MCI23 expressing the empty vector pASK-IBA2C have filamentous cells. Scale bars = 20 µm. D) Cell size of at least 960 cells from 30 pictures taken from six independent assays was measured by Image J. Boxes extend from the 25th to the 75th percentile of cell size distribution. The line in the middle of the box is the median. Whiskers represent 1st and 99th percentiles. Dots represents outliers. Statistical analysis was performed using Kruskal-Wallis test and Dunn's comparison post-hoc test, *** = P ≤ 0.001. E) Columns represent the mean ± SD occurrence of different phenotypes at 42 °C from five randomly chosen pictures from each of the six experiments.

Additionally, growth of *E. coli* was monitored to exclude that the different observed phenotypes resulted from potential cell arrests induced by protein induction. In three independent measurements, all cultures were growing exponentially after induction (Figure 62).

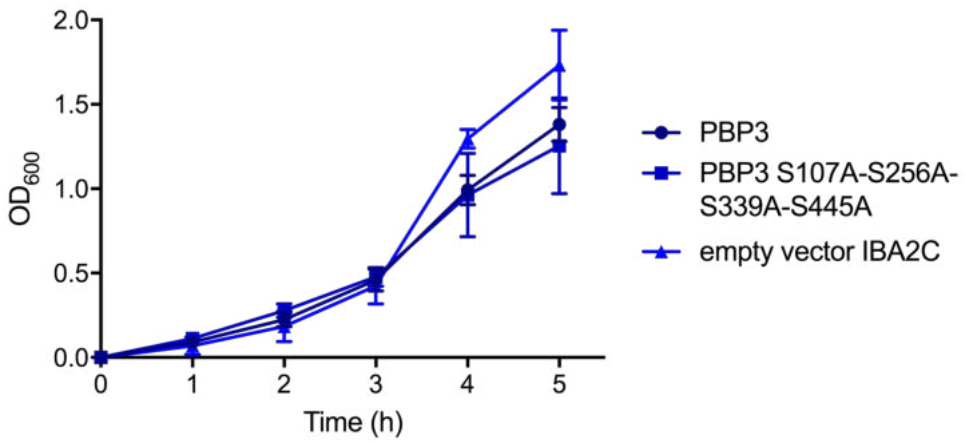

Figure 62: Growth kinetics of *E. coli* MCI23 during periplasmic expression of PBP3^{wMel}. Protein expression was induced at an OD_{600} of 0.5 with 100 ng/ml tetracycline. OD_{600} was measured every hour. Each point represents mean ± SD (n = 3).

3.5.4 Aztreonam treatment of PBP3^{wMel} *in vivo*

Aztreonam is a β-lactam with high affinity for PBP3 leading to arrested cell division and a filamentous phenotype (Weiss et al., 1997). To examine its effect on PBP3^{wMel} activity, the antibiotic was added to exponentially growing *E. coli* MCI23 cultures at 30 °C. *E. coli* MCI23 overexpressing PBP3^{wMel} were still able to partially maintain cell division in the presence of aztreonam indicating that PBP3^{wMel} activity cannot be blocked by aztreonam (Figure 63A). In contrast, addition of aztreonam to *E. coli* MCI23 overexpressing the empty vector at 30 °C resulted in filamentous cells indicating inhibition of the native *E. coli* PBP3 activity and divisome function (Figure 63B). Analysis of six independent assays revealed that untreated cells expressing PBP3^{wMel} or the empty vector had similar cell sizes at 30 °C (Figure 63C). In contrast, cells with the induced empty vector were significantly larger than cells expressing PBP3^{wMel} in the presence of aztreonam.

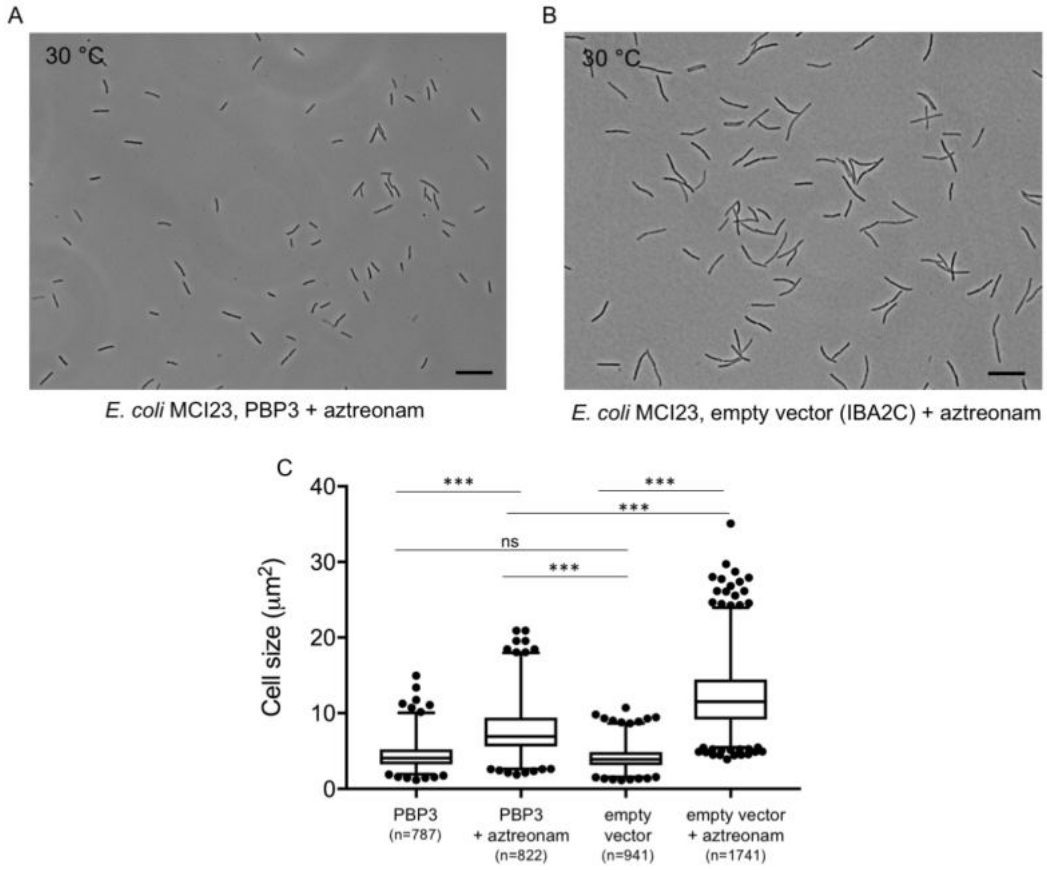

Figure 63: Cell division of *E. coli* MCI23 expressing PBP3^{wMel} is not inhibited by aztreonam, a specific inhibitor of PBP3. *E. coli* MCI23 harboring either PBP3^{wMel} or the empty vector were grown in LB medium at 30 °C containing chloramphenicol until an OD_{600} of 0.4. Cultures were induced with 100 ng/ml tetracycline and after 30 min, 8 µg/ml aztreonam were added. A) PBP3^{wMel} overexpressing cells partially divide in the presence of aztreonam, while B) cells expressing the empty vector pASK-IBA2C are elongated. Cultures without induction or without aztreonam served as controls. C) Cell size of at least 787 cells from 30 pictures taken from six independent assays was measured by Image J. Boxes extend from the 25th to the 75th percentile of cell size distribution. The line in the middle of the box is the median. Whiskers represent 1st and 99th percentiles, dots represent outliers. Statistical analysis was performed using Kruskal-Wallis test and Dunn's comparison post-hoc test, ns = not significant, *** = $P \leq 0.001$.

3.5.5 *In vivo* β-lactamase activity assay of PBP3^{wMel}

As PBP3^{wMel} was resistant to aztreonam *in vivo* (see chapter 3.5.4) and no penicillin-binding was observed *in vitro* (Ritzmann, 2016), a potential β-lactamase activity of this enzyme was examined. PBP3^{wMel} was expressed in *E. coli* C43 cultures supplemented with CENTA^{TM} and incubated for 16 h. In six independent experiments, absorbance λ_{405} increased of from 0.48 (± 0.04 SEM) to 1.36 (± 0.15 SEM) in cultures containing the positive control *E. coli* ML-35 pYC in six independent experiments, indicating CENTA^{TM} hydrolysis (Figure 64). In contrast, cultures expressing PBP3^{wMel} remained constant around $\lambda_{405} = 0.49$ (± 0.05 SEM). Cultures expressing the empty vector control slightly increased from $\lambda_{405} = 0.4$ (± 0.03 SEM) to 0.58 (± 0.07 SEM). In conclusion, no β-lactamase activity of PBP3^{wMel} was detected under the conditions tested.

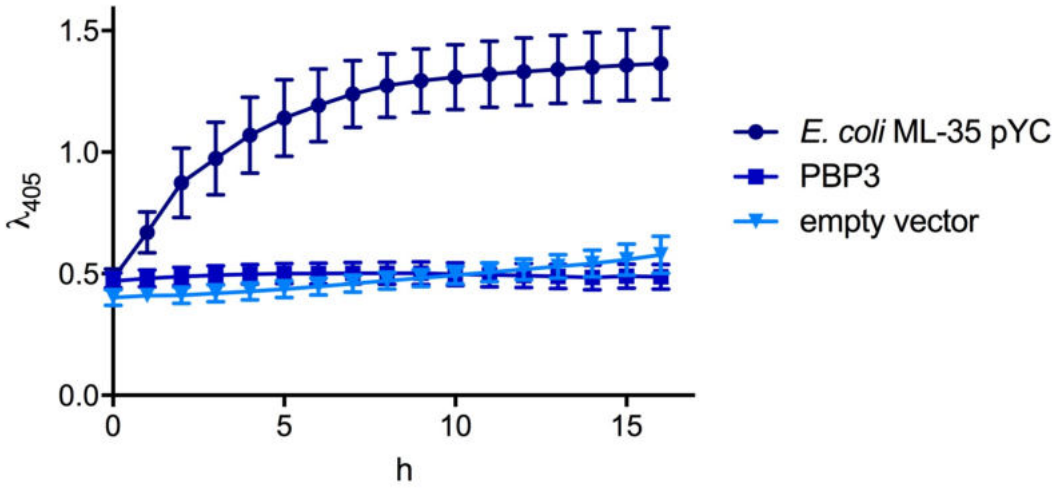

Figure 64: β-lactamase activity assay of PBP3^{wMel} *in vivo*. *E. coli* C43 carrying PBP3^{wMel} in pASK-IBA2C were induced with 200 ng/ml AHT. *E. coli* ML35-pYC constitutively expressing a periplasmic β-lactamase were used as a positive control, pASK-IBA2C (empty vector) served as a negative control. Data represent means from six independent assays. Error bars represent ± SEM.

3.5.6 *In silico* modeling of PBP3^{wMel}

In silico analysis predicted a binding of the β-lactam antibiotic cefoxitin at two serines (S256 and S445) of the four SXXK motifs (Figure 65). *In vivo* activity assays implied that SXXK motifs can substitute each other and recombinant PBP3^{wMel} was not impaired by the β-lactam aztreonam. Thus, PBP3^{wMel} might be functional in *Wolbachia* even in the presence of a β-lactam.

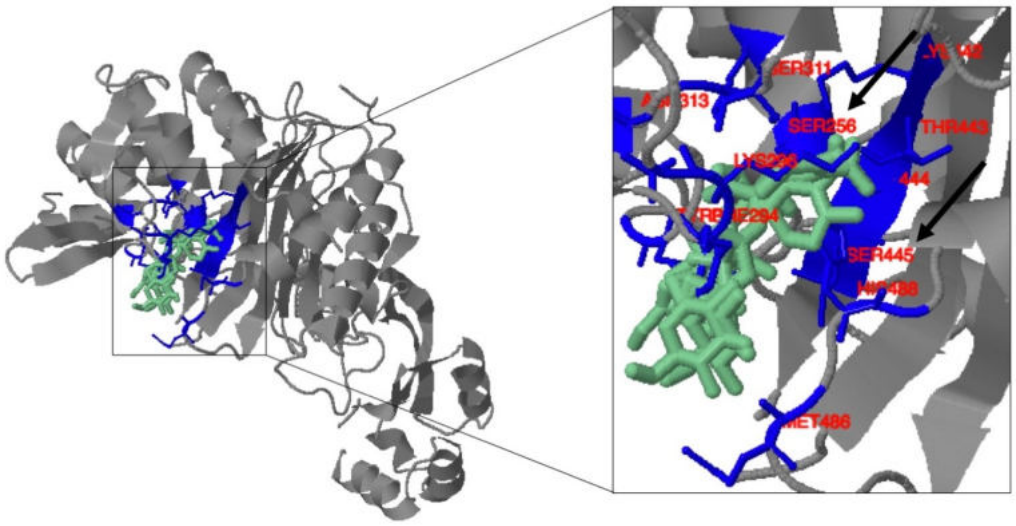

Figure 65: 3D structure of PBP3^{wMel} bound to cefoxitin as predicted by 3DLigandSite. The residues S256, K259, F294, K296, S311, N313, Y369, K442, T443, G444, S445, M486, H488 putatively involved in binding to cefoxitin (green) are marked in blue. Arrows point to the active site serines S256 and S445 of the SXXK motifs predicted to be involved in binding.

3.6 Fluorescent labeling of D-Ala-D-Ala dipeptides

3.6.1 Dipeptide labeling of *B. subtilis* 168 and *E. coli* W3110

A novel *in vivo* assay to fluorescently label lipid II using D-Ala-D-Ala dipeptide analogues revealed a ring-like peptidoglycan structure in *Chlamydia, Orientia* and *Planctomycetes* for the first time (Liechti et al., 2014; Jeske et al., 2015; Atwal et al., 2017). Ethynyl-D-Ala (EDA-DA) and Ethynyl-L-Ala (ELA-LA) dipeptides (synthesized by Pepmic Co., Ltd.) were applied to Gram-positive *B. subtilis* 168 and Gram-negative *E. coli* W3110 to verify that peptidoglycan was labeled specifically. In both strains, a binding of EDA-DA was observed, while ELA-LA labeled cells did not show a fluorescent signal (Figure 66A,B). Additionally, peptidoglycan sacculi from *B. subtilis* were prepared and digested with lysozyme resulting in a loss of the fluorescence signal (Figure 66C) providing further proof that the dipeptides were indeed specifically incorporated into peptidoglycan.

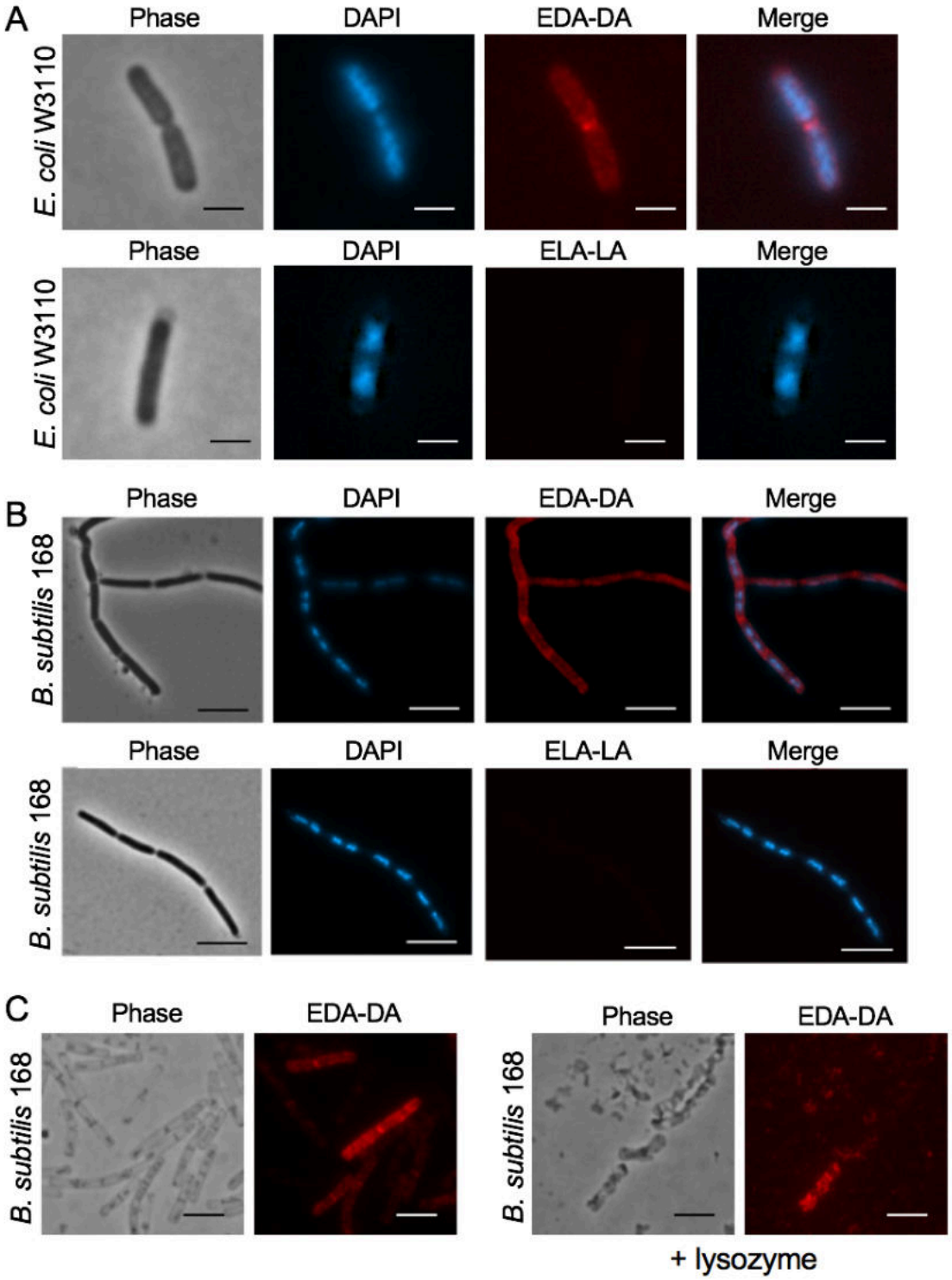

Figure 66: Dipeptide labeling in *E. coli* and *B. subtilis*. A) Fluorescent labeling of lipid II in *E. coli*. *E. coli* W3110 were incubated for 60 min in medium containing 1 mM of the dipeptide probe EDA-DA (top row) or ELA-LA (bottom row), respectively. Subsequent binding of the probe to an azide-modified Alexa Fluor® 594 (red) was achieved by click chemistry. DAPI (blue) was used for nuclear staining. Scale bar = 5 µm. B) Fluorescent labeling of lipid II in *B. subtilis*. *B. subtilis* 168 were incubated for 60 min in medium containing 1 mM of the dipeptide probe EDA-DA (top row) or ELA-LA (bottom row), respectively. Subsequent binding of the probe to an azide-modified Alexa Fluor® 594 (red) was achieved by click chemistry. DAPI (blue) was used for nuclear staining. Scale bar = 5 µm. C) Fluorescent labeling of lipid II in *B. subtilis* sacculi. *B. subtilis* 168 were incubated for 60 min in medium containing 1 mM of the dipeptide probe EDA-DA. Afterwards, the peptidoglycan sacculi were prepared and binding of the probe to an azide-modified Alexa Fluor® 594 was achieved by click chemistry. The cell wall sacculi were digested with 200 ng lysozyme resulting in a loss of the dipeptide signal. Scale bar = 5 µm.

3.6.2 Dipeptide labeling of *w*AlbB

A specific labeling of EDA-DA co-localized with *Wolbachia* specific antibodies *w*Pal and FtsZ was observed (Figure 67A) visualizing a lipid II-containing peptidoglycan-like structure in *Wolbachia* for the first time. Moreover, ELA-LA cells did not show a fluorescent signal indicating that *Wolbachia* might contain D-Ala in their lipid II peptide chain as already concluded previously (Vollmer et al., 2013) (Figure 67B). *Wolbachia* had a cell size varying between 0.45–1.8 µm, thus a detailed distribution of the labeled lipid II could not be determined with the microscope used (ZeissAxio VertA.1, Carl Zeiss AG). Attempts with a confocal microscope using Z-stacks and advanced microscope technologies (Zeiss LSM800 Airyscan, Carl Zeiss AG) to gain a higher resolution did not reveal a ring-like structure of the labeled dipeptides as shown for *Chlamydia* (Figure 67C). Notably, EDA-DA was detected only in some *Wolbachia* cells and the whole bacterial surface was labeled, which was also observed in *O. tsutsugamushi* (Atwal et al., 2017). Negative controls with EDA-DA applied on C6/36 insect cells without *w*AlbB did not show a fluorescent signal (Supplementary Figure 16).

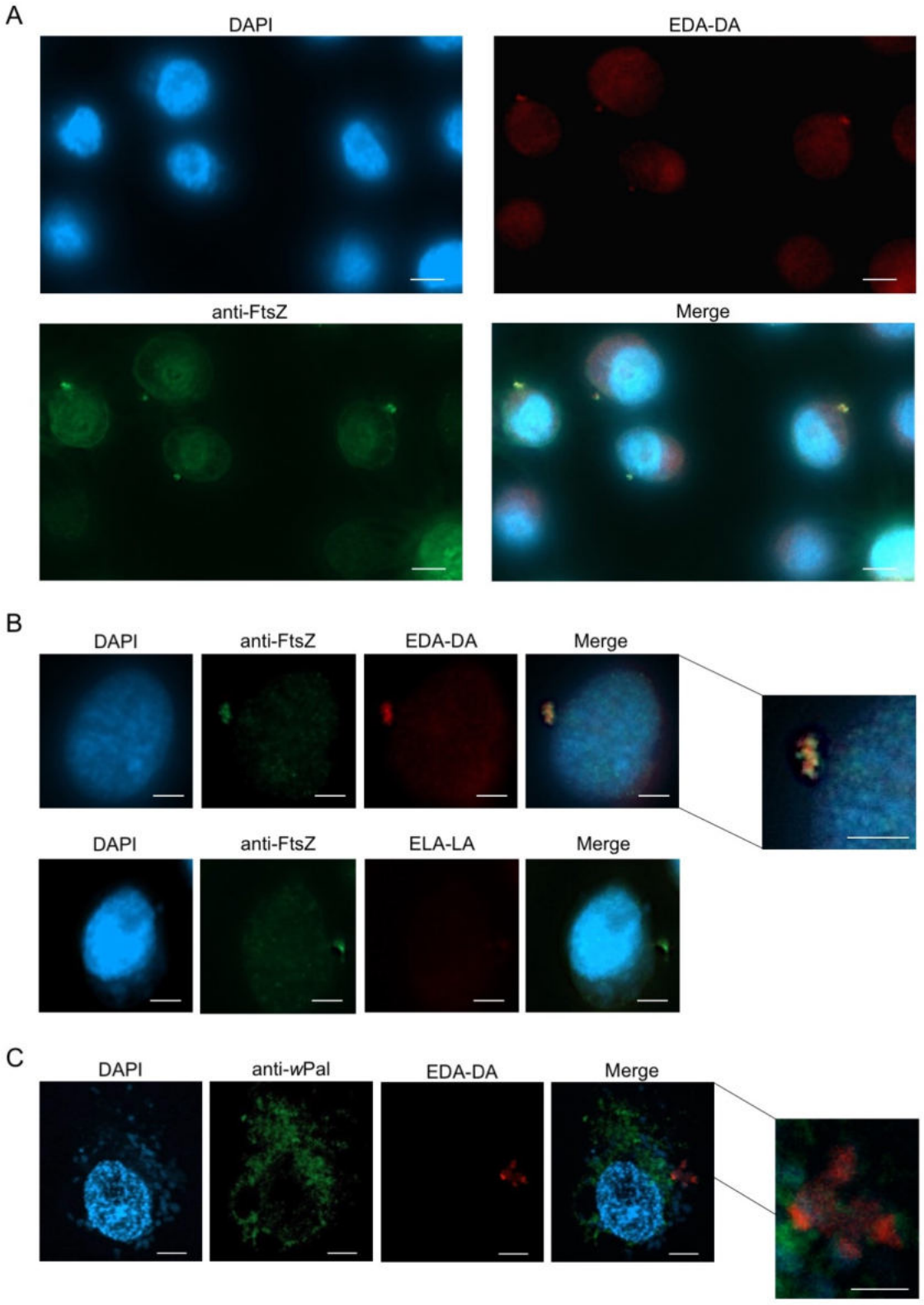

Figure 67: Fluorescent labeling of lipid II in *Wolbachia.* *w*AlbB infected C6/36 insect cells were incubated for 72 h with 1 mM of EDA-DA or ELA-LA, respectively. Binding of the probe to Alexa Fluor® 594 azide (red) was achieved by click chemistry. *w*AlbB were stained with anti-FtsZ or anti-*w*Pal antibody (green). DAPI (blue) was used for nuclear staining. A) Fluorescent labeling of lipid II by EDA-DA in *w*AlbB using anti-FtsZ antibody. Scale bar = 10 µm. B) Fluorescent labeling of lipid II by EDA-DA in one *w*AlbB infected C6/36 cell using anti-FtsZ antibody. Cells incubated with ELA-LA did not contain labeled lipid II. Scale bar = 5 µm, zoom: 2 µm. C) Fluorescent labeling of lipid II in one *w*AlbB infected C6/36 cell using anti-*w*Pal antibody. Scale bar = 5 µm, zoom = 2 µm. A,B) were observed with an epifluorescence microscope (ZeissAxio VertA.1, Carl Zeiss AG). C) were visualized using a confocal microscope (Zeiss LSM800 Airyscan, Carl Zeiss AG).

3.6.3 Dipeptide labeling of fosfomycin-treated *w*AlbB

To demonstrate specific incorporation of EDA-DA into *Wolbachia*, cells incubated with EDA-DA were pretreated with fosfomycin. This specific inhibitor of MurA, which catalyzes the first step of the lipid II biosynthesis from UDP-Glc*N*Ac, was demonstrated to result in an enlarged phenotype in *w*AlbB due to inhibited cell division (Vollmer et al., 2013). Here, treatment with fosfomycin led to the expected enlarged *Wolbachia* phenotype and no incorporation of EDA-DA into the cells (Figure 68).

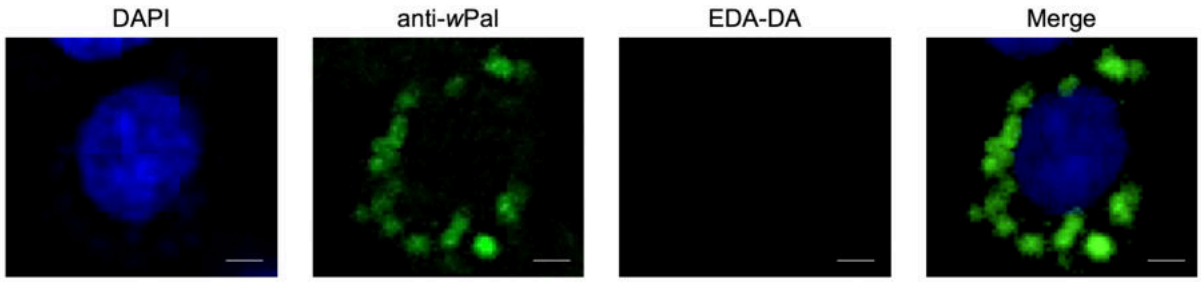

Figure 68: Fluorescent labeling of lipid II in *Wolbachia*. C6/36 insect cells infected with *w*AlbB were treated daily with 512 µg/ml fosfomycin for twelve days and then incubated for 72 h with 1 mM of the dipeptide probe EDA-DA. Subsequent binding of the probe to an azide-modified Alexa Fluor® 594 (red) was achieved by click chemistry. *Wolbachia* were stained with an anti-*w*PAL antibody (green). DAPI was used for nuclear staining (blue). Scale bar = 5 µm. Cells were visualized using a confocal microscope (Zeiss LSM710, Carl Zeiss AG).

3.6.4 Cell-free *w*AlbB viability in different media

Wolbachia can temporarily survive in an extracellular environment (Dobson et al., 2002; Frydman et al., 2006; Rasgon et al., 2006). To further demonstrate that *Wolbachia* have some form of peptidoglycan-like structure, *w*AlbB were purified from the C6/36 insect cells and suspended in ultrapure water, PBS or Leibovitz medium. *w*AlbB remained intact and viable in all media for at least one hour (Figure 69) indicating the presence of a mechanical stress-bearing structure as recently shown for *O. tsutsugamushi* in a similar assay (Atwal et al., 2017).

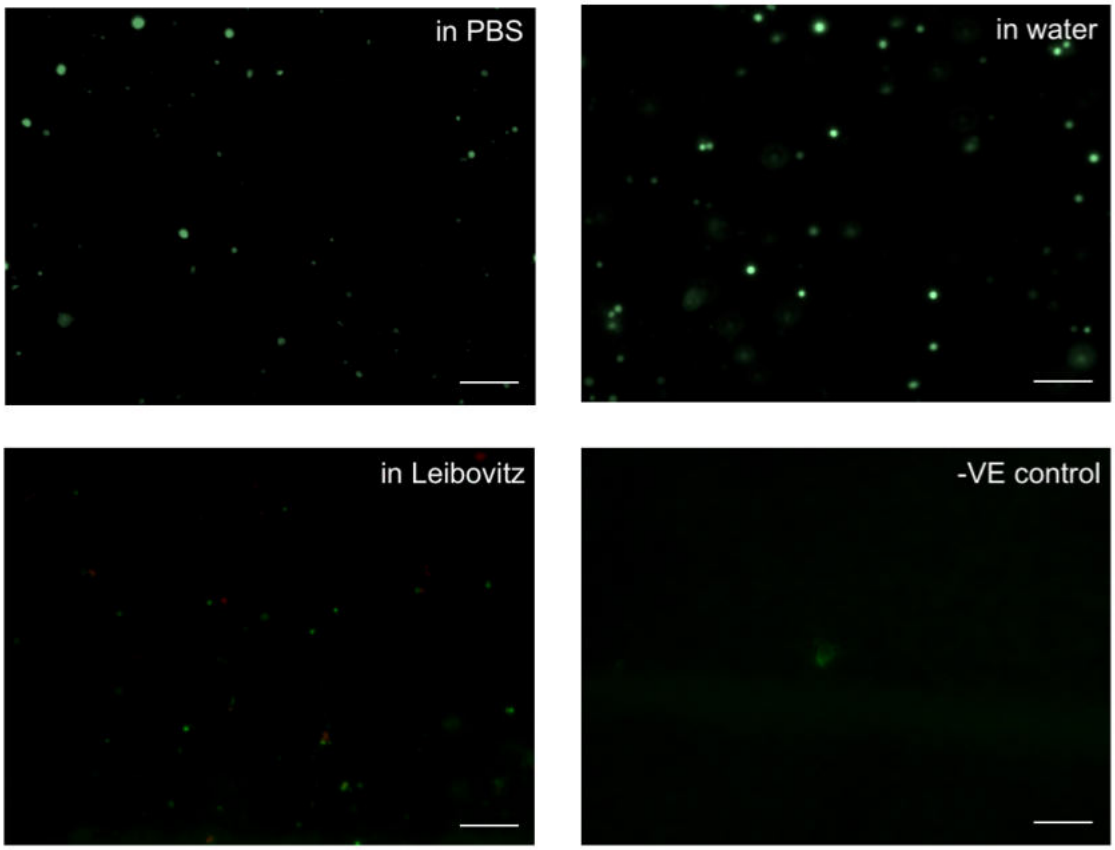

Figure 69: Viability of isolated *Wolbachia* suspended in different media. *w*AlbB infecting C6/36 insect cells were purified and resuspended in PBS, ultrapure water, or Leibovitz medium. LIVE/DEAD® *Bac*Light™ staining was added after 1 h incubation and cells were visualized under a fluorescence microscope. *w*AlbB remained viable in all media. A mock purification with uninfected C6/36 insect cells served as a negative control. Scale bar = 10 µm.

3.7 Cell-free *w*AlbB culture

The requirements for *Wolbachia* strain *w*AlbB growth in a host cell-free *in vitro* culture system were characterized in a former project (Vollmer, 2012). Supplementation with cell lysate derived from *Aedes albopictus* C6/36 insect cells allowed extracellular *w*AlbB replication rates in a mean of 6.4-fold. An insect cell lysate fraction containing cell membranes was identified as requisite for cell-free replication of *Wolbachia* (Vollmer, 2012). The required factors from this fraction were dependent on cultivation of the insect cells in medium containing fetal bovine serum. The endobacteria replicated for up to twelve days and could infect uninfected C6/36 cells (Vollmer, 2012). Replication rates in the insect cell-free culture were lower compared to *w*AlbB grown inside insect cells (Vollmer, 2012). In this work, the cell-free *w*AlbB culture was further studied and growth conditions were altered (e.g. by supplementation with substances) in order to enhance stability and growth. Moreover, cell-free *w*AlbB were

incubated with different antibiotics to test the efficacy and impact on proliferation and morphology.

3.7.1 Cell-free *w*AlbB with modified growth conditions

3.7.1.1 Incubation on actin-coated streptavidin plates

Cell-free *w*AlbB cells do not attach to the plate bottom impeding medium change of the culture. Centrifugation of the culture (18,400 g for 5 min) to separate *Wolbachia* from the cell culture medium harmed the bacteria (data not shown). To overcome this limiting factor of the cell-free culture, actin-coated streptavidin plates were used. Pal^{wBm} specifically binds to actin filaments of *B. malayi* and might be crucial in maintenance of endosymbiosis (Melnikow et al., 2013). Cell-free *w*AlbB were seeded on coated plates and kept in culture for twelve days. Cell-free *Wolbachia* incubated on the actin-coated plates were slightly increasing up to day six, but then decreased. Additionally, it was tested whether a medium change might enhance growth of the potentially adherent cells. However, resuspension in fresh culture medium on day six led to a loss of bacteria instead of enhancing growth (Supplementary Figure 17).

3.7.1.2 Cell-free growth in a lowered oxygen environment

Oxygen levels inside the C6/36 cells are unknown and growth of *w*AlbB might be adapted to lower levels of oxygen compared to the earth atmosphere. Using a carbonic gas chamber, oxygen levels were decreased from 20.9 % to 3 %, and carbonic gas increased from 0.004 % to 5 %. Additionally, cultures were maintained up to 15 days to test whether growth was enhanced in the carbonic gas chamber. Cell-free cultures incubated under lower levels of oxygen showed similar proliferation rates (6.9-fold ± 1 SD) compared to the standard cell-free *w*AlbB culture (7.2-fold ± 0.8 SD) and growth plateaued after twelve days (Supplementary Figure 18).

3.7.1.3 Supplementation of cell-free *w*AlbB standard culture medium

After 9–12 days of replication, cell-free *w*AlbB numbers decrease suggesting that substances necessary to replicate might be expended (Vollmer, 2012). To enhance growth, freshly prepared insect cell lysate (equivalent to 0.95 x 10^6 uninfected C6/36 cells) was applied to the culture and proliferation was monitored via qPCR. Proliferation rates were slightly higher after twelve days (4.9-fold ± 0.5 SD) compared to the standard cell-free culture (4-fold ± 0.3 SD) in the conducted assays, but growth was not elongated (Supplementary Figure 19).

Recent studies indicate that *Wolbachia*-infected insect cells might indeed incorporate cholesterol maybe as a substitute for lipopolysaccharide (Caragata et al., 2013; Geoghegan et

al., 2017). Therefore, insufficient amounts of cholesterol were considered as a potential limiting factor of cell-free *Wolbachia* growth. Freshly prepared water-soluble cholesterol was added to the cell-free culture, but no advantages regarding proliferation were observed compared to the standard conditions (Supplementary Figure 20).

Lipid Mixture Solution (PeproTech) contains non-animal-derived fatty acids and lipids to improve cell growth in serum-free media. The lipid mixture solution was added to the cell-free *w*AlbB culture to examine any beneficial effects, but supplementation inhibited cell-free growth rather than enhancing proliferation (Supplementary Figure 21).

To enhance cell-free *w*AlbB growth, biotin, cystine, glucose, PLP, and sodium bicarbonate, which are present in an optimized cell-free medium designed for intracellular *C. burnetii* (Omsland et al., 2009), were added to the cell-free *w*AlbB standard medium. Higher proliferation rates were observed in cultures supplemented with glucose (9.03-fold ± 1.6 SD) compared to the standard conditions (7.8-fold ± 2.7 SD), but replication decreased after nine days (Supplementary Figure 22). None of the other applied substances enhanced cell-free proliferation and moreover, supplementation of biotin and sodium bicarbonate inhibited *w*AlbB replication.

The co-cultivation of *B. malayi* and *B. pahangi* infective-stage L3 larvae with the yeast *R. minuta* supports molting to the fourth larval stage *in vitro* (Smith et al., 2000). It was suggested that the larvae are benefiting from an unknown secreted product of the yeast. This compound might also be beneficial for the growth of *Wolbachia*, thus *R. minuta* (10^4–10^7 cells/ml) were co-cultured with cell-free *w*AlbB. However, the presence of *R. minuta* harmed the cell-free culture leading to a depletion of *w*AlbB in a concentration-dependent manner (Supplementary Figure 23).

3.7.2 Growth of cell-free *w*AlbB in the presence of antibiotics

3.7.2.1 Cell-free growth in the presence and absence of penicillin/streptomycin

The standard insect cell culture medium includes the addition of 1 % penicillin and streptomycin to prevent growth of unwanted bacteria since *Wolbachia* were shown to be resistant to these two antibiotics (O'Neill et al., 1997). These experiments were never performed under cell-free conditions, thus it was tested whether penicillin or streptomycin potentially inhibit proliferation of cell-free *w*AlbB. Cell-free cultures were prepared as described in chapter 2.11.3 with or without 1 % penicillin/streptomycin and growth was monitored via qPCR. The results showed similar *w*AlbB proliferation rates under cell-free conditions in the presence

(9-fold ± 1.7 SD) or absence (9.3-fold ± 3.8 SD) of penicillin or streptomycin (Figure 70). Thus, these antibiotics were further used to prevent growth of other bacteria strains in the culture.

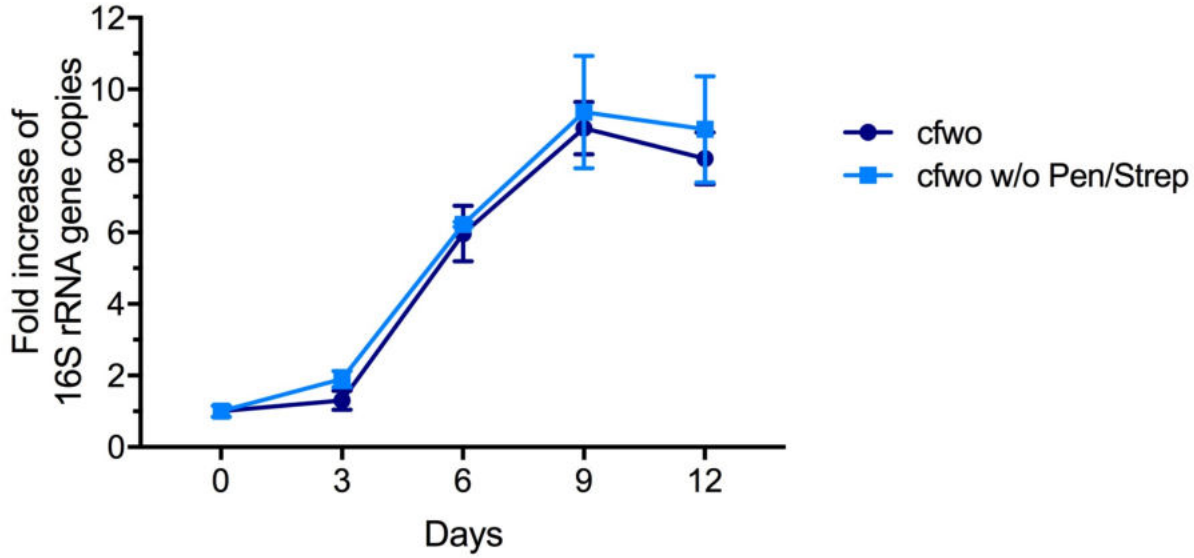

Figure 70: Cell-free *w*AlbB growth in the presence and absence of penicillin and streptomycin. Cell-free *Wolbachia* (cfwo) were incubated in medium with or without 1 % penicillin/streptomycin (Pen/Strep) for twelve days. Growth was monitored every three days by qPCR and data were normalized to day 0 (X-axis). For every time point the mean ± SEM of six samples from two independent experiments is shown.

3.7.2.2 Cell-free growth in the presence of antibiotics effective against *Wolbachia*

The extracellular cultivation of *Wolbachia* provides an excellent tool for understanding the biology and symbiosis of *Wolbachia* and allows treatment with antibiotics that do not pass the insect cell membranes. Cell-free growth in the presence and absence of corallopyronin A, doxycycline, fosfomycin and rifampicin was examined, four antibiotics which are known to affect *Wolbachia* (Volkmann et al., 2003; Schiefer et al., 2012; Vollmer et al., 2013). Untreated cell-free *w*AlbB cultures served as a positive control, *w*AlbB cultures incubated without cell lysate from insect cells only in culture medium served as a negative control, because this treatment does not facilitate cell-free replication. As growth rates showed a high variation in the conducted assays, one assay is exemplarily presented here (Figure 71). Untreated cell-free *w*AlbB cultures were able to replicate (4-fold ± 0.7 SD), while the growth rate of the medium control was low (1.2-fold ± 1 SD). All antibiotic-treated *Wolbachia* cultures replicated, albeit growth rates were decreased in rifampicin-treated cells (3.1-fold ± 1.5 SD). As no inhibition of cell-free *w*AlbB growth could be observed in the other three positive controls corallopyronin A (3.9-fold ± 1.1 SD), doxycycline (4.9-fold ± 1.2 SD) and fosfomycin (4.6-fold ± 0.2 SD), analysis of growth rates via gDNA and qPCR was considered as an improper tool to detect effects of antibiotics with unknown impact to *Wolbachia*.

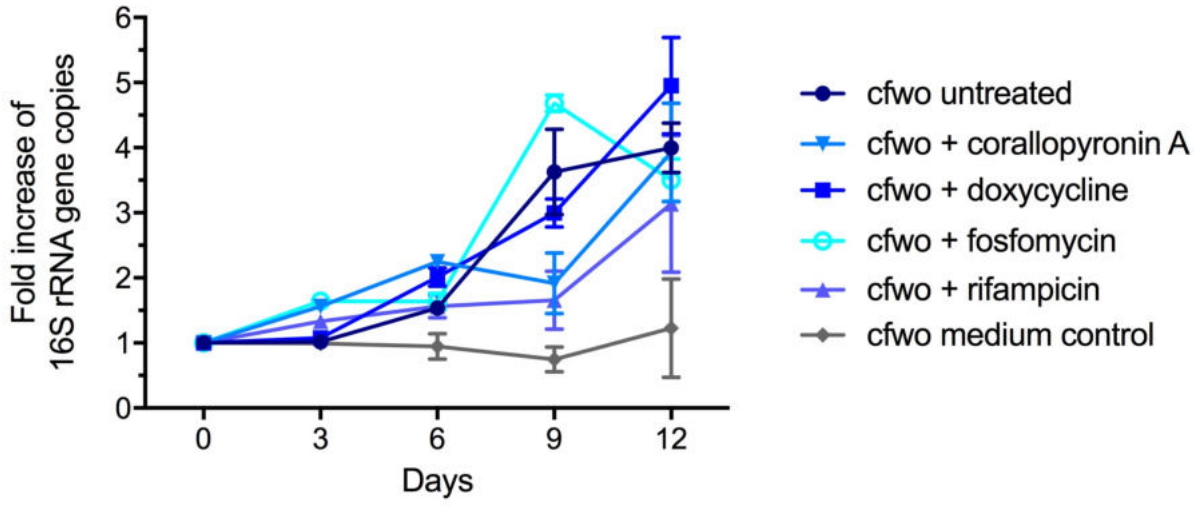

Figure 71: Cell-free *w*AlbB growth in the presence and absence of corallopyronin A, doxycycline, fosfomycin and rifampicin. Cell-free *Wolbachia* (cfwo) were incubated in growth medium with or without corallopyronin A, doxycycline, fosfomycin or rifampicin for twelve days. Cfwo incubated in medium served as a negative control. Growth was monitored every three days by qPCR and data were normalized to day 0 (X-axis). The graph is representative for six independent experiments. For every time point the mean ± SEM of three samples is shown.

A second approach to measure effects of antibiotics on cell-free *w*AlbB was the analysis of gene expression by isolation of total RNA of the culture, translation into cDNA and subsequent measurements via qPCR. Different experiments showed a high variance of expression levels of the 16S rRNA gene, thus the data from one experiment are exemplarily shown here (Figure 72). Since the 16S rRNA gene was not stably-expressed in untreated *w*AlbB, this attempt turned out as inappropriate and was rejected. Therefore, the effect of antibiotics on cell-free *w*AlbB was investigated by observing the phenotype of cells via microscopy.

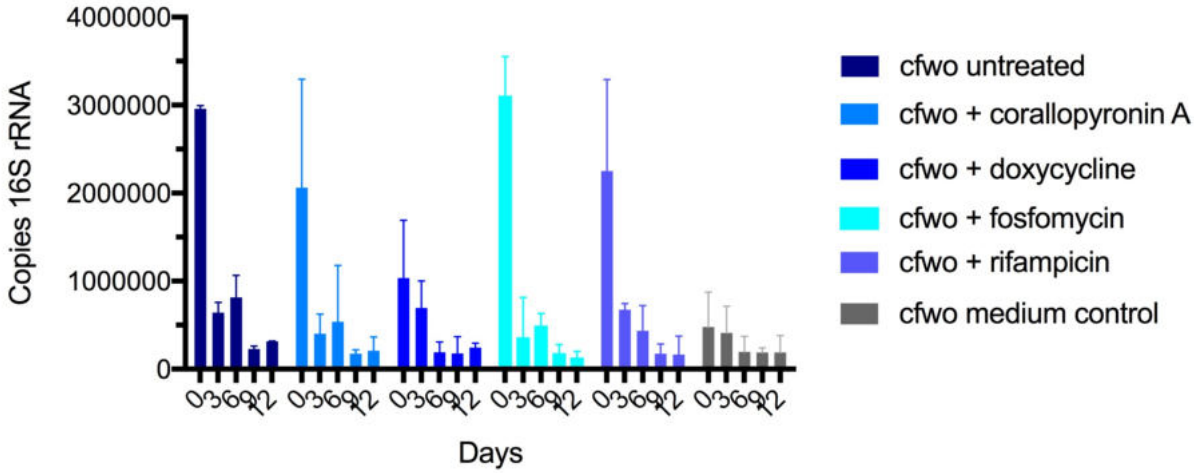

Figure 72: Levels of expressed 16S rRNA in cell-free *w*AlbB in the presence and absence of corallopyronin A, doxycycline and rifampicin. Cell-free *Wolbachia* (cfwo) were incubated with or without corallopyronin A, doxycycline, fosfomycin or rifampicin for twelve days. Cfwo incubated in medium without insect cell lysate served as a negative control. Every three days, RNA was extracted and transcribed into cDNA. Levels of 16S rRNA were monitored by qPCR of the transcribed cDNA. The graph is representative for six experiments. For every time point the mean ± SEM of three samples is shown.

3.7.3 Morphology of cell-free *w*AlbB in the presence of antibiotics

Cell-free *w*AlbB cultures were incubated with different antibiotics (see Table 28). After twelve days, fosfomycin-treated *Wolbachia* were significantly larger around 3.69 µm (± 1.35 SD) and *w*Pal was detected as a punctate staining pattern, whereas untreated cell-free *Wolbachia* had an average size of 1.06 µm (± 0.35 SD) and evenly distributed *w*Pal (Figure 73). These results confirm previous observations of enlarged fosfomycin-treated *Wolbachia* residing in host cells indicating sensitivity to this antibiotic (Vollmer et al., 2013).

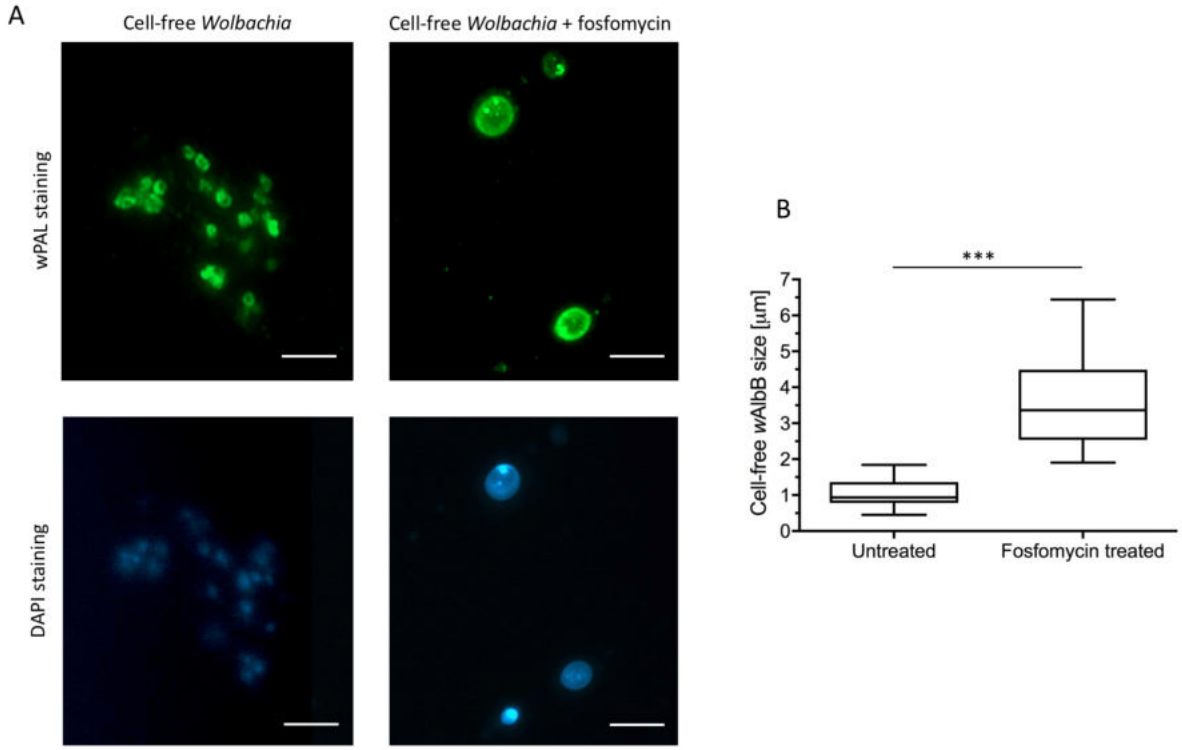

Figure 73: Cell-free cultured *Wolbachia* are sensitive to fosfomycin treatment. Cell-free *Wolbachia* cultures were incubated for twelve days without antibiotic or treated daily with 512 µg/ml fosfomycin. A) Cells were fixed and *Wolbachia* were visualized by immunofluorescence microscopy using *w*PAL anti-serum and an Alexa Fluor® 488 conjugated secondary goat anti-rabbit antibody as well as DAPI for DNA staining. Scale bar = 5 µm. B) Statistical difference (n = 22) was determined using Mann-Whitney test, *** = $P \leq 0.001$. Boxes extend from the 25th to the 75th percentile. The line in the middle of the box is plotted at the median. Whiskers extend from the smallest to the largest value.

However, none of the other tested antibiotics showed an aberrant phenotype including those targeting lipid II or peptidoglycan synthesis (ampicillin, bacitracin, vancomycin) (Figure 74).

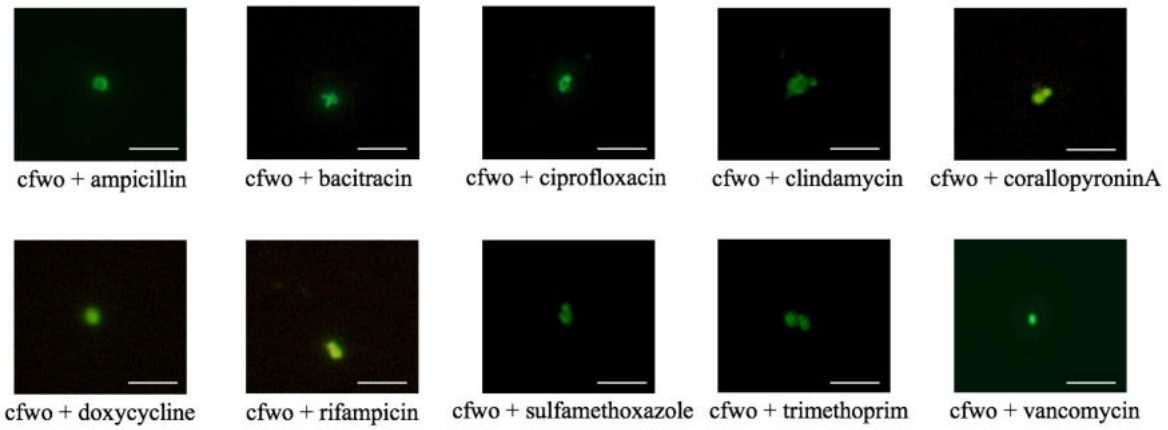

Figure 74: Cell-free *Wolbachia* morphology after antibiotic treatment. Cell-free *Wolbachia* cultures were incubated for twelve days with different antibiotics. Cells were fixed and *Wolbachia* visualized by immunofluorescence microscopy using *w*PAL anti-serum and an Alexa Fluor® 488 conjugated secondary goat anti-rabbit antibody. Scale bar = 5 µm.

4 Discussion

Wolbachia are obligate intracellular bacteria with a reduced genome and it is hypothesized that all genes retained are essential for *Wolbachia* survival (Wu et al., 2004; Foster et al., 2005). *Wolbachia* are not challenged by osmotic pressure and a peptidoglycan structure as present in free-living bacteria has not been detected, but *Wolbachia* possess all genes required for the synthesis of the peptidoglycan precursor lipid II. These genes are expressed *in vivo* and *Wolbachia* membrane preparations synthesize lipid II *ex vivo* (Henrichfreise et al., 2009). Furthermore, a crucial role of lipid II in the multi-enzyme machinery forming the divisome is estimated since inhibition of an early step of lipid II synthesis by fosfomycin leads to enlarged *Wolbachia* cells (Vollmer et al., 2013). The investigation of *Wolbachia* enzymes involved in lipid II metabolism does not only provide insight into *Wolbachia* biology but might identify novel targets for the development of antibiotics for use in depleting these essential endobacteria from filarial nematodes causing lymphatic filariasis and onchocerciasis in humans. Due to genetic intractability of *Wolbachia, E. coli* was used as surrogate host to investigate wolbachial enzyme activity *in vivo*.

4.1 Functional characterization of PBP6a$^{w\mathrm{Bm}}$

The final reaction in cell wall biosynthesis is the cleavage of the terminal D-Ala residue of the pentapeptide side chain accompanied by the formation of an interpeptide bridge (Peters et al., 2016). The degree of crosslinking is regulated by a monofunctional DD-carboxypeptidase cleaving the terminal D-Ala of the pentapeptide, thereby influencing the activities of the elongasome and the divisome due to their dependence on the presence of lipid II pentapeptide chains (Den Blaauwen et al., 2008). The function of the putative DD-carboxypeptidase PBP6a in *Wolbachia* is unknown thus far. In this thesis, a first insight into its role in wolbachial lipid II processing was gained by *in silico* analysis of the protein structure as well as *in vivo* and *in vitro* experiments. PBP6a$^{w\mathrm{Bm}}$ is a homolog of the DD-carboxypeptidase PBP6 from *E. coli*. *In silico* secondary structure analysis of PBP6a$^{w\mathrm{Bm}}$ predicted the presence of a putative active site center composed of SXXK, SX(D/N) and K(S/T)G motifs. However, it should be considered that this modeling was based on homologies to the presumed *E. coli* ortholog. Thus, the predicted structure can only give a hint of the putative protein architecture, but the exact structure of PBP6a$^{w\mathrm{Bm}}$ remains unclear at this point.

In this thesis, the *in vivo* activity of recombinant PBP6a^{wBm} was investigated in *E. coli*. The deletion of PBP6 in *E. coli* does not result in a detectable altered phenotype (Nelson and Young, 2001; Chowdhury et al., 2010). Still, the effect of this DD-carboxypeptidase on cell shape can be analyzed *in vivo* by overproducing the enzyme in the temperature-dependent PBP3-deficient *E. coli* strain MCI23 which leads to partial restoration of the normal cell shape (Begg et al., 1990; Otten, 2014). DD-carboxypeptidases cleave the terminal D-Ala from the pentapeptide side-chain of lipid II, yielding lipid II with a tetrapeptide. The subsequent cleavage of the lipid II tetrapeptide by the LD-carboxypeptidase A results in high levels of lipid II tripeptide that shifts the product equilibrium, thus favoring transpeptidation reactions by PBP3 (Beck and Park, 1977; Van Heijenoort, 2011). The high amount of lipid II tripeptide, which is the preferred substrate of PBP3, enables residual transpeptidation activity of this enzyme leading to partial complementation of cell division (Botta and Park, 1981; Pisabarro et al., 1986; Begg et al., 1990). Here, this assay was used to analyze the putative DD-carboxypeptidase activity of PBP6a^{wBm}. The growth defect of *E. coli* MCI23 at the non-permissive temperature of 42 °C was partially complemented in the presence of overexpressed recombinant PBP6a^{wBm}. Notably, long PBP6a^{wBm} expression of more than two hours resulted in formation of spherical cells and lysis (data not shown). Unregulated lipid II modification due to continuous overexpression of a DD-carboxypeptidase probably leads to an increased septation at the expense of elongation, resulting in spherical growth and cell lysis as shown during PBP3 and PBP5 overexpression in *E. coli* (Nelson and Young, 2001; Den Blaauwen et al., 2008). The observed mixture of phenotypes with variation in cell length of PBP6a^{wBm} expressing *E. coli* MCI23 might be due to lowered enzyme activity caused by the high temperature of 42 °C. As aforementioned, lipid II with a tripeptide is the preferred substrate of PBP3, but this enzyme is still impaired and only possesses residual activity at 42 °C. Additionally, it should be considered that peptidoglycan synthases are tightly regulated and show differential activity during different cell cycle stages. While the *E. coli* DD-carboxypeptidase PBP5 is highly active during exponential growth, PBP6a expression increases in the stationary phase (Sarkar et al., 2011). Hence, missing synchronization of cell cycles in this assay might lead to a mixture of phenotypes. Probably, single *E. coli* MCI23 cells might have been arrested during different cell cycle stages when the temperature was switched to 42 °C. This could have an influence on the degree of activity of recombinant PBP6a^{wBm} leading to mixed phenotypes. However, previous investigations on the activity of the DD-carboxypeptidase PBP5 in *E. coli* after synchronization of cell cycles revealed that synchronization was already lost after two divisions (Mirelman et al., 1977). Therefore, cell cycle synchronization was not reasonable for the complementation

assays and was neglected. Nevertheless, the results of the assays performed in this thesis provide a first hint that PBP6a^{wBm} is an active DD-carboxypeptidase *in vivo*.

The general mechanism of DD-carboxypeptidase activity is based on the conserved motifs SXXK, SX(D/N), and K(S/T)G. Although details of the exact catalytic mechanism of serine-based PBPs have not been elucidated yet, a general mechanism consisting of acylation and deacylation of the peptide substrates under involvement of all three conserved motifs has been predicted (Dougherty and Pucci, 2011). This prediction is mainly based on studies of the DD-carboxypeptidase PBP5 of *E. coli* (Nelson and Young, 2001; Sauvage et al., 2008). In this enzyme, the nucleophilic properties of the active site serine of the SXXK motif are enhanced by the abstraction of a proton by the hydroxylgroup of lysine of the same motif, promoting the nucleophilic attack on the terminal D-Ala carbonyl group of a pentapeptide. This leads to an acyl-enzyme intermediate and cleavage of the terminal D-Ala from the pentapeptide chain (Sauvage and Terrak, 2016). Subsequent deacylation is catalyzed by serine of the SX(D/N) motif and polarized by lysine of the K(S/T)G motif (Dougherty and Pucci, 2011). Since the nucleophilic attack during the first reaction step of a DD-carboxypeptidase requires the polarized hydroxyl group of the active site serine, amino acid substitution of serine by alanine within SXXK motifs was expected to impair PBP6a^{wBm} activity. A dependence of DD-carboxypeptidase activity on functional SXXK motifs was already demonstrated in PBP6 from *C. pneumoniae* (Otten, 2014). When PBP6a^{wBm} with a single mutated SXXK motif was expressed at the non-permissive temperature of 42 °C in *E. coli* MCI23, cell division was partially restored indicating that SXXK motifs can substitute each other. Mutation of both SXXK motifs present in PBP6a^{wBm} almost completely abolished enzyme activity resulting in filamentous *E. coli* MCI23 cells (mean: 91 %) unable to divide at 42 °C. However, more were filamentous (mean: 97 %) in the negative control with the induced empty vector. The remaining single and dividing cells in the double SXXK mutant of PBP6a^{wBm} were likely caused by expression stress as shown by control experiments with Pal^{wBm}.

The *in vitro* activity assays analyzed by TLC and MALDI-TOF showed lipid II with a tetrapeptide further supporting that PBP6a^{wBm} is a functional DD-carboxypeptidase. Mutation of SXXK motifs led to abolished activity of PBP6a^{wBm} indicating that activity might depend on functional SXXK motifs as shown for the chlamydial ortholog PBP6 (Otten, 2014). Enzyme activity of PBP6a^{wBm} was slower compared to the positive control VanY from *S. aureus*, which might be a result of suboptimal *in vitro* conditions for the recombinant wolbachial enzyme. Apart from that, *Wolbachia* have a slower metabolism with a generation time in cell culture of 14 h compared to free-living bacteria (e.g. less than one hour in *E. coli* and *B. subtilis*) and

therefore also enzyme activity might be slower (Fenollar et al., 2003; Taheri-Araghi et al., 2015). PBPs are the targets of β-lactam antibiotics as high affinity acylation of the SXXK active site serine blocks the enzyme into an inactive form (Sauvage and Terrak, 2016). Inhibition assays using β-lactams were only performed *in vitro*, because there is no specific inhibitor known for PBP6a. The application of broad spectra β-lactam antibiotics *in vivo* would impair a variety of PBPs in *E. coli* MCI23 potentially leading to false positive results. The applied β-lactams (ampicillin and penicillin G) did not inhibit PBP6a^{wBm} activity *in vitro* and moreover, the enzyme did not bind to fluorescent- or radiolabeled penicillin in binding assays. These results are in line with previous findings that *Wolbachia* are resistant to β-lactams (O'Neill et al., 1997). However, it should be considered that penicillin-binding assays were performed with purified recombinant enzymes. Due to a potential different folding of recombinant enzymes in *E. coli*, it is possible that the native PBP6a^{wBm} might bind β-lactams. *In silico* modeling predicted that the second and conserved SXXK binding motif of PBP6a^{wBm} might be accessible for β-lactams. As the first SXXK motif is not assumed to be involved in binding, PBP6a^{wBm} might still be active in the presence of a β-lactam, because *in vivo* assays indicate that one functional SXXK motif is sufficient to maintain activity of this enzyme. Further *in vivo* activity assays excluded that PBP6a^{wBm} resistance to β-lactams was caused by a potential β-lactamase activity of the enzyme. The conserved function of the PBP6a^{wBm} DD-carboxypeptidase activity provides first proof that wolbachial lipid II is further processed and this modification might be essential for the cell cycle in *Wolbachia*. In free-living bacteria, DD-carboxypeptidases regulate the degree of crosslinking of peptide stems to mature peptidoglycan, thus lipid II moieties in *Wolbachia* might at least be connected via peptide chains building a peptidoglycan-like structure.

4.2 Functional characterization of PBP2^{wBm}

Identical to DD-carboxypeptidases, DD-transpeptidase activity is based on the conserved motifs SXXK, SX(D/N), and K(S/T)G (Sauvage and Terrak, 2016). The active site serine of the SXXK motif plays a crucial role in the two-step crosslinking reaction. Firstly, it performs a nucleophile attack on the carbonyl group of the terminal D-Ala-D-Ala amide bond of a pentapeptide which leads to the formation of an acyl-enzyme intermediate and subsequent release of the terminal D-Ala. Secondly, an amino group of a peptide from a neighboring glycan chain attacks this complex building a cross bridge connecting both peptides with concomitant release of the DD-transpeptidase (Sauvage and Terrak, 2016). The role of PBP2^{wBm} in the cell cycle of *Wolbachia* is unknown and first assays to characterize this putative DD-transpeptidase

were performed in this thesis. Of note, PBP2^{wBm} was re-annotated in NCBI to a putative PBP3, a DD-transpeptidase involved in cell division. However, based on sequence alignments, PBP2^{wBm} showed a higher similarity to PBP2 from different species than to PBP3, thus the term PBP2^{wBm} was kept as a description for this enzyme in this study. Secondary structure analysis revealed a putative functional active site with SXXK, SX(D/N), and K(S/T)G motifs. PBP2^{wBm} was investigated *in vivo* using the temperature sensitive strain *E. coli* MCI23 with impaired PBP3 activity at 42 °C. Thereby, it was examined whether PBP2^{wBm} exhibits activity *in vivo* and if it is involved in cell elongation or cell division. In rod-shaped *E. coli*, PBP2 is an essential component of the peptidoglycan biosynthesis multi-enzyme complex and promotes cell elongation as well as shape maintenance (Den Blaauwen et al., 2008; Typas et al., 2010). Thus, it was unsurprising that PBP2^{wBm} with its native transmembrane domain was not active in the used *E. coli* MCI23 model. The transmembrane domain helps in the orientation of this enzyme and PBP2^{wBm} is expected to be recruited to the elongasome rather than to the divisome. In contrast, PBP2ΔTM^{wBm} restored complementation of *E. coli* MCI23 at 42 °C indicating enzyme activity *in vivo*. PBP2ΔTM^{wBm} without its native transmembrane domain might reach its target lipid II in the divisome due to solubility in the periplasm. PBP2ΔTM^{wBm} activity was presumably dependent on functional SXXK motifs as expression of the protein with mutated motifs led to decreased levels of *E. coli* MCI23 able to divide. Similar to PBP6a^{wBm}, an apparent remaining activity was observed, which was likely caused by protein expression stress. PBP2ΔTM^{wBm} was resistant to mecillinam showing wolbachial resistance to β-lactams on a molecular level. Further *in vivo* activity assays excluded that PBP2^{wBm} resistance was caused by a potential β-lactamase activity of the enzyme. *In silico* analysis predicted a binding of β-lactams only by the serine residue of the second SXXK motif. *In vivo* assays with a single mutated SXXK motif confirmed activity PBP2ΔTM^{wBm} with only one functional active site. Summing up, the *in vivo* results suggest that PBP2^{wBm} might be functional in the *E. coli* divisome or in the elongasome in a mecillinam-resistant manner. It should be noted that PBP2^{wBm} might also have DD-carboxypeptidase activity as the *in vivo* complementation assay cannot clearly distinguish between DD-carboxy- and DD-transpeptidase activity. But because PBP2^{wBm} was able to substitute for mecillinam-inhibited PBP2 from *E. coli*, it is likely that PBP2^{wBm} indeed has DD-transpeptidase activity. Since there was no *E. coli* strain available with a PBP2 knock-out during the study, additional control experiments could not be performed. A putative PBP3 which might act as a DD-transpeptidase specifically in the divisome is disrupted by multiple frameshifts in the genome of *w*Bm (Foster et al., 2005). Therefore, it might be speculated that PBP2^{wBm} can substitute PBP3 DD-transpeptidase function during division. This

would not automatically exclude a participation of this enzyme in cell elongation as it might have taken over both tasks in *Wolbachia* due to genome reduction. This was shown for *Chlamydia*, which harbor PBP2 and PBP3, where both enzymes were shown to be involved in cell division (Ouellette et al., 2012). The fact that PBP2 is present in the genome of *w*Bm and moreover, shows *in vivo* activity in assays with recombinant protein, strongly indicates that at least a rudimentary peptidoglycan might be present in *Wolbachia* of *Brugia malayi*. However, functional characterization of PBP2^{wBm} *in vitro* did not clearly reveal transpeptidation activity. In general, the cross-linking of lipid II peptide moieties by monofunctional DD-transpeptidases is poorly characterized *in vitro* even in well investigated bacteria due to a lack of established assays (Dougherty and Pucci, 2011). Furthermore, analysis of DD-transpeptidases can be cumbersome as most of these enzymes are membrane-anchored and difficult to purify in sufficient quality for biochemical characterization (Egan et al., 2015). In this thesis, reaction products resulting from PBP2^{wBm} *in vitro* activity were analyzed by TLC. A slight extinction of the lipid II band after incubation with PBP2^{wBm} was observed, which can be a hint for DD-transpeptidase activity, but generally this assay cannot detect cross-linked polymers. It should be considered that recombinant PBP2^{wBm} could only be stored for a couple of days after expression due to high instability and degradation of the protein. Thus, it cannot be excluded that some batches contained degraded protein, although they were used for activity assays immediately after purification. Still, the mechanism of DD-transpeptidase activity includes DD-carboxypeptidase activity resulting in a cleaved D-Ala and a lipid II tetrapeptide which can be detected *in vitro* as shown in this study for PBP6a^{wBm}. Lipid II with a tetrapeptide was not detected in the performed *in vitro* assays, thus the putative DD-transpeptidase activity of PBP2^{wBm} remains unclear and needs further study. In *E. coli*, peptidoglycan synthases were shown to be controlled by outer membrane proteins (Typas et al., 2010; Egan et al., 2014). Since an interaction between PBP2^{wBm} and Pal^{wBm} was measured, it was hypothesized that lipid II mDAP monomers might be cross-linked by the action of PBP2^{wBm} regulated by Pal^{wBm}. Thus, purified Pal^{wBm} was added to the *in vitro* DD-transpeptidase reaction mixture, but no activity of PBP2^{wBm} was observed by TLC under these conditions (data not shown). PBP2^{wBm} is predicted to be a monofunctional DD-transpeptidase suggesting that its activity might be dependent on the association with a bifunctional PBP with DD-transpeptidase and glycosyltransferase activity or with a monofunctional glycosyltransferase (Den Blaauwen et al., 2008). PBP2 from *S. aureus* is a bifunctional class A PBP (Barrett et al., 2005). A PBP2 mutant from *S. aureus* with knocked out DD-transpeptidase activity was kindly provided by Dr. Anna Müller (AG Tanja Schneider, University of Bonn) and *in vitro* DD-transpeptidase activity assays with

PBP2^{wBm} were repeated in the presence of the active glycosyltransferase. However, activity of PBP2^{wBm} was not observed under these conditions by TLC (data not shown). These results strongly indicate that PBP2^{wBm} activity might be dependent on other molecules which are lacking under *in vitro* conditions. Interestingly, the monofunctional DD-transpeptidase PBP2 from *E. coli* interacts with RodA, a transmembrane protein which was recently identified as a functional glycosyltransferase in *E. coli* and *B. subtilis* in absence of bifunctional PBPs (Cho et al., 2016; Meeske et al., 2016). The transmembrane protein FtsW, which builds a sub-complex with PBP3, is predicted to act as a glycosyltransferase in the divisome, but this hypothesis needs experimental validation (Cho et al., 2016; Meeske et al., 2016). FtsW and RodA belong to the so-called SEDS (shape, elongation, division and sporulation) cluster. Notably, SEDS proteins and monofunctional peptidoglycan DD-transpeptidases are spread wider among bacteria than bifunctional PBPs (Egan et al., 2015). Since RodA and FtsW interact with the monofunctional DD-transpeptidases PBP2 and PBP3, they might represent ancestral cognate enzyme pairs for peptidoglycan synthesis (Henrichfreise et al., 2016). In free-living bacteria, RodA-PBP2 and FtsW-PBP3 are specialized glycosyltransferase-transpeptidase pairs found in the elongasome or divisome, respectively (Henrichfreise et al., 2016). The absence of bifunctional PBPs for example in free-living *Planctomycetes* as well as in intracellular *Chlamydia* and *Wolbachia* suggests that monofunctional peptidoglycan SEDS-transpeptidase pairs might have been retained as principal peptidoglycan polymerase systems (Henrichfreise et al., 2016). A putative RodA protein is annotated in the *w*Bm genome (NCBI: WP_011256217.1). *In vitro* activity assays with PBP2^{wBm} in combination with RodA^{wBm} and subsequent measurements by TLC and MALDI-TOF might be reasonable approaches to reveal glycosyltransferase and DD-transpeptidase activity and consequently to detect a peptidoglycan-like polymer. Notably, it was already demonstrated that *Wolbachia* strain *w*AlbB expresses FtsW and RodA (Vollmer et al., 2013). It remains to be seen if the RodA/FtsW homolog in *Wolbachia* has such an activity for the assembly of peptidoglycan together with a monofunctional DD-transpeptidase.

4.3 Functional characterization of PBP3^{w}Mel

Filarial *Wolbachia* like *w*Bm only harbor one putative monofunctional DD-transpeptidase, whereas *Wolbachia* residing in insect cells, e.g. *w*Mel, encode both PBP2 and PBP3. In free-living bacteria, PBP3 is part of the divisome driving the septation process by transpeptidation of lipid II with peptidoglycan at the septation site (Den Blaauwen et al., 2008), but the role of this enzyme in *Wolbachia* is unknown. *In silico* analysis of the primary and secondary structure predicted a putative active site for DD-transpeptidase activity. The

purification of recombinant PBP3^{wMel} and functional characterization *in vivo* and *in vitro* were performed as part of a master thesis (Ritzmann, 2016). In this study, the *in vivo* activity of recombinant PBP3^{wMel} was further investigated. Overexpressed PBP3^{wMel} partially restored the growth defects of *E. coli* MCI23 at the non-permissive temperature. Although cell complementation was not restored completely, which might be explained by sub-optimal conditions for the wolbachial enzyme at 42 °C, the results indicate that PBP3^{wMel} exhibits activity *in vivo* and is capable of lipid II modification. To provide evidence that PBP3^{wMel} *in vivo* activity is based on the typical mode of action described for PBPs, the serine residues from all four SXXK motifs identified in PBP3^{wMel} were substituted by alanine by site-directed mutagenesis. Single SXXK mutations did not result in an altered phenotype, indicating normal cell division of *E. coli* MCI23 (Ritzmann, 2016). Simultaneous mutation of all four SXXK motifs resulted in an increase of filamentous cells indicating impaired PBP3^{wMel} activity. In PBP3 from *C. pneumoniae*, the ability to complement cell division of *E. coli* MCI23 at the non-permissive temperature was dependent on all functional SXXK motifs, but in contrast, the single SXXK motifs were able to substitute each other *in vitro* (Otten, 2014).

To confirm the mode of action of PBP3^{wMel} as a DD-transpeptidase within the *in vivo* model, additional experiments using the specific PBP3 inhibitor aztreonam were conducted. This antibiotic leads to a filamentous phenotype due to impaired cell division (Georgopapadakou et al., 1982). When aztreonam was added to the exponentially growing *E. coli* MCI23 cells overexpressing PBP3^{wMel} at the permissive temperature of 30 °C, cell sizes increased compared to the untreated controls. Of note, cell sizes (median: 6.9 µm) were similar to those observed in the complementation assays at 42 °C with overexpressed PBP3^{wMel} (median: 6.1 µm). In contrast, cells expressing the empty vector were significantly larger (median: 11.5 µm) in the presence of aztreonam. This result confirms an inhibition of the *E. coli* PBP3 and supports the conclusion that partial restoration of division in cells overexpressing PBP3^{wMel} originated from the wolbachial enzyme. Aztreonam is a β-lactam, thus the low affinity of aztreonam to PBP3^{wMel} supports previous findings of *Wolbachia* resistance to this antibiotic class (O'Neill et al., 1997; Fenollar et al., 2003). Aztreonam resistance was shown in some *E. coli* strains which is manifested by a four-amino-acid insertion (YRIK or YRIN) in PBP3 (Alm et al., 2015). Structural analysis revealed that this insertion impacts the accessibility of some β-lactam drugs to the DD-transpeptidase pocket (Alm et al., 2015). Neither YRIK nor YRIN are present in PBP3^{wMel}, but *in silico* analysis predicted a possible binding of the β-lactam cefoxitin only at two of the four active site serines of SXXK motifs. This indicates an inaccessibility of the other two SXXK motifs, which could maintain enzyme activity. Further

in vivo activity assays excluded that PBP3$^{w\text{Mel}}$ resistance to β-lactams was caused by a potential β-lactamase activity of the enzyme.

4.4 Interaction of Pal$^{w\text{Bm}}$ with lipid II and PBP2ΔTM$^{w\text{Bm}}$

In Gram-negative bacteria, the predominantly single-layered peptidoglycan sacculus is connected to the outer membrane by covalent and noncovalent interactions with various outer membrane proteins (Typas et al., 2010). Pal is an outer membrane protein which binds specifically to uncross-linked mDAP and is part of the membrane-spanning Tol-Pal complex (Gerding et al., 2007; Yeh et al., 2010). The Tol-Pal complex is essential for proper constriction of the outer membrane during cell division and interacts with other outer membrane proteins to connect the outer membrane, peptidoglycan and the inner membrane, thus facilitating membrane integrity (Godlewska et al., 2009). *Wolbachia* lack peptidoglycan-binding proteins that promote the maintenance of the peptidoglycan sacculus in other Gram-negative bacteria except for Pal (Wu et al., 2004; Turner et al., 2009; Typas et al., 2012). Pal is one of two identified lipoproteins in *Wolbachia* (Voronin et al., 2014). In filarial infections, the pro-inflammatory capacity of *B. malayi* and *O. volvulus* is higher in the presence of *Wolbachia* and their lipoproteins have been identified as key ligands (Hise et al., 2007; Turner et al., 2009; Tamarozzi et al., 2011). In *Wolbachia* of *B. malayi*, Pal$^{w\text{Bm}}$ was found to be among the most abundant proteins and is localized in the outer membrane (Voronin et al., 2014). It is likely that wolbachial Pal is necessary to connect the inner and outer membrane, especially during cell division, and this interaction partner might be lipid II (Vollmer et al., 2013). First evidence for this was shown in the *Wolbachia* strain *w*AlbB which was treated with fosfomycin, an antibiotic blocking lipid II synthesis, resulting in a perturbed localization of wolbachial Pal and enlarged cells unable to divide (Vollmer et al., 2013). The protein-lipid II interaction studies shown in this thesis suggest that lipid II might be connected to the outer membrane via Pal$^{w\text{Bm}}$. The preferred substrate of Pal$^{w\text{Bm}}$ was lipid II containing mDAP, giving a further hint of the *Wolbachia* lipid II composition. Noteworthy, *Wolbachia* retained the ability to synthesize mDAP *de novo*, indicating that mDAP is found at position three of the lipid II pentapeptide chain like in other Gram-negative bacteria as well as in Gram-positive bacteria of the genus *Bacillus* (Foster et al., 2005; Henrichfreise et al., 2009). During cell division, lipid II or a further processed form of the molecule possibly anchored in the inner membrane might be linked to the outer membrane by interacting with wolbachial Pal, forming a ring-like structure necessary for constriction of the outer membrane. A second potential interaction partner of the wolbachial Pal was PBP2. In *E. coli*, it was demonstrated that the outer membrane-anchored lipoproteins

LpoA and LpoB control peptidoglycan synthases (Paradis-Bleau et al., 2010; Typas et al., 2010). Each Lpo protein stimulates the DD-transpeptidase activity of its cognate PBP by binding and concomitantly inducing conformational changes (Egan et al., 2014). The protein-protein interaction studies conducted in this thesis revealed an interaction between the lipoprotein Pal$^{w\mathrm{Bm}}$ and PBP2ΔTM$^{w\mathrm{Bm}}$. The N-terminus containing the transmembrane domain of PBP2$^{w\mathrm{Bm}}$ might be anchored in the inner membrane, while the C-terminus harboring the active site might be stimulated by binding to Pal$^{w\mathrm{Bm}}$. Moreover, it can be speculated that the PBP2$^{w\mathrm{Bm}}$-Pal$^{w\mathrm{Bm}}$ complex might maintain membrane integrity by connecting the inner and outer membrane.

4.5 Functional characterization of AmiD$^{w\mathrm{Mel}}$

The genome of arthropod *Wolbachia* such as *w*Mel encode one putative peptidoglycan hydrolase, homologous to the N-acetylmuramoyl-L-alanine amidase AmiD from *E. coli*, although a functional cell wall has not been detected (Wu et al., 2004). In contrast to all other characterized amidases (AmiA, AmiB, AmiC) from *E. coli*, AmiD has a broad substrate specificity and its exact role is unclear (Kerff et al., 2010). Park and Uehara (2007) proposed that the breakdown of cell wall fragments in the periplasm by AmiD is a secondary strategy to prevent immune responses in the host. The enzyme belongs to the amidase 2 family (PF01510 in the Pfam database). Eukaryotic peptidoglycan recognition proteins (PGRPs) have at least one carboxyterminal PGRP domain, which is homologous to bacteriophage and bacterial type 2 amidases (Dziarski and Gupta, 2006). PGRPs are involved in innate immune responses against bacteria (Dziarski and Gupta, 2006). *Drosophila* relies entirely on innate immunity and two pathways respond to different classes of microorganisms (Buchon et al., 2014). The Toll pathway is mainly activated in response to Gram-positive bacteria and fungi, whereas the immune deficiency (Imd) pathway is mostly triggered by Gram-negative bacteria. Here, recognition of bacteria is mostly achieved by PGRPs. The membrane anchored receptor PGRP-LC and the cytoplasmic receptor PGRP-LE upstream of the Imd pathway sense peptidoglycan fragments containing mDAP in the peptide side chains (Myllymäki et al., 2014). The minimum structure for recognition by PGRP-LC is a monomer of Glc*N*Ac-Mur*N*Ac with an internal 1,6-anhydro-bond attached to a tripeptide (Stenbak et al., 2004). In this study, AmiD$^{w\mathrm{Mel}}$ was functionally characterized to better understand its role in insect *Wolbachia* biology. The presence of an N-terminal signal peptide predicted a periplasmic localization of AmiD$^{w\mathrm{Mel}}$ but no insertion into the outer membrane like its *E. coli* homolog (Uehara and Park, 2007). The periplasmic localization was confirmed *in vitro*, and activity assays revealed that

AmiD$^{w\text{Mel}}$ hydrolyzes the amide bond between Mur*N*Ac and L-alanine of the peptide stem of various substrates like monomeric lipid II, polymeric peptidoglycan and anhydromuropeptides. This activity was inhibited by the exchange of one of the zinc-coordinating residues as well as by the non-specific metal chelator EDTA and the zinc-specific inhibitor 1,10-phenanthroline. A zinc-dependent activity was also shown in AmiD from *E. coli* (Uehara and Park, 2007). *In vivo* assays using an *E. coli* strain with knocked-out AmiA, B and C demonstrated an involvement in cell division of AmiA from *C. pneumoniae* (Klöckner et al., 2014). Due to rapid degradation of AmiD$^{w\text{Mel}}$ in the used *E. coli* strain, this assay was not suitable for this study. Thus, it cannot be ruled out that AmiD$^{w\text{Mel}}$ is involved in the turnover of a rudimentary peptidoglycan-like structure as the recycling pathway of C_{55}-P remains unclear in *Wolbachia* (Henrichfreise et al., 2009; Vollmer et al., 2013). However, the question remains why AmiD is only conserved in *Wolbachia* found in arthropods. AmiD$^{w\text{Mel}}$ was able to hydrolyze anhydromuropeptides like its *E. coli* homolog (Uehara and Park, 2007). Notably, the 1,6-anhydro bonds of anhydromuropeptides are generated by periplasmic lytic transglycosylases cleaving the glycosidic bond between Mur*N*Ac and Glc*N*Ac units. The conservation of the capability to cleave anhydromuropeptides gives a first hint that *Wolbachia* may contain a peptidoglycan-like structure with connected glycan strands. However, neither a bifunctional PBP with DD-transpeptidase and peptidoglycan glycosyltransferase activity that could link the sugar moieties of lipid II nor a lytic transglycosylase that could catalyze glycan chain cleavage during bacterial growth have been identified in the *Wolbachia* genomes (Wu et al., 2004; Foster et al., 2005). Nevertheless, the aforementioned identification of RodA as a glycosyltransferase supports the hypothesis of a potential peptidoglycan structure in *Wolbachia*.

The size of AmiD$^{w\text{Mel}}$ with 497 amino acids is striking (AmiD from *E. coli*: 257 amino acids) leading to the assumption of a potential additional function of this enzyme. Contrary to homologs from free-living bacteria, AmiD$^{w\text{Mel}}$ contains conserved SXXK, SX(D/N) and K(S/T)G motifs in its C-terminus typically found in PBPs and also in AmiA from *C. pneumoniae*. This chlamydial AmiA is an amidase involved in septum cleavage and additionally functions as a DD-carboxypeptidase (Klöckner et al., 2014). Thus, AmiD$^{w\text{Mel}}$ was investigated for a putative additional DD-carboxypeptidase activity *in vivo* and *in vitro*. *In vivo* assays with *E. coli* MCI23 provided first hints of DD-carboxypeptidase activity, which was dependent on the functional active site serine S400. These results suggested that AmiD$^{w\text{Mel}}$ is an enzyme with dual activity having N-acetylmuramoyl-L-alanine amidase activity in the N-terminal and DD-carboxypeptidase activity in the C-terminal part of the protein. Additionally, an interaction between fluorescent penicillin and AmiD$^{w\text{Mel}}$ was observed *in vitro* indicating

that the PBP active site motifs are indeed present in this enzyme and accessible to β-lactams. However, DD-carboxypeptidase activity was not confirmed *in vitro*. Analysis of the reaction products of AmiD^{wMel} by TLC and MALDI-TOF did not reveal lipid II containing a tetrapeptide. Possibly, the DD-carboxypeptidase activity was too low which might explain why lipid II containing a tetrapeptide was not detected by these methods. Additional assays, in which free D-Ala is detected even in low concentrations, turned out to be inappropriate to reliably measure DD-carboxypeptidase activity as no significant differences between the negative and the positive control could be calculated. Thus, further assays are necessary to investigate and confirm the putative DD-carboxypeptidase activity of AmiD^{wMel}. Nevertheless, the functional conservation of N-acetylmuramoyl-L-alanine amidase activity indicates that AmiD^{wMel} plays an important role in the lifecycle of insect *Wolbachia*, but its involvement in cell division remains unclear. Likely, AmiD^{wMel} might suppress host immune responses by removing the peptide chain from the sugar moieties. Because insect *Wolbachia* are parasites and can horizontally infect other insects (Werren et al., 2008), this enzyme may have been maintained for example in *w*Mel, *w*Ri and *w*Pip to aid this specific endosymbiotic lifestyle and protect these endobacteria. In contrast, genomes of sequenced *Wolbachia* from filarial nematodes show that these strains have lost the ability to synthesize AmiD. Moreover, nematodes do not express homologs of PGRP-LC or Imd (Irazoqui et al., 2010; Ermolaeva and Schumacher, 2014) and thus would not recognize the same peptidoglycan metabolism/recycling products, allowing *Wolbachia* of filarial nematodes to lose AmiD during evolution as mutualistic endosymbionts. In conclusion, the enzymatic activity of AmiD^{wMel} may have a crucial role in cleavage of a peptidoglycan-like structure and allow *Wolbachia* to avoid host organism immune responses by degrading cell wall fragments in the periplasm that could be recognized by innate immune receptors (Buchon et al., 2014).

4.6 Growth requirements of *Wolbachia w*AlbB in a cell-free culture

The examination of *Wolbachia* is challenging as they live well protected from the environment by four lipid membrane layers: the host cell membrane, the membrane of the vacuole in which *Wolbachia* reside in the cytoplasm and the bacterial outer and inner membrane. *In vitro* culture systems are few and attempts to culture *Wolbachia* of filarial nematodes have not been successful (Slatko et al., 2014). Only strains naturally occurring in arthropods have been established in cell cultures (O'Neill et al., 1997; Turner et al., 2006). Therefore, possibilities to investigate *Wolbachia* are limited. An extracellular culture system would open the door for the application of a broad spectrum of molecular biological techniques

and facilitate the elucidation of *Wolbachia* biology. For example, the efficacy of large antibiotics, which are not able to pass all four lipid membrane layers, could be examined. First steps towards a cell-free system were made by Rasgon et al. (2006). *Wolbachia* strain *w*AlbB purified from an insect cell line was maintained in a cell-free culture medium for up to one week, but could not proliferate outside the host cell. Further attempts regarding *ex-vivo* growth failed, but some components were advantageous regarding survival of *Wolbachia*, e.g. compatible solutes, actin and mammal blood (Uribe-Alvarez et al., 2018). A host cell-free culture of *w*AlbB with viable cells which were replicating and infective up to twelve days was established in a former project (Vollmer, 2012). An insect cell lysate fraction containing cell membranes was identified as requisite for cell-free replication of *Wolbachia*, but replication was limited to 9-12 days (Vollmer, 2012). Further experiments on single components of the membrane fraction were performed, for example with certain membrane lipids. However, the results were ambiguous and it was assumed that there are several positive and negative factors influencing the culture in a complex manner (J. Vollmer, pers. communication). Usage and insufficient supply of nutrients might be a reasonable explanation, but as *Wolbachia* replicate slowly, a competition for nutrients seems unlikely (Vollmer, 2012).

Part of this thesis was to examine if additional supplemented substances that are not present in the standard cell culture medium might enhance growth and stability of cell-free *w*AlbB. The survival of *Anaplasma phagocytophilum* and *Ehrlichia chaffeensis*, which are closely related to *Wolbachia*, is dependent on the incorporation of cholesterol derived from their host to maintain membrane integrity (Lin and Rikihisa, 2003). Like *Wolbachia*, *A. phagocytophilum* and *E. chaffeensis* do not synthesize lipid A and it was proposed that cholesterol might be necessary to promote membrane stability as a substitute for lipopolysaccharide (Lin and Rikihisa, 2003; Wu et al., 2004). Recent studies indicate that *Wolbachia*-infected insect cells might indeed incorporate cholesterol (Caragata et al., 2013; Geoghegan et al., 2017). Further, *Wolbachia* reside in cholesterol-rich Golgi-related vesicles derived from the host forming a vacuole surrounding each bacterium (Cho et al., 2011). Insects assimilate cholesterol from their environment which is incorporated into the plasma membrane and into internal membranes like those from the Golgi apparatus (Rolls et al., 1997). Thus, cholesterol might be a limiting factor for cell-free *w*AlbB proliferation and supplementation with the membrane fraction of an insect cell lysate might not be sufficient to keep up growth for more than twelve days. The supplementation of water-soluble cholesterol did not lead to elongated replication of cell-free *w*AlbB. The application of fresh cell lysate after nine days showed higher cell-free *w*AlbB proliferation after twelve days compared to the standard culture

in the performed assays, but taken as a whole, proliferation rates were not higher than the observed mean of 6.4-fold from previous assays (see chapter 3.7). Based on these results, cholesterol and certain components from the insect cell membrane that are potentially taken up by *Wolbachia* were concluded not to be key factor for limited proliferation. Since *Wolbachia* replication was high between days 3–9, a complete medium change after nine days to supply *Wolbachia* with fresh culture medium was reasonable. This was challenging as the bacteria did not attach to the plate surface. Centrifugation of the culture to separate *Wolbachia* from the cell culture medium led to a loss of the bacteria. Thus, cell culture plates were coated with actin to allow attachment of the *Wolbachia* to the surface and to potentially facilitate medium change. Several studies demonstrate a close association of *Wolbachia* and other intracellular bacteria with the host cell cytoskeleton (Ferree et al., 2005; Galán and Cossart, 2005; Melnikow et al., 2013; Landmann et al., 2014; Reed et al., 2014; Souza Santos and Orth, 2015). In *Drosophila*, *Wolbachia* localize at the anterior pole of the mosquito`s oocytes using microtubules, thus ensuring transmission to the next generation (Ferree et al., 2005). In *B. malayi*, wolbachial surface proteins form a complex with actin and tubulin and this binding is supposed to be crucial in maintenance of endosymbiosis (Melnikow et al., 2013). Moreover, the supplementation of actin was shown to improve survival of isolated *Wolbachia* (Uribe-Alvarez et al., 2018). In this thesis, cell-free *w*AlbB were cultured on an actin-coated streptavidin plate to examine if the bacteria benefit from actin and if they attach to the substrate, which would have facilitated medium change. However, cell-free growth on actin-coated plates was decreased compared to the standard conditions. It cannot be excluded that substances from the wash buffer used for actin-coating on the streptavidin plates were harmful to the bacteria, although plates were rinsed several times with culture medium before use. Medium change after six days led to a loss of bacteria leading to the conclusion that *Wolbachia* were not attached to the actin-coated plates. The binding of *Wolbachia* to actin might be more crucial to keep maintenance in the host cell culture rather than to be involved in replication itself.

As shown for other intracellular bacteria, culturing in a lowered oxygen environment can increase cell-free growth (Omsland et al., 2009). Here, proliferation rates were similar in cell-free *w*AlbB incubated under a lower oxygen level compared to standard conditions. Thus, oxygen levels are presumably not the limiting factor of cell-free *Wolbachia* growth. Of note, the variance of *w*AlbB replication rates in cell-free cultures between different experiments was similar to those of *Wolbachia* cultured inside insect cells reflecting growth variability that might originate from variances in temperature, cell culture passage and culture medium. An optimized culture medium was already designed for cell-free growth of the obligate endobacteria

C. burnetii using expression microarrays, genomic reconstruction and metabolite typing (Omsland et al., 2009). The cell-free *w*AlbB medium was compared to the optimized cell-free medium for *C. burnetii* and substances, which were present in the medium for *C. burnetii*, were supplemented to the cell-free *w*AlbB medium. An increase of proliferation was observed in cultures supplemented with glucose. The glucose and glycogen metabolism in *B. malayi* is associated with *Wolbachia* symbiont fitness and it was shown that the disaccharide sucrose, consisting of glucose and fructose, improves survival of isolated *Wolbachia* (Voronin et al., 2016; Uribe-Alvarez et al., 2018). Thus, this compound might be beneficial for wolbachial growth. Indeed, growth rates slightly increased in the presence of glucose, but proliferation could not be elongated. Moreover, biotin and sodium bicarbonate harmed the culture. To determine exact nutrient requirements and to design a *Wolbachia*-specific cell-free medium, differences in gene expression of *Wolbachia* cultured in insect cells and cell-free should be examined in a future project.

Another possible explanation why cell-free *Wolbachia* replication stops after 9-12 days might be the regulation of *Wolbachia* densities by an unknown intrinsic or host-derived mechanism. It is striking that cell-free *w*AlbB were only proliferating at an initial concentration of 0.5 – 1 x 10^3 cells/µl. In contrast, in cell-free cultures containing higher densities of *Wolbachia* with 10^4 or 10^5 cells/µl, *Wolbachia* numbers rarely increased (Vollmer, 2012). This indicates that *Wolbachia* might sense cell densities and regulate cell division by internal communication patterns. The two-component regulatory system (TCS) is the predominant form of signaling used in a majority of prokaryotes, including bacteria (Beier and Gross, 2006). It is composed of a sensor histidine kinase and a paired response regulator (Mitrophanov and Groisman, 2008; Jung et al., 2012). Stimuli such as nutrients, osmolarity, oxygen, salinity and quorum sensing cues are recognized by sensor histidine kinases (Mascher et al., 2006). This activates cognate response regulators which for example coordinate induction of sporulation, regulation of bacterial differentiation or formation of biofilms (Stock et al., 2000). TCS genes are highly conserved in various *Wolbachia* strains, but very little is known about their function to date (Cheng et al., 2006; Brilli et al., 2010). A bioinformatic study showed that wolbachial TCS genes are consistently found clustered with metabolic genes within different *Wolbachia* strains including *w*AlbB and *w*Bm (Christensen and Serbus, 2015). Considering these findings, it might be hypothesized that *Wolbachia* are able to sense for example nutrients or quorum sensing molecules and consequently regulate cell division. This could explain why cell-free *Wolbachia* growth stops after 9-12 days of incubation and could further explain the observation that *Wolbachia* cell numbers inside the C6/36 insect cells do not reach a density that would

negatively affect the survival of the insect cell. In *Drosophila*, *Wolbachia* replication was indicated to be tissue-dependent as growth rates differ significantly between head and ovaries (McGraw et al., 2002). *Wolbachia* replication is also dependent on the stage of the host life cycle. In *A. albopictus*, *Wolbachia* replication stops during the diapause of mosquito eggs in which no host cell division occurs, highlighting the dependence of *Wolbachia* proliferation on host cell division (Ruang-Areerate et al., 2004). In the filarial nematode *B. malayi*, *Wolbachia* numbers are low and remain constant in microfilaria and insect-borne larval stages, but proliferation increases suddenly after the infection of a vertebrate host (McGarry et al., 2004; Taylor et al., 2013). This seems to play an essential role in larval development as demonstrated by the arrested larval growth and development in response to antibiotic treatment (Taylor et al., 2012). *B. malayi* and *B. pahangi* infective-stage larvae co-cultured *in vitro* with the yeast *R. minuta* have been shown to support consistent and reproducible molting to the fourth larval stage (Smith et al., 2000). It was suggested that the larvae are benefiting from an unknown secreted product of the yeast. Since proliferation rates of *Wolbachia* severely increase in this phase of the larvae (McGarry et al., 2004; Taylor et al., 2013), the bacteria might also benefit from secretion products of *R. minuta*. In this thesis, cell-free *w*AlbB were co-cultured with viable *R. minuta*. The co-cultivation harmed the *Wolbachia* leading to a concentration-dependent decrease of bacteria rather than enhanced growth. Thus, it might be assumed that the secreted yeast product might be more beneficial for the viability of filarial larvae than for *Wolbachia*. In a future experiment, *R. minuta* lysate in different concentrations might be used. This would prevent that bacteria are overgrown by the yeast. Notably, it was recently shown that *w*AlbB is able to grow in artificially infected *Saccharomyces cerevisiae* (Uribe-Alvarez et al., 2018). Compared to controls, infected yeast lost viability early, but this system might potentially provide a promising future model of interactions that occur in a naturally infected eukaryote host (Uribe-Alvarez et al., 2018).

Summing up, these findings provide insight into the complexity of *Wolbachia* replication and endosymbiont-host dependency. Further research will be necessary to elucidate the multiple mechanisms that influence and regulate *Wolbachia* replication and to enhance growth as well as stability of the *w*AlbB cell-free culture.

4.7 Antibiotic treatment of *Wolbachia w*AlbB in a cell-free culture

Several antibiotics tested in *Wolbachia*-infected cell cultures did not deplete the bacteria and it was a matter of debate whether they were ineffective because they could not reach their

target or because *Wolbachia* are indeed resistant. The cell-free system meets all requirements to examine antibiotics directly applied to *Wolbachia.* Thus, another part of this thesis was the application of antibiotics to the cell-free *w*AlbB culture. Different antibiotics were supplemented to the cell-free culture medium, gDNA was prepared and growth rates were monitored via qPCR of the 16S rRNA gene. To exclude that penicillin or streptomycin, which are supplements of the normal cell culture medium, have an inhibitory effect on cell-free *w*AlbB proliferation, cultures with and without these antibiotics were tested. Here, no differences in growth rates were observed supporting previous findings that *Wolbachia* are resistant to β-lactams (O'Neill et al., 1997). Proliferation rates were also examined with the *Wolbachia*-affecting antibiotics corallopyronin A, doxycycline, fosfomycin and rifampicin. However, cell-free *w*AlbB growth rates were not decreased in the presence of corallopyronin A, doxycycline or fosfomycin. Only treatment with rifampicin led to decreased cell-free growth, but a complete inhibition of growth was not observed here as well. It might be assumed that an effect on growth would only be observed using antibiotics with bactericidal activity like rifampicin, but this assumption does not hold true as fosfomycin also acts bactericidal (Michalopoulos et al., 2011). Generally, it should be considered that gDNA was prepared and measured from the whole culture and it is possible that DNases are lower or absent in the cell-free culture. Thus, gDNA fragments of dead cells were potentially measured by qPCRs leading to a seemingly increase of *Wolbachia*. To solve this issue, expression levels of the 16S rRNA gene prepared from the cell-free culture were measured. However, no differences between antibiotic treated and untreated cultures were revealed due to low expression after twelve days also in untreated controls. A study in *w*Mel confirmed that rRNA expression levels are high and variable among samples (Gutzwiller et al., 2015). Thus, this approach is not suitable to reliably compare antibiotic treated and untreated *w*AlbB cultures.

Another approach to determine bacteria numbers is counting of cells under a microscope and discrimination between living and dead bacteria by LIVE/DEAD® staining. This was applied to the cell-free *Wolbachia*, but in the majority of experiments, only few cells were detected after twelve days also in the controls cultures without antibiotic treatment. Other previous attempts to count cell-free *Wolbachia* also turned out to be inappropriate as a high variance between measured cells per qPCR and actually counted cells was revealed (J. Vollmer, pers. communication). Therefore, this approach was rejected and the impact on the morphology of antibiotic-treated *w*AlbB was investigated to reveal potential antibiotic-effects on *Wolbachia*. Cell-free *Wolbachia* were fixed, stained and visualized under a microscope. In a previous study, *w*AlbB residing in C6/36 insect host cells were treated with the lipid II-synthesis

blocking antibiotic fosfomycin, which led to enlarged bacteria (Vollmer et al., 2013). This finding indicated that lipid II is essential for cell division in *Wolbachia*. Moreover, fosfomycin treatment on *Wolbachia* revealed a perturbed localization of *w*Pal suggesting an interaction of this lipoprotein with lipid II or its processed form (Vollmer et al., 2013). This assumption is supported by the results of the interaction assays in this thesis (see chapter 4.4). The incubation of cell-free *w*AlbB with fosfomycin also showed an aberrant phenotype with enlarged cells and delocalized *w*Pal appearing in a spot-like pattern. None of the other antibiotics tested revealed a visible aberrant phenotype. Ciprofloxacin, clindamycin, corallopyronin A, doxycycline, rifampicin, sulfamethoxazole and trimethoprim do not target cell wall biosynthesis, thus an impact on cell morphology was unlikely. For antibiotics targeting the cell wall or synthesis steps (ampicillin, bacitracin, vancomycin) an aberrant phenotype was more likely. For example, ampicillin-treated *C. trachomatis* have aberrant, enlarged reticulate bodies (Liechti et al., 2014). Here, no changes compared to the control cells were observed after twelve days of incubation with the respective antibiotic. On the one hand, it can be proposed that *Wolbachia* are indeed resistant to these antibiotics and therefore no change of morphology was detected. On the other hand, it might be assumed that antibiotics were unstable and thus ineffective. Since stability, solubility and shelf life of antibiotics were considered while preparing the assays, this possibility can be neglected. Another explanation for the inefficacy of the substances might be an inaccessibility of their targets. For instance, most Gram-negative bacteria are naturally resistant to vancomycin as this molecule cannot pass the outer membrane (Geraci, 1977). *Wolbachia* likely have an unusual outer membrane since they are unable to synthesize lipid A, a key moiety of lipopolysaccharide (Foster et al., 2005). Thus, certain compounds, which are too large to pass the outer membrane of Gram-negative bacteria, might pass the unique *Wolbachia* outer membrane. This was already demonstrated for corallopyronin A which normally depletes only Gram-positive bacteria, but is also highly active against *Wolbachia* (Schiefer et al., 2012). In contrast, it should be considered that compounds that normally pass the Gram-negative outer membrane might not be able to reach their target in *Wolbachia* due to their unique outer membrane.

In conclusion, the investigation of *Wolbachia* cultures in terms of antibiotic susceptibility remains challenging. To establish rapid and reliable tools to analyze antibiotic assays, several attempts could be beneficial. The amplification of genes like the wolbachial surface protein (wsp) WD1063 might be more eligible than 16S rRNA to measure replication or depletion of cell-free *Wolbachia*. Wsp is stably-expressed in *Wolbachia* making it suitable to compare expression levels of antibiotic treated and untreated cells (Gutzwiller et al., 2015).

Wolbachia growth inside yeast cells can be determined by PCR of wsp and this approach might be applied to the cell-free *w*AlbB culture (Uribe-Alvarez et al., 2018). Additionally, *Wolbachia* replication or depletion can also be estimated by the detection of wsp by Western Blot and analysis of band intensity (Uribe-Alvarez et al., 2018). As another approach, fluorescence-activated cell sorting of LIVE/DEAD® stained *Wolbachia* after antibiotic treatment might lead to more detailed and accurate results instead of analysis with a microscope.

4.8 Lipid II labeling of *w*AlbB

Wolbachia possess all genes to build the peptidoglycan precursor lipid II and a previous study confirmed that recombinant proteins and purified *Wolbachia* membranes synthesize lipid I and II *in vitro* and that the pathway is essential for *Wolbachia* cell division (Henrichfreise et al., 2009). It was proposed that *Wolbachia* might have a peptidoglycan-like molecule built of peptide cross-links and that lipid II might be needed for the coordination of cell division (Foster et al., 2005; Henrichfreise et al., 2009). However, the exact molecular structure and further processing of *Wolbachia* lipid II is unknown. *Wolbachia* have lost most genes for amino acid biosynthesis *de novo*, but retained the genes for mDAP biosynthesis (Foster et al., 2005). *Wolbachia* most likely maintained the mDAP pathway because this amino acid is essential for the synthesis of lipid II and cannot be provided by the eukaryotic host. In this thesis, Pal^{wBm} was shown to preferentially bind to lipid II containing mDAP, giving a hint that this amino acid is found in the peptide moiety. Although *Wolbachia* lack typical amino acid racemases, they express MetC, which was shown to have an alternative alanine racemase activity in *E. coli* (Kang et al., 2011). MetC^{wBm} also possesses L-alanine racemase activity *in vitro*, giving a first hint that *Wolbachia* might provide D-Ala for the terminal dipeptide in the pentapeptide of lipid II (Vollmer et al., 2013). *Wolbachia* such as *w*Bm harbor the gene for the D-Ala-D-Ala ligase Ddl required to synthesize the D-Ala dipeptide that is linked to the UDP-Mur*N*Ac-tripeptide by MurF (Foster et al., 2005). The expression of Ddl has already been shown in *w*AlbB (Vollmer et al., 2013). An *in vivo* assay with fluorescently labeled lipid II using D-Ala-D-Ala dipeptide analogues revealed a ring-like peptidoglycan structure for the first time in *Chlamydia*, *Orientia* and *Planctomycetes* (Liechti et al., 2014; Jeske et al., 2015; Atwal et al., 2017). In this thesis, this technique was established in a C6/36 insect cell line infected with *w*AlbB. Fluorescent labeling showed a specific co-localization of anti-*Wolbachia* sera and the labeled D-amino acid dipeptide visualized a lipid II-containing and putative peptidoglycan-like structure in *Wolbachia* for the first time. The results further demonstrate that the cell wall

precursor lipid II is synthesized *in vivo* and most likely contains D-Ala-D-Ala. No labeling was monitored after fosfomycin treatment confirming the specific visualization of lipid II by EDA-DA. Isolated *Wolbachia* from the insect cell culture remained viable in different media (water, PBS and Leibovitz medium). Previous studies also demonstrated that *Wolbachia* can temporarily survive in an extracellular environment (Dobson et al., 2002; Frydman et al., 2006; Rasgon et al., 2006). The viability of isolated intracellular bacteria in different media has also been shown in *O. tsutsugamushi* and has been interpreted as an indicator for the presence of a mechanical stress-bearing structure as provided by peptidoglycan (Atwal et al., 2017).

The examination of a dipeptide antibody via highly resolving transmission electron microscopy could provide further insights into cell wall localization and structure in *Wolbachia*. Similar to *Orientia*, only few *Wolbachia* cells contained detectable dipeptides leading to the speculation it might only be synthesized at division sites (Atwal et al., 2017). In free-living bacteria, FtsZ recruits divisome proteins and confers the inner contractile force for the cell, whilst the outer force is provided by the peptidoglycan sacculus (Ghosh and Sain, 2008). In *Wolbachia*, FtsZ might constitute the inner contractile force, but the outer contractile force is unknown. Concluding that the observed lipid II structure consists of a polymer, it might be postulated that this confers the outer force in cell division. This hypothesis is in accordance with previous findings that lipid II plays a crucial role during cell division in *Wolbachia* (Foster et al., 2005; Henrichfreise et al., 2009; Vollmer et al., 2013).

4.9 Lipid II metabolism and its role in *Wolbachia* biology

In free-living bacteria, synthesized lipid II is flipped across the cytoplasmic membrane into the periplasm (Ruiz, 2016). To date, the identity of the enzyme translocating lipid II across the cell membrane remains a matter of debate. Several enzymes (FtsW, MurJ and RodA) might function as flippases and are discussed controversially (Ruiz, 2016). As *Wolbachia* annotate all three potential flippases, it is likely that the wolbachial lipid II molecule is translocated across the cytoplasmic membrane into the periplasm by one of these enzymes (Vollmer et al., 2013). Recent studies indicate glycosyltransferase activity of RodA in *E. coli* and *B. subtilis* in absence of bifunctional PBPs, and FtsW is hypothesized to have similar activity (Cho et al., 2016; Meeske et al., 2016). Thus, FtsW and RodA might be glycosyltransferases rather than flippases concluding that lipid II is likely translocated into the periplasm by MurJ. Once in the periplasm, lipid II is incorporated into the growing peptidoglycan by glycosyltransferases, DD-carboxypeptidases and DD-transpeptidases in free-living bacteria. The genome from *w*Mel contains the lipid II processing enzymes PBP2, PBP3, PBP6a, and AmiD, whereas filarial *w*Bm

only encodes the genes for PBP2 and PBP6a. The results of this thesis are a first characterization of wolbachial lipid II processing enzymes and give a hint why they have been maintained in the genome. Lipid II of *w*Bm is likely processed by the DD-transpeptidase PBP2 leading to connected peptide moieties. The degree of crosslinking might be regulated by the DD-carboxypeptidase PBP6a. In *w*Mel, the DD-transpeptidase PBP3 might lead to additional amounts of connected lipid II peptide moieties during cell division which could be recycled by AmiD to suppress host immune responses. In *E. coli*, PBP2 is mainly involved in the elongasome building peptidoglycan, while PBP3 is only functional in the divisome (Goffin et al., 1996; Höltje, 1998). In case of *Wolbachia*, a distinct separation of these multi-enzyme complexes might not hold true. Here, orchestration of lipid II processing as well as cell division may be achieved by the formation of overlapping multi-enzyme complexes (Figure 75).

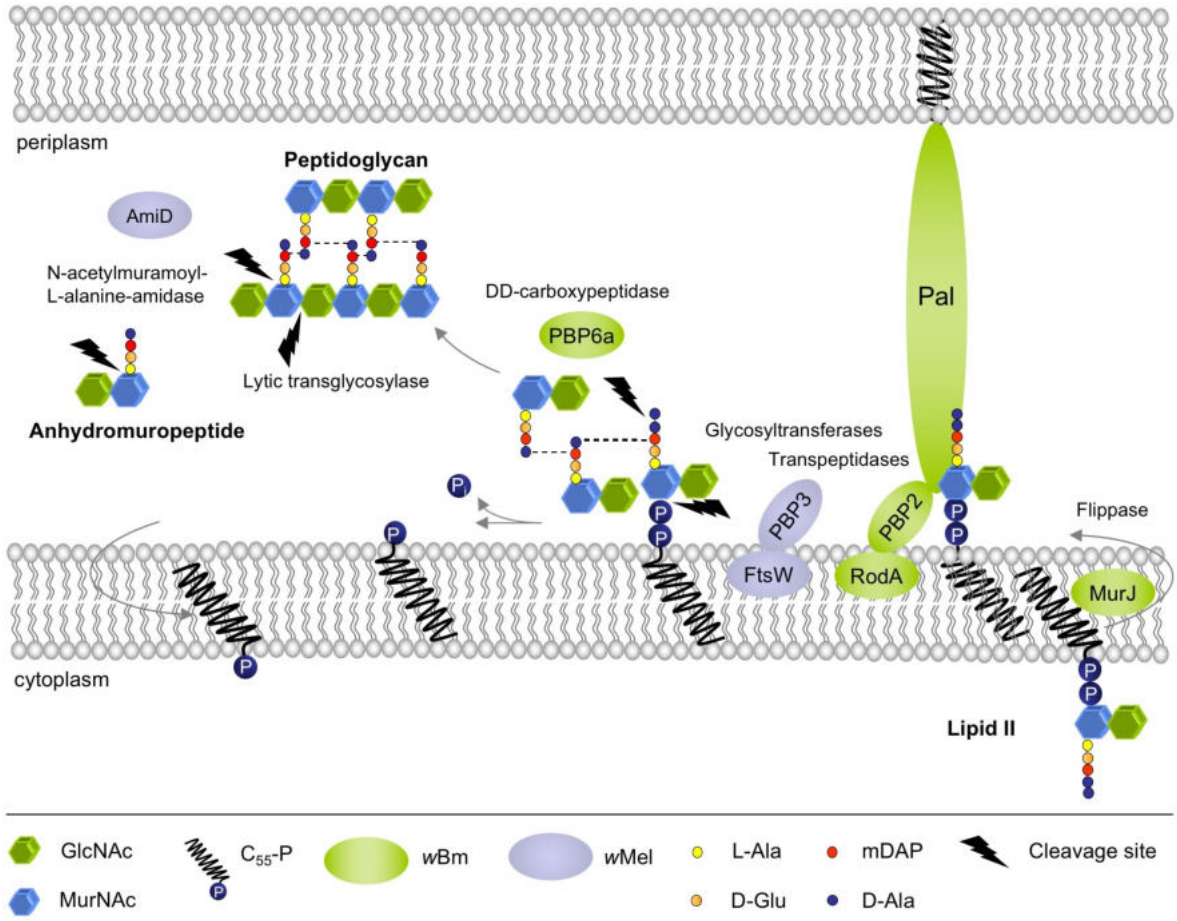

Figure 75: Proposed model of lipid II processing in *Wolbachia*. Lipid II might be flipped into the periplasm by MurJ. Pal (*w*Bm) might interact with lipid II and PBP2 (*w*Bm). PBP2 DD-transpeptidase activity might be catalyzed by the putative glycosyltransferase RodA building glycan chains with concomitant cleavage of the undecaprenyl phosphate (C_{55}-P) from Mur*N*Ac. The degree of crosslinking might be regulated by the DD-carboxypeptidase PBP6a (*w*Bm). PBP3 (*w*Mel) might have DD-transpeptidase activity during cell division together with the putative glycosyltransferase FtsW in insect *Wolbachia*. Peptidoglycan is cleaved by an unknown lytic transglycosylase resulting in anhydromurepeptides. AmiD (*w*Mel) cleaves the bond between peptide chain and sugars in peptidoglycan, lipid II and anhydromurepeptides. AmiD might furthermore have additional DD-carboxypeptidase activity. However, almost all peptidoglycan recycling enzymes are missing from annotated *Wolbachia* genomes and the further processing of C_{55}-P remains unclear.

Pal might interact with lipid II and PBP2 connecting the inner and outer membrane (see chapter 4.4). Active monofunctional PBPs together with RodA and FtsW might synthesize at least a peptidoglycan-like macromolecule putatively essential for cell division, which would confirm previous hypotheses (Foster et al., 2005; Henrichfreise et al., 2009; Vollmer et al., 2013). Investigating more enzymes involved in the orchestration of lipid II will further unravel cell wall metabolism in *Wolbachia*. In *w*Bm, MurJ (NCBI: WP_011256323) and RodA are encoded, while the homolog of FtsW is disrupted by multiple frameshifts (Foster et al., 2005). In *w*Mel, the sequences of MurJ, RodA and FtsW were found (Foster et al., 2005). The characterization of these enzymes is part of current and future studies. In *Chlamydia*, MreB is essential for growth and cell division (Ouellette et al., 2012). This rod shape-determining protein forms actin-like filaments and interacts with PBP2 to direct its synthesis of peptidoglycan as shown in free-living bacteria (Jones et al., 2001; Divakaruni et al., 2005). As MreB is present in *w*Bm (NCBI: WP_011256355) and can specifically be inhibited by S-(3,4-dichlorobenzyl) isothiourea, it might be a potential point of application to deplete *Wolbachia* (Noritaka et al., 2002). Thus, the characterization of wolbachial MreB might be reasonable.

The lipid II processing enzymes of this study were also investigated regarding their potential as targets for antibiotics. β-lactams react with the serine of the SXXK motif forming a long-lived acyl-enzyme covalent complex, consequently blocking enzyme activity (Nicola et al., 2010). The results of this thesis demonstrated that the activity of wolbachial PBPs is dependent on functional SXXK motifs, but *Wolbachia* are resistant to β-lactam antibiotics (O'Neill et al., 1997). The application of β-lactams to cell-free *Wolbachia* and to wolbachial PBPs confirmed resistance to this class of antibiotics. The underlying molecular mechanism is probably an inaccessibility of some SXXK motifs to β-lactams. *Wolbachia* PBPs all have more SXXK motifs than their *E. coli* orthologs and the active site serines were demonstrated to potentially substitute each other in function. This might be an advantage in terms of resistance when a β-lactam is present and not bound to all SXXK motifs. Surprisingly, AmiD^{wMel} showed binding to penicillin. Its putative additional DD-carboxypeptidase activity needs further validation (see chapter 4.5), and now it can only be speculated whether this activity is inhibited by β-lactams. However, as cells remained unaffected by applied β-lactams in the cell-free *w*AlbB culture, wolbachial PBPs and AmiD appear not to be suitable targets for β-lactam antibiotics. Apart from β-lactams, other antibiotics such as glycopeptides or lantibiotics inhibit the last stage of peptidoglycan polymerization by binding to the lipid II substrate (Sauvage and Terrak, 2016). Notably, a newly discovered natural product, teixobactin, isolated from *Eleftheria terrae*, inhibits cell wall synthesis in Gram-positive bacteria by binding to lipid II

and lipid III (precursor of teichoic acid) (Ling et al., 2015). Teixobactin is also active against an *E. coli* mutant with a defective outer membrane permeability barrier (Ling et al., 2015). *Wolbachia* most probably have an unusual outer membrane due to missing lipid A (Foster et al., 2005). Thus, antibiotics like teixobactin that are only active against Gram-positive bacteria might also be effective against *Wolbachia* and should be considered in antibiotic assays.

*w*Mel have two more enzymes (AmiD and PBP3) involved in cell wall metabolism that are absent in *w*Bm, suggesting differences of a putative peptidoglycan structure (Foster et al., 2005). These differences might reflect the occurrence of a mutualistic lifestyle and in contrast to a parasitic lifestyle (Foster et al., 2005). After the identification of RodA as an active glycosyltransferase (Cho et al., 2016; Meeske et al., 2016) it should be taken in account that *Wolbachia* might have a mature cell wall. Even more, the explanation that these bacteria have incomplete peptidoglycan machineries does not hold true anymore as the truly minimal maybe ancestral sets (RodA-PBP2 and FtsW-PBP3) remained concealed (Henrichfreise et al., 2016). Supporting this hypothesis, recent studies demonstrate that a peptidoglycan-like structure can be detected in intracellular *Chlamydia* and *Orientia* which also do not have all peptidoglycan synthesizing enzymes, but possess homologs of the SEDS proteins FtsW and RodA (Pilhofer et al., 2013; Liechti et al., 2014; Jeske et al., 2015; Van Teeseling et al., 2015; Atwal et al., 2017). In this study, a lipid II-containing and putative peptidoglycan-like structure was detected in *w*AlbB for the first time (see chapter 4.8). Moreover, it was demonstrated that AmiD$^{w\text{Mel}}$ is a peptidoglycan hydrolase capable of cleaving structures specifically obtained by lytic transglycosylases from glycan strands (see chapter 4.5). These results strongly indicate that at least insect *Wolbachia* may contain peptidoglycan with connected glycan strands. *E. coli* L-forms are assumed to lack peptidoglycan due to inhibited PBP1a and PBP1b (Joseleau-Petit et al., 2007). Still, they grow in isotonic medium which is blocked after additional inhibition of PBP2 or PBP3, suggesting that at least a basal level of peptidoglycan synthesis is essential for cell division (Joseleau-Petit et al., 2007). Presumably, cell wall biosynthesis and cell division are tightly connected and cannot be separately eliminated in the course of evolution (Otten, 2014). Comparative analysis of major obligate intracellular bacteria predicted some sort of peptidoglycan-like structure in *Wolbachia* termed into a group of "peptidoglycan-intermediate" organisms along with *Chlamydia*, *O. tsutsugamushi* and *Anaplasma marginale* (Otten et al., 2017). In conclusion, the results of this study together with latest research findings regarding peptidoglycan in intracellular bacteria and newly discovered SEDS glycosyltransferases support the assumption that *Wolbachia* are not cell wall-less bacteria, but rather have a physical structure composed of lipid II that can interact with outer membrane proteins.

Supplement

```
PBP6a wBm       MLDKLVILLLVSTLPFSSYSYQFRTKAKQAVVLDLASDLFIFEHNSDEKMSPSSMSKLMT   60
PBP6a wMel      MLSRLVILLLVFILPFSSYSYQFRTKAKQAVVLDLASDSFIFDHNSDEKMAPSSMSKLMT   60
                **.:*******  ************************ ***:*******:*********
PBP6a wBm       LYVAFDYLKAGIIDMKDKFRVSRKAWERKGSSMFLKEGQSVSVKELLEGVTTVSGNDACI  120
PBP6a wMel      LYIAFDYLKAGIIHMEDKFRVSRKAWERRGSSMFLKEGQSVTVRELLEGITIVSGNDACI  120
                **:**********.*:************:************:*:*****:* ********
PBP6a wBm       TLAEGIAGSEENFVVEMNEVAQNLNLSDSYFVNSSGWPDKDHFMSAKDLVVLAKRIFTDF  180
PBP6a wMel      TLAEGIAGSEENFVAEMNEVAQNLNLNDSHFVNSSGWPDEDHFMNAKDLVMLAKRIFTDF  180
                **************.***********.**:*********:****.*****:*********
PBP6a wBm       PEYYDLFSKQYLTYNDIIQKNKNLLLFHDIGVDGLKTGYTNAGGYGIVISAKRNDRRIFA  240
PBP6a wMel      PEYYDLFSEQYLTYNEIVQKNKNLLLFHDIGVDGLKTGYTNAGGYGIVASAKRNDRRIFA  240
                ********:******:*:****************************** ***********
PBP6a wBm       VVNGLNTEKERIEEAKRLIQYSFNHFNTKKIFAKDSVVEEINVLYGKERKVSATVANDVT  300
PBP6a wMel      VVNGLNTEKERIEEAKRLIQYSLNHFNTKKIFVKDSVVEEVNVLYGKDRKVPITVANDVT  300
                **********************:*********.********:******:***  *******
PBP6a wBm       ITYNRNLRDKIKVRVEYKDMIPAPIKKGQEVGKIFIEIPGIEQQTIPLYAVNDVQELNYV  360
PBP6a wMel      ITYNRKLHDQIKVRIEYKDMIPAPIKKGQEVGKVFVEIPGIEQQTTPLYAANDVQELNFV  360
                *****:*:*:****:******************:*:********* ****.*******:*
PBP6a wBm       EKFFRILF   368
PBP6a wMel      EKFFRMLF   368
                *****:**
```

Supplementary Figure 1: Amino acid alignment of PBP6a^{wBm} and PBP6a^{wMel}. * fully conserved residue; **:** conservation between groups of strongly similar properties; **.** conservation between groups of weakly similar properties. Conserved SXXK, SX(D/N) and K(S/T)G motifs found in PBP6a^{wBm} and PBP6a^{wMel} are written in bold letters, motif alignments are framed in black.

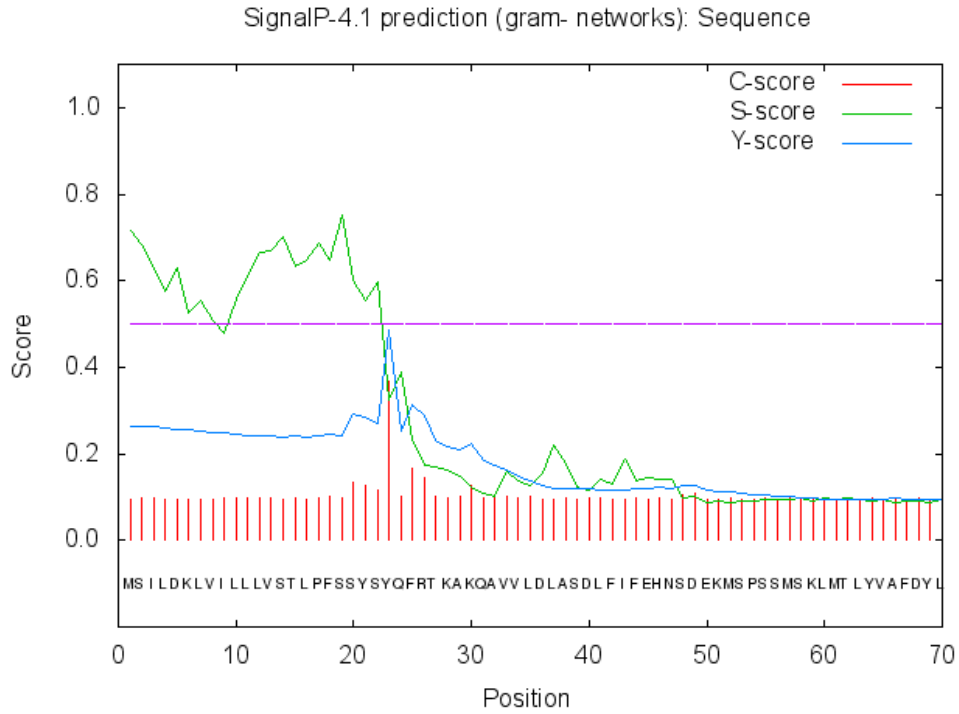


```
# Measure  Position  Value    Cutoff   signal peptide?
  max. C    23       0.366
  max. Y    23       0.487
  max. S    19       0.751
  mean S     1-22    0.619
       D     1-22    0.549   0.420   YES
Name = Sequence  SP = 'YES' Cleavage site between pos. 22 and 23: SYS-YQ D = 0.549
D-cutoff = 0.420 Networks = SignalP-noTM
```

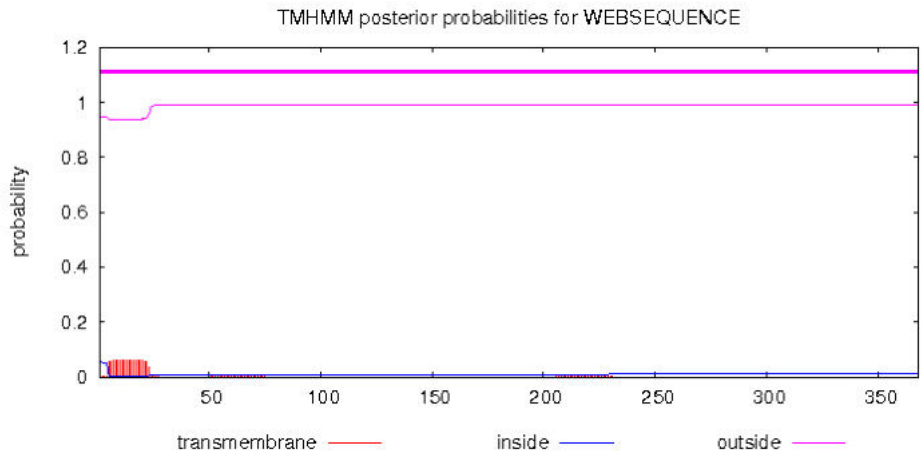


```
# WEBSEQUENCE Length: 368
# WEBSEQUENCE Number of predicted TMHs:  0
# WEBSEQUENCE Exp number of AAs in TMHs: 1.17651
# WEBSEQUENCE Exp number, first 60 AAs:  1.13184
# WEBSEQUENCE Total prob of N-in:        0.05357
# WEBSEQUENCETMHMM2.0     outside           1   368
```

Supplementary Figure 2: Prediction of a signal peptide in PBP6a^{wBm} (Signal P) for secretion in the periplasm, but no transmembrane domain (TMHMM).

```
PBP6a         --------ATGA---------GTATATTAGACAAAT-------T----GGTAATCCTGCT   32
PBP6a_SP      TCTAGATAACGAGGGCAAAAAATGAAAAAGACAGCTATCGCGATTGCAGTGGCACTGGCT   60
                      * **         .*.:*::*****..*       *    *  ..:*  ***
PBP6a         GTTAGTTTCTACGCTTCCTTTTTC--------TTCATATTCATACCAATTTAGAACTAAA   84
PBP6a_SP      G------GTTTCGCTACCGTAGCGCAGGCCGGAGACCATGGTTACCAATTTAGAACTAAA   114
              *        *:****:** *:           : .. **  :******************
PBP6a         GCAAAGCAAGCAGTAGTTTTAGATTTAGCCTCAGACTTGTTCATTTTTGAGCATAATTCC   144
PBP6a_SP      GCAAAGCAAGCAGTAGTTTTAGATTTAGCCTCAGACTTGTTCATTTTTGAGCATAATTCC   174
              ************************************************************
PBP6a         GACGAAAAGATGTCTCCATCTTCAATGAGCAAGCTAATGACTTTATATGTAGCCTTCGAT   204
PBP6a_SP      GACGAAAAGATGTCTCCATCTTCAATGAGCAAGCTAATGACTTTATATGTAGCCTTCGAT   234
              ************************************************************
PBP6a         TATTTAAAAGCTGGAATAATAGACATGAAGGATAAATTTCGAGTAAGTAGAAAAGCGTGG   264
PBP6a_SP      TATTTAAAAGCTGGAATAATAGACATGAAGGATAAATTTCGAGTAAGTAGAAAAGCGTGG   294
              ************************************************************
PBP6a         GAAAGAAAAGGCTCTTCTATGTTTTTAAAGGAAGGTCAATCTGTTTCGGTGAAAGAATTG   324
PBP6a_SP      GAAAGAAAAGGCTCTTCTATGTTTTTAAAGGAAGGTCAATCTGTTTCGGTGAAAGAATTG   354
              ************************************************************
PBP6a         CTTGAAGGAGTTACAACGGTCTCGGGTAACGATGCCTGCATAACGTTAGCTGAGGGCATT   384
PBP6a_SP      CTTGAAGGAGTTACAACGGTCTCGGGTAACGATGCCTGCATAACGTTAGCTGAGGGCATT   414
              ************************************************************
PBP6a         GCCGGGTCAGAAGAGAATTTCGTGGTTGAAATGAACGAAGTTGCACAAAATTTGAACCTA   444
PBP6a_SP      GCCGGGTCAGAAGAGAATTTCGTGGTTGAAATGAACGAAGTTGCACAAAATTTGAACCTA   474
              ************************************************************
PBP6a         AGCGACAGTTACTTTGTCAATTCAAGCGGGTGGCCAGATAAAGATCATTTCATGAGTGCA   504
PBP6a_SP      AGCGACAGTTACTTTGTCAATTCAAGCGGGTGGCCAGATAAAGATCATTTCATGAGTGCA   534
              ************************************************************
PBP6a         AAAGATTTGGTAGTACTAGCAAAAAGGATTTTTACTGATTTCCCTGAATATTATGATTTA   564
PBP6a_SP      AAAGATTTGGTAGTACTAGCAAAAAGGATTTTTACTGATTTCCCTGAATATTATGATTTA   594
              ************************************************************
PBP6a         TTTTCTAAACAATATCTAACATATAACGATATCATACAAAAAAATAAAAATCTTTTACTT   624
PBP6a_SP      TTTTCTAAACAATATCTAACATATAACGATATCATACAAAAAAATAAAAATCTTTTACTT   654
              ************************************************************
PBP6a         TTTCATGATATTGGAGTTGATGGCTTAAAGACCGGTTATACAAACGCTGGTGGTTACGGC   684
PBP6a_SP      TTTCATGATATTGGAGTTGATGGCTTAAAGACCGGTTATACAAACGCTGGTGGTTACGGC   714
              ************************************************************
PBP6a         ATTGTAATTTCTGCAAAACGAAACGATAGGAGAATTTTCGCTGTTGTAAATGGCTTAAAC   744
PBP6a_SP      ATTGTAATTTCTGCAAAACGAAACGATAGGAGAATTTTCGCTGTTGTAAATGGCTTAAAC   774
              ************************************************************
PBP6a         ACTGAAAAAGAGCGAATAGAAGAAGCAAAAAGACTGATACAATATTCCTTCAATCATTTT   804
PBP6a_SP      ACTGAAAAAGAGCGAATAGAAGAAGCAAAAAGACTGATACAATATTCCTTCAATCATTTT   834
```

```
             ************************************************************
PBP6a        AATACTAAGAAGATATTTGCTAAGGATAGTGTAGTTGAGGAAATAAATGTTCTATACGGA  864
PBP6a_SP     AATACTAAGAAGATATTTGCTAAGGATAGTGTAGTTGAGGAAATAAATGTTCTATACGGA  894
             ************************************************************
PBP6a        AAGGAGAGAAAAGTATCTGCCACAGTTGCAAATGATGTCACCATAACTTATAACCGCAAT  924
PBP6a_SP     AAGGAGAGAAAAGTATCTGCCACAGTTGCAAATGATGTCACCATAACTTATAACCGCAAT  954
             ************************************************************
PBP6a        CTACGTGATAAAATTAAGGTGCGTGTTGAATATAAAGATATGATACCTGCACCTATTAAA  984
PBP6a_SP     CTACGTGATAAAATTAAGGTGCGTGTTGAATATAAAGATATGATACCTGCACCTATTAAA  1014
             ************************************************************
PBP6a        AAAGGGCAAGAAGTAGGTAAAATTTTTATAGAAATACCAGGTATAGAGCAGCAAACTATA  1044
PBP6a_SP     AAAGGGCAAGAAGTAGGTAAAATTTTTATAGAAATACCAGGTATAGAGCAGCAAACTATA  1074
             ************************************************************
PBP6a        CCACTTTATGCAGTGAATGATGTACAGGAATTAAATTACGTAGAAAAGTTTTTTAGAATA  1104
PBP6a_SP     CCACTTTATGCAGTGAATGATGTACAGGAATTAAATTACGTAGAAAAGTTTTTTAGAATA  1134
             ************************************************************
PBP6a        TTGTTTTAA-----------------------------------------------------  1113
PBP6a_SP     TTGTTTGACCATGGTCTCAGCGCTTGGAGCCACCCGCAGTTCGAAAAATAATAAGCTTGA  1194
             ****** *.
PBP6a        ----------- 1113
PBP6a_SP     CCTGTGAAGTG 1205
```

Supplementary Figure 3: Nucleic acid alignment of PBP6a^{wBm} and cloned PBP6a^{wBm} (_SP) in pASK-IBA2C.

```
Mut12        CAANNTCTAGATMACGAGGGCAAAAAATGAAAAAGACAGCTATCGCGATTGCAGTGGCAC
PBP6a        -------------ATGAG---------TATATTAGACAAAT-------T----GGTAATC
                         * ***         *.:*::*****..*       *    *  ..:*
Mut12        TGGCTG------GTTTCGCTACCGTAGCGCAGGCCGGAGACCATGGTTACCAATTTAGAA
PBP6a        CTGCTGTTAGTTTCTACGCTTCCTTTTTC--------TTCATATTCATACCAATTTAGAA
               ****        *:****:** *:           : .. **  :**************
Mut12        CTAAAGCAAAGCAAGCAGTAGTTTTAGATTTAGCCTCAGACTTGTTCATTTTTGAGCATA
PBP6a        CTAAAGCAAAGCAAGCAGTAGTTTTAGATTTAGCCTCAGACTTGTTCATTTTTGAGCATA
             ************************************************************
Mut12        ATGCCGACGAAAAGATGTCTCCATCTGCAATGAGCAAGCTAATGACTTTATATGTAGCCT
PBP6a        ATTCCGACGAAAAGATGTCTCCATCTTCAATGAGCAAGCTAATGACTTTATATGTAGCCT
             ** ********************** ***********************************
Mut12        TCGATTATTTAAAAGCTGGAATAATAGACATGAAGGATAAATTTCGAGTAAGTAGAAAAG
PBP6a        TCGATTATTTAAAAGCTGGAATAATAGACATGAAGGATAAATTTCGAGTAAGTAGAAAAG
             ************************************************************
Mut12        CGTGGGAAAGAAAAGGCTCTTCTATGTTTTTAAAGGAAGGTCAATCTGTTTCGGTGAAAG
PBP6a        CGTGGGAAAGAAAAGGCTCTTCTATGTTTTTAAAGGAAGGTCAATCTGTTTCGGTGAAAG
             ************************************************************
Mut12        AATTGCTTGAAGGAGTTACAACGGTCTCGGGTAACGATGCCTGCATAACGTTAGCTGAGG
PBP6a        AATTGCTTGAAGGAGTTACAACGGTCTCGGGTAACGATGCCTGCATAACGTTAGCTGAGG
             ************************************************************
Mut12        GCATTGCCGGGTCAGAAGAGAATTTCGTGGTTGAAATGAACGAAGTTGCACAAAATTTGA
PBP6a        GCATTGCCGGGTCAGAAGAGAATTTCGTGGTTGAAATGAACGAAGTTGCACAAAATTTGA
             ************************************************************
Mut12        ACCTAAGCGACAGTTACTTTGTCAATTCAAGCGGGTGGCCAGATAAAGATCATTTCATGA
PBP6a        ACCTAAGCGACAGTTACTTTGTCAATTCAAGCGGGTGGCCAGATAAAGATCATTTCATGA
             ************************************************************
Mut12        GTGCAAAAGATTTGGTAGTACTAGCAAAAAGGATTTTTACTGATTTCCCTGAATATTATG
PBP6a        GTGCAAAAGATTTGGTAGTACTAGCAAAAAGGATTTTTACTGATTTCCCTGAATATTATG
             ************************************************************
Mut12        ATTTATTTTCTAAACAATATCTAACATATAACGATATCATACAAAAAAATAAAAATCTTT
PBP6a        ATTTATTTTCTAAACAATATCTAACATATAACGATATCATACAAAAAAATAAAAATCTTT
             ************************************************************
Mut12        TACTTTTTCATGATATTGGAGTTGATGGCTTAAAGACCGGTTATACAAACGCTGGTGGTT
PBP6a        TACTTTTTCATGATATTGGAGTTGATGGCTTAAAGACCGGTTATACAAACGCTGGTGGTT
             ************************************************************
Mut12        ACGGCATTGTAATTTCTGCAAAACGAAACGATAGGAGAATTTTCGCTGTTGTAAATGGCT
PBP6a        ACGGCATTGTAATTTCTGCAAAACGAAACGATAGGAGAATTTTCGCTGTTGTAAATGGCT
             ************************************************************
Mut12        TAAACACTGAAAAAGAGCGAATAGAAGAAGCAAAAAGACTGATACAATATTCCTTCAATC
PBP6a        TAAACACTGAAAAAGAGCGAATAGAAGAAGCAAAAAGACTGATACAATATTCCTTCAATC
             ************************************************************
Mut12        ATTTTAATACTAAGAAGATATTTGCTAAGGATAGTGTAGTTGAGGAAATAAATGTTCTAT
PBP6a        ATTTTAATACTAAGAAGATATTTGCTAAGGATAGTGTAGTTGAGGAAATAAATGTTCTAT
             ************************************************************
```

```
Mut12         ACGGAAAGGAGAGAAAAGTATCTGCCACAGTTGCAAATGATGTCACCATAACTTATAACC
PBP6a         ACGGAAAGGAGAGAAAAGTATCTGCCACAGTTGCAAATGATGTCACCATAACTTATAACC
              ************************************************************
Mut12         GCAATCTACGTGATAAAATTAAGGTGCGTGTTGAATATAAAGATATGATACCTGCACCTA
PBP6a         GCAATCTACGTGATAAAATTAAGGTGCGTGTTGAATATAAAGATATGATACCTGCACCTA
              ************************************************************
Mut12         TTAAAAAAGGGCAAGAAGTAGGTAAAATTTTTATAGAAATACCAGGTATAGAGCAGCAAA
PBP6a         TTAAAAAAGGGCAAGAAGTAGGTAAAATTTTTATAGAAATACCAGGTATAGAGCAGCAAA
              ************************************************************
Mut12         CTATACCACTTTATGCAGTGAATGATGTACAGGAATTAAATTACGTAGAAAAGTTTTTTA
PBP6a         CTATACCACTTTATGCAGTGAATGATGTACAGGAATTAAATTACGTAGAAAAGTTTTTTA
              ************************************************************
Mut12         GAATATTGTTTGACCATGGTCTCAGCGCTTGGAGCCACCCGCAGTTCGAAAAATAATAAG
PBP6a         GAATATTGTTTTAA----------------------------------------------
              *********** *.
Mut12         CTTGACCTGTGAAGTGAAAAA
PBP6a         ---------------------
```

Supplementary Figure 4: Nucleic acid alignment of PBP6a^{wBm} and cloned PBP6a^{wBm} active site mutant S48A-S56A (Mut12) in pASK-IBA2C. Mutated bases are highlighted gray.

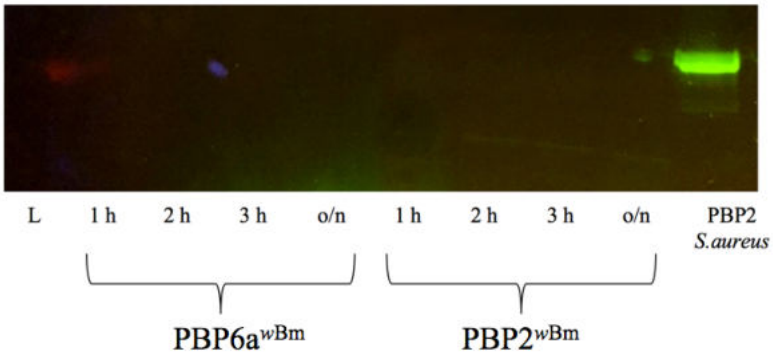

Supplementary Figure 5: Penicillin-binding assay. PBP2^{wBm} and PBP6a^{wBm} were incubated for 1 h, 2 h, 3 h or overnight (o/n) with Bocillin^{TM} FL. PBP2 from *S. aureus* served as a positive control.

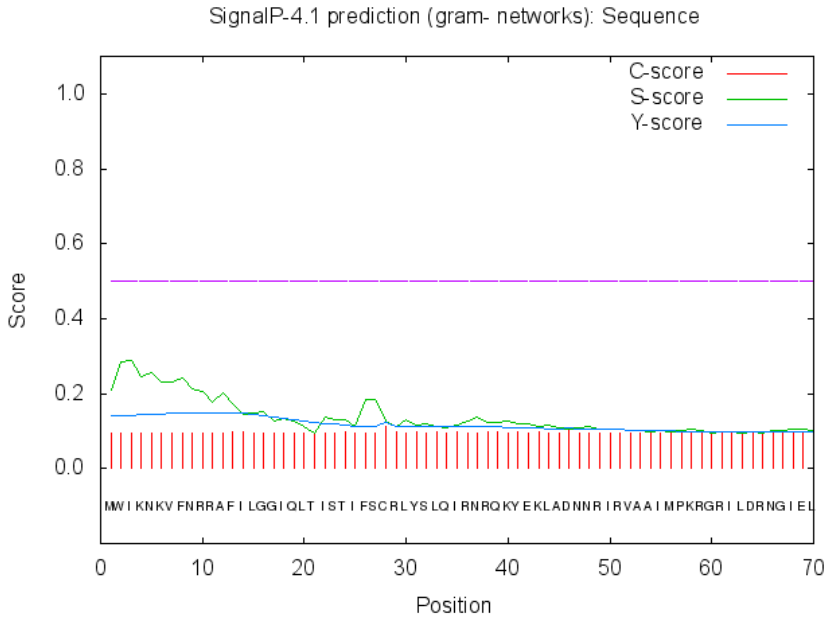


```
# Measure  Position  Value    Cutoff   signal peptide?
  max. C    28        0.111
  max. Y    13        0.150
  max. S     3        0.289
  mean S     1-12     0.232
       D     1-12     0.180   0.420   NO
Name = Sequence  SP = 'NO' D = 0.180 D-cutoff = 0.420 Networks = SignalP-TM
```

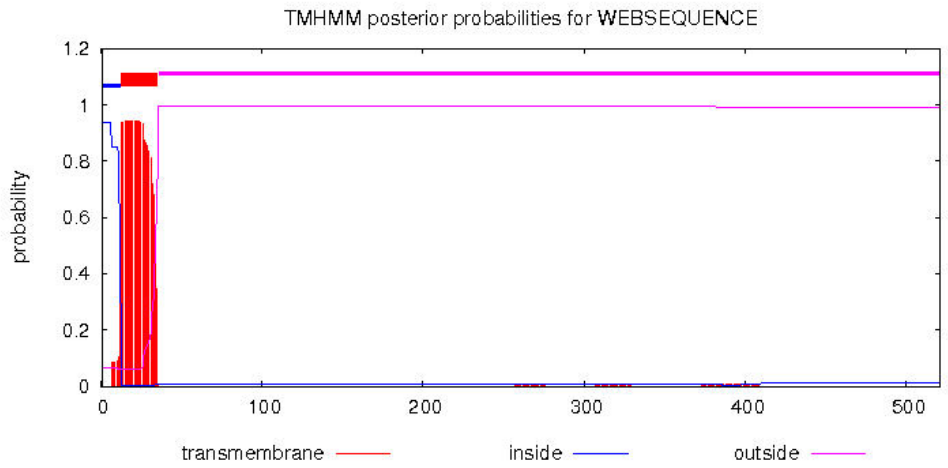


```
# WEBSEQUENCE Length: 521
# WEBSEQUENCE Number of predicted TMHs:  1
# WEBSEQUENCE Exp number of AAs in TMHs: 20.64977
# WEBSEQUENCE Exp number, first 60 AAs:  20.49195
# WEBSEQUENCE Total prob of N-in:        0.93602
# WEBSEQUENCE POSSIBLE N-term signal sequence
WEBSEQUENCE      TMHMM2.0 inside       1    12
WEBSEQUENCE      TMHMM2.0 TMhelix     13    35
WEBSEQUENCE      TMHMM2.0 outside     36   521
```

Supplementary Figure 6: Prediction for a transmembrane domain in PBP3^{wBm} by TMHMM, but not for a signal peptide as predicted by Signal P.

```
PBP2 wBm      MWIKNKVFNRRAFILGGIQLTISTIFSCRLYSLQIRNRQKYEKLADNNRIRVAAIMPKRG   60
PBP2 wMel     MWTKNKVFNRRAFILGGIQLTISAVFSCRLYNLQIRNRQKYEALSNSNRIRVATIMPKRG   60
              ** ********************::******.********** *::.******:******
PBP2 wBm      RILDRNGIELAVDKISYIVLFDKQKISSEEVDWETLSEIESNVTKSSETKITALYKRHYP   120
PBP2 wMel     KILDRNSIELAVNKISYVVLFDGS---GKEVDLQTLSEVESKIAKSS-EKITALYKRYYP   116
              :******.*****:****:**** .   .:*** :****:**:::***  ********:**
PBP2 wBm      FGSICSHTLGYTKKQQGINEAGISGIEYTYDHILKGKPGRSEQEINSKKRIVRELSSIPQ   180
PBP2 wMel     FGSMCSHVIGYTKRQQGISEVGISGIEYTYDHILKGKSGKSEQEINSKKRFIKELSSIPQ   176
              ***:***.:****:****.*.*************** *:**********:::*******
PBP2 wBm      QDGQDVQLTIDIDLQEKIAEIFKGHKGSVTAIDVGNGEILTLYNSPSYDNNLFANKLSNE   240
PBP2 wMel     QDGQDVQLTIDINLQEKTAEVFKDHQGSAVVIDVNNGEILALYNSPSYDNNLFASRLSNE   236
              ************:**** **:**.*:**...***.*****:*************.:****
PBP2 wBm      AWEGLNTPSLPLVNRALSYQIPPGSIFKIIVALAGLKDGIITPEEKFSCVGYMKIGERRF   300
PBP2 wMel     TWESLNAPSLPLVNRALSYQIPPGSIFKVIVALAGLKDGIITPEEKFSCKGYMKIGERKF   296
              :**.**:**********************:******************** ********:*
PBP2 wBm      CCLKSKVHGYVSLNEAMALSCNTYFYNIGKKISVDSLVEMARKFGIGSGPLIGAFKEEAP   360
PBP2 wMel     RCLKSKVHGYVSLNEAMALSCNTYFYNIGKKISVDSLVEMARKFGIGSGPLIGTFKEEAP   356
               ****************************************************:******
PBP2 wBm      GLLPDKDWRTRKLYSEWYLGDTVNLVIGQGYVLTTPLQLAVLAARIATGKEVIPRIEMSK   420
PBP2 wMel     GLLPDRDWRTRKLYSQWYLGDTINLVIGQGYMLTTPLQLAVLAARIATGKEVIPRIKMNE   416
              *****:*********:******:********:************************:*.:
PBP2 wBm      TMQDFPDIDIAHEHLSIVRKAMFNMVNIKAGTYRKGLSSIRIAGKTGTPEINSKGESHKL   480
PBP2 wMel     TIQDFPDIDVDCEHLSIVRKAMFDVVNSKTGTYKKGLSGIQIAGKTGTPEINSKGESHKL   476
              *:*******:  ***********::** *:***:****.*:******************
PBP2 wBm      FIAYGPYHDPRYAISVFIEYGKAPRQDVAMANEILRYMLKG-------      521
PBP2 wMel     FIAYGPYHNPRYAISVFIEHGKAPRQDVAIANEIFQYMLETMSIKLLA      524
              ********:**********:*********:****::***:
```

Supplementary Figure 7: Amino acid alignment of PBP2^{wBm} and PBP2^{wMel} (WP_010962786.1). ***** fully conserved residue; **:** conservation between groups of strongly similar properties; **.** conservation between groups of weakly similar properties. Conserved SXXK, SX(D/N) and K(S/T)G motifs found in PBP2^{wBm} and PBP2^{wMel} are written in bold letters, motif alignments are framed in black.

```
PBP2 wBm      --MWIKNKVFNRRAFILGGIQLTISTIFSCRLYSLQIRNRQKYEKLADNNRIRVAAIMPK   58
PBP3 wMel     MQALLKNKL-RSLCFIVPLFIFY--IIIIFRIFSL------TFDQLTTSENFRKDNIVHK   51
                  :***: .  .**:  : :    *:  *::**      .:::*: .:.:*   *: *
PBP2 wBm      RGRILDRNGIELAVDKISYIVLFDKQKISS--------------------------EEV   91
```

```
PBP3 wMel     QPDILDRNGVVIATNVPTTSLYIDATKVKNPESIAAQLCSTLHDLEYKNLYRVLTSEKKF  111
              :  ******: :*.:  :  : :*  *:..                              ::.
PBP2 wBm      DWETLSEIESN-----VTKSSETKITALYKRHYPFGSICSHTLGYTKKQQGINEAGISGI  146
PBP3 wMel     AWIKRHLTPKELLAIKNAGVPGVNFDDDIKRIYPHSNLFSHVLGYTDID----GNGIAGV  167
               * .     .:      :    .::    ** **...: **.****. :      **:*:
PBP2 wBm      EYTYDHILKGKPGRSEQEINSKKRIVRELSSIPQQDGQDVQLTIDIDLQEKIAEIFKGHK  206
PBP3 wMel     EAYISKN-----N--EQ----EKPIILSLDT-------RVQSIVHEEL-TKAVRRYQALG  208
              *   .:      .  **    :* *: .*.:        **  :. :*  * .. ::.
PBP2 wBm      GSVTAIDVGNGEILTLYNSPSYDNNLFANKLSNEAWEGLNTPSLPLVNRALSYQIPPGSI  266
PBP3 wMel     GVGIVLNVRNSEVISMVSLPDFNPNLQNKAEDVQKF---NRASLG--------VYEMGSV  257
              *   .::* *.*:::: . *.:: **  :  . : :   *  **           **:
PBP2 wBm      FKIIVALAGLKDGIITPEEKFSCVGYMKIGERRFCCLKSKVHGYVSLNEAMALSCNTYFY  326
PBP3 wMel     LKYFTIAAALDANATKTSDLYDVSTPITIGKYKIQDFHKSKIPKITVQDIFVKSSNIGAA  317
              :* :.  *.*. .  . .: :.    :.**: ::  ::..    ::::: :. *.*
PBP2 wBm      NIGKKISVDSLVEMARKFGIGSGPLIGAFKEEAPGLLPDKDWRTRKLYSEWYLGDTVNLV  386
PBP3 wMel     KIAVKLGIEKQVEYFKAMKL-FSPLKIEIPEKSTPIIPD-KWSETTLITA---------S  366
              :*. *:.::. **  : : :  .**   : *::  ::** .*   .* :
PBP2 wBm      IGQGYVLTTPLQLAVLAARIA----------------TGKEVIPRIEMSKTMQDFPDIDI  430
PBP3 wMel     YGYGIA-VTPIHLAQTAAALINNGIFHNATLMLNKRSIGEQIISRRT-SREMR-------  417
               * * . .**::**  ** :                  *:::* *   *: *:
PBP2 wBm      AHEHLSIVRKAMFNMVNIKAGTY-RKGLSSIRIAGKTGTPEINSKGE-----SHKLFIAY  484
PBP3 wMel     -----KLLRAA------VTDGTGRKAKIKAYSIGGKTGSAEKVVDGKYSKDANIASFIGV  466
                   .::* *      :. **  :  :.:  *.****: *   .*:     .   **.
PBP2 wBm      GPYHDPRYAISVFIEYGKAPRQDV-AMANEILRYMLKG-----------     521
PBP3 wMel     LTMLDPRYIVLIAIDEPQGMHHTGGIIAAPIVKNIINRIAPILNVTPEM     515
                  **** : : *:  :. ::    :*  *:: :::
```

Supplementary Figure 8: Amino acid alignment of PBP2^{wBm} and PBP3^{wMel} (WP_010963147.1). ***** fully conserved residue; **:** conservation between groups of strongly similar properties; **.** conservation between groups of weakly similar properties. Conserved SXXK, SX(D/N) and K(S/T)G motifs found in PBP2$_{wBm}$ and PBP3$_{wMel}$ are written in bold letters, motif alignments are framed in black.

```
PBP2_TM    AAAATCTAGATAACGAGGGCAAAAAATGAAAAAGACAGCTATCGCGATTGCAGTG-GCAC
PBP2       ------------ATGTGGATAAA---AAACAAAGTCTTTAATCGTAG-GGCATTTATATT
                        * *:**. ***   :.*.****:*:  :**** ..  *** *   .:
PBP2_TM    TGGCTGGTTTCGCTACCGTAGCGCAGGCCGCTAGCTGGAGCCACCCGC------AGTTCG
PBP2       AGGCGGTAT-----------------TCAGCTTACCATTTCCACAATTTTTAGTTGTAGG
           :*** * :*                  *.***:.* . : ****..        :**: *
PBP2_TM    AAA-AAATCGAAGGGCGCCGAAACAGACAAAAATACGAAAAGCTGGCTGACAATAACAGG
PBP2       TTATATAGTTTACAAATACGAAACAGACAAAAATACGAAAAGCTGGCTGACAATAACAGG
           ::* *:*   :* ... .****************************************
PBP2_TM    ATACGAGTTGCTGCTATTATGCCTAAGCGTGGCAGAATTTTAGATAGGAATGGCATTGAA
PBP2       ATACGAGTTGCTGCTATTATGCCTAAGCGTGGCAGAATTTTAGATAGGAATGGCATTGAA
           ************************************************************
PBP2_TM    CTTGCAGTAGACAAAATTTCGTACATTGTTTTGTTCGATAAGCAAAAAATTTCTAGTGAA
PBP2       CTTGCAGTAGACAAAATTTCGTACATTGTTTTGTTCGATAAGCAAAAAATTTCTAGTGAA
           ************************************************************
PBP2_TM    GAAGTTGATTGGGAAACATTATCAGAAATTGAATCTAATGTAACAAAATCGTCAGAAACA
PBP2       GAAGTTGATTGGGAAACATTATCAGAAATTGAATCTAATGTAACAAAATCGTCAGAAACA
           ************************************************************
PBP2_TM    AAAATAACCGCTCTTTATAAACGTCACTATCCGTTCGGTTCAATATGTTCTCATACACTA
PBP2       AAAATAACCGCTCTTTATAAACGTCACTATCCGTTCGGTTCAATATGTTCTCATACACTA
           ************************************************************
PBP2_TM    GGATATACGAAAAAACAGCAAGGCATAAACGAAGCAGGAATCAGTGGTATTGAATATACA
PBP2       GGATATACGAAAAAACAGCAAGGCATAAACGAAGCAGGAATCAGTGGTATTGAATATACA
           ************************************************************
PBP2_TM    TATGATCATATATTGAAAGGCAAGCCAGGGAGATCTGAGCAGGAAATAAATTCTAAAAAA
PBP2       TATGATCATATATTGAAAGGCAAGCCAGGGAGATCTGAGCAGGAAATAAATTCTAAAAAA
           ************************************************************
PBP2_TM    CGCATCGTGAGAGAATTATCAAGCATACCACAACAGGACGGACAAGATGTACAGCTAACA
PBP2       CGCATCGTGAGAGAATTATCAAGCATACCACAACAGGACGGACAAGATGTACAGCTAACA
           ************************************************************
PBP2_TM    ATTGATATTGATCTGCAAGAGAAAATTGCAGAGATATTTAAAGGTCACAAAGGTTCTGTA
PBP2       ATTGATATTGATCTGCAAGAGAAAATTGCAGAGATATTTAAAGGTCACAAAGGTTCTGTA
           ************************************************************
PBP2_TM    ACGGCGATTGATGTAGGTAACGGAGAAATTTTAACATTATATAATTCACCTTCTTACGAT
PBP2       ACGGCGATTGATGTAGGTAACGGAGAAATTTTAACATTATATAATTCACCTTCTTACGAT
           ************************************************************
```

```
PBP2_TM    AATAACCTTTTTGCTAACAAACTATCAAATGAGGCTTGGGAAGGTTTAAATACTCCTTCA
PBP2       AATAACCTTTTTGCTAACAAACTATCAAATGAGGCTTGGGAAGGTTTAAATACTCCTTCA
           ************************************************************
PBP2_TM    TTACCACTTGTAAATCGTGCATTATCGTATCAAATTCCACCTGGTTCGATATTTAAAATA
PBP2       TTACCACTTGTAAATCGTGCATTATCGTATCAAATTCCACCTGGTTCGATATTTAAAATA
           ************************************************************
PBP2_TM    ATAGTTGCACTTGCGGGTCTAAAGGATGGAATAATCACTCCAGAAGAGAAATTTTCATGT
PBP2       ATAGTTGCACTTGCGGGTCTAAAGGATGGAATAATCACTCCAGAAGAGAAATTTTCATGT
           ************************************************************
PBP2_TM    GTAGGCTATATGAAAATAGGTGAGCGGAGGTTTTGTTGCTTGAAAAGCAAAGTCCATGGA
PBP2       GTAGGCTATATGAAAATAGGTGAGCGGAGGTTTTGTTGCTTGAAAAGCAAAGTCCATGGA
           ************************************************************
PBP2_TM    TATGTATCTTTAAATGAAGCAATGGCTTTATCATGTAACACTTACTTTTATAATATAGGA
PBP2       TATGTATCTTTAAATGAAGCAATGGCTTTATCATGTAACACTTACTTTTATAATATAGGA
           ************************************************************
PBP2_TM    AAAAAAATAAGTGTAGACTCTCTAGTAGAAATGGCAAGAAAATTTGGTATCGGAAGTGGG
PBP2       AAAAAAATAAGTGTAGACTCTCTAGTAGAAATGGCAAGAAAATTTGGTATCGGAAGTGGG
           ************************************************************
PBP2_TM    CCACTAATTGGAGCATTTAAAGAAGAAGCTCCAGGATTGTTGCCTGATAAAGATTGGCGT
PBP2       CCACTAATTGGAGCATTTAAAGAAGAAGCTCCAGGATTGTTGCCTGATAAAGATTGGCGT
           ************************************************************
PBP2_TM    ACACGAAAGCTATATTCGGAGTGGTATTTAGGTGACACTGTCAACTTAGTTATAGGGCAA
PBP2       ACACGAAAGCTATATTCGGAGTGGTATTTAGGTGACACTGTCAACTTAGTTATAGGGCAA
           ************************************************************
PBP2_TM    GGGTATGTGCTTACAACACCACTGCAGCTTGCAGTTCTTGCGGCAAGAATTGCAACAGGA
PBP2       GGGTATGTGCTTACAACACCACTGCAGCTTGCAGTTCTTGCGGCAAGAATTGCAACAGGA
           ************************************************************
PBP2_TM    AAGGAGGTGATTCCCCGCATTGAAATGAGTAAAACGATGCAAGATTTTCCTGATATTGAT
PBP2       AAGGAGGTGATTCCCCGCATTGAAATGAGTAAAACGATGCAAGATTTTCCTGATATTGAT
           ************************************************************
PBP2_TM    ATAGCTCATGAGCATCTCAGTATAGTTCGAAAAGCTATGTTTAACATGGTGAATATTAAA
PBP2       ATAGCTCATGAGCATCTCAGTATAGTTCGAAAAGCTATGTTTAACATGGTGAATATTAAA
           ************************************************************
PBP2_TM    GCTGGAACCTATAGAAAAGGGCTAAGCAGTATACGAATTGCCGGCAAAACCGGTACACCA
PBP2       GCTGGAACCTATAGAAAAGGGCTAAGCAGTATACGAATTGCCGGCAAAACCGGTACACCA
           ************************************************************
PBP2_TM    GAGATAAACTCTAAGGGTGAAAGTCATAAATTATTCATCGCTTATGGCCCTTACCATGAC
PBP2       GAGATAAACTCTAAGGGTGAAAGTCATAAATTATTCATCGCTTATGGCCCTTACCATGAC
           ************************************************************
PBP2_TM    CCGCGCTATGCAATCTCTGTATTCATAGAGTACGGCAAAGCCCCACGCCAAGATGTTGCT
PBP2       CCGCGCTATGCAATCTCTGTATTCATAGAGTACGGCAAAGCCCCACGCCAAGATGTTGCT
           ************************************************************
PBP2_TM    ATGGCCAATGAAATATTGCGGTATATGCTTAAAGGGTGATATCTAACTAAGCTTGA
PBP2       ATGGCCAATGAAATATTGCGGTATATGCTTAAAGGGTGA----------------
           ************************************
```

Supplementary Figure 9: Nucleic acid alignment of PBP2^{wBm} and cloned PBP2ΔTM^{wBm} in pASK-IBA6C.

```
PBP2          CAAAAATCTAGATAACGAGGGCAAAAAATGAAAAAGACAGCTATCGCGATTGCAGTGGCA  60
PBP2orig      ------------------------------------------------------------  0

PBP2          CTGGCTGGTTTCGCTACCGTAGCGCAGGCCGCTAGCTGGAGCCACCCGCAGTTCGAAAAA  120
PBP2orig      ------------------------------------------------------------  0

PBP2          ATCGAAGGGCGCTGGATAAAAAACAAAGTCTTTAATCGTAGGGCATTTATATTAGGCGGT  180
PBP2orig      ---------ATGTGGATAAAAAACAAAGTCTTTAATCGTAGGGCATTTATATTAGGCGGT  51
                        *********************************************

PBP2          ATTCAGCTTACCATTTCCACAATTTTTAGTTGTAGGTTATATAGTTTACAAATACGAAAC  240
PBP2orig      ATTCAGCTTACCATTTCCACAATTTTTAGTTGTAGGTTATATAGTTTACAAATACGAAAC  111
              ************************************************************

PBP2          AGACAAAAATACGAAAAGCTGGCTGACAATAACAGGATACGAGTTGCTGCTATTATGCCT  300
PBP2orig      AGACAAAAATACGAAAAGCTGGCTGACAATAACAGGATACGAGTTGCTGCTATTATGCCT  171
              ************************************************************

PBP2          AAGCGTGGCAGAATTTTAGATAGGAATGGCATTGAACTTGCAGTAGACAAAATTTCGTAC  360
PBP2orig      AAGCGTGGCAGAATTTTAGATAGGAATGGCATTGAACTTGCAGTAGACAAAATTTCGTAC  231
              ************************************************************

PBP2          ATTGTTTTGTTCGATAAGCAAAAAATTTCTAGTGAAGAAGTTGATTGGGAAACATTATCA  420
PBP2orig      ATTGTTTTGTTCGATAAGCAAAAAATTTCTAGTGAAGAAGTTGATTGGGAAACATTATCA  291
              ************************************************************
```

```
PBP2          GAAATTGAATCTAATGTAACAAAATCGTCAGAAACAAAAATAACCGCTCTTTATAAACGT  480
PBP2orig      GAAATTGAATCTAATGTAACAAAATCGTCAGAAACAAAAATAACCGCTCTTTATAAACGT  351
              ************************************************************
PBP2          CACTATCCGTTCGGTTCAATATGTTCTCATACACTAGGATATACGAAAAAACAGCAAGGC  540
PBP2orig      CACTATCCGTTCGGTTCAATATGTTCTCATACACTAGGATATACGAAAAAACAGCAAGGC  411
              ************************************************************
PBP2          ATAAACGAAGCAGGAATCAGTGGTATTGAATATACATATGATCATATATTGAAAGGCAAG  600
PBP2orig      ATAAACGAAGCAGGAATCAGTGGTATTGAATATACATATGATCATATATTGAAAGGCAAG  471
              ************************************************************
PBP2          CCAGGGAGATCTGAGCAGGAAATAAATTCTAAAAAACGCATCGTGAGAGAATTATCAAGC  660
PBP2orig      CCAGGGAGATCTGAGCAGGAAATAAATTCTAAAAAACGCATCGTGAGAGAATTATCAAGC  531
              ************************************************************
PBP2          ATACCACAACAGGACGGACAAGATGTACAGCTAACAATTGATATTGATCTGCAAGAGAAA  720
PBP2orig      ATACCACAACAGGACGGACAAGATGTACAGCTAACAATTGATATTGATCTGCAAGAGAAA  591
              ************************************************************
PBP2          ATTGCAGAGATATTTAAAGGTCACAAAGGTTCTGTAACGGCGATTGATGTAGGTAACGGA  780
PBP2orig      ATTGCAGAGATATTTAAAGGTCACAAAGGTTCTGTAACGGCGATTGATGTAGGTAACGGA  651
              ************************************************************
PBP2          GAAATTTTAACATTATATAATTCACCTTCTTACGATAATAACCTTTTTGCTAACAAACTA  840
PBP2orig      GAAATTTTAACATTATATAATTCACCTTCTTACGATAATAACCTTTTTGCTAACAAACTA  711
              ************************************************************
PBP2          TCAAATGAGGCTTGGGAAGGTTTAAATACTCCTTCATTACCACTTGTAAATCGTGCATTA  900
PBP2orig      TCAAATGAGGCTTGGGAAGGTTTAAATACTCCTTCATTACCACTTGTAAATCGTGCATTA  771
              ************************************************************
PBP2          TCGTATCAAATTCCACCTGGTTCGATATTTAAAATAATAGTTGCACTTGCGGGTCTAAAG  960
PBP2orig      TCGTATCAAATTCCACCTGGTTCGATATTTAAAATAATAGTTGCACTTGCGGGTCTAAAG  831
              ************************************************************
PBP2          GATGGAATAATCACTCCAGAAGAGAAATTTTCATGTGTAGGCTATATGAAAATAGGTGAG  1020
PBP2orig      GATGGAATAATCACTCCAGAAGAGAAATTTTCATGTGTAGGCTATATGAAAATAGGTGAG  891
              ************************************************************
PBP2          CGGAGGTTTTGTTGCTTGAAAAGCAAAGTCCATGGATATGTATCTTTAAATGAAGCAATG  1080
PBP2orig      CGGAGGTTTTGTTGCTTGAAAAGCAAAGTCCATGGATATGTATCTTTAAATGAAGCAATG  951
              ************************************************************
PBP2          GCTTTATCATGTAACACTTACTTTTATAATATAGGAAAAAAAATAAGTGTAGACTCTCTA  1140
PBP2orig      GCTTTATCATGTAACACTTACTTTTATAATATAGGAAAAAAAATAAGTGTAGACTCTCTA  1011
              ************************************************************
PBP2          GTAGAAATGGCAAGAAAATTTGGTATCGGAAGTGGGCCACTAATTGGAGCATTTAAAGAA  1200
PBP2orig      GTAGAAATGGCAAGAAAATTTGGTATCGGAAGTGGGCCACTAATTGGAGCATTTAAAGAA  1071
              ************************************************************
PBP2          GAAGCTCCAGGATTGTTGCCTGATAAAGATTGGCGTACACGAAAGCTATATTCGGAGTGG  1260
PBP2orig      GAAGCTCCAGGATTGTTGCCTGATAAAGATTGGCGTACACGAAAGCTATATTCGGAGTGG  1131
              ************************************************************
PBP2          TATTTAGGTGACACTGTCAACTTAGTTATAGGGCAAGGGTATGTGCTTACAACACCACTG  1320
PBP2orig      TATTTAGGTGACACTGTCAACTTAGTTATAGGGCAAGGGTATGTGCTTACAACACCACTG  1191
              ************************************************************
PBP2          CAGCTTGCAGTTCTTGCGGCAAGAATTGCAACAGGAAAGGAGGTGATTCCCCGCATTGAA  1380
PBP2orig      CAGCTTGCAGTTCTTGCGGCAAGAATTGCAACAGGAAAGGAGGTGATTCCCCGCATTGAA  1251
              ************************************************************
PBP2          ATGAGTAAAACGATGCAAGATTTTCCTGATATTGATATAGCTCATGAGCATCTCAGTATA  1440
PBP2orig      ATGAGTAAAACGATGCAAGATTTTCCTGATATTGATATAGCTCATGAGCATCTCAGTATA  1311
              ************************************************************
PBP2          GTTCGAAAAGCTATGTTTAACATGGTGAATATTAAAGCTGGAACCTATAGAAAAGGGCTA  1500
PBP2orig      GTTCGAAAAGCTATGTTTAACATGGTGAATATTAAAGCTGGAACCTATAGAAAAGGGCTA  1371
              ************************************************************
PBP2          AGCAGTATACGAATTGCCGGCAAAACCGGTACACCAGAGATAAACTCTAAGGGTGAAAGT  1560
PBP2orig      AGCAGTATACGAATTGCCGGCAAAACCGGTACACCAGAGATAAACTCTAAGGGTGAAAGT  1431
              ************************************************************
PBP2          CATAAATTATTCATCGCTTATGGCCCTTACCATGACCCGCGCTATGCAATCTCTGTATTC  1620
PBP2orig      CATAAATTATTCATCGCTTATGGCCCTTACCATGACCCGCGCTATGCAATCTCTGTATTC  1491
              ************************************************************
PBP2          ATAGAGTACGGCAAAGCCCCACGCCAAGATGTTGCTATGGCCAATGAAATATTGCGGTAT  1680
PBP2orig      ATAGAGTACGGCAAAGCCCCACGCCAAGATGTTGCTATGGCCAATGAAATATTGCGGTAT  1551
              ************************************************************
PBP2          ATGCTTAAAGGGTGATATCTAACTAAGCTTGACCTGTGAA      1720
PBP2orig      ATGCTTAAAGGGTGA-------------------------      1566
              ***************
```

Supplementary Figure 10: Nucleic acid alignment of PBP2$^{w\mathrm{Bm}}$ (PBP2orig) and cloned PBP2$^{w\mathrm{Bm}}$ in pASK-IBA6C.

```
Mut12          ANNTAACGAGGGCAAAAAATGAAAAAGACAGCTATCGCGATTGCAGTGGCACTGGCTGGT
PBP2           -----ATGTGGAT---AAAAAACAAAGTCTTTAATCGT-AGGGCATTTATATT-------
                    * * **     ***  * **** *    ****  *  *** *   * *
Mut12          TTCGCTACCGTAGCGCAGGCCGCTAGCTGGAGCCACCCGCAGTTCGAAAAAATCGAAGGG
PBP2           --AGGCGGTATTCAGCTTACCATTTCCACAATTTTTAGTTGTAGGTTATATAGTTTACAA
                  *      *   **   **  *  *   *                 * * *    *
Mut12          CGCCGAAACAGACAAAAATACGAAAAGCTGGCTGACAATAACAGGATACGAGTTGCTGCT
PBP2           ATACGAAACAGACAAAAATACGAAAAGCTGGCTGACAATAACAGGATACGAGTTGCTGCT
                  ************************************************************
Mut12          ATTATGCCTAAGCGTGGCAGAATTTTAGATAGGAATGGCATTGAACTTGCAGTAGACAAA
PBP2           ATTATGCCTAAGCGTGGCAGAATTTTAGATAGGAATGGCATTGAACTTGCAGTAGACAAA
               ************************************************************
Mut12          ATTTCGTACATTGTTTTGTTCGATAAGCAAAAAATTTCTAGTGAAGAAGTTGATTGGGAA
PBP2           ATTTCGTACATTGTTTTGTTCGATAAGCAAAAAATTTCTAGTGAAGAAGTTGATTGGGAA
               ************************************************************
Mut12          ACATTATCAGAAATTGAATCTAATGTAACAAAATCGGCGGAAACAAAAATAACCGCTCTT
PBP2           ACATTATCAGAAATTGAATCTAATGTAACAAAATCGTCAGAAACAAAAATAACCGCTCTT
               ********************************** * ********************
Mut12          TATAAACGTCACTATCCGTTCGGTTCAATATGTTCTCATACACTAGGATATACGAAAAAA
PBP2           TATAAACGTCACTATCCGTTCGGTTCAATATGTTCTCATACACTAGGATATACGAAAAAA
               ************************************************************
Mut12          CAGCAAGGCATAAACGAAGCAGGAATCAGTGGTATTGAATATACATATGATCATATATTG
PBP2           CAGCAAGGCATAAACGAAGCAGGAATCAGTGGTATTGAATATACATATGATCATATATTG
               ************************************************************
Mut12          AAAGGCAAGCCAGGGAGATCTGAGCAGGAAATAAATTCTAAAAAACGCATCGTGAGAGAA
PBP2           AAAGGCAAGCCAGGGAGATCTGAGCAGGAAATAAATTCTAAAAAACGCATCGTGAGAGAA
               ************************************************************
Mut12          TTATCAAGCATACCACAACAGGACGGACAAGATGTACAGCTAACAATTGATATTGATCTG
PBP2           TTATCAAGCATACCACAACAGGACGGACAAGATGTACAGCTAACAATTGATATTGATCTG
               ************************************************************
Mut12          CAAGAGAAAATTGCAGAGATATTTAAAGGTCACAAAGGTTCTGTAACGGCGATTGATGTA
PBP2           CAAGAGAAAATTGCAGAGATATTTAAAGGTCACAAAGGTTCTGTAACGGCGATTGATGTA
               ************************************************************
Mut12          GGTAACGGAGAAATTTTAACATTATATAATTCACCTTCTTACGATAATAACCTTTTTGCT
PBP2           GGTAACGGAGAAATTTTAACATTATATAATTCACCTTCTTACGATAATAACCTTTTTGCT
               ************************************************************
Mut12          AACAAACTATCAAATGAGGCTTGGGAAGGTTTAAATACTCCTTCATTACCACTTGTAAAT
PBP2           AACAAACTATCAAATGAGGCTTGGGAAGGTTTAAATACTCCTTCATTACCACTTGTAAAT
               ************************************************************
Mut12          CGTGCATTATCGTATCAAATTCCACCTGGTGCGATATTTAAAATAATAGTTGCACTTGCG
PBP2           CGTGCATTATCGTATCAAATTCCACCTGGTTCGATATTTAAAATAATAGTTGCACTTGCG
               ****************************** ******************************
Mut12          GGTCTAAAGGATGGAATAATCACTCCAGAAGAGAAATTTTCATGTGTAGGCTATATGAAA
PBP2           GGTCTAAAGGATGGAATAATCACTCCAGAAGAGAAATTTTCATGTGTAGGCTATATGAAA
               ************************************************************
Mut12          ATAGGTGAGCGGAGGTTTTGTTGCTTGAAAAGCAAAGTCCATGGATATGTATCTTTAAAT
PBP2           ATAGGTGAGCGGAGGTTTTGTTGCTTGAAAAGCAAAGTCCATGGATATGTATCTTTAAAT
               ************************************************************
Mut12          GAAGCAATGGCTTTATCATGTAACACTTACTTTTATAATATAGGAAAAAAAATAAGTGTA
PBP2           GAAGCAATGGCTTTATCATGTAACACTTACTTTTATAATATAGGAAAAAAAATAAGTGTA
               ************************************************************
Mut12          GACTCTCTAGTAGAAATGGCAAGAAAATTTGGTATCGGAAGTGGGCCACTAATTGGAGCA
PBP2           GACTCTCTAGTAGAAATGGCAAGAAAATTTGGTATCGGAAGTGGGCCACTAATTGGAGCA
               ************************************************************
Mut12          TTTAAAGAAGAAGCTCCAGGATTGTTGCCTGATAAAGATTGGCGTACACGAAAGCTATAT
PBP2           TTTAAAGAAGAAGCTCCAGGATTGTTGCCTGATAAAGATTGGCGTACACGAAAGCTATAT
               ************************************************************
Mut12          TCGGAGTGGTATTTAGGTGACACTGTCAACTTAGTTATAGGGCAAGGGTATGTGCTTACA
PBP2           TCGGAGTGGTATTTAGGTGACACTGTCAACTTAGTTATAGGGCAAGGGTATGTGCTTACA
               ************************************************************
Mut12          ACACCACTGCAGCTTGCAGTTCTTGCGGCAAGAATTGCAACAGGAAAGGAGGTGATTCCC
PBP2           ACACCACTGCAGCTTGCAGTTCTTGCGGCAAGAATTGCAACAGGAAAGGAGGTGATTCCC
               ************************************************************
Mut12          CGCATTGAAATGAGTAAAACGATGCAAGATTTTCCTGATATTGATATAGCTCATGAGCAT
PBP2           CGCATTGAAATGAGTAAAACGATGCAAGATTTTCCTGATATTGATATAGCTCATGAGCAT
               ************************************************************
Mut12          CTCAGTATAGTTCGAAAAGCTATGTTTAACATGGTGAATATTAAAGCTGGAACCTATAGA
PBP2           CTCAGTATAGTTCGAAAAGCTATGTTTAACATGGTGAATATTAAAGCTGGAACCTATAGA
               ************************************************************
```

```
Mut12          AAAGGGCTAAGCAGTATACGAATTGCCGGCAAAACCGGTACACCAGAGATAAACTCTAAG
PBP2           AAAGGGCTAAGCAGTATACGAATTGCCGGCAAAACCGGTACACCAGAGATAAACTCTAAG
               ************************************************************
Mut12          GGTGAAAGTCATAAATTATTCATCGCTTATGGCCCTTACCATGACCCGCGCTATGCAATC
PBP2           GGTGAAAGTCATAAATTATTCATCGCTTATGGCCCTTACCATGACCCGCGCTATGCAATC
               ************************************************************
Mut12          TCTGTATTCATAGAGTACGGCAAAGCCCCACGCCAAGATGTTGCTATGGCCAATGAAATA
PBP2           TCTGTATTCATAGAGTACGGCAAAGCCCCACGCCAAGATGTTGCTATGGCCAATGAAATA
               ************************************************************
Mut12          TTGCGGTATATGCTTAAAGGGTGATATCTAACTAAG
PBP2           TTGCGGTATATGCTTAAAGGGTGA------------
               ***********************************
```

Supplementary Figure 11: Nucleic acid alignment of PBP2^{wBm} and cloned PBP2^{wBm} active site mutant S107A-S265A (Mut12) in pASK-IBA6C. Mutated bases are highlighted gray.

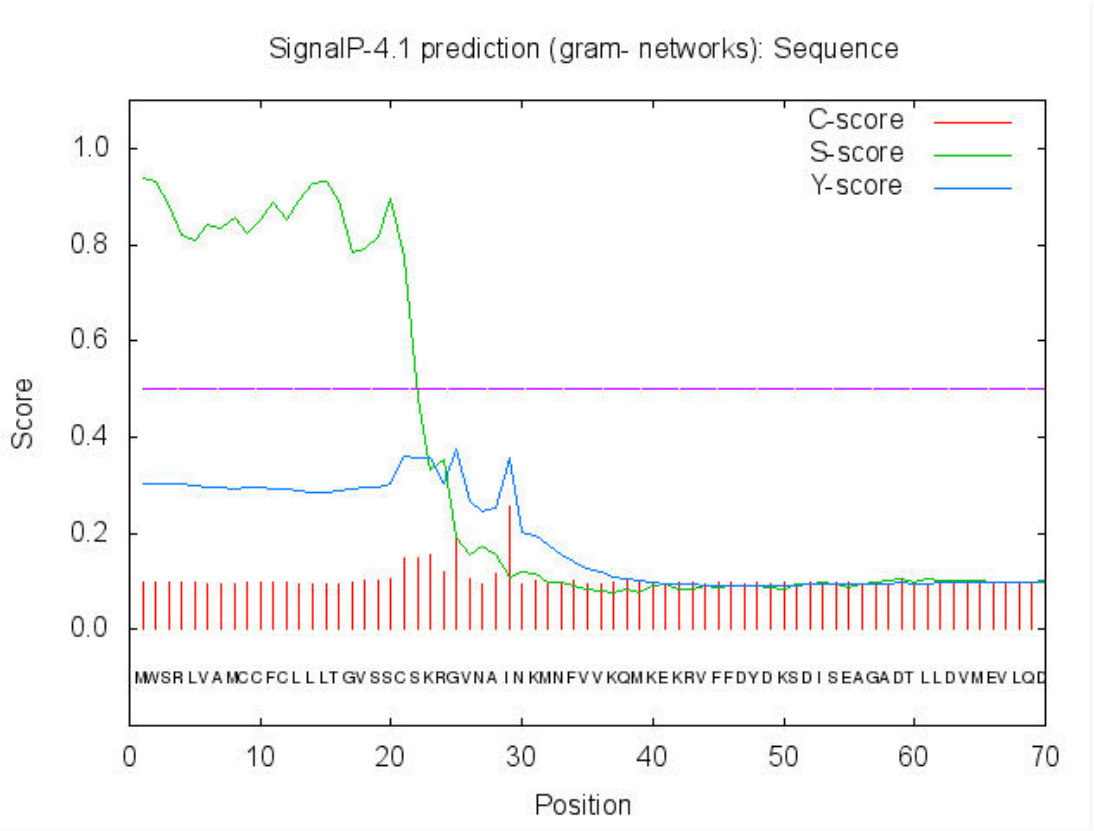


```
# Measure  Position  Value    Cutoff   signal peptide?
  max. C    29        0.257
  max. Y    25        0.375
  max. S     1        0.940
  mean S     1-24     0.800
       D     1-24     0.574   0.570    YES
Name = Sequence  SP = 'YES' Cleavage site between pos. 24 and 25: SKR-GV D = 0.574
D-cutoff = 0.570 Networks = SignalP-noTM
```

Supplementary Figure 12: Prediction for a signal peptide as predicted in Pal^{wBm} by Signal P.

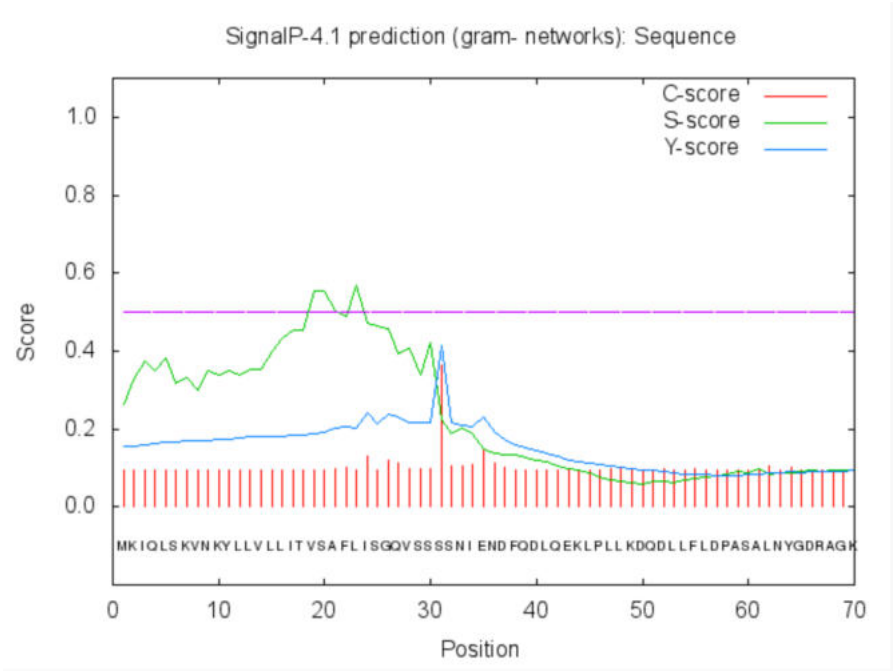


```
# Measure  Position  Value    Cutoff   signal peptide?
  max. C    31        0.363
  max. Y    31        0.413
  max. S    23        0.568
  mean S     1-30     0.403
       D     1-30     0.409   0.400    YES
Name = Sequence  SP = 'YES' Cleavage site between pos. 30 and 31: VSS-SS D = 0.409
D-cutoff = 0.400 Networks = SignalP-TM
```

Supplementary Figure 13: Prediction for a signal peptide as predicted in AmiD^{wMel} by Signal P.

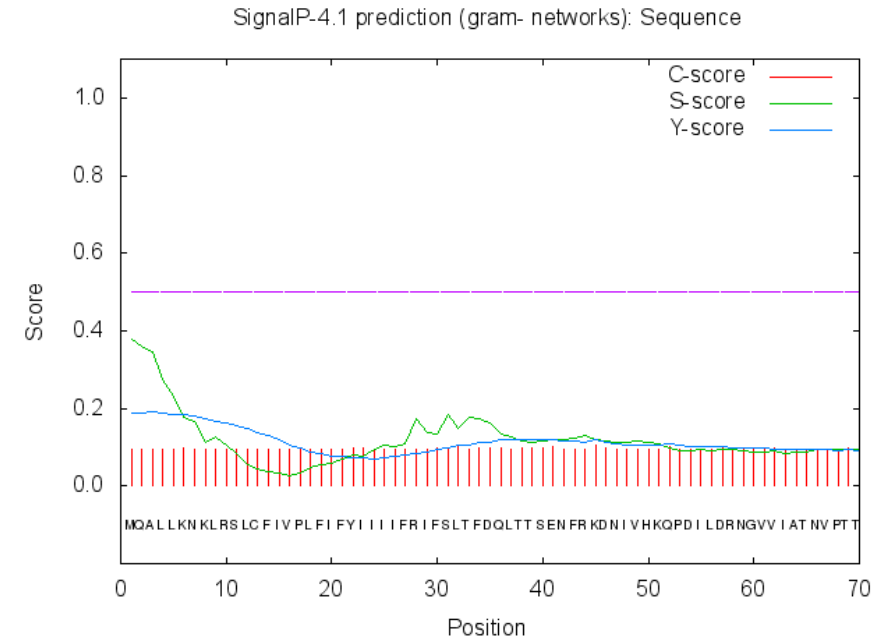


```
# Measure  Position  Value    Cutoff   signal peptide?
  max. C    45        0.106
  max. Y    11        0.156
  max. S     1        0.379
  mean S     1-10     0.227
       D     1-10     0.182   0.420    NO
Name = Sequence  SP = 'NO' D = 0.182 D-cutoff = 0.420 Networks = SignalP-TM
```

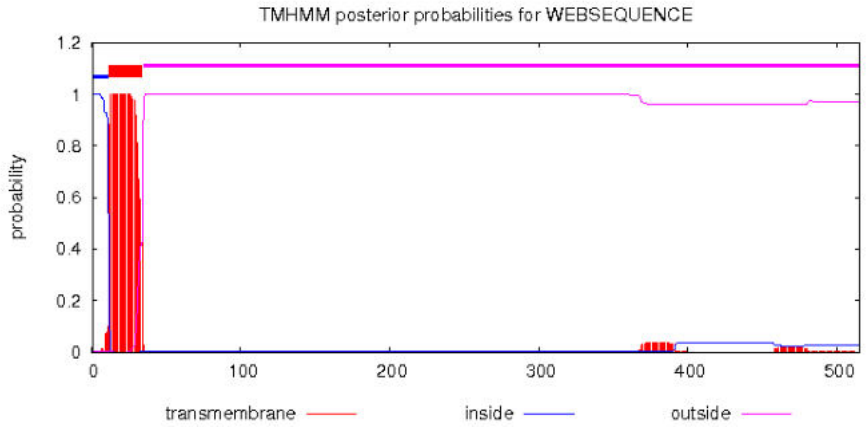


```
# WEBSEQUENCE Length: 515
# WEBSEQUENCE Number of predicted TMHs:  1
# WEBSEQUENCE Exp number of AAs in TMHs: 22.94915
# WEBSEQUENCE Exp number, first 60 AAs:  21.68864
# WEBSEQUENCE Total prob of N-in:        0.99859
# WEBSEQUENCE POSSIBLE N-term signal sequence
WEBSEQUENCE      TMHMM2.0 inside        1    11
WEBSEQUENCE      TMHMM2.0 TMhelix      12    34
WEBSEQUENCE      TMHMM2.0 outside      35   515
```

Supplementary Figure 14: Prediction for a transmembrane domain in PBP3^{wMel}, but not for a signal peptide.

```
PBP3      ------------------------------------------------------------
Mut1234   CAAAAATCTAGATAACGAGGGCAAAAAATGAAAAAGACAGCTATCGCGATTGCAGTGGCA

PBP3      ---------------------------ATGCAAGCATTACTTAAAAATAAGCTCCGCTCA
Mut1234   CTGGCTGGTTTCGCTACCGTAGCGCAGGCCCAAGCATTACTTAAAAATAAGCTCCGCTCA
                               .        ******************************
PBP3      CTGTGTTTTATAGTACCATTATTTATATTTTATATAATAATTATTTTTCGCATATTCTCT
Mut1234   CTGTGTTTTATAGTACCATTATTTATATTTTATATAATAATTATTTTTCGCATATTCTCT
          ************************************************************
PBP3      TTAACATTTGATCAACTTACTACTTCAGAAAATTTTAGAAAAGATAATATAGTACATAAA
Mut1234   TTAACATTTGATCAACTTACTACTTCAGAAAATTTTAGAAAAGATAATATAGTACATAAA
          ************************************************************
PBP3      CAACCTGATATTTTAGATAGAAATGGAGTGGTAATAGCAACAAATGTGCCCACAACATCA
Mut1234   CAACCTGATATTTTAGATAGAAATGGAGTGGTAATAGCAACAAATGTGCCCACAACATCA
          ************************************************************
PBP3      CTATATATAGATGCAACCAAAGTAAAGAATCCGGAAAGTATAGCAGCACAACTGTGTTCT
Mut1234   CTATATATAGATGCAACCAAAGTAAAGAATCCGGAAAGTATAGCAGCACAACTGTGTTCT
          ************************************************************
PBP3      ACTTTGCATGACCTCGAATACAAGAACTTATATAGAGTACTTACTTCAGAAAAGAAATTT
Mut1234   ACTTTGCATGACCTCGAATACAAGAACTTATATAGAGTACTTACTGCCGAAAAGAAATTT
          ******************************************** *.************
PBP3      GCTTGGATAAAGCGGCACTTGACTCCAAAAGAATTACTAGCGATCAAAAACGCTGGTGTA
Mut1234   GCTTGGATAAAGCGGCACTTGACTCCAAAAGAATTACTAGCGATCAAAAACGCTGGTGTA
          ************************************************************
PBP3      CCAGGAGTAAATTTTGATGACGACATAAAGCGTATATATCCTCACAGTAATTTATTTTCA
Mut1234   CCAGGAGTAAATTTTGATGACGACATAAAGCGTATATATCCTCACAGTAATTTATTTTCA
          ************************************************************
PBP3      CACGTGCTTGGTTACACTGACATAGATGGCAATGGTATTGCAGGAGTTGAGGCGTATATA
Mut1234   CACGTGCTTGGTTACACTGACATAGATGGCAATGGTATTGCAGGAGTTGAGGCGTATATA
          ************************************************************
PBP3      AGTAAAAACAATGAGCAAGAAAAGCCCATAATACTATCCTTAGATACACGAGTGCAAAGC
Mut1234   AGTAAAAACAATGAGCAAGAAAAGCCCATAATACTATCCTTAGATACACGAGTGCAAAGC
          ************************************************************
PBP3      ATAGTGCATGAAGAGCTAACTAAAGCTGTAAGAAGATATCAGGCACTTGGCGGAGTAGGA
Mut1234   ATAGTGCATGAAGAGCTAACTAAAGCTGTAAGAAGATATCAGGCACTTGGCGGAGTAGGA
          ************************************************************
PBP3      ATTGTTTTAAATGTGAGAAATAGTGAAGTTATCTCGATGGTCAGCCTACCTGATTTTAAT
Mut1234   ATTGTTTTAAATGTGAGAAATAGTGAAGTTATCTCGATGGTCAGCCTACCTGATTTTAAT
          ************************************************************
```

```
PBP3      CCCAACTTACAGAATAAGGCAGAAGACGTACAAAAGTTTAATCGCGCCAGTCTTGGGGTA
Mut1234   CCCAACTTACAGAATAAGGCAGAAGACGTACAAAAGTTTAATCGCGCCAGTCTTGGGGTA
          ************************************************************
PBP3      TATGAGATGGGGTCGGTATTAAAATACTTTACAATAGCCGCAGCGCTTGATGCAAACGCT
Mut1234   TATGAGATGGGGGCGGTATTAAAATACTTTACAATAGCCGCAGCGCTTGATGCAAACGCT
          ************ ************************************************
PBP3      ACAAAAACTAGCGATTTATATGACGTATCAACACCAATCACCATCGGAAAGTATAAAATT
Mut1234   ACAAAAACTAGCGATTTATATGACGTATCAACACCAATCACCATCGGAAAGTATAAAATT
          ************************************************************
PBP3      CAGGATTTTCATAAATCTAAAATTCCAAAAATTACTGTGCAAGATATATTTGTAAAATCA
Mut1234   CAGGATTTTCATAAATCTAAAATTCCAAAAATTACTGTGCAAGATATATTTGTAAAATCA
          ************************************************************
PBP3      TCCAACATTGGTGCAGCAAAAATTGCAGTCAAACTAGGTATTGAAAAACAGGTAGAATAC
Mut1234   TCCAACATTGGTGCAGCAAAAATTGCAGTCAAACTAGGTATTGAAAAACAGGTAGAATAC
          ************************************************************
PBP3      TTTAAAGCTATGAAGCTATTTTCTCCTTTGAAAATAGAAATACCAGAAAAATCCACACCG
Mut1234   TTTAAAGCTATGAAGCTATTTGCGCCTTTGAAAATAGAAATACCAGAAAAATCCACACCG
          ********************* * ************************************
PBP3      ATAATCCCGGATAAATGGAGTGAAACCACTTTAATAACAGCATCTTATGGTTATGGCATA
Mut1234   ATAATCCCGGATAAATGGAGTGAAACCACTTTAATAACAGCATCTTATGGTTATGGCATA
          ************************************************************
PBP3      GCTGTAACTCCTATACATCTTGCACAAACTGCAGCAGCATTAATCAACAATGGGATATTT
Mut1234   GCTGTAACTCCTATACATCTTGCACAAACTGCAGCAGCATTAATCAACAATGGGATATTT
          ************************************************************
PBP3      CATAACGCAACCTTGATGTTGAATAAAAGAAGTATAGGAGAGCAAATTATCTCAAGAAGA
Mut1234   CATAACGCAACCTTGATGTTGAATAAAAGAAGTATAGGAGAGCAAATTATCTCAAGAAGA
          ************************************************************
PBP3      ACTTCCAGGGAAATGAGAAAATTATTACGTGCAGCAGTAACAGATGGCACTGGCAGAAAA
Mut1234   ACTTCCAGGGAAATGAGAAAATTATTACGTGCAGCAGTAACAGATGGCACTGGCAGAAAA
          ************************************************************
PBP3      GCAAAAATAAAGGCATATTCAATAGGAGGAAAAACTGGATCGGCGGAAAAAGTTGTAGAT
Mut1234   GCAAAAATAAAGGCATATTCAATAGGAGGAAAAACTGGAGCGGCGGAAAAAGTTGTAGAT
          ************************************ ************************
PBP3      GGTAAATATAGCAAAGATGCAAACATAGCATCATTTATAGGAGTGCTAACTATGCTTGAC
Mut1234   GGTAAATATAGCAAAGATGCAAACATAGCATCATTTATAGGAGTGCTAACTATGCTTGAC
          ************************************************************
PBP3      CCAAGGTACATAGTGCTAATTGCTATTGATGAGCCTCAAGGGATGCACCATACCGGGGGA
Mut1234   CCAAGGTACATAGTGCTAATTGCTATTGATGAGCCTCAAGGGATGCACCATACCGGGGGA
          ************************************************************
PBP3      ATAATTGCTGCGCCTATAGTAAAGAACATTATAAATAGAATAGCGCCTATACTAAATGTT
Mut1234   ATAATTGCTGCGCCTATAGTAAAGAACATTATAAATAGAATAGCGCCTATACTAAATGTT
          ************************************************************
PBP3      ACACCTGAGATGTAA-----------------------------
Mut1234   ACACCTGAGATGAGCGCTTGGAGCCACCCGCAGTTCGAAAAATAA
```

Supplementary Figure 15: Nucleic acid alignment of PBP3^{wMel} and cloned PBP3^{wMel} active site mutant S107A-S256A-S339A-S445A (Mut1234) in pASK-IBA2C. Mutated bases are highlighted gray.

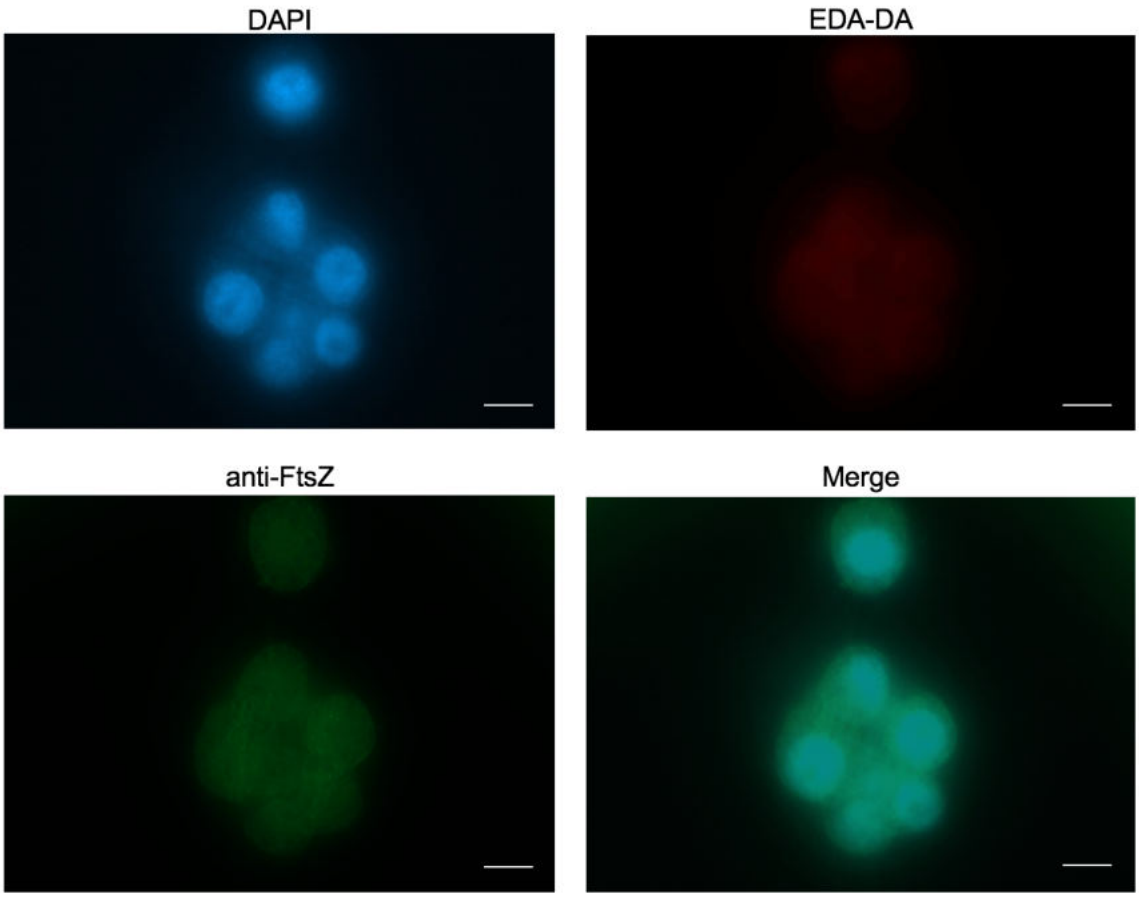

Supplementary Figure 16: C6/36 insect cells without *w*AlbB were incubated for 72 h in medium containing 1 mM of the dipeptide probe EDA-DA. Subsequent binding of the probe to an azide-modified Alexa Fluor 594 (red) was achieved by click chemistry. *Wolbachia* were stained with an anti-FtsZ antibody (green). DAPI (blue) was used for nuclear staining. Scale bar = 10 µm.

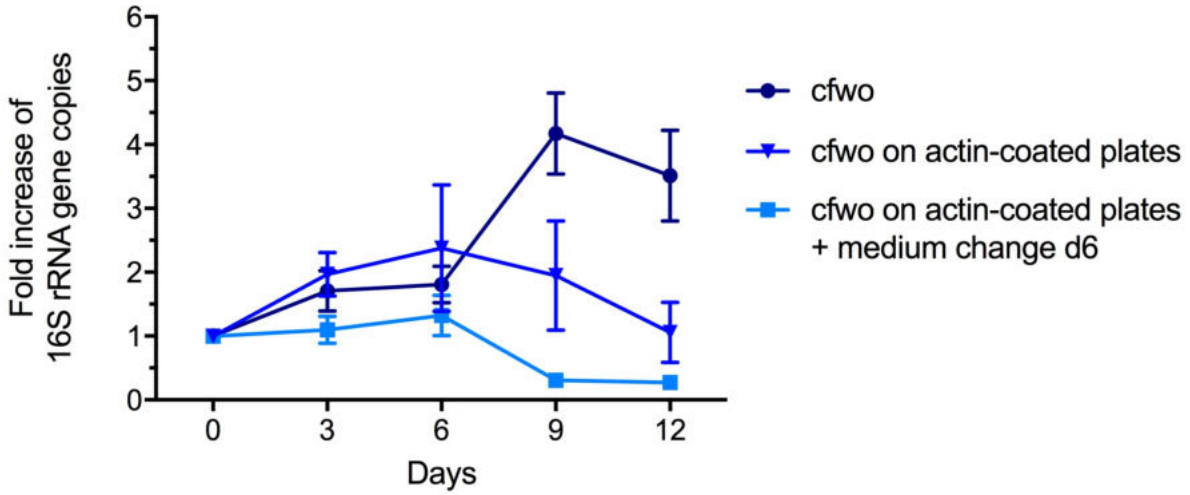

Supplementary Figure 17: Cell-free *w*AlbB growth on actin-coated streptavidin plates. Cell-free *Wolbachia* (cfwo) were incubated in growth medium either on untreated or actin-coated 96-well plates for twelve days. Growth was monitored every three days by qPCR and data were normalized to day 0 (X-axis). The graph is representative for two experiments. For every time point the mean ± SEM of six samples is shown.

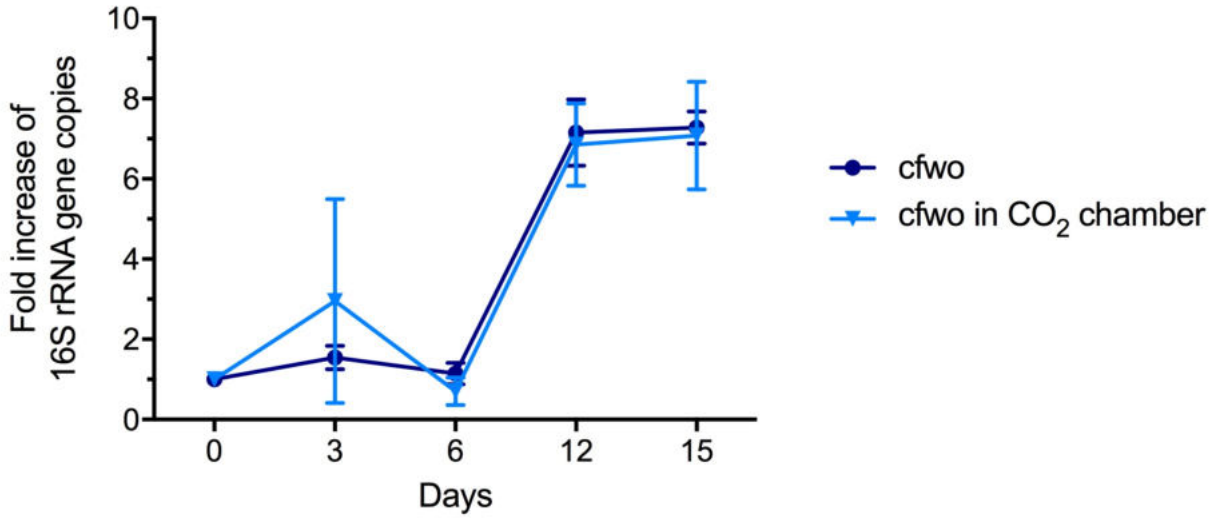

Supplementary Figure 18: Cell-free *w*AlbB growth in a lowered oxygen environment. Cell-free *Wolbachia* (cfwo) were incubated in growth medium under standard conditions or in a carbonic gas chamber for twelve days. Growth was monitored every three days by qPCR and data were normalized to day 0 (X-axis). The graph is representative for three experiments. For every time point the mean ± SEM of three samples is shown.

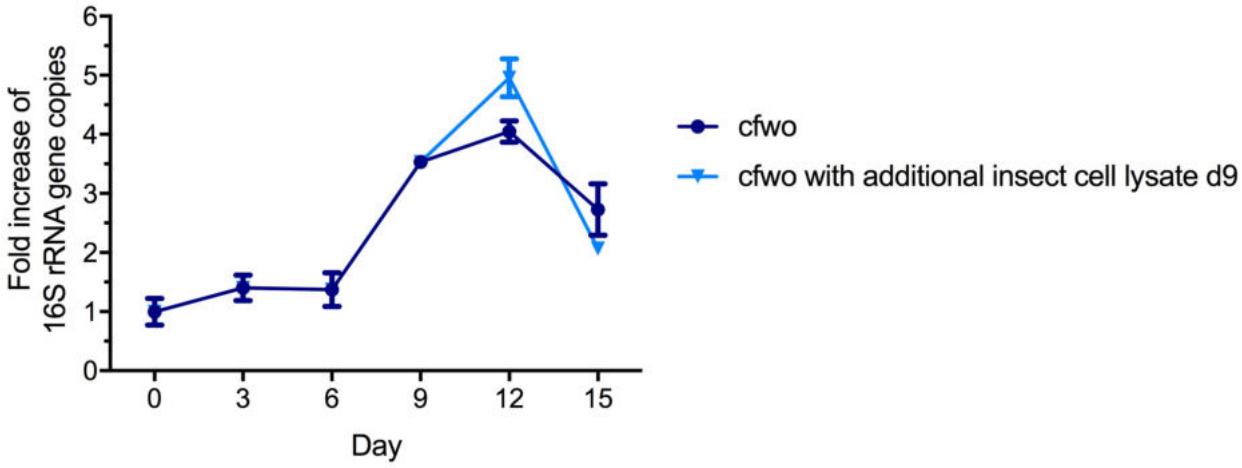

Supplementary Figure 19: Addition of fresh insect cell lysate to cell-free *w*AlbB. Cell-free *Wolbachia* (cfwo) were incubated in growth medium for twelve days. One culture was supplemented with additional cell lysate (equivalent to 0.95 x 10^6 uninfected C6/36 cells) after nine days (d9). Growth was monitored every three days by qPCR and data were normalized to day 0 (X-axis). The graph is representative for two experiments. For every time point the mean ± SEM of three samples is shown.

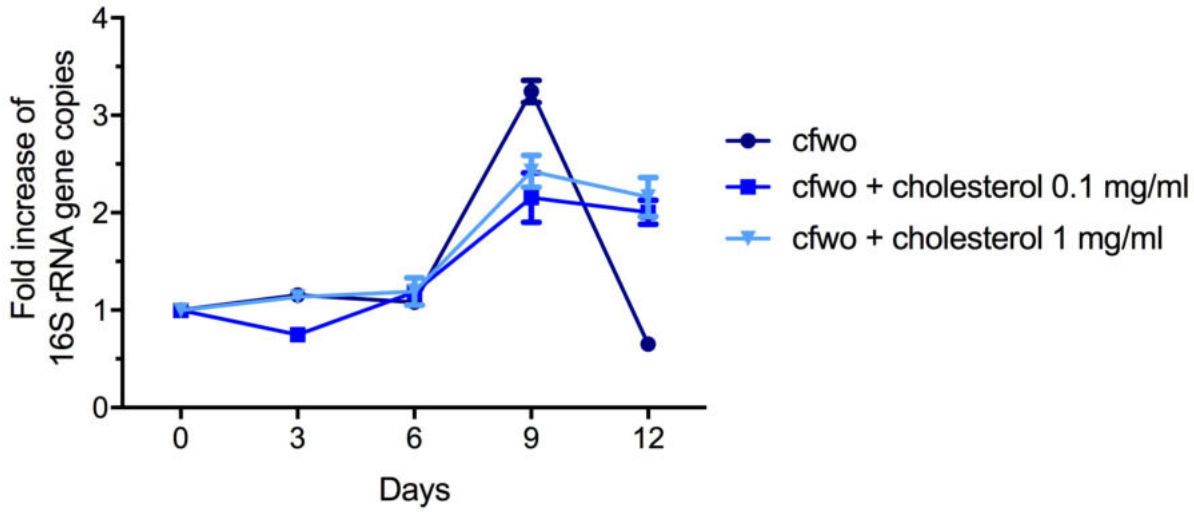

Supplementary Figure 20: Cell-free *Wolbachia* growth supplemented with cholesterol. Cell-free *Wolbachia* (cfwo) were incubated in growth medium for twelve days in the presence or absence of water-soluble cholesterol (0.1 or 1 mg/ml). Growth was monitored every three days by qPCR and data were normalized to day 0 (X-axis). The graph is representative for two experiments. For every time point the mean ± SEM of six samples is shown.

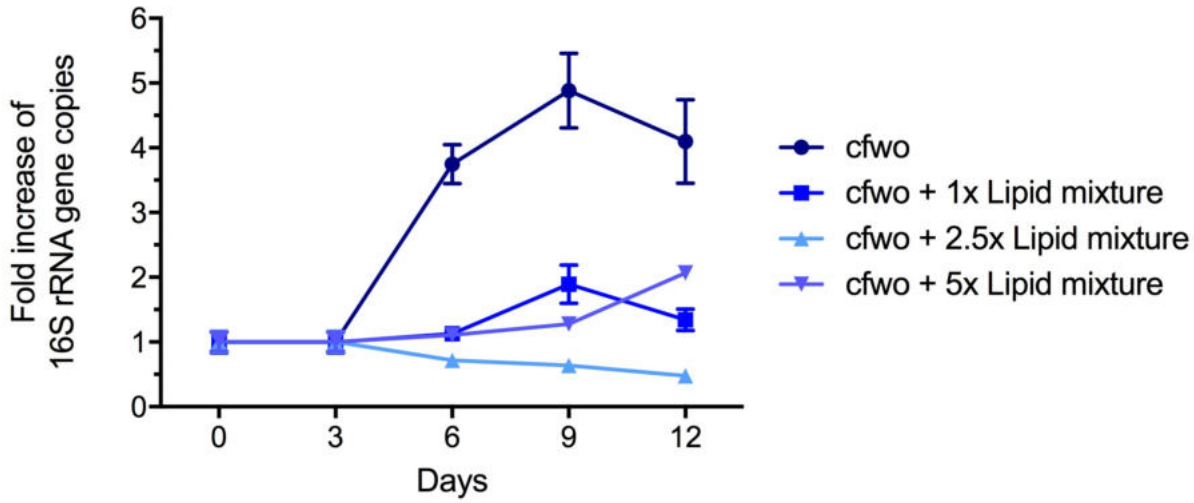

Supplementary Figure 21: Supplementation of culture medium with lipid mixture solution. Cell-free *Wolbachia* (cfwo) were incubated in growth medium for twelve days in the presence or absence of a lipid mixture solution (PeproTech). Growth was monitored every three days by qPCR and data were normalized to day 0 (X-axis). The experiment was performed once. For every time point the mean ± SEM of three samples is shown.

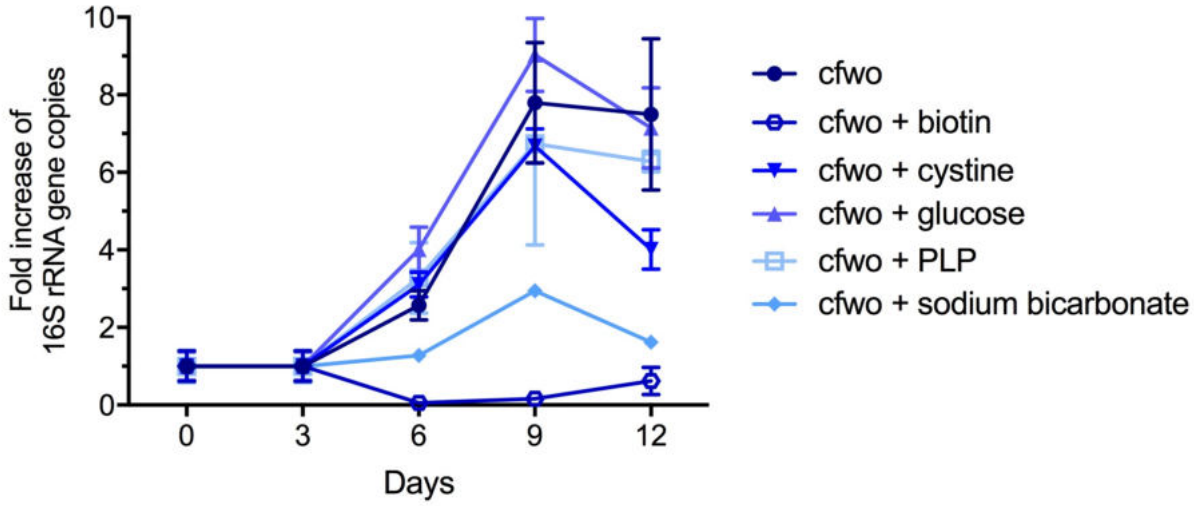

Supplementary Figure 22: Addition of supplements to the cell-free *w*AlbB culture medium. Cell-free *Wolbachia* (cfwo) were incubated in growth medium for twelve days in the presence or absence of biotin, cystine, glucose, PLP, sodium bicarbonate. Growth was monitored every three days by qPCR and data were normalized to day 0 (X-axis). The graph is representative for two experiments. For every time point the mean ± SEM of three samples is shown.

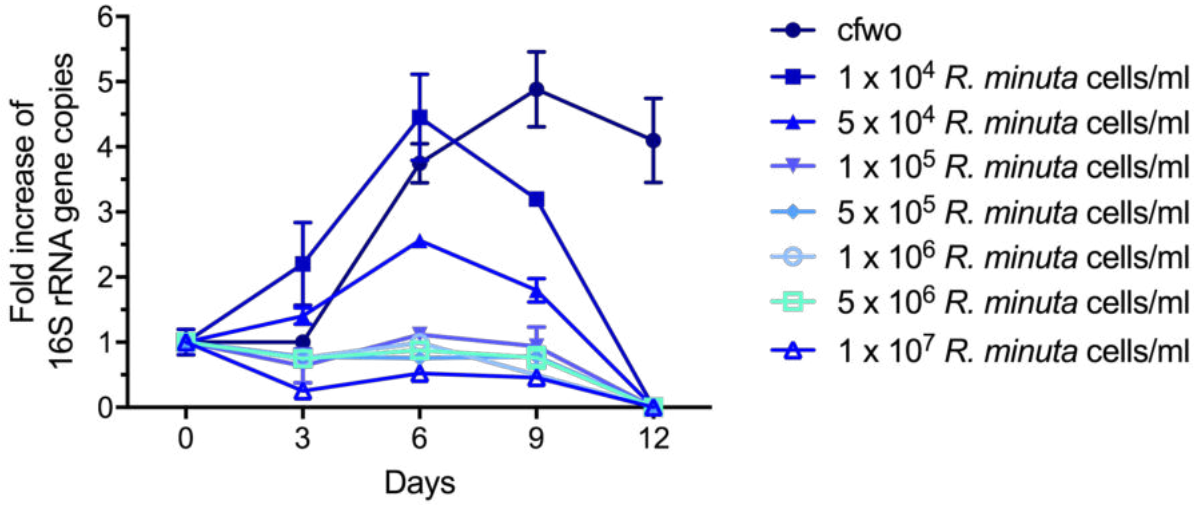

Supplementary Figure 23: Co-cultivation of *Rhodotorula minuta* and cell-free *w*AlbB. Cell-free *Wolbachia* (cfwo) were incubated in growth medium for twelve days in absence or presence of $1x10^4$-$1x10^7$ *Rhodotorula minuta* cells/ml. Growth was monitored every three days by qPCR and data were normalized to day 0 (X-axis). The experiment was performed once. For every time point the mean ± SEM of six samples is shown.

Literature

Adam, M., Damblon, C., Jamin, M., Zorzi, W., Dusart, V., Galleni, M., et al. (1991). Acyltransferase activities of the high-molecular-mass essential penicillin-binding proteins. Biochemical Journal 279(2), 601-604.

Ajendra, J., Specht, S., Ziewer, S., Schiefer, A., Pfarr, K., Parčina, M., et al. (2016). NOD2 dependent neutrophil recruitment is required for early protective immune responses against infectious *Litomosoides sigmodontis* L3 larvae. Scientific Reports 6.

Alm, R. A., Johnstone, M. R. and Lahiri, S. D. (2015). Characterization of *Escherichia coli* NDM isolates with decreased susceptibility to aztreonam/avibactam: role of a novel insertion in PBP3. Journal of Antimicrobial Chemotherapy 70(5), 1420-1428.

Anderson, J. S., Matsuhashi, M., Haskin, M. A. and Strominger, J. L. (1967). Biosynthesis of the peptidoglycan of bacterial cell walls II. Phospholipid carriers in the reaction sequence. Journal of Biological Chemistry 242(13), 3180-3190.

Atwal, S., Giengkam, S., Chaemchuen, S., Dorling, J., Kosaisawe, N., VanNieuwenhze, M., et al. (2017). Evidence for a peptidoglycan-like structure in *Orientia tsutsugamushi*. Molecular Microbiology 105(3), 440-452.

Awadzi, K. and Gilles, H. (1992). Diethylcarbamazine in the treatment of patients with onchocerciasis. British journal of clinical pharmacology 34(4), 281-288.

Bandi, C., Anderson, T. J., Genchi, C. and Blaxter, M. L. (1998). Phylogeny of *Wolbachia* in filarial nematodes. Proceedings of the Royal Society of London B: Biological Sciences 265(1413), 2407-2413.

Bandi, C., McCall, J. W., Genchi, C., Corona, S., Venco, L. and Sacchi, L. (1999). Effects of tetracycline on the filarial worms *Brugia pahangi* and *Dirofilaria immitis* and their bacterial endosymbionts *Wolbachia*. International Journal for Parasitology 29(2), 357-364.

Bandi, C., Trees, A. J. and Brattig, N. W. (2001). *Wolbachia* in filarial nematodes: evolutionary aspects and implications for the pathogenesis and treatment of filarial diseases. Veterinary Parasitology 98(1), 215-238.

Baquero, M.-R., Bouzon, M., Quintela, J. C., Ayala, J. A. and Moreno, F. (1996). DacD, an *Escherichia coli* gene encoding a novel penicillin-binding protein (PBP6b) with DD-carboxypeptidase activity. Journal of Bacteriology 178(24), 7106-7111.

Barrett, D., Leimkuhler, C., Chen, L., Walker, D., Kahne, D. and Walker, S. (2005). Kinetic characterization of the glycosyltransferase module of *Staphylococcus aureus* PBP2. Journal of Bacteriology 187(6), 2215-2217.

Beck, B. D. and Park, J. T. (1977). Basis for the observed fluctuation of carboxypeptidase II activity during the cell cycle in BUG 6, a temperature-sensitive division mutant of *Escherichia coli*. Journal of Bacteriology 130(3), 1292-1302.

Begg, K., Takasuga, A., Edwards, D., Dewar, S., Spratt, B., Adachi, H., et al. (1990). The balance between different peptidoglycan precursors determines whether *Escherichia coli* cells will elongate or divide. Journal of Bacteriology 172(12), 6697-6703.

Beier, D. and Gross, R. (2006). Regulation of bacterial virulence by two-component systems. Current Opinion in Microbiology 9(2), 143-152.

Bian, G., Xu, Y., Lu, P., Xie, Y. and Xi, Z. (2010). The endosymbiotic bacterium *Wolbachia* induces resistance to dengue virus in *Aedes aegypti*. PLoS Pathogens 6(4), e1000833.

Bird, A., el-Sheikh, H., Anderson, J. and Fuglsang, H. (1980). Changes in visual function and in the posterior segment of the eye during treatment of onchocerciasis with diethylcarbamazine citrate. British Journal of Ophthalmology 64(3), 191-200.

Boatin, B. A. and Richards, F. O. (2006). Control of onchocerciasis. Advances in Parasitology 61, 349-394.

Bockarie, M. J. and Deb, R. M. (2010). Elimination of lymphatic filariasis: do we have the drugs to complete the job? Current Opinion in Infectious Diseases 23(6), 617-620.

Born, P., Breukink, E. and Vollmer, W. (2006). *In vitro* synthesis of cross-linked murein and its attachment to sacculi by PBP1A from *Escherichia coli*. Journal of Biological Chemistry 281(37), 26985-26993.

Bos, M. P., Robert, V. and Tommassen, J. (2007). Biogenesis of the gram-negative bacterial outer membrane. Annual Review of Microbiology 61, 191-214.

Botta, G. A. and Park, J. T. (1981). Evidence for involvement of penicillin-binding protein 3 in murein synthesis during septation but not during cell elongation. Journal of Bacteriology 145(1), 333-340.

Bradford, M. M. (1976). A rapid and sensitive method for the quantitation of microgram quantities of protein utilizing the principle of protein-dye binding. Analytical Biochemistry 72(1-2), 248-254.

Brilli, M., Fondi, M., Fani, R., Mengoni, A., Ferri, L., Bazzicalupo, M., et al. (2010). The diversity and evolution of cell cycle regulation in alpha-proteobacteria: a comparative genomic analysis. BMC Systems Biology 4(1), 52.

Broadbent, A. D. (2001). Basic principles of textile coloration. Society of Dyers and Colorists West Yorkshire.

Buchon, N., Silverman, N. and Cherry, S. (2014). Immunity in *Drosophila melanogaster* from microbial recognition to whole-organism physiology. Nature Reviews Immunology 14(12), 796-810.

Bui, N. K., Gray, J., Schwarz, H., Schumann, P., Blanot, D. and Vollmer, W. (2009). The peptidoglycan sacculus of *Myxococcus xanthus* has unusual structural features and is degraded during glycerol-induced myxospore development. Journal of Bacteriology 191(2), 494-505.

Campbell, W. (2012). History of avermectin and ivermectin, with notes on the history of other macrocyclic lactone antiparasitic agents. Current Pharmaceutical Biotechnology 13(6), 853-865.

Caragata, E. P., Rancès, E., Hedges, L. M., Gofton, A. W., Johnson, K. N., O'Neill, S. L., et al. (2013). Dietary cholesterol modulates pathogen blocking by *Wolbachia*. PLoS Pathogens 9(6), e1003459.

Cheng, Z., Kumagai, Y., Lin, M., Zhang, C. and Rikihisa, Y. (2006). Intra-leukocyte expression of two-component systems in *Ehrlichia chaffeensis* and *Anaplasma phagocytophilum* and effects of the histidine kinase inhibitor closantel. Cellular microbiology 8(8), 1241-1252.

Cho, H., Wivagg, C. N., Kapoor, M., Barry, Z., Rohs, P. D., Suh, H., et al. (2016). Bacterial cell wall biogenesis is mediated by SEDS and PBP polymerase families functioning semi-autonomously. Nature Microbiology 1(10), 16172.

Cho, K.-O., Kim, G.-W. and Lee, O.-K. (2011). *Wolbachia* bacteria reside in host Golgi-related vesicles whose position is regulated by polarity proteins. PLoS One 6(7), e22703.

Chowdhury, C., Nayak, T. R., Young, K. D. and Ghosh, A. S. (2010). A weak DD-carboxypeptidase activity explains the inability of PBP 6 to substitute for PBP 5 in maintaining normal cell shape in *Escherichia coli*. FEMS Microbiology Letters 303(1), 76-83.

Christensen, S. and Serbus, L. R. (2015). Comparative analysis of *Wolbachia* genomes reveals streamlining and divergence of minimalist two-component systems. G3: Genes, Genomes, Genetics 5(5), 983-996.

Clare, R. H., Cook, D. A., Johnston, K. L., Ford, L., Ward, S. A. and Taylor, M. J. (2015). Development and validation of a high-throughput anti-*Wolbachia* whole-cell screen: a route to macrofilaricidal drugs against onchocerciasis and lymphatic filariasis. Journal of Biomolecular Screening 20(1), 64-69.

Clark, M. (2007). "*Wolbachia* symbiosis in arthropods," in *Wolbachia*: A bug's life in another bug. Karger Publishers, 90-123.

Cloud-Hansen, K. A., Peterson, S. B., Stabb, E. V., Goldman, W. E., McFall-Ngai, M. J. and Handelsman, J. (2006). Breaching the great wall: peptidoglycan and microbial interactions. Nature Reviews Microbiology 4(9), 710-716.

Cooper, M. A. (2006). Optical biosensors: where next and how soon? Drug Discovery Today 11(23), 1061-1067.

Crump, A. and Ōmura, S. (2011). Ivermectin, 'wonder drug' from Japan: the human use perspective. Proceedings of the Japan Academy, Series B 87(2), 13-28.

Dai, D. and Ishiguro, E. E. (1988). MurH, a new genetic locus in *Escherichia coli* involved in cell wall peptidoglycan biosynthesis. Journal of Bacteriology 170(5), 2197-2201.

Dai, K., Xu, Y. and Lutkenhaus, J. (1993). Cloning and characterization of ftsN, an essential cell division gene in *Escherichia coli* isolated as a multicopy suppressor of ftsA12 (Ts). Journal of Bacteriology 175(12), 3790-3797.

De Benedetti, S., Bühl, H., Gaballah, A., Klöckner, A., Otten, C., Schneider, T., et al. (2014). Characterization of serine hydroxymethyltransferase GlyA as a potential source of D-alanine in *Chlamydia pneumoniae*. Frontiers in Cellular and Infection Microbiology 4, 19.

Den Blaauwen, T., Aarsman, M. E., Vischer, N. O. and Nanninga, N. (2003). Penicillin-binding protein PBP2 of *Escherichia coli* localizes preferentially in the lateral wall and at mid-cell in comparison with the old cell pole. Molecular Microbiology 47(2), 539-547.

Den Blaauwen, T., De Pedro, M. A., Nguyen-Distèche, M. and Ayala, J. A. (2008). Morphogenesis of rod-shaped sacculi. FEMS Microbiology Reviews 32(2), 321-344.

Divakaruni, A. V., Loo, R. R. O., Xie, Y., Loo, J. A. and Gober, J. W. (2005). The cell-shape protein MreC interacts with extracytoplasmic proteins including cell wall assembly complexes in *Caulobacter crescentus*. Proceedings of the National Academy of Sciences of the United States of America 102(51), 18602-18607.

Dobson, S. L., Marsland, E. J., Veneti, Z., Bourtzis, K. and O'Neill, S. L. (2002). Characterization of *Wolbachia* host cell range via the *in vitro* establishment of infections. Applied and environmental microbiology 68(2), 656-660.

Dougherty, T. J. and Pucci, M. J. (2011). Antibiotic discovery and development. Springer Science & Business Media.

Dreyer, G., Noroes, J., Figueredo-Silva, J. and Piessens, W. (2000). Pathogenesis of lymphatic disease in bancroftian filariasis: a clinical perspective. Parasitology Today 16(12), 544-548.

Dutra, H. L. C., Rocha, M. N., Dias, F. B. S., Mansur, S. B., Caragata, E. P. and Moreira, L. A. (2016). *Wolbachia* blocks currently circulating zika virus isolates in brazilian *Aedes aegypti* mosquitoes. Cell Host & Microbe 19(6), 771-774.

Dziarski, R. and Gupta, D. (2006). The peptidoglycan recognition proteins (PGRPs). Genome Biology 7(8), 232.

Egan, A. J., Biboy, J., van't Veer, I., Breukink, E. and Vollmer, W. (2015). Activities and regulation of peptidoglycan synthases. Philosphical Transactions of the Royal Society B 370(1679), 20150031.

Egan, A. J., Jean, N. L., Koumoutsi, A., Bougault, C. M., Biboy, J., Sassine, J., et al. (2014). Outer-membrane lipoprotein LpoB spans the periplasm to stimulate the peptidoglycan synthase PBP1B. Proceedings of the National Academy of Sciences of the United States of America 111(22), 8197-8202.

Ermolaeva, M. A. and Schumacher, B. (2014). Insights from the worm: the *C. elegans* model for innate immunity. Seminars in Immunology 26(4), 303-309.

Fenollar, F., Maurin, M. and Raoult, D. (2003). *Wolbachia pipientis* growth kinetics and susceptibilities to 13 antibiotics determined by immunofluorescence staining and real-time PCR. Antimicrobial Agents and Chemotherapy 47(5), 1665-1671.

Ferree, P. M., Frydman, H. M., Li, J. M., Cao, J., Wieschaus, E. and Sullivan, W. (2005). *Wolbachia* utilizes host microtubules and dynein for anterior localization in the *Drosophila* oocyte. PLoS Pathogens 1(2), e14.

Fischer, P. U., King, C. L., Jacobson, J. A. and Weil, G. J. (2017). Potential value of triple drug therapy with ivermectin, diethylcarbamazine, and albendazole (IDA) to accelerate elimination of lymphatic filariasis and onchocerciasis in Africa. PLOS Neglected Tropical Diseases 11(1), e0005163.

Foltz, J. L., Makumbi, I., Sejvar, J. J., Malimbo, M., Ndyomugyenyi, R., Atai-Omoruto, A. D., et al. (2013). An epidemiologic investigation of potential risk factors for nodding syndrome in Kitgum District, Uganda. PloS One 8(6), e66419.

Foster, J., Ganatra, M., Kamal, I., Ware, J., Makarova, K., Ivanova, N., et al. (2005). The *Wolbachia* genome of *Brugia malayi*: endosymbiont evolution within a human pathogenic nematode. PLos Biology 3(4), e121.

Francis, H., Awadzi, K. and Ottesen, E. (1985). The Mazzotti reaction following treatment of onchocerciasis with diethylcarbamazine: clinical severity as a function of infection intensity. The American Journal of Tropical Medicine and Hygiene 34(3), 529-536.

Frydman, H. M., Li, J. M., Robson, D. N. and Wieschaus, E. (2006). Somatic stem cell niche tropism in *Wolbachia*. Nature 441(7092), 509.

Galán, J. E. and Cossart, P. (2005). Host–pathogen interactions: a diversity of themes, a variety of molecular machines. Current Opinion in Microbiology 8(1), 1-3.

Gallup, J. L. and Sachs, J. D. (2000). Agriculture, climate, and technology: why are the tropics falling behind? American Journal of Agricultural Economics 82(3), 731-737.

Gardon, J., Gardon-Wendel, N., Kamgno, J., Chippaux, J.-P. and Boussinesq, M. (1997). Serious reactions after mass treatment of onchocerciasis with ivermectin in an area endemic for *Loa loa* infection. The Lancet 350(9070), 18-22.

Geoghegan, V., Stainton, K., Rainey, S. M., Ant, T. H., Dowle, A. A., Larson, T., et al. (2017). Perturbed cholesterol and vesicular trafficking associated with dengue blocking in *Wolbachia*-infected *Aedes aegypti* cells. Nature Communications 8(1), 526. doi: 10.1038/s41467-017-00610-8.

Georgopapadakou, N., Smith, S. and Sykes, R. (1982). Mode of action of azthreonam. Antimicrobial Agents and Chemotherapy 21(6), 950-956.

Geraci, J. (1977). Vancomycin. Mayo Clinic Proceedings 52(10), 631-634.

Gerding, M. A., Ogata, Y., Pecora, N. D., Niki, H. and De Boer, P. A. (2007). The trans-envelope Tol–Pal complex is part of the cell division machinery and required for proper outer-membrane invagination during cell constriction in *E. coli*. Molecular Microbiology 63(4), 1008-1025.

Ghosh, A. S., Chowdhury, C. and Nelson, D. E. (2008). Physiological functions of D-alanine carboxypeptidases in *Escherichia coli*. Trends in Microbiology 16(7), 309-317.

Ghosh, B. and Sain, A. (2008). Origin of contractile force during cell division of bacteria. Physical Review Letters 101(17), 178101.

Ghuysen, J.-M. (1991). Serine beta-lactamases and penicillin-binding proteins. Annual Reviews in Microbiology 45(1), 37-67.

Glauner, B., Höltje, J. and Schwarz, U. (1988). The composition of the murein of *Escherichia coli*. Journal of Biological Chemistry 263(21), 10088-10095.

Godlewska, R., Wiśniewska, K., Pietras, Z. and Jagusztyn-Krynicka, E. K. (2009). Peptidoglycan-associated lipoprotein (Pal) of Gram-negative bacteria: function, structure, role in pathogenesis and potential application in immunoprophylaxis. FEMS Microbiology Letters 298(1), 1-11.

Goffin, C., Fraipont, C., Ayala, J., Terrak, M., Nguyen-Distèche, M. and Ghuysen, J.-M. (1996). The non-penicillin-binding module of the tripartite penicillin-binding protein 3 of *Escherichia coli* is required for folding and/or stability of the penicillin-binding module and the membrane-anchoring module confers cell septation activity on the folded structure. Journal of Bacteriology 178(18), 5402-5409.

Goffin, C. and Ghuysen, J.-M. (1998). Multimodular penicillin-binding proteins: an enigmatic family of orthologs and paralogs. Microbiology and Molecular Biology Reviews 62(4), 1079-1093.

Goffin, C. and Ghuysen, J.-M. (2002). Biochemistry and comparative genomics of SxxK superfamily acyltransferases offer a clue to the mycobacterial paradox: presence of penicillin-susceptible target proteins versus lack of efficiency of penicillin as therapeutic agent. Microbiology and molecular biology reviews 66(4), 702-738.

Gordon, A., Martin, A. and Synge, R. (1943). Partition chromatography in the study of protein constituents. Biochemical Journal 37(1), 79.

Gutzwiller, F., Carmo, C. R., Miller, D. E., Rice, D. W., Newton, I. L., Hawley, R. S., et al. (2015). Dynamics of *Wolbachia pipientis* gene expression across the *Drosophila melanogaster* life cycle. G3: Genes, Genomes, Genetics, g3. 115.021931.

Guzman, L.-M., Belin, D., Carson, M. J. and Beckwith, J. (1995). Tight regulation, modulation, and high-level expression by vectors containing the arabinose PBAD promoter. Journal of Bacteriology 177(14), 4121-4130.

Heidrich, C., Templin, M. F., Ursinus, A., Merdanovic, M., Berger, J., Schwarz, H., et al. (2001). Involvement of N-acetylmuramyl-L-alanine amidases in cell separation and antibiotic-induced autolysis of *Escherichia coli*. Molecular Microbiology 41(1), 167-178.

Henrichfreise, B., Brunke, M. and Viollier, P. H. (2016). Bacterial surfaces: the wall that SEDS built. Current Biology 26(21), 1158-1160.

Henrichfreise, B., Schiefer, A., Schneider, T., Nzukou, E., Poellinger, C., Hoffmann, T. J., et al. (2009). Functional conservation of the lipid II biosynthesis pathway in the cell wall-less bacteria

Chlamydia and *Wolbachia*: why is lipid II needed? Molecular Microbiology 73(5), 913-923. doi: 10.1111/j.1365-2958.2009.06815.x.

Hertig, M. (1936). The rickettsia, *Wolbachia pipientis* (gen. et sp. n.) and associated inclusions of the mosquito, *Culex pipiens*. Parasitology 28(4), 453-486.

Hertig, M. and Wolbach, S. B. (1924). Studies on rickettsia-like micro-organisms in insects. The Journal of Medical Research 44(3), 329.

Hise, A. G., Daehnel, K., Gillette-Ferguson, I., Cho, E., McGarry, H. F., Taylor, M. J., et al. (2007). Innate immune responses to endosymbiotic *Wolbachia* bacteria in *Brugia malayi* and *Onchocerca volvulus* are dependent on TLR2, TLR6, MyD88, and Mal, but not TLR4, TRIF, or TRAM. The Journal of Immunology 178(2), 1068-1076.

Hoerauf, A., Mand, S., Adjei, O., Fleischer, B. and Büttner, D. W. (2001). Depletion of *Wolbachia* endobacteria in *Onchocerca volvulus* by doxycycline and microfilaridermia after ivermectin treatment. The Lancet 357(9266), 1415-1416.

Hoerauf, A., Mand, S., Volkmann, L., Büttner, M., Marfo-Debrekyei, Y., Taylor, M., et al. (2003). Doxycycline in the treatment of human onchocerciasis: kinetics of *Wolbachia* endobacteria reduction and of inhibition of embryogenesis in female *Onchocerca* worms. Microbes and Infection 5(4), 261-273.

Hoerauf, A., Specht, S., Büttner, M., Pfarr, K., Mand, S., Fimmers, R., et al. (2008). *Wolbachia* endobacteria depletion by doxycycline as antifilarial therapy has macrofilaricidal activity in onchocerciasis: a randomized placebo-controlled study. Medical Microbiology and Immunology 197(3), 295-311.

Hoerauf, A., Volkmann, L., Hamelmann, C., Adjei, O., Autenrieth, I. B., Fleischer, B., et al. (2000). Endosymbiotic bacteria in worms as targets for a novel chemotherapy in filariasis. The Lancet 355(9211), 1242-1243.

Hoffmann, A., Montgomery, B., Popovici, J., Iturbe-Ormaetxe, I., Johnson, P., Muzzi, F., et al. (2011). Successful establishment of *Wolbachia* in *Aedes* populations to suppress dengue transmission. Nature 476(7361), 454-457.

Höltje, J.-V. (1998). Growth of the stress-bearing and shape-maintaining murein sacculus of *Escherichia coli*. Microbiology and Molecular Biology Reviews 62(1), 181-203.

Horvath, C. G. and Lipsky, S. (1966). Use of liquid ion exchange chromatography for the separation of organic compounds. Nature 211(5050), 748-749.

Hotez, P. J., Pecoul, B., Rijal, S., Boehme, C., Aksoy, S., Malecela, M., et al. (2016). Eliminating the neglected tropical diseases: translational science and new technologies. PLOS Neglected Tropical Diseases 10(3), e0003895.

Idro, R., Opar, B., Wamala, J., Abbo, C., Onzivua, S., Mwaka, D. A., et al. (2016). Is nodding syndrome an *Onchocerca volvulus*-induced neuroinflammatory disorder? Uganda's story of research in understanding the disease. International Journal of Infectious Diseases 45, 112-117.

Irazoqui, J. E., Urbach, J. M. and Ausubel, F. M. (2010). Evolution of host innate defence: insights from *Caenorhabditis elegans* and primitive invertebrates. Nature Reviews Immunology 10(1), 47-58.

Irschik, H., Jansen, R., Höfle, G., Gerth, K. and Reichenbach, H. (1985). The corallopyronins, new inhibitors of bacterial RNA synthesis from *Myxobacteria*. The Journal of Antibiotics 38(2), 145-152.

Jadaun, G. P. S., Dixit, S., Saklani, V., Mendiratta, S., Jain, R. and Singh, S. (2017). HPLC for peptides and proteins: principles, methods and applications. Pharmaceutical Methods 8(1).

Jeske, O., Schüler, M., Schumann, P., Schneider, A., Boedeker, C., Jogler, M., et al. (2015). *Planctomycetes* do possess a peptidoglycan cell wall. Nature Communications 6, 7116.

Jiggins, F. M. (2002). The rate of recombination in *Wolbachia* bacteria. Molecular Biology and Evolution 19(9), 1640-1643. doi: 10.1093/oxfordjournals.molbev.a004228.

Johnson, J. W., Fisher, J. F. and Mobashery, S. (2013). Bacterial cell-wall recycling. Annals of the New York Academy of Sciences 1277(1), 54-75.

Johnson, T. P., Tyagi, R., Lee, P. R., Lee, M.-H., Johnson, K. R., Kowalak, J., et al. (2017). Nodding syndrome may be an autoimmune reaction to the parasitic worm *Onchocerca volvulus*. Science Translational Medicine 9(377), eaaf6953.

Johnston, K. L., Wu, B., Guimarães, A., Ford, L., Slatko, B. E. and Taylor, M. J. (2010). Lipoprotein biosynthesis as a target for anti-*Wolbachia* treatment of filarial nematodes. Parasites & Vectors 3(1), 1.

Jones, L. J., Carballido-López, R. and Errington, J. (2001). Control of cell shape in bacteria: helical, actin-like filaments in *Bacillus subtilis*. Cell 104(6), 913-922.

Jones, R. N., Wilson, H., Novick, W., Barry, A. and Thornsberry, C. (1982). *In vitro* evaluation of CENTA, a new beta-lactamase-susceptible chromogenic cephalosporin reagent. Journal of Clinical Microbiology 15(5), 954-958.

Joseleau-Petit, D., Liébart, J.-C., Ayala, J. A. and D'Ari, R. (2007). Unstable *Escherichia coli* L forms revisited: growth requires peptidoglycan synthesis. Journal of Bacteriology 189(18), 6512-6520.

Jung, K., Fried, L., Behr, S. and Heermann, R. (2012). Histidine kinases and response regulators in networks. Current Opinion in Microbiology 15(2), 118-124.

Kamgno, J., Pion, S. D., Mackenzie, C. D., Thylefors, B. and Boussinesq, M. (2009). *Loa loa* microfilarial periodicity in ivermectin-treated patients: comparison between those developing and those free of serious adverse events. The American Journal of Tropical Medicine and Hygiene 81(6), 1056-1061.

Kang, L., Shaw, A. C., Xu, D., Xia, W., Zhang, J., Deng, J., et al. (2011). Upregulation of MetC is essential for D-alanine-independent growth of an alr/dadX-deficient *Escherichia coli* strain. Journal of Bacteriology 193(5), 1098-1106.

Karas, M., Bachmann, D., Bahr, U. e. and Hillenkamp, F. (1987). Matrix-assisted ultraviolet laser desorption of non-volatile compounds. International Journal of Mass Spectrometry and Ion Processes 78, 53-68.

Karlsson, R., Michaelsson, A. and Mattsson, L. (1991). Kinetic analysis of monoclonal antibody-antigen interactions with a new biosensor based analytical system. Journal of Immunological Methods 145(1-2), 229-240.

Katabarwa, M. N., Eyamba, A., Nwane, P., Enyong, P., Yaya, S., Baldiagaï, J., et al. (2011). Seventeen years of annual distribution of ivermectin has not interrupted onchocerciasis transmission in North Region, Cameroon. The American Journal of Tropical Medicine and Hygiene 85(6), 1041-1049.

Kawai, T. and Akira, S. (2007). Signaling to NF-κB by Toll-like receptors. Trends in Molecular Medicine 13(11), 460-469.

Kelly, J. A. and Kuzin, A. P. (1995). The refined crystallographic structure of a DD-peptidase penicillin-target enzyme at 1.6 Å resolution. Journal of Molecular Biology 254(2), 223-236.

Kerff, F., Petrella, S., Mercier, F., Sauvage, E., Herman, R., Pennartz, A., et al. (2010). Specific structural features of the N-acetylmuramoyl-L-alanine amidase AmiD from *Escherichia coli* and mechanistic implications for enzymes of this family. Journal of Molecular Biology 397(1), 249-259.

Khatri, V., Chauhan, N., Vishnoi, K., von Gegerfelt, A., Gittens, C. and Kalyanasundaram, R. (2018). Prospects of developing a prophylactic vaccine against human lymphatic filariasis–evaluation of protection in non-human primates. International Journal for Parasitology.

Kirby, W. (1977). Pharmacokinetics of fosfomycin. Chemotherapy 23(1), 141-151.

Klarmann-Schulz, U., Specht, S., Debrah, A. Y., Batsa, L., Ayisi-Boateng, N. K., Osei-Mensah, J., et al. (2017). Comparison of doxycycline, minocycline, doxycycline plus albendazole and albendazole alone in their efficacy against onchocerciasis in a randomized, open-label, pilot trial. PLOS Neglected Tropical Diseases 11(1), e0005156.

Klöckner, A., Otten, C., Derouaux, A., Vollmer, W., Bühl, H., De Benedetti, S., et al. (2014). AmiA is a penicillin target enzyme with dual activity in the intracellular pathogen *Chlamydia pneumoniae*. Nature Communications 5, 4201.

Komlan, K., Vossberg, P. S., Gantin, R. G., Solim, T., Korbmacher, F., Banla, M., et al. (2018). *Onchocerca volvulus* infection and serological prevalence, ocular onchocerciasis and parasite transmission in northern and central Togo after decades of *Simulium damnosum* sl vector control and mass drug administration of ivermectin. PLoS Neglected Tropical Diseases 12(3), e0006312.

Kozek, W. J. (1977). Transovarially-transmitted intracellular microorganisms in adult and larval stages of *Brugia malayi*. The Journal of Parasitology, 992-1000.

Laemmli, U. and Favre, M. (1970). SDS polyacrylamide gel electrophoresis. Nature 227, 680-682.

Landmann, F., Foster, J. M., Michalski, M. L., Slatko, B. E. and Sullivan, W. (2014). Co-evolution between an endosymbiont and its nematode host: *Wolbachia* asymmetric posterior localization and AP polarity establishment. PLoS Neglected Tropical Diseases 8(8), e3096.

Lee, J., Tattoli, I., Wojtal, K. A., Vavricka, S. R., Philpott, D. J. and Girardin, S. E. (2009). PH-dependent internalization of muramyl peptides from early endosomes enables Nod1 and Nod2 signaling. Journal of Biological Chemistry 284(35), 23818-23829.

Lehrer, R. I., Barton, A. and Ganz, T. (1988). Concurrent assessment of inner and outer membrane permeabilization and bacteriolysis in *E. coli* by multiple-wavelength spectrophotometry. Journal of Immunological Methods 108(1-2), 153-158.

Lentz, C. S., Halls, V., Hannam, J. S., Niebel, B., Strübing, U., Mayer, G., et al. (2013). A selective inhibitor of heme biosynthesis in endosymbiotic bacteria elicits antifilarial activity *in vitro*. Chemistry & Biology 20(2), 177-187.

LePage, D. and Bordenstein, S. R. (2013). *Wolbachia*: can we save lives with a great pandemic? Trends in Parasitology 29(8), 385-393.

Liechti, G., Kuru, E., Hall, E., Kalinda, A., Brun, Y., VanNieuwenhze, M., et al. (2014). A new metabolic cell-wall labelling method reveals peptidoglycan in *Chlamydia trachomatis*. Nature 506(7489), 507-510.

Lin, M. and Rikihisa, Y. (2003). *Ehrlichia chaffeensis* and *Anaplasma phagocytophilum* lack genes for lipid A biosynthesis and incorporate cholesterol for their survival. Infection and Immunity 71(9), 5324-5331.

Lindsey, A. R., Werren, J. H., Richards, S. and Stouthamer, R. (2016). Comparative genomics of a parthenogenesis-inducing *Wolbachia* symbiont. G3: Genes, Genomes, Genetics 6(7), 2113-2123.

Ling, L. L., Schneider, T., Peoples, A. J., Spoering, A. L., Engels, I., Conlon, B. P., et al. (2015). A new antibiotic kills pathogens without detectable resistance. Nature 517(7535), 455-459.

Louis, C. and Nigro, L. (1989). Ultrastructural evidence of *Wolbachia* rickettsiales in *Drosophila simulans* and their relationships with unidirectional cross-incompatibility. Journal of Invertebrate Pathology 54(1), 39-44.

Mackey, T. K., Liang, B. A., Cuomo, R., Hafen, R., Brouwer, K. C. and Lee, D. E. (2014). Emerging and reemerging neglected tropical diseases: a review of key characteristics, risk factors, and the policy and innovation environment. Clinical Microbiology Reviews 27(4), 949-979.

Makepeace, B. L., Rodgers, L. and Trees, A. J. (2006). Rate of elimination of *Wolbachia pipientis* by doxycycline in vitro increases following drug withdrawal. Antimicrobial Agents and Chemotherapy 50(3), 922-927.

Malanovic, N. and Lohner, K. (2016). Gram-positive bacterial cell envelopes: the impact on the activity of antimicrobial peptides. Biochimica et Biophysica Acta (BBA)-Biomembranes 1858(5), 936-946.

Mariner, K., McPhillie, M., Trowbridge, R., Smith, C., O'Neill, A. J., Fishwick, C. W., et al. (2011). Activity of and development of resistance to corallopyronin A, an inhibitor of RNA polymerase. Antimicrobial Agents and Chemotherapy 55(5), 2413-2416.

Markovski, M., Bohrhunter, J. L., Lupoli, T. J., Uehara, T., Walker, S., Kahne, D. E., et al. (2016). Cofactor bypass variants reveal a conformational control mechanism governing cell wall polymerase activity. Proceedings of the National Academy of Sciences 113(17), 4788-4793.

Mascher, T., Helmann, J. D. and Unden, G. (2006). Stimulus perception in bacterial signal-transducing histidine kinases. Microbiology and Molecular Biology Reviews 70(4), 910-938.

Massova, I. and Mobashery, S. (1998). Kinship and diversification of bacterial penicillin-binding proteins and β-lactamases. Antimicrobial Agents and Chemotherapy 42(1), 1-17.

McGarry, H. F., Egerton, G. L. and Taylor, M. J. (2004). Population dynamics of *Wolbachia* bacterial endosymbionts in *Brugia malayi*. Molecular and Biochemical Parasitology 135(1), 57-67.

McGraw, E., Merritt, D., Droller, J. and O'Neill, S. (2002). *Wolbachia* density and virulence attenuation after transfer into a novel host. Proceedings of the National Academy of Sciences of the United States of America 99(5), 2918-2923.

Meeske, A. J., Riley, E. P., Robins, W. P., Uehara, T., Mekelanos, J. J., Kahne, D., et al. (2016). SEDS proteins are a widespread family of bacterial cell wall polymerases. Nature 537(7622), 634-638.

Melnikow, E., Xu, S., Liu, J., Bell, A. J., Ghedin, E., Unnasch, T. R., et al. (2013). A potential role for the interaction of *Wolbachia* surface proteins with the *Brugia malayi* glycolytic enzymes and cytoskeleton in maintenance of endosymbiosis. PLoS Neglected Tropical Diseases 7(4), e2151.

Michalopoulos, A. S., Livaditis, I. G. and Gougoutas, V. (2011). The revival of fosfomycin. International Journal of Infectious Diseases 15(11), e732-e739.

Mirelman, D., Yashouv-Gan, Y. and Schwarz, U. (1977). Regulation of murein biosynthesis and septum formation in filamentous cells of *Escherichia coli* PAT 84. Journal of Bacteriology 129(3), 1593-1600.

Misra, S., Sharma, V. and Srivastava, A. K. (2015). Bacterial polysaccharides: an overview. Polysaccharides: Bioactivity and Biotechnology, 81-108.

Mitrophanov, A. Y. and Groisman, E. A. (2008). Signal integration in bacterial two-component regulatory systems. Genes & Development 22(19), 2601-2611.

Moreira, L. A., Iturbe-Ormaetxe, I., Jeffery, J. A., Lu, G., Pyke, A. T., Hedges, L. M., et al. (2009). A *Wolbachia* symbiont in *Aedes aegypti* limits infection with dengue, Chikungunya, and *Plasmodium*. Cell 139(7), 1268-1278.

Mueller-Langer, F. (2013). Neglected infectious diseases: are push and pull incentive mechanisms suitable for promoting drug development research? Health Economics, Policy and Law 8(02), 185-208.

Mullis, K., Faloona, F., Scharf, S., Saiki, R., Horn, G. and Erlich, H. (Year). "Specific enzymatic amplification of DNA i*n vitro*: the polymerase chain reaction", in: Cold Spring Harbor Symposia on Quantitative Biology: Cold Spring Harbor Laboratory Press), 263-273.

Myllymäki, H., Valanne, S. and Rämet, M. (2014). The *Drosophila* imd signaling pathway. The Journal of Immunology 192(8), 3455-3462.

Nelson, D. E. and Young, K. D. (2001). Contributions of PBP 5 and DD-carboxypeptidase penicillin binding proteins to maintenance of cell shape in *Escherichia coli*. Journal of Bacteriology 183(10), 3055-3064.

Nguyen, H. H., Park, J., Kang, S. and Kim, M. (2015). Surface plasmon resonance: a versatile technique for biosensor applications. Sensors 15(5), 10481-10510.

Nicola, G., Tomberg, J., Pratt, R., Nicholas, R. A. and Davies, C. (2010). Crystal structures of covalent complexes of β-lactam antibiotics with *Escherichia coli* penicillin-binding protein 5: toward an understanding of antibiotic specificity. Biochemistry 49(37), 8094-8104.

Noma, M., Nwoke, B., Nutall, I., Tambala, P., Enyong, P., Namsenmo, A., et al. (2013). Rapid epidemiological mapping of onchocerciasis (REMO): its application by the African Programme for Onchocerciasis Control (APOC). Pathogens and Global Health 96(Sup.1), S29-S39.

Noritaka, I., Nagai, K. and Wachi, M. (2002). Novel S-benzylisothiourea compound that induces spherical cells in *Escherichia coli* probably by acting on a rod-shape-determining protein(s) other than penicillin-binding protein 2. Bioscience, Biotechnology, and Biochemistry 66(12), 2658-2662.

O'Neill, S., M Pettigrew, M., Sinkins, S., Braig, H., Andreadis, T. and Tesh, R. (1997). *In vitro* cultivation of *Wolbachia pipientis* in an *Aedes albopictus* cell line. Insect Molecular Biology 6(1), 33-39.

Olrichs, N. K. (2010). Bugging the cell wall of bacteria: novel insights into the biosynthesis of peptidoglycan and its inhibition. Dissertation, Utrecht University.

Omsland, A., Cockrell, D. C., Howe, D., Fischer, E. R., Virtaneva, K., Sturdevant, D. E., et al. (2009). Host cell-free growth of the Q fever bacterium *Coxiella burnetii*. Proceedings of the National Academy of Sciences of the United States of America 106(11), 4430-4434.

Ōmura, S. and Crump, A. (2004). The life and times of ivermectin—a success story. Nature Reviews Microbiology 2(12), 984-989.

Osei-Atweneboana, M. Y., Awadzi, K., Attah, S. K., Boakye, D. A., Gyapong, J. O. and Prichard, R. K. (2011). Phenotypic evidence of emerging ivermectin resistance in *Onchocerca volvulus*. PLoS Negl Trop Dis 5(3), e998.

Otten, C., Brilli, M., Vollmer, W., Viollier, P. H. and Salje, J. (2017). Peptidoglycan in obligate intracellular bacteria. Molecular Microbiology.

Otten, C., De Benedetti, S., Gaballah, A., Bühl, H., Klöckner, A., Brauner, J., et al. (2015). Co-Solvents as stabilizing agents during heterologous overexpression in *Escherichia coli*–application to chlamydial penicillin-binding protein 6. PloS one 10(4), e0122110.

Otten, C. F. (2014). Processing of the cell wall precursor lipid II in *Chlamydia pneumoniae*. Dissertation, University of Bonn.

Ottesen, E. A. (2000). Editorial: the global programme to eliminate lymphatic filariasis. Tropical Medicine & International Health 5(9), 591-594.

Ouellette, S. P., Karimova, G., Subtil, A. and Ladant, D. (2012). *Chlamydia* co-opts the rod shape-determining proteins MreB and Pbp2 for cell division. Molecular Microbiology 85(1), 164-178.

Paradis-Bleau, C., Markovski, M., Uehara, T., Lupoli, T. J., Walker, S., Kahne, D. E., et al. (2010). Lipoprotein cofactors located in the outer membrane activate bacterial cell wall polymerases. Cell 143(7), 1110-1120.

Park, J. T. and Uehara, T. (2008). How bacteria consume their own exoskeletons (turnover and recycling of cell wall peptidoglycan). Microbiology and Molecular Biology Reviews 72(2), 211-227.

Parsons, L. M., Lin, F. and Orban, J. (2006). Peptidoglycan recognition by Pal, an outer membrane lipoprotein. Biochemistry 45(7), 2122-2128.

Pennartz, A., Généreux, C., Parquet, C., Mengin-Lecreulx, D. and Joris, B. (2009). Substrate-induced inactivation of the *Escherichia coli* AmiD N-acetylmuramoyl-L-alanine amidase highlights a new strategy to inhibit this class of enzyme. Antimicrobial Agents and Chemotherapy 53(7), 2991-2997.

Peters, K., Kannan, S., Rao, V. A., Biboy, J., Vollmer, D., Erickson, S. W., et al. (2016). The redundancy of peptidoglycan carboxypeptidases ensures robust cell shape maintenance in *Escherichia coli*. mBio 7(3), e00819-00816.

Pfarr, K., Debrah, A., Specht, S. and Hoerauf, A. (2009). Filariasis and lymphoedema. Parasite Immunology 31(11), 664-672.

Phaff, H., Mrak, E. and Williams, O. (1952). Yeasts isolated from shrimp. Mycologia 44(4), 431-451.

Pham, K., LaForge, K. and Kreek, M. (1998). Sticky-end PCR: new method for subcloning. Biotechniques 25, 206-208.

Pilhofer, M., Aistleitner, K., Biboy, J., Gray, J., Kuru, E., Hall, E., et al. (2013). Discovery of chlamydial peptidoglycan reveals bacteria with murein sacculi but without FtsZ. Nature Communications 4, 2856.

Pinho, M. G. and Errington, J. (2005). Recruitment of penicillin-binding protein PBP2 to the division site of *Staphylococcus aureus* is dependent on its transpeptidation substrates. Molecular Microbiology 55(3), 799-807.

Pisabarro, A. G., Prats, R. A., Vaquez, D. and Rodríguez-Tébar, A. (1986). Activity of penicillin-binding protein 3 from *Escherichia coli*. Journal of Bacteriology 168(1), 199-206.

Ramaiah, K. and Ottesen, E. A. (2014). Progress and impact of 13 years of the global programme to eliminate lymphatic filariasis on reducing the burden of filarial disease. PLOS Neglected Tropical Diseases 8(11), e3319.

Rasgon, J. L., Gamston, C. E. and Ren, X. (2006). Survival of *Wolbachia pipientis* in cell-free medium. Applied and Environmental Microbiology 72(11), 6934-6937. doi: 10.1128/AEM.01673-06

Rebollo, M. P. and Bockarie, M. J. (2014). Shrinking the lymphatic filariasis map: update on diagnostic tools for mapping and transmission monitoring. Parasitology 141(14), 1912-1917.

Reed, S. C., Lamason, R. L., Risca, V. I., Abernathy, E. and Welch, M. D. (2014). *Rickettsia* actin-based motility occurs in distinct phases mediated by different actin nucleators. Current Biology 24(1), 98-103.

Renart, J., Reiser, J. and Stark, G. R. (1979). Transfer of proteins from gels to diazobenzyloxymethyl-paper and detection with antisera: a method for studying antibody specificity and antigen structure. Proceedings of the National Academy of Sciences 76(7), 3116-3120.

Rick, P. D., Hubbard, G. L., Kitaoka, M., Nagaki, H., Kinoshita, T., Dowd, S., et al. (1998). Characterization of the lipid-carrier involved in the synthesis of enterobacterial common antigen (ECA) and identification of a novel phosphoglyceride in a mutant of *Salmonella typhimurium* defective in ECA synthesis. Glycobiology 8(6), 557-567.

Ritzmann, N. (2016). Functional characterization of a putative metallo-beta-lactamase and the penicillin-binding- proteins PBP6a from *Wolbachia* endosymbiont of *Brugia malayi* (*w*Bm) and

PBP3 from *Wolbachia* endosymbiont of *Drosophila melanogaster* (*w*Mel). Master thesis, University of Bonn.

Rolls, M. M., Marquardt, M. T., Kielian, M. and Machamer, C. E. (1997). Cholesterol-independent targeting of Golgi membrane proteins in insect cells. Molecular Biology of the Cell 8(11), 2111-2118.

Rouser, G., Fleischer, S. and Yamamoto, A. (1970). Two dimensional thin layer chromatographic separation of polar lipids and determination of phospholipids by phosphorus analysis of spots. Lipids 5(5), 494-496.

Ruang-Areerate, T., Kittayapong, P., McGraw, E. A., Baimai, V. and O'Neill, S. L. (2004). *Wolbachia* replication and host cell division in *Aedes albopictus*. Current Microbiology 49(1), 10-12.

Ruiz, N. (2016). Filling holes in peptidoglycan biogenesis of *Escherichia coli*. Current Opinion in Microbiology 34, 1-6.

Rusche, J. R. and Howard-Flanders, P. (1985). Hexamine cobalt chloride promotes intermolecular ligation of blunt end DNA fragments by T4 DNA ligase. Nucleic acids research 13(6), 1997-2008.

Sahl, H.-G. and Brandis, H. (1981). Production, purification and chemical properties of an antistaphylococcal agent produced by *Staphylococcus* epidermidis. Microbiology 127(2), 377-384.

Saint André, A. v., Blackwell, N. M., Hall, L. R., Hoerauf, A., Brattig, N. W., Volkmann, L., et al. (2002). The role of endosymbiotic *Wolbachia* bacteria in the pathogenesis of river blindness. Science 295(5561), 1892-1895.

Sambrook, J., Fritsch, E. F. and Maniatis, T. (1989). Molecular cloning. Cold spring harbor laboratory press New York.

Sangoro, O., Kelly, A. H., Mtali, S. and Moore, S. J. (2014). Feasibility of repellent use in a context of increasing outdoor transmission: a qualitative study in rural Tanzania. Malaria journal 13(1), 1.

Sarkar, P., Yarlagadda, V., Ghosh, C. and Haldar, J. (2017). A review on cell wall synthesis inhibitors with an emphasis on glycopeptide antibiotics. MedChemComm 8(3), 516-533.

Sarkar, S. K., Dutta, M., Chowdhury, C., Kumar, A. and Ghosh, A. S. (2011). PBP5, PBP6 and DacD play different roles in intrinsic β-lactam resistance of *Escherichia coli*. Microbiology 157(9), 2702-2707.

Sauvage, E., Kerff, F., Terrak, M., Ayala, J. A. and Charlier, P. (2008). The penicillin-binding proteins: structure and role in peptidoglycan biosynthesis. FEMS Microbiology Reviews 32(2), 234-258.

Sauvage, E. and Terrak, M. (2016). Glycosyltransferases and transpeptidases/penicillin-binding proteins: valuable targets for new antibacterials. Antibiotics 5(1), 12.

Schäberle, T. F., Schiefer, A., Schmitz, A., König, G. M., Hoerauf, A. and Pfarr, K. (2014). Corallopyronin A – A promising antibiotic for treatment of filariasis. International Journal of Medical Microbiology 304(1), 72-78.

Scheffers, D.-J. and Pinho, M. G. (2005). Bacterial cell wall synthesis: new insights from localization studies. Microbiology and Molecular Biology Reviews 69(4), 585-607.

Schiefer, A., Schmitz, A., Schäberle, T. F., Specht, S., Lämmer, C., Johnston, K. L., et al. (2012). Corallopyronin A specifically targets and depletes essential obligate *Wolbachia* endobacteria from filarial nematodes *in vivo*. Journal of Infectious Diseases 206(2), 249-257.

Schneider, T. and Sahl, H.-G. (2010). An oldie but a goodie–cell wall biosynthesis as antibiotic target pathway. International Journal of Medical Microbiology 300(2), 161-169.

Schneider, T., Senn, M. M., Berger-Bächi, B., Tossi, A., Sahl, H. G. and Wiedemann, I. (2004). *In vitro* assembly of a complete, pentaglycine interpeptide bridge containing cell wall precursor (lipid II-Gly5) of *Staphylococcus aureus*. Molecular Microbiology 53(2), 675-685.

Schwechheimer, C. and Kuehn, M. J. (2015). Outer-membrane vesicles from Gram-negative bacteria: biogenesis and functions. Nature Reviews Microbiology 13(10), 605-619.

Sironi, M., Bandi, C., Sacchi, L., Di Sacco, B., Damiani, G. and Genchi, C. (1995). Molecular evidence for a close relative of the arthropod endosymbiont *Wolbachia* in a filarial worm. Molecular and Biochemical Parasitology 74(2), 223-227.

Slatko, B. E., Luck, A. N., Dobson, S. L. and Foster, J. M. (2014). *Wolbachia* endosymbionts and human disease control. Molecular and Biochemical Parasitology 195(2), 88-95.

Slatko, B. E., Taylor, M. J. and Foster, J. M. (2010). The *Wolbachia* endosymbiont as an anti-filarial nematode target. Symbiosis 51(1), 55-65.

Smith, H. L., Paciorkowski, N., Babu, S. and Rajan, T. (2000). Development of a serum-free system for the *in vitro* cultivation of *Brugia malayi* infective-stage larvae. Experimental Parasitology 95(4), 253-264.

Smith, J. D., Kumarasiri, M., Zhang, W., Hesek, D., Lee, M., Toth, M., et al. (2013). Structural analysis of the role of *Pseudomonas aeruginosa* penicillin-binding protein 5 in β-lactam resistance. Antimicrobial Agents and Chemotherapy 57(7), 3137-3146.

Smits, H. L. (2009). Prospects for the control of neglected tropical diseases by mass drug administration. Expert Review of Anti-Infective Therapy 7(1), 37-56.

Souza Santos, M. and Orth, K. (2015). Subversion of the cytoskeleton by intracellular bacteria: lessons from *Listeria*, *Salmonella* and *Vibrio*. Cellular Microbiology 17(2), 164-173.

Specht, S., Mand, S., Marfo-Debrekyei, Y., Debrah, A. Y., Konadu, P., Adjei, O., et al. (2008). Efficacy of 2- and 4-week rifampicin treatment on the *Wolbachia* of *Onchocerca volvulus*. Parasitology Research 103(6), 1303-1309.

Spratt, B. G. and Pardee, A. B. (1975). Penicillin-binding proteins and cell shape in *E. coli*. Nature 254(5500), 516.

Stenbak, C. R., Ryu, J.-H., Leulier, F., Pili-Floury, S., Parquet, C., Hervé, M., et al. (2004). Peptidoglycan molecular requirements allowing detection by the *Drosophila* immune deficiency pathway. The Journal of Immunology 173(12), 7339-7348.

Stock, A. M., Robinson, V. L. and Goudreau, P. N. (2000). Two-component signal transduction. Annual Review of Biochemistry 69(1), 183-215.

Suginaka, H., Blumberg, P. M. and Strominger, J. L. (1972). Multiple penicillin-binding components in *Bacillus subtilis*, *Bacillus cereus*, *Staphylococcus aureus*, and *Escherichia coli*. Journal of Biological Chemistry 247(17), 5279-5288.

Taheri-Araghi, S., Bradde, S., Sauls, J. T., Hill, N. S., Levin, P. A., Paulsson, J., et al. (2015). Cell-size control and homeostasis in bacteria. Current Biology 25(3), 385-391.

Tamarozzi, F., Halliday, A., Gentil, K., Hoerauf, A., Pearlman, E. and Taylor, M. J. (2011). Onchocerciasis: the role of *Wolbachia* bacterial endosymbionts in parasite biology, disease pathogenesis, and treatment. Clinical Microbiology Reviews 24(3), 459-468.

Tambo, E., Khater, E. I., Chen, J.-H., Bergquist, R. and Zhou, X.-N. (2015). Nobel prize for the artemisinin and ivermectin discoveries: a great boost towards elimination of the global infectious diseases of poverty. Infectious Diseases of Poverty 4(1), 1.

Taylor, M. and Hoerauf, A. (1999). *Wolbachia* bacteria of filarial nematodes. Parasitology Today 15(11), 437-442.

Taylor, M. J., Ford, L., Hoerauf, A., Pfarr, K., Foster, J. M., Kumar, S., et al. (2012). Drugs and targets to perturb the symbiosis of *Wolbachia* and filarial nematodes. Parasitic Helminths: Targets, Screens, Drugs and Vaccines, 251-265.

Taylor, M. J., Hoerauf, A. and Bockarie, M. (2010). Lymphatic filariasis and onchocerciasis. The Lancet 376(9747), 1175-1185.

Taylor, M. J., Hoerauf, A., Townson, S., Slatko, B. E. and Ward, S. A. (2014). Anti-*Wolbachia* drug discovery and development: safe macrofilaricides for onchocerciasis and lymphatic filariasis. Parasitology 141(1), 119-127.

Taylor, M. J., Voronin, D., Johnston, K. L. and Ford, L. (2013). *Wolbachia* filarial interactions. Cellular Microbiology 15(4), 520-526.

Thomsen, E. K., Sanuku, N., Baea, M., Satofan, S., Maki, E., Lombore, B., et al. (2015). Efficacy, safety, and pharmacokinetics of co-administered diethylcarbamazine, albendazole, and ivermectin for the treatment of bancroftian filariasis. Clinical Infectious Diseases 62(3), 334-341.

Tisch, D. J., Michael, E. and Kazura, J. W. (2005). Mass chemotherapy options to control lymphatic filariasis: a systematic review. The Lancet Infectious Diseases 5(8), 514-523.

Tram, U., Ferree, P. M. and Sullivan, W. (2003). Identification of *Wolbachia*–host interacting factors through cytological analysis. Microbes and Infection 5(11), 999-1011.

Turner, J. D., Langley, R. S., Johnston, K. L., Egerton, G., Wanji, S. and Taylor, M. J. (2006). *Wolbachia* endosymbiotic bacteria of *Brugia malayi* mediate macrophage tolerance to TLR-and CD40-

specific stimuli in a MyD88/TLR2-dependent manner. The Journal of Immunology 177(2), 1240-1249.

Turner, J. D., Langley, R. S., Johnston, K. L., Gentil, K., Ford, L., Wu, B., et al. (2009). *Wolbachia* lipoprotein stimulates innate and adaptive immunity through Toll-like receptors 2 and 6 to induce disease manifestations of filariasis. Journal of Biological Chemistry 284(33), 22364-22378.

Turusov, V., Rakitsky, V. and Tomatis, L. (2002). Dichlorodiphenyltrichloroethane (DDT): ubiquity, persistence, and risks. Environmental Health Perspectives 110(2), 125.

Typas, A., Banzhaf, M., Gross, C. A. and Vollmer, W. (2012). From the regulation of peptidoglycan synthesis to bacterial growth and morphology. Nature Reviews Microbiology 10(2), 123-136.

Typas, A., Banzhaf, M., van Saparoea, B. v. d. B., Verheul, J., Biboy, J., Nichols, R. J., et al. (2010). Regulation of peptidoglycan synthesis by outer-membrane proteins. Cell 143(7), 1097-1109.

Uehara, T. and Park, J. T. (2007). An anhydro-N-acetylmuramyl-L-alanine amidase with broad specificity tethered to the outer membrane of *Escherichia coli*. Journal of Bacteriology 189(15), 5634-5641.

Uehara, T., Parzych, K. R., Dinh, T. and Bernhardt, T. G. (2010). Daughter cell separation is controlled by cytokinetic ring-activated cell wall hydrolysis. The EMBO Journal 29(8), 1412-1422.

UN (2015). Sixty-ninth session of the United National General Assembly: Draft outcome document of the United Nations summit for the adoption of the post-2015 development agenda. Available: http://www.un.org/ga/search/view_doc.asp?symbol=A/69/L.85&Lang=E [Online].[Accessed 02.05.2018].

Uribe-Alvarez, C., Chiquete-Félix, N., Morales-García, L., Bohórquez-Hernández, A., Delgado-Buenrostro, N. L., Vaca, L., et al. (2018). *Wolbachia pipientis* grows in *Saccharomyces cerevisiae* evoking early death of the host and deregulation of mitochondrial metabolism. MicrobiologyOpen, e00675.

Van der Linden, M., De Haan, L., Hoyer, M. and Keck, W. (1992). Possible role of *Escherichia coli* penicillin-binding protein 6 in stabilization of stationary-phase peptidoglycan. Journal of Bacteriology 174(23), 7572-7578.

Van Heijenoort, J. (2011). Peptidoglycan hydrolases of *Escherichia coli*. Microbiology and Molecular Biology Reviews 75(4), 636-663.

Van Teeseling, M. C., Mesman, R. J., Kuru, E., Espaillat, A., Cava, F., Brun, Y. V., et al. (2015). Anammox planctomycetes have a peptidoglycan cell wall. Nature Communications 6, 6878.

Volkmann, L., Fischer, K., Taylor, M. and Hoerauf, A. (2003). Antibiotic therapy in murine filariasis (*Litomosoides sigmodontis*): comparative effects of doxycycline and rifampicin on *Wolbachia* and filarial viability. Tropical Medicine & International Health 8(5), 392-401.

Vollmer, J. (2012). *Wolbachia*, endosymbionts of arthropods and filarial nematodes: requirement of cell wall biosynthesis for cell division and replication in a host cell-free culture. Dissertation, University of Bonn.

Vollmer, J., Schiefer, A., Schneider, T., Jülicher, K., Johnston, K. L., Taylor, M. J., et al. (2013). Requirement of lipid II biosynthesis for cell division in cell wall-less *Wolbachia*, endobacteria of arthropods and filarial nematodes. International Journal of Medical Microbiology 303(3), 140-149.

Vollmer, W., Joris, B., Charlier, P. and Foster, S. (2008). Bacterial peptidoglycan (murein) hydrolases. FEMS Microbiology Reviews 32(2), 259-286.

Voronin, D., Bachu, S., Shlossman, M., Unnasch, T. R., Ghedin, E. and Lustigman, S. (2016). Glucose and glycogen metabolism in *Brugia malayi* Is associated with *Wolbachia* symbiont fitness. PloS One 11(4), e0153812.

Voronin, D., Guimarães, A. F., Molyneux, G. R., Johnston, K. L., Ford, L. and Taylor, M. J. (2014). *Wolbachia* lipoproteins: abundance, localisation and serology of *Wolbachia* peptidoglycan associated lipoprotein and the Type IV Secretion System component, VirB6 from *Brugia malayi* and *Aedes albopictus*. Parasites & Vectors 7(1), 1.

Walker, M., Specht, S., Churcher, T. S., Hoerauf, A., Taylor, M. J. and Basáñez, M.-G. (2015). Therapeutic efficacy and macrofilaricidal activity of doxycycline for the treatment of river blindness. Clinical Infectious Diseases 60(8), 1199-1207.

Wass, M. N., Kelley, L. A. and Sternberg, M. J. (2010). 3DLigandSite: predicting ligand-binding sites using similar structures. Nucleic Acids Research 38(Suppl 2), W469-W473.

Weiss, D. S., Chen, J. C., Ghigo, J.-M., Boyd, D. and Beckwith, J. (1999). Localization of FtsI (PBP3) to the septal ring requires its membrane anchor, the Z ring, FtsA, FtsQ, and FtsL. Journal of Bacteriology 181(2), 508-520.

Weiss, D. S., Pogliano, K., Carson, M., Guzman, L. M., Fraipont, C., Nguyen-Distèche, M., et al. (1997). Localization of the *Escherichia col*i cell division protein FtsI (PBP3) to the division site and cell pole. Molecular Microbiology 25(4), 671-681.

Wenk, P. and Renz, A. (2003). Parasitologie: Biologie der Humanparasiten; 12 Tabellen. Thieme.

Werren, J. H., Baldo, L. and Clark, M. E. (2008). *Wolbachia*: master manipulators of invertebrate biology. Nature Reviews Microbiology 6(10), 741-751.

Wheeler, R., Chevalier, G., Eberl, G. and Gomperts Boneca, I. (2014). The biology of bacterial peptidoglycans and their impact on host immunity and physiology. Cellular Microbiology 16(7), 1014-1023.

WHO (2012). Roadmap approved by the Strategic and Technical Advisory Group for Neglected Tropical Diseases in 2011. Available: http://www.who.int/neglected_diseases/NTD_RoadMap_2012_Fullversion.pdf [Online]. [Accessed: 02.05.2018].

WHO (2016a). Weekly Epidemiological Record, 23 September 2016, vol. 91, 39 (pp. 441–460).

WHO (2016b). Weekly Epidemiological Record, 28 October 2016, vol. 91, 43 (pp. 501–516).

Wu, M., Sun, L. V., Vamathevan, J., Riegler, M., Deboy, R., Brownlie, J. C., et al. (2004). Phylogenomics of the reproductive parasite *Wolbachia pipientis w*Mel: a streamlined genome overrun by mobile genetic elements. PLoS Biology 2(3), e69.

Yeats, C., Finn, R. D. and Bateman, A. (2002). The PASTA domain: a β-lactam-binding domain. Trends in Biochemical Sciences 27(9), 438-440.

Yeh, Y.-C., Comolli, L. R., Downing, K. H., Shapiro, L. and McAdams, H. H. (2010). The *Caulobacter* Tol-Pal complex is essential for outer membrane integrity and the positioning of a polar localization factor. Journal of Bacteriology 192(19), 4847-4858.

Zapun, A., Vernet, T. and Pinho, M. G. (2008). The different shapes of cocci. FEMS Microbiology Reviews 32(2), 345-360.

Zhao, G., Meier, T. I., Kahl, S. D., Gee, K. R. and Blaszczak, L. C. (1999). Bocillin FL, a sensitive and commercially available reagent for detection of penicillin-binding proteins. Antimicrobial Agents and Chemotherapy 43(5), 1124-1128.

Zug, R. and Hammerstein, P. (2012). Still a host of hosts for *Wolbachia*: analysis of recent data suggests that 40% of terrestrial arthropod species are infected. PloS One 7(6), e38544.

Zug, R. and Hammerstein, P. (2015). Bad guys turned nice? A critical assessment of *Wolbachia* mutualisms in arthropod hosts. Biological Reviews 90(1), 89-111.

List of abbreviations

µg	Microgram
µl	Microliter
µm	Micrometer, micron
µM	Micromolar
ad	Adjust volume to
AHT	Anhydrotetracycline
AmiD^{wMel}	N-acetylmuramoyl-L-alanine amidase from *Wolbachia* endosymbiont of *Drosophila melanogaster*
Aqua dest.	Aqua destillata
BCIP	(5-bromo-4-chloro-1H-indol-3-yl) dihydrogen phosphate
BLI	Biolayer interferometry
bp	Base pair(s)
BSA	Bovine serum albumin
°C	Degree Celsius
C_{55}-P	Undecaprenyl phosphate
d	Day
Da	Dalton
DAAO	D-amino acid oxidase
D-Ala	D-alanine
D-Ala-D-Ala	D-alanyl-D-alanine
DAPI	4′,6-Diamidin-2-phenylindol
DMSO	Diethyl sulfoxide
DNA	Deoxyribonucleic acid
dNTP	Deoxynucleotide triphosphate
EDA-DA	Ethynyl-D-alanyl-D-alanine
EDTA	Ethylenediaminetetraacetic acid
ELA-LA	Ethynyl-L-alanyl-L-alanine
FCS	Fetal calf serum
g	Gravimetric force
Glc*N*Ac	N-acetylglucosamine
h	Hour
HMW	High molecular weight

HPLC	High performance liquid chromatography
kb	Kilobase
kDa	Kilodalton
l	Liter
L-Ala	L-alanine
LB-medium	Lysogeny broth medium
Lipid II	Undecaprenyl-pyrophosphoryl-Mur*N*Ac-pentapeptide-Glc*N*Ac
L-Lys	L-lysine
LMW	Low molecular weight
M	Molar
MALDI-TOF	Matrix-assisted laser desorption/ionization time-of-flight
MDA	Mass drug administration
min	Minute
m-DAP	Meso-diaminopimelic acid
mg	Milligram
ml	Milliliter
mM	Millimolar
Mur*N*Ac	N-acetylmuramic acid
MW	Molecular weight
NaOH	Sodium hydroxide
NBT	Nitro blue tetrazolium chloride
NCBI	National Center for Biotechnology Information
ng	Nanogram
nm	Nanometer
nM	Nanomolar
NOD	Nucleotide-binding oligomerization domain
OD_{600}	Optical density at 600nm
Pal^{wBm}	Peptidoglycan-associated outer membrane lipoprotein from *Wolbachia* endosymbionts of *Brugia malayi*
PAMP	Pathogen-associated molecular pattern
PBP	Penicillin-binding protein
$PBP2^{wBm}$	Penicillin-binding protein 2 from *Wolbachia* endosymbionts of *Brugia malayi*
$PBP3^{wMel}$	Penicillin-binding protein 3 from *Wolbachia* endosymbionts of *Drosophila melanogaster*

PBP6a^{wBm}	Penicillin-binding protein 6a from *Wolbachia* endosymbionts of *Brugia malayi*
PCR	Polymerase chain reaction
PFA	Paraformaldehyde
pH	Pondus hydrogenii, hydrogen ion concentration
Pi	Inorganic phosphate
PMA	Phosphomolybdic acid
qPCR	Quantitative real-time PCR
RBB	Remazol brilliant blue
RNA	Ribonucleic acid
rpm	Rotations per minute
RT	Room temperature
s	Second
SD	Standard deviation
SDS	Sodium dodecyl sulfate
SDS-PAGE	Sodium dodecyl sulfate polyacrylamide gel electrophoresis
SEM	Standard error of the mean
SPR	Surface plasmon resonance
TEMED	Tetramethylethylenediamine
TLC	Thin layer chromatography
TLR	Toll-Like-Receptor
Tris	Tris(hydroxymethyl)aminomethan
UDP	Uridine diphosphate
UDP-Glc*N*Ac	Uridine diphosphate N-acetylglucosamine
UDP-Mur*N*Ac	Uridine diphosphate N-acetylmuramic acid
V	Volt
v/v	Volume per volume
***w*ALB B**	*Wolbachia pipientis* strain *Aedes albopictus* B
***w*Bm**	*Wolbachia* endosymbionts of *Brugia malayi*
WHO	World Health Organization
***w*Mel**	*Wolbachia* endosymbionts of *Drosophila melanogaster*
w/v	Weight per volume